

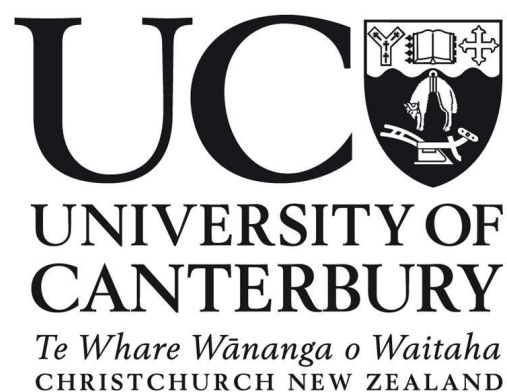
# The geomorphological response of uplifted unconsolidated coastal environments, Kaikōura, New Zealand

---

A thesis submitted in partial fulfilment of the  
requirements for the degree of  
**Master of Science in Environmental Science**  
at the University of Canterbury

**Kate MacDonald**  
University of Canterbury  
February 2019

---



# Abstract

Earthquakes can significantly warp coastlines and induce sudden changes in relative sea level. Along the northeast coast of New Zealand's South Island, a 7.8  $M_w$  earthquake on the 14<sup>th</sup> of November 2016 induced instantaneous uplift of approximately 1 m around the Kaikōura Peninsula, and deformation along 110 km of coastline. This uplift induced a relative sea level fall, and two years after the earthquake, mixed sand and gravel (MSG) beach responses have now been documented. The overarching aim of this thesis is to further understand how MSG coastal environments respond to a large tectonic events where there is an earthquake-induced change in relative sea level, using the Kaikōura Earthquake as a case study.

As a baseline from which to understand the MSG beach response, pre-earthquake trends of 18 profiles along the Kaikōura coastline were calculated and a cluster analysis of geomorphic parameters was undertaken to determine the within-type variations of MSG beaches within the study area. Common post-earthquake surveying techniques were analysed using both pre and post-earthquake data to determine the most appropriate method of surveying following an event that causes deformation of the geodetic system. Global Navigation Satellite System (GNSS) surveying equipment was then used to re-survey 18 beach profiles, and sedimentology data was collected using Digital Grain Size (DGS) analysis methods, at the same locations as pre-earthquake data for comparability. Methodology investigations identified that following an earthquake, damage to the geodetic system can make obtaining short-term data difficult. Such data, therefore, is either rarely collected because of the complexities involved, or data is collected knowing there will need to be future pre-use adjustments. A mixed method approach, using both Digital Elevation Models (DEM) generated by Light Detection and Ranging (LiDAR) data and beach profile surveys, was determined to be the most appropriate approach to use in a post-earthquake coastal environment, given the complimentary spatial and temporal attributes of these two techniques.

The results of this study showed that Kaikōura beaches can be classified into three within-type variations: (1) accretionary South Bay beaches; (2) open coast and rivermouth beaches; and (3) narrow and steep beaches. The three different within-type beach groups then responded to the earthquake in similar ways, as revealed by resurveys in both 2017 and 2018. Volume increase, progradation and berm redevelopment relative to sea level occurred at all profiles that were resurveyed in January 2017. However, these responses between within-type variations had altered again by the September 2018 re-survey. Conceptual response pathway models were developed using the results from the beach surveying collected in this study, combined with historical response studies to inform a longer term response. Predominantly, there were



two main response pathways: (1) accretional and (2) erosional. The conceptual models detail that the rate at which the beaches respond following the earthquake depends on the amount of sediment supply at a profile, as well the environmental conditions which were driving pre-earthquake long-term trends at the different profiles. Overall, profiles which had a long-term accretionary trend pre-earthquake are predicted to take longer to return to pre-earthquake profile extents, whilst profiles which showed pre-earthquake erosional trends tend to very rapidly erode back to their pre-earthquake extent and shape. The latter types of profile began to return to their pre-earthquake extent within the first two years of the Kaikōura event.

Prior to this research, few studies have examined in detail the field response of MSG beaches to instantaneous changes in relative sea level, especially in the initial years following an earthquake. Furthermore, there has been no commonly accepted protocol identifying a best-approach to surveying coastal environments following earthquakes. Poorly informed ideas of how coastal systems respond to earthquakes can result in poor resource management decisions, which can have significant impacts on coastal communities for many future decades. This research has contributed to bridging this knowledge gap, by developing a best-approach method to coastal surveying post-earthquake, as well as in acknowledging the errors which can be involved in both collection and processing. The results of this study have contributed to the response model of MSG beaches to earthquakes and to relative sea level fall by addressing the short-term responses. Future research includes the continued monitoring of the 18 beach profiles to bridge the temporal gap between this study and Single's (1985) long-term response model.



Mixed sand and gravel beaches of Kaikōura, 19<sup>th</sup> August 2018. Photo credit: K MacDonald

# Table of Contents

|  |           |
|--|-----------|
| Abstract . . . . .   | i         |
| Acknowledgements . . . . .   | xix       |
| <b>1 Introduction</b>  | <b>1</b>  |
| 1.1 Background . . . . .   | 1         |
| 1.2 Research aims and objectives . . . . .                               | 3         |
| 1.3 Thesis structure . . . . .   | 4         |
| <b>2 Literature Review</b>   | <b>6</b>  |
| 2.1 Introduction . . . . .   | 6         |
| 2.2 Mixed sand and gravel coastal environments . . . . .                 | 6         |
| 2.2.1 Mixed sand and gravel beaches . . . . .                            | 7         |
| 2.2.2 Hapua lagoons . . . . .  | 10        |
| 2.3 Coasts and earthquakes . . . . .                                     | 11        |
| 2.4 Coastal response to relative sea level fall . . . . .                | 14        |
| 2.5 Surveying in a post-earthquake environment . . . . .                 | 18        |
| 2.6 Conclusions . . . . .  | 21        |
| <b>3 Study area: Kaikōura, New Zealand</b>                               | <b>23</b> |
| 3.1 Introduction . . . . .   | 23        |
| 3.2 Field sites . . . . .  | 23        |
| 3.3 Fluvial environment . . . . .  | 25        |
| 3.4 Coastal environment . . . . .  | 26        |
| 3.5 Tectonic history . . . . .   | 33        |
| <b>4 Methodology</b>   | <b>37</b> |
| 4.1 Introduction . . . . .   | 37        |
| 4.2 Data and methods: Pre-earthquake Kaikōura beaches analysis . . . . . | 39        |
| 4.2.1 Beach profile surveying data . . . . .                             | 39        |
| 4.2.2 Classification of Kaikōura MSG beaches . . . . .                   | 40        |

|          |  |           |
|----------|--|-----------|
| 4.2.3    | Cluster analysis of geomorphic parameters . . . . .                      | 40        |
| 4.3      | Data and methods: Critiquing post-earthquake survey techniques . . . . . | 43        |
| 4.3.1    | Digital elevation model (DEM) . . . . .                                  | 43        |
| 4.3.2    | Aerial imagery . . . . .   | 45        |
| 4.4      | Data and methods: Post-earthquake Kaikōura beaches analysis . . . . .    | 46        |
| 4.4.1    | Beach profile surveying . . . . .  | 47        |
| 4.4.2    | Sedimentology . . . . .  | 52        |
| <b>5</b> | <b>Kaikōura's Mixed Sand and Gravel Beaches</b>                          | <b>58</b> |
| 5.1      | Introduction . . . . .   | 58        |
| 5.2      | A review of geomorphic parameters . . . . .                              | 60        |
| 5.3      | Classification of Kaikōura MSG beaches . . . . .                         | 66        |
| 5.3.1    | Group 1: Accretionary South Bay beaches . . . . .                        | 67        |
| 5.3.2    | Group 2: Wide and flat open coast and rivermouth beaches . . . . .       | 71        |
| 5.3.3    | Group 3: Steep and narrow beaches . . . . .                              | 72        |
| 5.4      | Conclusions . . . . .  | 74        |
| <b>6</b> | <b>Surveying in a Post-Earthquake Environment</b>                        | <b>76</b> |
| 6.1      | Introduction . . . . .   | 76        |
| 6.2      | Results . . . . .  | 77        |
| 6.2.1    | Beach profile surveying . . . . .  | 77        |
| 6.2.2    | Digital Elevation Model . . . . .  | 78        |
| 6.2.3    | Aerial imagery . . . . .   | 81        |
| 6.3      | Discussion . . . . .   | 84        |
| 6.4      | Conclusions . . . . .  | 87        |
| <b>7</b> | <b>Post-earthquake geomorphological response</b>                         | <b>89</b> |
| 7.1      | Introduction . . . . .   | 89        |
| 7.2      | Investigating differences in post-earthquake surveying data . . . . .    | 91        |
| 7.3      | Geomorphological response . . . . .                                      | 95        |
| 7.3.1    | Differential coastal uplift . . . . .                                    | 96        |
| 7.3.2    | Volume change . . . . .  | 97        |
| 7.3.3    | Progradation and transgression . . . . .                                 | 101       |
| 7.3.4    | Berm redevelopment . . . . .   | 103       |
| 7.3.5    | Sedimentology . . . . .  | 105       |
| 7.4      | Discussion . . . . .   | 108       |
| 7.4.1    | Geomorphological response . . . . .                                      | 108       |

|          |   |            |
|----------|---|------------|
| 7.4.2    | Sedimentological response . . . . .                                   | 111        |
| 7.5      | Conclusions . . . . .   | 112        |
| <b>8</b> | <b>Discussion</b>   | <b>114</b> |
| 8.1      | Introduction . . . . .  | 114        |
| 8.2      | Conceptual response pathways . . . . .                                | 114        |
| 8.2.1    | Accretional profile response pathway . . . . .                        | 116        |
| 8.2.2    | Erosional profile response pathway . . . . .                          | 120        |
| 8.2.3    | Rock shore platform accretionary response pathway . . . . .           | 122        |
| 8.2.4    | Rock shore platform erosional response pathway . . . . .              | 125        |
| 8.2.5    | Environmental conditions influencing response rate . . . . .          | 127        |
| 8.3      | Consideration of seismic hazards in coastal environments . . . . .    | 128        |
| 8.4      | Implications for Kaikōura coastal resource management . . . . .       | 132        |
| 8.5      | Surveying in post-earthquake environments . . . . .                   | 134        |
| 8.6      | Conclusions . . . . .   | 135        |
| <b>9</b> | <b>Conclusions</b>  | <b>137</b> |
| 9.1      | Key findings . . . . .  | 137        |
| 9.2      | Limitations . . . . .   | 140        |
| 9.3      | Future research . . . . .   | 141        |
|          | <b>Appendices</b>   | <b>157</b> |
| A        | Site descriptions for Environment Canterbury beach profiles . . . . . | 157        |
| B        | Methods for calculating geomorphic parameters . . . . .               | 176        |
| C        | Methods for calculating environmental parameters . . . . .            | 179        |
| D        | Sedimentology results . . . . .                                       | 181        |

# List of Figures

|     |   |    |
|-----|---|----|
| 2.1 | MSG beach morphology and zonation. Adapted from Kirk (1980). . . . .  | 8  |
| 2.2 | Classification of rivermouth environments based on process agents dominating the interface environment, showing Hapua lagoons to be wave dominated environments. Taken from Hart (2007). . . . .  | 10 |
| 2.3 | Morphological states of a hapua environment. Behavioural change over time depends on wave and river influences, closing and breaching the gravel barrier. Taken from Hart (2009). . . . .   | 11 |
| 2.4 | Profile response of an uplifted beach where there is a relative sea level fall. As the beach responds, the berm reforms relative to sea level. Adapted from Single (1985). . . . .  | 16 |
| 2.5 | Aftershocks in the Canterbury Earthquake Sequence (CES) following three main earthquake events, which highlights the decay in frequency and magnitude of aftershocks following the event. Aftershocks were still occurring over 400 days after the initial earthquake in September 2010. Taken from Shcherbakov et al. (2012). . . . .  | 20 |
| 3.1 | 18 Environment Canterbury beach profile sites, which have been surveyed annually from 1997–2015, and used for analysis in this study. Contains data sourced from the LINZ Data Service. . . . .   | 24 |
| 3.2 | The Kowhai River historically flowed across the fan beneath the Mount Fyffe catchment. The mouth was once located on the northern side of the Peninsula near the Kaikōura Township. The Kowhai River currently flows south of the Kaikōura Peninsula, and is contained by stop banks, but after periods of heavy prolonged rainfall, the Kowhai River can flood old channel and exit the township at the Lyall Creek outflow which runs through the township. Taken from Dawe (2001). . . . . | 26 |

|     |   |    |
|-----|---|----|
| 3.3 | Wave conditions north and south of the Peninsula when a strong southerly is taking place. The left image is taken in South Bay, while the right image shows the contrasting calmer conditions at Gooches Beach, north of the Peninsula, demonstrating the buffering effect of the Peninsula. Image taken 24 <sup>th</sup> August 2018. Photo credit: K MacDonald . . . . .  | 28 |
| 3.4 | Tidal cycles measured in 2017, showing The high tide extents throughout the years (above MSL) and the low tide extents (below MSL), where MSL in Kaikōura is approximately 1.2 m. Data sourced from NIWA Tide forecaster. . . . .   | 29 |
| 3.5 | Schematic of the Kaikōura coastline showing the main sediment transport systems along rivers, creeks and tributaries. Longshore transport in the swash zone is the main process of moving sediment alongshore. Wave refraction around the Pensinsula, as well as prevailing north-easterly winds, help drive longshore transport south from the Hāpuku River. . . . .   | 30 |
| 3.6 | Distribution of fault lines across New Zealand, confined largely to the central North and South islands. (Left) New Zealand sits on the plate boundary of the Pacific and Australian Plates. (Right) Faults which affect Kaikōura, with the red faults detailing the faults which ruptured in the 2016 November earthquake. Data is provided from New Zealand GeoNet project and its sponsors EQC, GNS Science and LINZ. Basemaps are sourced from the LINZ Data Service. . . . .   | 34 |
| 3.7 | Two of the estimated >10,000 landslides which occurred as a result of the 7.8 Kaikōura Earthquake. The left image shows a landslide which was located approximately 10 km south of the Peninsula. The landslide at Ohau Point (right), is located approximately 25 km north of the Peninsula. Seawalls have now been put at both locations to protect the recovery efforts from intense wave action. Images sourced from the LINZ Data Service. . . . .   | 35 |
| 4.1 | Research framework of the overall methodological approach. Two time periods are studied, pre-earthquake and post-earthquake. The pre-earthquake analysis uses both desktop analysis and data analysis to determine pre-earthquake beach trends, and the within-type variations of MSG beaches in the Kaikōura area. Post-earthquake beach response is determined through the collection of beach profile surveying and sedimentology data. An overall synthesis of results uses the pre-earthquake beach states to investigate the changes in the post-earthquake environment, and develop conceptual pathway models to illustrate how the MSG beaches responded post-earthquake. . . . . | 38 |

|     |   |    |
|-----|---|----|
| 4.2 | Framework of pre-earthquake classification of MSG beaches. The flow chart outlines the different methods and data used to calculate the different geomorphic and environmental parameters for the MSG classification component of this study. Adapted from Scott et al. (2011) . . . . .  | 41 |
| 4.3 | Schematic of a MSG beach profile showing the extent and occurrence of the geomorphic parameters calculated used in the classification component of this study in a simplified MSG environment. Adapted from Kirk (1980). . . . .  | 42 |
| 4.4 | The subtraction tool in <i>ArcGIS</i> is used to determine the elevation differences between the 2012 and 2018 DEM. The tool subtracts one raster dataset from the other, and its output is the elevation difference between the two data sets. The red boxes represent an elevation fall from 2012-2018, which could be a result of subsidence, or in a coastal setting, erosion. The green boxes are calculated as a rise in elevation between 2012 and 2018, indicative of uplift or in a coastal setting, accretion. . . . .                      | 44 |
| 4.5 | Two lines analysed on the aerial imagery are the vegetation line, marked where the last line of vegetation is before the beach turns into complete sediment. The second line is the wet water line, which is measured with consideration of a margin of error (MOE). The slope of the foreshore between the high tide and the low tide mark (x) is measured as the MOE to account for the differences in tides when the images were captured. If the change in a shoreline is more than the MOE, then the change in shoreline is significant. . . . . | 46 |
| 4.6 | Profiles KCK2470 (left), KCK2486 (middle) and KCK2496 (right) profile lines, with control points intersecting the profile line in their pre-earthquake positions. Basemap sourced from the LINZ Data Service. . . . .   | 48 |
| 4.7 | Sequence of diagrams showing the changing of survey planes following a major tectonic event. (A) Pre-earthquake survey line, which runs through two control points to the edge of the shoreline. (B) Uplift and horizontal translation moves the physical control points, which moves the physical survey line. (C) Two survey lines now exist following a large tectonic event. . . . .  | 49 |
| 4.8 | Four different profile lines are shown here on a simplified MSG beach profile, which are used for analysis in Chapter 7. The four lines are: pre-earthquake (2015), uplifted 2015 profile to represent an immediate uplifted profile after the earthquake, January 2017 survey profile, and September 2018 survey profile. . .  | 50 |



|      |  |    |
|------|--|----|
| 4.9  | Location of base station set up and radio repeater set up over the 19 <sup>th</sup> to 21 <sup>st</sup> September 2018 fieldwork. Insets (left) shows the base station set up on the South Bay Wharf, and (right) the radio repeater set up at the northern end of Gooches Beach. Basemap sourced from the LINZ Data Service. Photo credit: K MacDonald. . . . .   | 53 |
| 4.10 | Annotated diagram of a screenshot of profile KCK3800 survey showing how the survey data was processed using <i>ArcGIS</i> . The geospatially correct location of the control points and known distance between control points meant that survey points collected along the geospatial plane could be comparable to 1997–2015 ECan surveys. . . . .   | 54 |
| 4.11 | (A) Sediment sampling box in the field, showing dimensions and where the camera and flash is placed. (B) Example of a sediment sample image taken in the upper foreshore at profile KCK2510, showing that the box enables natural light to be excluded from the image, but the flash gives a consistent light source to the sample. Photo credit: K MacDonald. . . . .   | 55 |
| 4.12 | Screen capture of the DGS user interface, where images of sediment can be loaded into, a region of interest can be selected, filters can be applied, and a resolution can be set. Size distribution is then calculated, and a more extensive set of grainsize statistics is exported into <i>Microsoft Excel</i> . . . . .   | 56 |
| 5.1  | Volume and 1m horizontal contour changes over the 1997–2015 period for profile KCK2200 (left) and KCK3684 (right). The figures show that the 1m contour and the volume track very similarly at profiles which are less dynamic, however at profile KCK2200, the 1 m contour can vary significantly, while its volume is undergoes much less significant year to year changes. . . . .                          | 63 |
| 5.2  | Results of Hierarchical Cluster analysis showing three main clusters, and profile KCK4200 as an outlier. Group 1 consists of profiles which are located in South Bay which have a strong accretionary trend. Group 2 profiles are predominantly located in open coast and rivermouth environments. Group 3 consists of profiles which are steep an narrow, and distributed widely throughout the study area. . | 67 |
| 5.3  | Distribution of groups based on the cluster analysis using geomorphic parameters. The cluster analysis results showed that there were 3 main variations of MSG beaches found in the study area, and they are predominantly distributed in geographically similar areas with common environmental conditions acting on the profiles. Basemap sourced from the LINZ Data Service. . . . .                        | 68 |

|     |   |    |
|-----|---|----|
| 5.4 | Images taken August 2018 of the three different beach groups: (Top) Group 1 accretionary South Bay beaches, taken at KCK2486 and KCK2550; (middle) Group 2 wide and flat open coast and rivermouth beaches, taken at KCK2200 by the Kowhai rivermouth and KCK4220 by the oxidation ponds; and (bottom) Group 3 steep and narrow beaches, taken at KCK3737 and KCK5025. Photo credit: K MacDonald . . . . .  | 69 |
| 5.5 | MSD ordinations of beach profiles from the similarities matrix, showing the variation of each parameter for each group, as per the scale at the top right of each graph. The dashed lines represent the grouping of profiles as per the MSD ordinations and hierarchical cluster analysis. . . . .  | 70 |
| 6.1 | Beach profile survey collected using GNSS surveying equipment at profile KCK3855 near the railway station. The four different lines represent different time periods: 2015, immediately after the earthquake, January 2017, and September 2018. . .   | 78 |
| 6.2 | Two differential DEM's showing the difference in elevation from 2012 to 2018 by the Kaikōura township (left) and the South Bay area (right). Green indicates uplift/accretion of sediment on the beach over the 4 year period, and red represents the subsidence/erosion. Grey represents the error margin of 1 m resolution LiDAR which is 0.15–0.25 m. Light green represents what may be considered as a direct result of the uplift as over these two areas, they were uplifted approximately 1 m. Beyond the 1 m uplift (dark green) may be a result of accretion, human modification or translation of land in steep areas. . . . . | 80 |
| 6.3 | Profiles from profile KCK3684 extracted from the 2018 DEM using the 3D analyst tool in <i>ArcGIS</i> (left) and beach profile survey collected using GNSS surveying equipment (right). The raw data is represented with a black solid line. Red dotted lines account for the error in the technique, where DEM will have a 0.2 m (0.15 to 0.25 m) vertical accuracy, and GNSS beach profile surveys will have 0.02 m vertical accuracy. . . . .   | 81 |
| 6.4 | Four different areas of shoreline analysis using aerial photography are shown here. (A) KCK2200; (B) KCK2470 to KCK2550; (C) KCK3712 and KCK3737; and (D) KCK3800 and KCK3855. Each image has 6 lines present, 3 representing the wet water line extent for 1999, 2014 and 2016; and 3 representing the vegetation line extent for 1999, 2014 and 2016. Basemaps sourced from the LINZ Data Service. . . . .  | 83 |

- 6.5 Explanatory diagram showing the effect tides have on the interpretation of shore-line analysis using aerial imagery. This diagram shows the foreshore profile lines of profile KCK2550 for 1999, 2014 and 2017, the profiles closest to the time of capture of aerial imagery. The shaded blue area represents the tidal range. If the images in 1999 and 2014 were captured at low tide, the beach profile data shows the same wet water line change as the aerial imagery results. The 2016 aerial imagery must have been therefore taken at high tide in order for aerial imagery to have shown a retreat of 3 m. If the 2016 image was taken at low tide, aerial imagery would have shown progradation of 10 m between 2014 and 2016. . 87
- 7.1 Differential uplift in the study area predominantly caused by the 14<sup>th</sup> of November 2016 earthquake, showing that areas closer to the Peninsula uplifted between 0.8-1m, matching the Clark et al. (2017) study, whereas profiles further away from the Peninsula, both north and south, experienced different degrees of uplift. Both profile KCK1870 and KCK5025 experienced 0.5-0.6m of uplift, while profile KCK4700 experienced no change in elevation of control points. Imagery from Google, Digital Globe. . . . . 90
- 7.2 Manual adjustment in *Microsoft Excel* to match the ‘raw’ 2017 survey to the backshore of the 2018 survey taken in this study. This figure shows how the uplifting of the backshore can affect perceived trends between 2017-2018 on the beach profile. Where the dotted red (raw 2017) and the solid red (adjusted 2017) appear on the same side of the black solid line (2018), there was no change in trend from year to year between the two surveys when the 2017 survey is manually adjusted. The lower foreshore shows a change in trend where the raw data shows a stable trend from 2017-2018 where both profiles stay the same, whereas the adjusted 2017 profile shows erosion in this area from 2017 to 2018. . 92

|     |   |     |
|-----|---|-----|
| 7.3 | Magnitude, depth and location of earthquakes and aftershocks with epicentres in the study area (top) and larger rupture region (bottom) following the November 2016 earthquake. (Top row) the occurrence of aftershocks and earthquakes in the six months following the earthquake, and subsequent images show the 6 month periods in sequence. The images show that most aftershocks are $<3 M_w$ , and the frequency of aftershocks drops from 1453 in the six months after the earthquake, to 167 between May 2017 and November 2017, to 107 between November 2017 and May 2018; and 79 between May 2018 and November 2018. (Bottom row) the occurrence of aftershocks $> 3 M_w$ in the larger region from the November earthquake to the January 2017 survey (bottom left), compared with aftershocks between the January 2017 survey and the September 2018 survey (bottom right). The red box highlights the study area, showing most aftershocks in the study area occurred before the first survey. Data is provided from New Zealand GeoNet project and its sponsors EQC, GNS Science and LINZ. Basemap is sourced from OpenStreetMap. . . . . | 94  |
| 7.4 | Summary of post-earthquake volume changes between each survey following the earthquake. All profiles surveyed in 2017 experienced an increase in subaerial volume. The 2018 survey showed some profiles had begun to erode, but profiles still maintained an overall net gain of subaerial sediment volume. Profile KCK4700 was not surveyed in 2017, however the overall volume change from 2015-2018 shows a significant loss of subaerial volume. This profile also experienced no uplift. No profiles showed volume loss between 2015–2017. . . . .   | 98  |
| 7.5 | Two graphs showing the rate of volume change following the earthquake (red) in relation to its pre-earthquake trend. Profile KCK2200 (left) showed a strong accretionary trend following the earthquake, as the volume of sediment at the profile has far exceeded any volume previously seen at the profile. Profile KCK3737 (right) shows that initially the volume increased beyond any volume seen at the profile pre-earthquake, however from January 2017 to September 2018 volume has begun to decline back to pre-earthquake figures. . . . .   | 99  |
| 7.6 | A summary of horizontal 1 m contour changes following the earthquake. The 2017 survey showed progradation at all profiles following the earthquake. 50% of profiles surveyed in both 2017 and 2018 showed shoreline transgression from 2017 to 2018. Profile KCK2200 showed continued progradation at a high rate in 2018, while profile KCK4700 has undergone a substantial amount of shoreline transgression. No profiles that were surveyed in 2017 showed transgression between 2015–2017. . . . .  | 102 |

|     |   |     |
|-----|---|-----|
| 7.7 | Berm morphology changes seen in post-earthquake surveys, representative of the three different geomorphic groups. Group 1 and 3 show the berms redevelopment at pre-earthquake elevations, while Group 2 profiles have redeveloped the storm berm but the lower foreshore continues to grow and flatten out. . . . .  | 104 |
| 7.8 | Differences in 1997 and 2018 graphic mean beach sediment sizes (mm), shown from south to north along the horizontal axis. A negative value implies that the mean grain size has decreased since 1997, and a positive grain size change implies that the mean grain size has increased since 1997. Most profiles have undergone change to some degree. The raw graphic mean results are found in Appendix D.   | 107 |
| 8.1 | Conceptual model showing accretional beach response following an earthquake with their associated sediment budget on the right. This model indicates that when uplift occurs, the position of maximum wave effect steps out, there is an increase in sediment supply as fines move down the catchment. Over the subsequent months, berms build with the increased sediment budget at elevations lower than pre-earthquake berm elevations. In the years following the earthquake (Stage 3), there is still an increase in gravel sediment moving down the catchment and promoting further accretion of the beach. Stages 4 and 5 are faded out to represent the uncertainty of these model outcomes, due to the knowledge of pre-earthquake accretional trends. Single's (1985) model informs these two stages, however its unknown how accurate the fully response will be in this setting. Slowly, the nearshore will erode from the concentration of the wave energy in a seaward position, and the point of maximum wave effect will move landward. The old storm berm becomes a paleo beach, and undergoes no further changes. . | 118 |

- 8.2 Conceptual response pathway for erosional beach profiles, which had poor sediment supplies and erosional trends pre-earthquake. Stages 1–2 demonstrate the immediate and short-term effects of the earthquake, where the old storm berm is lifted out of the wave action zone, and the foreshore is reworked to form berms relative to sea level, at elevations similar to pre-earthquake. Stages 3 shows the response in the years following the earthquake, where the uplifted profile is eroding back to the pre-earthquake position, where it will still continue to erode due to the lack of sediment reaching the profiles, and the pre-earthquake trends resuming. Stages 4 and 5 are informed by the Single (1985) model, however due to the knowledge that these beaches were eroding pre-earthquake, it is uncertain whether they will respond in the same way as Single’s (1985) model. The continued erosion may erode away at the beach below the limit of wave process action, and cause scarping. . . . . 121
- 8.3 Conceptual response pathway for accretional beaches which are located on top of limestone platforms. The position of maximum wave effect is stepped out into the nearshore, and the rate of response is dependent on the rate at which the nearshore can be eroded, which is very long due to the nearshore being consolidated limestone. The new position of the position of maximum wave effect is promotes onshore accretion as wave energy is dissipated further seaward than pre-earthquake. The erosion of the nearshore profile takes a long time because of slow erosion rate of consolidated rock. The max wave effect position slowly moves landward, and in doing so wave energy reaches closer to the beach, and as this happens, the profile slowly retreats to the pre-earthquake profile extent. This response is likely to be on a several decades to century scale. Stages 4 and 5 are based on Single’s (1985) model, and are faded out to represent the uncertainty that these responses will occur due to the differences in circumstances between the Kaikōura and Napier coastal environments. . . . . 124

|     |  |     |
|-----|--|-----|
| 8.4 | Conceptual response model for erosional beaches on limestone platforms. Uplift makes the position of max wave effect step out, and has to erode the limestone platform to return back to its pre-earthquake position. Progradation and accretion occurs in the initial months after the earthquake because there is more suspended sediment in the nearshore from distant sediment sources, and wave energy is dissipated further seaward than before the earthquake. The position of maximum wave energy very slowly begins to move landward. Over time, the lack of sediment supply to the profiles and the increased wave energy acting on the subaerial environment leads to erosion of the profile back to the pre-earthquake profile extents, potentially creating a scarp as it continues to erode back into the sediment below the limit of wave process action. . . . . | 126 |
| 8.5 | A temporal and spatial representation of coastal processes which affect the coastal morphology. Earthquake disturbances has been added to the conceptual diagram in the geological section due to the long return interval of earthquakes, and the response period of its sub-sequential hazards and impacts. Earthquake disturbances encompasses all short and long-term effects of the earthquake, including tsunami inundation to river aggradation, to long-term nearshore adjustments. Adapted from Woodroffe (2003) after Cowell and Thom (1994). . . . .  | 130 |
| 8.6 | Seismic Staircase model that shows that immediate and delayed responses of the sand beach environment following an earthquake. The responses of humans are variable, but can be both immediate and delayed (Taken from Goff and McFadgen, 2002) . . . . .  | 131 |

# List of Tables

|     |  |    |
|-----|--|----|
| 3.1 | Beach renourishment volumes which took place between 1997 and 2016 along the Kaikōura Esplanade by the Kaikōura District Council (KDC) to slow erosion rates in this area. Sediment was taken from South Bay and relocated to various locations along the Esplanade throughout the 19 year period. Information sourced from OCEL Consultants NZ Ltd (2016) and Bruce Gabites, ECan Coastal Scientist (Pers comm, 2018). . . . .  | 32 |
| 5.1 | Literature review of studies which have classified different beach types, and the parameters used in these study to classify the beach type and within-type variations. . . . .  | 61 |
| 5.2 | A summary of the environmental conditions measured and acting on the different beach groups. This shows the break down of the three main within-type variations, describing the contributing factors to their geomorphic states. Within-type variations can be sub-categorised again based on environmental conditions, and refining groups based on their geographic distribution within the study area. . .  | 73 |
| 6.1 | A summary table of the benefits, drawbacks, and accuracy/errors of each method analysed in Chapter 6. . . . .  | 85 |
| 7.1 | Adjustment of the ECan January 2017 survey to match the backshore elevations of the 2018 survey taken in this study to minimise the unexplained differential ‘error’. Calculations of volume and 1 m horizontal contour were recalculated for the adjusted surveys and are shown here compared as ‘raw’ (ECan survey) and ‘adjusted’ (ECan survey backshore adjusted to September 2018 survey backshore) to identify significant differences which would affect the perception of the results. Shaded numbers are the figures which their adjusted value did not have the same relationship (Progradation or Transgression) with the 2018 survey as the raw 2017 survey. . . . . | 96 |



|     |  |     |
|-----|--|-----|
| 7.2 | Rates of volume change per year, from 1997–2015 (Pre-Earthquake), compared with 2015–2018 (Post-Earthquake), demonstrating the changes in volume at most profiles being excessively more over the 3 year period since the 2015 survey. The rate of change at most profiles was more extreme during the 2015–2017 stage, however most profiles demonstrated continued growth at a rate higher than pre-earthquake during the 2017–2018 period. It is important to note that the pre-earthquake columns is averaged over a 17 year period, whilst the post-earthquake columns is only representative of a 2 year period. . . . . | 99  |
| 7.3 | Comparison of sand/gravel composition percentages between 1997 and 2018 for both the upper foreshore (UF) and the mid tide zone (MT). . . . .  | 106 |

# Acknowledgements

I would like to start by thanking my supervisors Dr Deirdre Hart and Dr Seb Pitman. It has been a pleasure working alongside you both. Thank you for the constant advise, feedback and insightful chats about anything and everything coastal. Your passion for coasts is very inspiring, and your support throughout the whole process has been invaluable. I could not have picked a better supervisory team, and am eternally grateful for all of the knowledge and opportunities you have both passed onto me.

I would like to thank the Waterways Centre for Freshwater Management for providing funding for this project through the Masters Scholarship for 2018. It was a real privilege to receive this scholarship and present at the post-graduate conference. A big thank you to Suellen for all of your help with organising funding for fieldwork away. Thank you also to University of Canterbury for providing funding through the UC Masters Scholarship.

Thank you to the geography department technician team - Paul, Justin and Nick. A special thanks to Paul Bealing for helping with everything surveying in Kaikōura, and giving me a crash course using a trimble. Your expertise and guidance was very much appreciated throughout the project.

Thank you to Bruce and Justin from Environment Canterbury for providing beach survey and sedimentology data, as well as for the initial discussions around the project. A special thanks to Bruce Gabites, for always answering my questions patiently and for helping with the fixing of the initial survey data. I really appreciated all of your advise on a topic which was unfamiliar to us all! Thank you to Martin Single and Derek Todd for the thought provoking discussions towards the end of the project, which came at a great time to pull me out of tunnel vision and broaden my thinking. Thank you also to Rachel Musgrove from NCTIR for supplying the 2018 LiDAR data.

Thank you to Laura and Euan for being the most joyful field assistants I could have asked for, and for all the laughs in the stressful times out in the field. Dr Jolley, thanks for proof reading in the final days (and the emotional support throughout my entire university journey!). To my friends, the Paroa Gang, the Dream team, the Girls, and the Geol crew, thanks for always giving me a good excuse to leave the office for a boogie. I am forever in debt to all of your kindness, friendship and inspiration to do awesome things. You all 'rock'.

Finally to my family. Mum, Dad, Sam, Lucas, Nana and Gryphon. Thanks for everything you do and continue to do. I wouldn't be where I am without you all, and I'm so lucky to have you.

# Chapter 1

## Introduction

### 1.1 Background

New Zealand is a tectonically activity country due to its location on the Australian and Pacific plate boundary. Despite the known seismic risks surrounding the high density of populations living near New Zealand coastlines, few studies have looked at how unconsolidated environments on coasts respond to a change in relative sea level following an earthquake event, and more specifically, mixed sand and gravel (MSG) beaches (Single, 1985; Paterson, 2000; Olson, 2010; Hart et al., 2015; Brown, 2017). While subsidence following an earthquake can accelerate relative sea level rise and increase the flood hazard in low lying developments (Hart et al., 2015), seismic uplift can have a temporary positive effect, where the backshore is elevated and more material is supplied to the subaerial beach profile, creating a impermanent buffer for the effects of sea level rise and masking previously known erosional trends at a coastline (Single, 1985). Following an earthquake event with significant uplift, there is a common public misconception that uplift of a coastline will suppress or eliminate long-term coastal hazards such as erosion, sea level rise and flooding associated with low lying developments. An example of this misconception was seen in 1931 following the 7.8  $M_w$  Napier earthquake, where an area of the coastline was uplifted and a backshore lagoon was drained as a result (Single, 1985; Komar, 2010). Poor understanding of the long-term response of MSG beaches at the time resulted in the newly uplifted land being used for residential development. 50 years on from the earthquake, Single (1985) noted in his research the erosion of the coastline which was beginning to effect the residents who lived on this uplifted land, as the nearshore had eroded back to pre-earthquake conditions, and the subaerial beach profile began to erode. An erosional scarp was 20 m away from residential houses and threatening the coastal development. The long time period between

the event and the response of the beach means that often a historic event is not attributed to a modern problem, especially in such a dynamic and changing environment. Other studies on the MSG beaches of the Wellington coastline have shown that over 150 years on from the Wairarapa 8.2  $M_w$  earthquake in 1855 the coastline is still responding (Olson, 2010). The aim of this research is to further our understanding of how MSG coastal environments respond to a large tectonic events where there is an earthquake-induced change in relative sea level, to further inform the existing response model which only addresses beach response on a historical time scale. This research uses the Kaikōura MSG beaches, and the 14<sup>th</sup> of November 2016 earthquake as a case study to record and analyse the short-term geomorphological changes.

The public and government misconception of the impacts of earthquakes on coastal systems is largely due to the lack of data which can properly inform longer term response models. There is a greater understanding now of the long-term response of these beaches following earthquakes (Single, 1985; Olson, 2010), however fewer studies detail the beach changes in the immediate aftermath of the event to the decadal response period (Stanley, 1968; Villagran et al., 2013). There are various issues which accompany the collection of data in the short-term following an earthquake, including the prioritising of recovering infrastructure, the threat of subsequent hazards from the event, as well as the process of adapting common surveying techniques and the geodetic system to the post-earthquake environment (Winefield et al., 2010). Earthquake events are unpredictable and infrequent, and therefore the short time frame for data to be collected following a significant event which causes enough change to prompt data collection, on a human time scale, is rare. In the past decade, the South Island has been affected by the Canterbury Earthquake Sequence (CES) from 2010 (Duffy et al., 2013), and more recently, the 7.8  $M_w$  November 14<sup>th</sup> 2016 Kaikōura Earthquake (Clark et al., 2017). Prior to these earthquakes, the only earthquake located in a densely populated centre which caused significant deformation and destruction was the 1931 Napier earthquake. The advancement of technology since the Napier earthquake means that some techniques used for cadastral surveying (property boundaries) or for council monitoring, had never been tested in a post-earthquake environment in New Zealand, where the changes to the geodetic system were so significant that geodetic marks previously used for surveying could not be used. Furthermore, there is no commonly accepted post-earthquake surveying protocols in a coastal environment. This thesis will explicitly address this issue by analysing a series of different post-earthquake techniques on their suitability and ability to contribute useful data for post-earthquake analysis.

The mixed sand and gravel (MSG) beaches of Kaikōura sit on a high wave energy, tectonically active coastline. Similar to many New Zealand beaches, it is located in close proximity to an actively uplifting and eroding mountain range, which provides large amounts of sediment to

the coastline for nourishment. When the sediment reaches the coastline from the catchment, the high wave energy of the coastline transports the sediment alongshore, nourishing a coast of MSG beaches and hapua environments. Globally, MSG beaches are typically found at high latitudes where glacial debris and tectonics play a vital role in influencing the geomorphology of the coastline. This beach type is common along the East Coast of New Zealand, as well as the West Coast of the South Island. As noted by Jennings and Shulmeister (2002), there may be within-type variations of MSG beaches, as there is with sand beaches (Short, 1979), in which the geomorphic characteristics of the beach fall within the category of MSG beach, but small variations in environmental conditions acting on a profile are reflected in the differences in the geomorphic properties of a beach. The commonality of these beaches in tectonically active environments, and New Zealand, means that this beach type is likely to be subjected to tectonic events and subsequent changes in the future, and therefore there is a vested interest in understanding how this beach type responds to changes.

This research will use Kaikōura as a case study, for a tectonically active area with MSG environments that underwent tectonic deformation on the 14<sup>th</sup> of November 2018 in a 7.8  $M_w$  earthquake. Deformation from the event lead to approximately 1 m of uplift around the Kaikōura Peninsula (Stephenson et al., 2017; Clark et al., 2017), and as a result there was a fall in relative sea level. This study will aim to better inform a short-term response model, in which details how MSG beaches respond to a change in relative sea level. Currently, only long-term morphodynamic trends are understood, and are informed using historical, low resolution data. This study will highlight the complexities involved in collecting data after an earthquake which can effectively inform a short-term conceptual response model along an entire stretch of coastline which varies in environmental conditions and geomorphic properties. A thorough investigation of the Kaikōura Coastline, both pre and post-earthquake is undertaken to ensure that coastal resource management decisions are well informed as the Kaikōura region moves forward with its recovery.

## 1.2 Research aims and objectives

As previously stated, the aim of this research is to further understand how MSG coastal environments respond to a large tectonic event when there is an earthquake-induced change in relative sea level. In order to develop a conceptual response model, investigations into pre-earthquake coastline trends, as well as appropriate post-earthquake surveying techniques are undertaken to inform the collection and analysis of post-earthquake survey data. The overall aim of this thesis is achieved through the following three objectives:

**Objective 1** To establish the pre-earthquake long-term trends of the unconsolidated coastal environments in Kaikōura, through the means of geomorphology and sedimentology.

**Objective 2** To evaluate post-earthquake surveying techniques and the data captured through the use of different methods.

**Objective 3** To identify what the short-term responses are in a MSG coastal environment following an earthquake-induced change in relative sea level.

These objectives were achieved using the study area of Kaikōura, and the November 14<sup>th</sup> 2016 earthquake as a case study for a tectonic event which induced a change in relative sea level. To address Objective 1, parameters for a series of 18 beach profiles are determined and used for a classification of MSG beaches to identify within-type variations of MSG beaches along the Kaikōura coastline, and the associated environmental conditions which influence the geomorphology of these profiles before the earthquake.

To address Objective 2, common post-earthquake techniques using remotely sensed data, including LiDAR and aerial imagery, are applied to the Kaikōura coastline to identify what information can be extracted from these surveys to inform geomorphic beach response after an earthquake.

Having identified the pre-earthquake coastal trends, and undertaken method development to determine a ‘best-approach’ post-earthquake data collection technique, Objective 3 is addressed by analysing post-earthquake surveying data. Key geomorphic parameters such as volume, shoreline and beach shape are used to inform the short-term geomorphic response of different within-type variations of MSG beaches, to determine the predominant trends following the earthquake. This information will then be used to inform various conceptual response pathway models to illustrate the short-term responses of the Kaikōura beaches.

## 1.3 Thesis structure

This chapter has introduced the research topic and identified the research objectives for this study, and has outlined the structure of this thesis.

Chapter 2 provides a summary of literature surrounding coastal processes and geomorphology of MSG coastal environments, as well as how these environments are known to respond to changes in relative sea level, and how this information is collected in a post-earthquake environment.

Chapter 3 will provide an overview of the Kaikōura study area, including the environmental parameters acting on the area, and the geological history of the region.

Chapter 4 will identify the methods used for this study to achieve the overall aim of this thesis.

Chapter 5, 6 and 7 are used to address the three research objectives in turn.

Chapter 8 discusses the conceptual response pathways informed by this study, and identifies the implications of this research in a resource management context.

Chapter 9 summarises the findings of this research, states the limitations of this study and suggests areas for future research.

# Chapter 2

## Literature Review

### 2.1 Introduction

This chapter will provide a broad overview of the types of MSG coastal environments present in the Kaikōura study area, including MSG beaches and hapua lagoons. It will also examine literature which addresses coastal geomorphic responses to earthquake events, and more specifically, how MSG beaches respond to relative sea level fall. Finally, this chapter will look at different surveying techniques in a post-earthquake environment, and how these techniques can be applied in a coastal setting.

### 2.2 Mixed sand and gravel coastal environments

MSG coastal environments in the Kaikōura study area are inclusive of both beaches and river-mouth barriers enclosing small coastal hydrosystems, known as hapua lagoons (Hart, 2007). Whilst both of these environments differ significantly in term of process and response, they are both composed of a wide range of sediment size, from sand to boulder (Kirk, 1980; Hume et al., 2016). The environments are usually indicative of a high energy wave climate, where MSG environments found on the east coast of the South Island are subject to the East Coast Swell Environment (Davies, 1964). Jennings and Shulmeister (2002) suggests that there is a relationship between sediment supply, wave regime and beach shape, alluding to the fact that the Kaikōura coastline is subject to a high energy wave climate and is supplied with a wealth of sediment from the Kaikōura Seaward Ranges, and therefore can produce MSG environments. The following will look at what determines these environments to be defined as MSG beaches



and hapua lagoons, and the process/response regime working in these environments.

### **2.2.1 Mixed sand and gravel beaches**

A coarse clastic beach is a broad brush term for a series of variations of beaches in which their composition is inclusive of gravel. The difference between a sand and a coarse clastic beach is primarily determined by the sediment composition of the beach. Sand beaches comprise of sediment ranging from 0.0625 mm (very fine sand) to 2 mm (coarse sand), whilst various coarse clastic beaches can contain a range of sediment sizes from 0.0625 mm (very fine sand) to > 2 mm (gravels) (Wentworth, 1922). Comparatively, coarse clastic beaches are less commonly studied than sand beach types, as they are plentiful at high/low latitudes, such as New Zealand, Canada and Alaska, where there is a high wave energy and cold climate (Buscombe and Masselink, 2006). These beaches are often located away from cities, making it a less attractive setting to undertake research than warmer, calm sand beaches located closer to cities. Coarse clastic beaches require either glacial processes to supply sediment to the nearshore for reworking, or a high magnitude of nearby mountain erosion where sediment is supplied from the mountains to the coast by rivers (Jennings and Shulmeister, 2002). Jennings and Shulmeister (2002) suggest that coarse clastic beach types can be divided into three categories: pure gravel, composite, and MSG. A composite beach contains sand and gravel, but is hydraulically sorted into two parts, with a gravelly backshore and a sand beach face and nearshore (Karunaratna et al., 2012). A MSG beach is mixed in sediment size and composition both horizontally and vertically across the whole profile (Kirk, 1980; Jennings and Shulmeister, 2002). MSG beaches are, relative to other beach types, typically neglected in international coastal research (Mason and Coates, 2001). However, existing literature surrounding MSG beaches is highly localised to New Zealand, in particular Hawke's Bay (Single, 1985; Paterson, 2000; Ivamy and Kench, 2006; Komar, 2010; Dickson et al., 2011; Brown, 2017), the Canterbury Bight (McLean and Kirk, 1969; Kirk, 1969) and Kaikōura (McLean and Kirk, 1969; McLean, 1970; Kirk, 1975; Dawe, 1997, 2001).

Morphology of a MSG beach is variable within its own classification, but overall differs from a pure gravel or composite beach (Jennings and Shulmeister, 2002). Jennings and Shulmeister (2002) stated that MSG beaches could have within-type variations, but there was no evidence to suggest that it would change from MSG to pure gravel or composite following an event. The composition ratio of sand to gravel in a MSG beach shows variability when documented in literature, from 50% sand (McLean, 1970), to 30% sand (Pontee et al., 2004), to anywhere between 15–68% sand (Mason and Coates, 2001). Kirk (1980) proposed that there were four main morphological zones on a MSG beach. As shown in Figure 2.1, these zones are: (1)

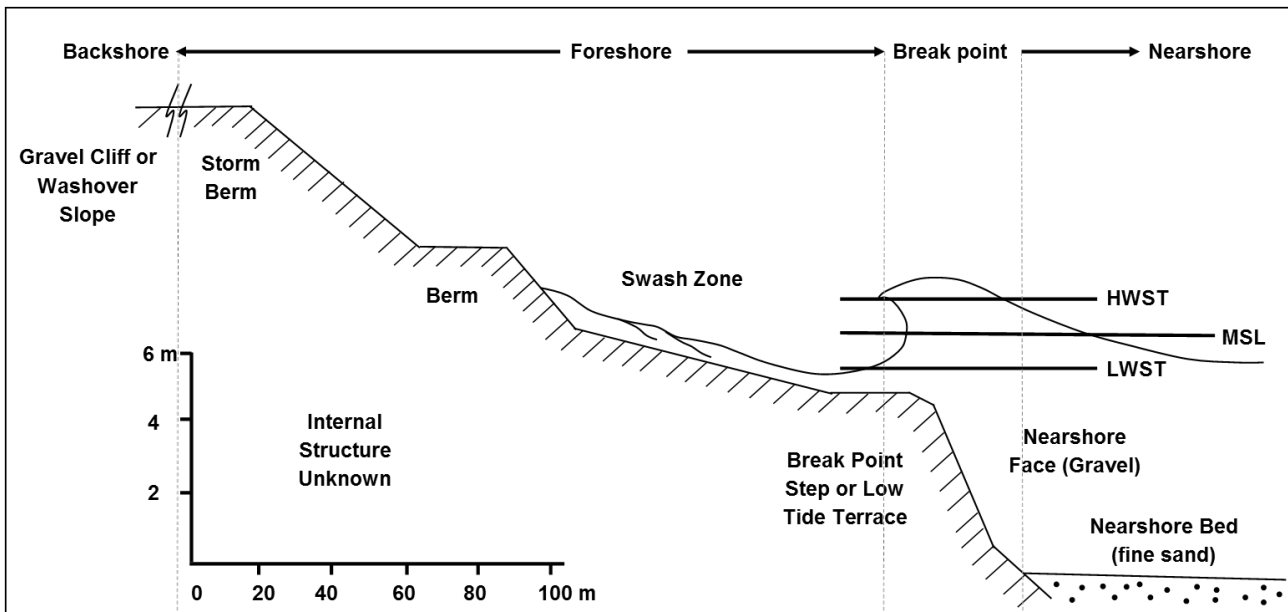


Figure 2.1: MSG beach morphology and zonation. Adapted from Kirk (1980).

backshore; (2) foreshore (3) break point step; and (4) nearshore.

The backshore zone is the area landward of the storm berm, located at the edge of the active profile. It is often composed of relict sediment (Dawe, 1997), overwash from storms (Kirk, 1980), and often some vegetation. The zone is out of the everyday active beach profile, and can sometimes be backed by a cliff or a hard structure (eg. seawall) (Pontee et al., 2004). The backshore is a good indicator of historical long-term change or events, as often there are paleo terraces present. These are abandoned berms in the backshore due to a change in environmental conditions, or an event with significant uplift (Orford et al., 1996).

The foreshore comprises of multiple berms, usually one at the landward edge of the zone, the storm berm, which marks the storm wave runup on a progradational beach. Further down the profile, subsequent smaller berms form with different wave energy and sediment supply (Pontee et al., 2004). There is no set number of berms a MSG profile will have, nor is there a set elevation the berms will commonly appear at, as they usually form at the top of wave runup, which varies with different beaches depending on slope and wave energy (Jennings and Shulmeister, 2002). The lower foreshore, which extends out to the break point step, is known as the ‘swash zone’. Wave energy is concentrated here when it reaches the beach, and as a result this zone usually contains coarser sediment than the high tide mark (Jennings and Shulmeister, 2002). The swash zone is dominated by swash and backwash of waves, and is the zone on the profile responsible for longshore gravel sediment transport (Kirk, 1980). MSG beaches have complex sediment patterns which are not yet fully understood. There is no linear longshore transport relationship suggesting a decrease in grain size with distance from a sediment source (McLean, 1970). The micro-tidal (to lower meso-tidal) nature of MSG beach types means that

there is a narrow zone of wave energy concentration on the foreshore (Kirk, 1980).

The break point step feature, unique to coarse clastic beaches, means the surf zone is confined to a single line of breakers close to the swash zone (Kirk, 1980). The step, built up of cobble and gravel, changes at its base to fine sand on the nearshore bed and gives the beach a ‘reflective’ nature, reflecting a considerable amount of wave energy off the beach face (Kirk, 1980; Wright and Short, 1984). The lack of surf zone means that there is a lack of offshore energy dissipation (Olson, 2010), and the plunging waves are at a high velocity when they are breaking on the foreshore, where the energy is then dissipated (Anthony, 2009).

The nearshore environment is the fine sandy bed which extends seaward of the break point step, gently sloping offshore. There is no periodic onshore–offshore re-circulation between the beach face and the nearshore environment, in which sediment transport is shore-parallel (Kirk, 1980). Sediment transport is therefore predominantly alongshore and highly localised to the swash zone for gravel transport, but fine sediments can be transported in the nearshore environment with long shore drift. Kirk (1980) stated that Adams (1978) pebble abrasion study lead him to believe that New Zealand MSG beaches would follow an erosional trend, with an estimated loss of 3-5% of sediment offshore. Environment Canterbury (2005) showed that the Canterbury Bight along the Canterbury coastline exhibited an erosional trend, Berger (2017) showed there were variable trends present along MSG beaches in Kaikōura, as was there varying trends along the Hawke’s Bay coastline (Carruth, 2017). The beaches’ coarse sediment alludes to the idea that these beaches are found in high energy environments, in which higher wave heights are also thought to be associated with erosion (Saville and Watts, 1969), however the long-term trend is highly dependent on the sediment budget and sediment availability. The lack of onshore–offshore movement also means that MSG beaches do not respond to storms the same as sand beach systems which undergo bar building in the nearshore (Pontee et al., 2004), and the major changes are documented in the subaerial beach profile (Kirk, 1980). The break point step feature means that if gravel is transported by backwash beyond this zone, it will likely be lost offshore as it requires a lot of energy to transport gravel over the break point step. The single breaker line creates a dangerous environment to study the processes in the nearshore, however as stated by Kirk (1980), because of the lack of onshore-offshore movements, most changes in the MSG beach environment can be seen in the subaerial profile of the beach. When considering changes in a MSG beach environment, particular regard should be given to longshore transport barriers and other interruptions in the swash zone which could hinder gravel sediment transport in the swash zone.

### 2.2.2 Hapua lagoons

Rivermouth environments occur at the interface of freshwater and marine environments, where the interaction can create complex dynamics and unique interface features. The type of interface environment is determined by its primary process agent as shown in Figure 2.2, where an estuary is primarily tide dominated; a delta is river dominated; and a hapua lagoon is wave dominated (Hart, 2007). There are three main braided rivers located in the Kaikōura area that contribute sediment to the coastal environment. These are the Kahutara River and the Kowhai River (south of the Kaikōura Peninsula); and the Hāpuku River (north of the Kaikōura Peninsula). The rivermouths of all three rivers exhibit complex dynamics as they approach the coastline, in the form of small hapuas. Hapuas in the past were often grouped with other rivermouth environments, for example, Hume and Herdendorf (1988) grouped hapua type lagoons with estuaries, despite hapua lagoons lacking the characteristic of being estuarine, or having tidal ingress or a tidal prism. The term hapua was introduced by Kirk and Lauder (1994) in an attempt to distinguish hapua environments from other rivermouth environments. Prior to the introduction of this term, hapua had been described in multiple studies, especially along the Canterbury coast, although they were primarily described as freshwater lagoon features (Kelk, 1974; Kirk, 1991; Todd, 1992). Since the introduction of this term, multiple studies have been undertaken to better understand hapua coastal lagoon environments (Kirk and Lauder, 1994; Hart, 1999, 2007, 2009; Creed, 2014; Hume et al., 2016).

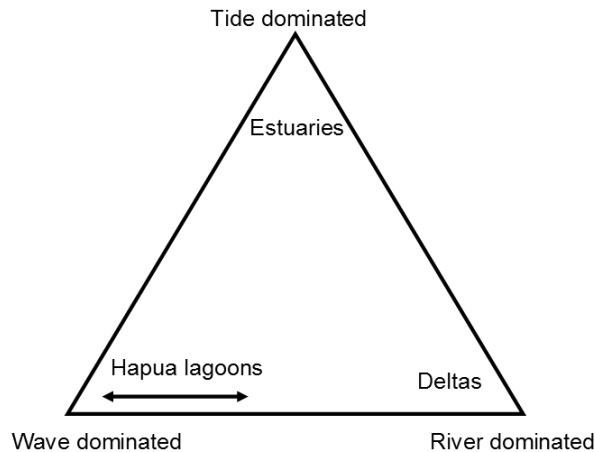


**Figure 2.2:** Classification of rivermouth environments based on process agents dominating the interface environment, showing Hapua lagoons to be wave dominated environments. Taken from Hart (2007).

The Hume et al. (2016) classification scheme of coastal hydrosystem environments classifies over 550 of New Zealand coastal hydrosystems into different geomorphic classes. In this classification scheme, hapua type lagoons are recognised as a coastal hydrosystem and are described as narrow, elongated and shallow rivermouth lagoons that are enclosed by a coarse gravel barrier,

with a single outlet. They are commonly found on high energy wave dominated coastlines, with no tidal prism, but can experience backwater effects during high tides (Hume et al., 2016). The backwater effect is the increase in water level due to a decrease in outlet and percolation efficiency at higher tidal stages, without any tidal ingress. Hapua lagoons are primarily freshwater features, which experience saltwater entry by spray and wave over-topping in storm events (Hart, 2007; Hume et al., 2016), and for short periods post storm breaching, but not daily.

The cyclical nature of hapua lagoons promotes morphological change of the hapua outlet over time, as shown in Figure 2.3, and tends to migrate with the longshore drift of gravel along the coast. The channel migrates alongshore under the influence of fluvial and littoral processes. As the channel migrates north, it elongates and weakens. A high energy wave or flooding event will change the course of the outlet by breaching of the barrier as a result of the weak channel not being able to cope with the outflow of the lagoon (Hart, 1999).

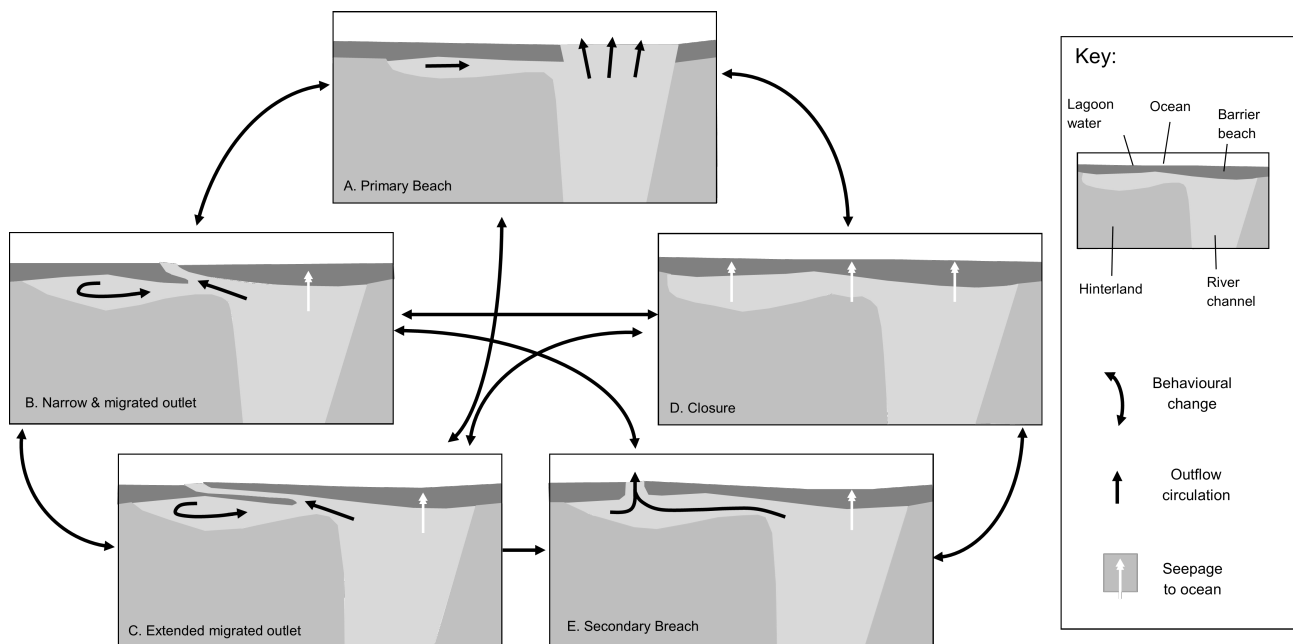


**Figure 2.3:** Morphological states of a hapua environment. Behavioural change over time depends on wave and river influences, closing and breaching the gravel barrier. Taken from Hart (2009).

## 2.3 Coasts and earthquakes

Many low lying coasts situated around the Pacific Ocean along faults lines share the common subjection to the phenomena of earthquakes, including New Zealand, Japan, China, Indonesia, America and South America (Hart et al., 2015). Earthquakes of a large magnitude around the Pacific Rim are not uncommon, where historically earthquakes both onshore and offshore

have lead to devastation in low lying coastal communities. Literature surrounding coasts and earthquakes largely focuses on the hazardous nature of earthquake and the impacts of lives, infrastructure, and the societal recovery following these events (Coburn et al., 1992; Athukorala and Resosudarmo, 2005; Kazama and Noda, 2012; Doocy et al., 2013). The recordings of changes in a geomorphological sense in a coastal post-earthquake environment largely coincide with earthquake events which have induced tsunamis (Pari et al., 2008; Paris et al., 2009; Goto et al., 2011; Tanaka et al., 2012; Villagran et al., 2013). A significant amount of tsunami research and its affects on coastal morphology surrounds the 2004 Indian Ocean tsunami (Paris et al., 2009) and the 2011 Tohoku, Japan tsunami (Udo et al., 2012; Tanaka et al., 2012). Short-term geomorphological studies following these earthquake events which induced tsunamis showed that not only were there significant impacts onshore to the coastal, fluvial and interface systems, but morphologically it was shown that there were also significant changes to the nearshore topography of the seabed, especially in the wave breaking region (Goto et al., 2011). The morphological onshore changes were largely a result of erosion caused by initial wave energy reaching the beaches, but also from the return flow of the water moving back to the ocean, which deposited eroded onshore sediment into the nearshore bed (Tanaka et al., 2007). Tanaka et al. (2012) showed in their aerial imagery analysis of the coastline following the 2011 Tohoku tsunami that the coastline suffered significant erosion, and hard coastal structures which have spaced gaps resulted in concentrated erosion around these structures. The recovery of these eroded coastlines back to their pre-tsunami extents and states were found to be dependent on the available sediment supply. Coasts that have large rivers nearby with good sediment budgets have appeared to morphologically recover quickly, whereas coasts which do not have good sediment supplies were found to erode back to rocky shorelines (Tanaka et al., 2012). A study by Villagran et al. (2013) looked at the morphological response of an erosive sand beach and accretionary sandy spit following the 8.8  $M_w$  earthquake in Chile, 2010, and its subsequent tsunami. The two beaches underwent co-seismic deformation, in which the erosional beach underwent subsidence. The study showed that within three years, the sandy spit had completely recovered its sediment volume post-earthquake and tsunami, due to the close proximity to the rivermouth and large sediment supply coming from the catchment, though the rivermouth outlet had migrated from its pre-earthquake position along the spit (Villagran et al., 2013). In contrast to this, the pre-earthquake erosional trending beach which experienced 1 m of subsidence, showed that its erosional trends were accelerated by the relative rise in sea level, and there was a continuous reduction in beach width following the earthquake three years on (Villagran et al., 2013).

There is large variation throughout literature suggesting how long it takes for a coast to respond to earthquakes, and this is likely a result of the different definitions of response in a coastal

system. As seen in Villagran et al. (2013), three years following the earthquake the sandy spit was believed to have been recovered, defined by the re-establishment of the subaerial sediment volume. Single (1985) believed at the time of his study, the Napier coastline was almost fully recovered from the 1 m uplift on the MSG beach 54 years on from the earthquake; however, Olson (2010) believed that the Wellington coastline was still recovering from its 1860s earthquake which generated 6 m of uplift. For Single (1985) and Olson (2010), recovery of the coastal environment meant the return of a beach back to its pre-earthquake form, with a similar beach profile to its pre-earthquake profile, which these studies showed occurs on a decadal to century time scale after the nearshore has recovered from the uplift and also eroded back to pre-earthquake positions. These studies also considered the response of the nearshore environment to be driving long-term responses, an important factor to acknowledge when detailing the recovery of coarse clastic coastal system. Single's (1985) and Olson's (2010) studies could have recorded longer response times also due to the fact they were observing MSG beaches, whilst Villagran et al. (2013) was observing sand beaches. The finer sediment in a sand beach would require less energy to move, and therefore morphological response could take place under lower energy conditions.

New landscapes form in the coastal environment as it responds to a change in relative sea level. These changes can be a result of the increase in sediment budget due to landslide debris coming down from a nearby catchment (Ramsey, 2007). Generally finer sediment from the catchment will reach the coastline before gravels and sands due to the light weight and mobility of finer sediment. Hart et al. (2015) found that following the CES in 2010, there was an increased amount of fine sediment in the beach sedimentology samples, and this resulted in beach scarping and erosion as the fines moved through the coastal system (Hart et al., 2015). This change was found in the initial months following the earthquake, and by 3 years after the earthquake, the fine sediments had winnowed out of the beach profiles and moved through the system. In terms of sedimentology, beaches have shown to recover quickly.

The biological impacts felt from earthquakes and associated relative sea level change in a coastal environment were first noted by Darwin (1851) where 3 m of uplift on the Chilean coast had left mussels dead along a rocky coastline. Following the Kaikōura Earthquake, similar scenarios were seen when intertidal biomes were used to measure the amount of uplift from the event (Clark et al., 2017). As noted by Marsden et al. (2015), inter-tidal biomes will migrate following an earthquake to relocate to where their desirable tidal range is. In the 2010 Canterbury earthquake, the southern two thirds of the Avon-Heathcote estuary uplifted, while the northern third subsided. The impacts on the estuarine environment included the migration of species in adjustment to their new tidal range, as a result of the change in relative sea level

(Marsden et al., 2015). The subsiding areas meant that some areas were now closer to the water table than pre-earthquake, and were more vulnerable to liquefaction. Following the earthquake, there were other factors species in the coastal and estuarine environment had to adjust to follow the Christchurch Earthquake Sequence, including increased pollution from contaminated water entering the waterways due to pluvial flooding, as well as increased sedimentation, from both liquefaction, as well as around Banks Peninsula where the loess caps on top of the volcanic rocks broke off into the coastal environment (Hart et al., 2015). Borja et al. (2010) believed that the recovery of estuarine environments following such event was 4 to 10 years, however Marsden et al. (2015) believes that the time period of recovery is difficult to determine, and could take from days to years to decades, and up to 25 years for different species. The recovery depends on the factors involved, where biological responses will be at a different rate to geomorphic responses.

In conclusion, there is a large seismic hazard in New Zealand due to its location along a plate boundary, and as seen in other countries, coastal settlements have an additional risk of tsunamis following an earthquake. There are various cascading effects which stem from an earthquake which will impact a coasts ability to recovery, both biologically and geomorphically. Trying to attach a time scale in which a tectonically disturbed coastal environment will recover is extremely difficult, especially in modern environments when the coasts are densely populated, and anthropogenic factors specific to the cities infrastructure, geology and geomorphology will have a considerable affect on the recovery of the environment. The different dynamics, mobile processes and biomes which occur in coastal and interface environments mean there are many different factors that need to be considered when analysing these environments following an earthquake. Analysing the geomorphic and biological responses following an earthquake is extremely relevant given the dense populations, both society and ecologically, that reside in these locations. It is important to further identify how these environments should be expected to respond following these events in the future.

## **2.4 Coastal response to relative sea level fall**

The following section will discuss relative sea level change in terms of relative sea level fall, as this is the change that the Kaikōura study area experienced following the November 2016 earthquake.

Relative sea level is the measurement of the mean sea level in relation to local land elevation. Changes in relative sea level can be a result of various short and long-term events which causes land to uplift or subside. Long-term relative sea level change is usually a result of isostasy,



or tectonic uplift/subsidence occurring over hundreds to thousands of years (Rovere et al., 2016). Short-term relative sea level change is caused by more instantaneous change in a coastal environment, and is attributed to activities such as mining or ground water extraction, causing subsidence and a relative sea level rise; or in the context of this study, a relative sea level change can be attributed to uplift or subsidence of the coastal environment, through a tectonic event (Single, 1985; Olson et al., 2012).

Globally, literature has a strong focus on coastal response to a change in eustatic sea level, as a result of climate change induced sea level rise (Cowell et al., 1992; Leatherman et al., 2000; Cooper and Pilkey, 2004; FitzGerald et al., 2008). Early studies of beach response to sea level rise are largely overshadowed by the development of the Bruun Rule (Bruun, 1954, 1962). The Bruun rule demonstrates that with sea level rise under certain constrained conditions, a sand beach will translate upward and landward at the same rate, maintaining morphological features (Bruun, 1962). The Bruun Rule has been seen as contentious since its development (see Rosati et al. (2013) and Cooper and Pilkey (2004)), mostly due to its two dimensional nature not taking into account differences in sediment budgets (Everts, 1985; Rosati et al., 2013). It was also found that the model was not validated through many field observations (Schwartz, 1967; Rosen, 1978; Pilkey and Davis, 1987; Bruun, 1988). A modified version of the rule is still used in New Zealand, as well as other countries, to calculate set back distances in regards to coastal planning around sea level rise, as there is no commonly accepted alternative (Rosati et al., 2013).

Relative sea level fall, as experienced in the Kaikōura study area, can result from uplifting land in a local area. Bruun (1983) stated that the Bruun rule could be reversed to two-dimensionally model how a gravel beach would respond following relative sea level fall. Single (1985) argued that relative sea level fall as a result of instantaneous coastal uplift caused by a tectonic event could not be represented in full by the reverse Bruun Rule. Single (1985) states that MSG beach response following relative sea level fall can be modelled in two stages. The first stage is the vertical adjustment of the coastline as a result of the uplift, causing instantaneous progradation, in which the new foreshore is the pre-earthquake sea bed and additional volume of sediment has been uplifted into the active beach affected by marine processes. The second stage is the response stage in which the newly uplifted profile adjusts to its pre-earthquake equilibrium state. The adjustment occurs firstly with removal of sediment in the nearshore as the position of maximum wave effort is translated seaward with uplift, causing relative sea level rise in the nearshore profile due to the erosion. The position of maximum wave effort is the seaward extent in the nearshore profile where wave energy is interacting with the nearshore bed to move sediment. The rest of the profile continues to adjust as the position of maximum wave

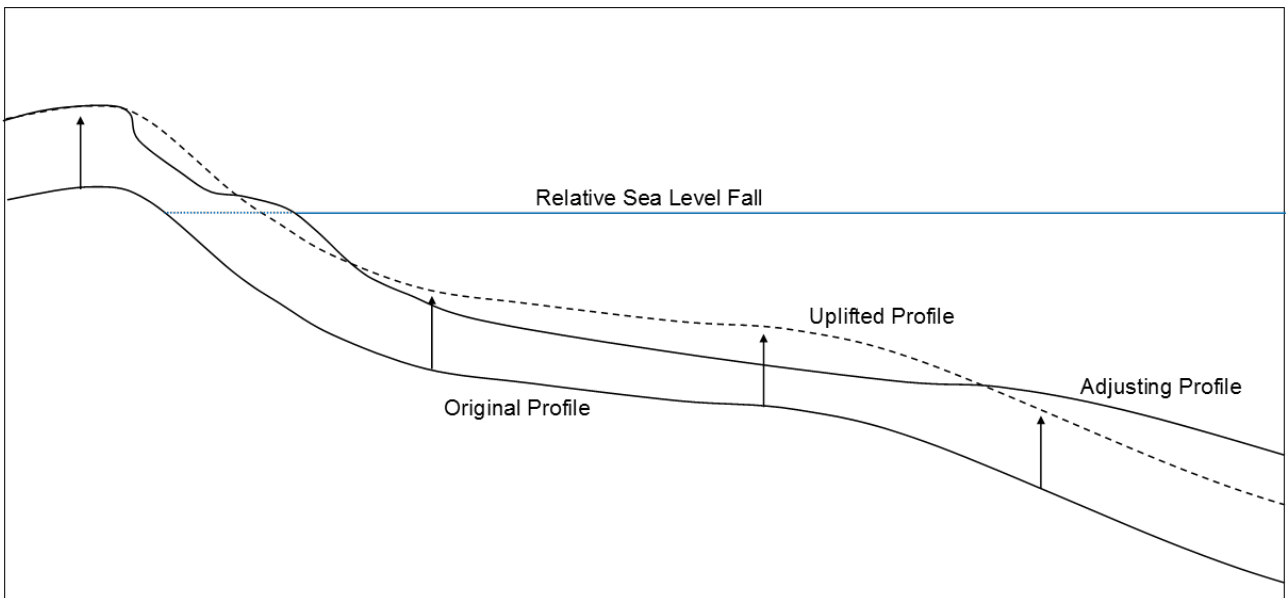


**Figure 2.4:** Profile response of an uplifted beach where there is a relative sea level fall. As the beach responds, the berm reforms relative to sea level. Adapted from Single (1985).

effort retreats landward with the relative sea level rise in the nearshore, until the profile adjusts back to its pre-state equilibrium (Single, 1985). The duration of response will be dependent on the amount of sediment added to the budget following the earthquake, as well as sediment composition in the nearshore, and the amount of uplift which occurred. Single (1985) believed that the response in the second stage could be likened to the reversal of the Bruun Rule, as demonstrated in Figure 2.4.

Few long-term studies have been conducted on tectonically induced sea level fall on gravelly beaches, however the majority of studies are focused on MSG beaches in New Zealand. Following on from Single's (1985) study on the uplifted Napier beaches from the 7.8  $M_w$  earthquake in 1931, Paterson (2000) continued to assess the long-term changes on the Hawke's Bay beaches. Paterson (2000) determined from his study that the Bruun Rule greatly underestimated any shoreline change observations by a factor of 38. He believed that following the earthquake, there would be an initial period of progradation because the uplifted nearshore would dissipate wave energy, and promote onshore movement of sediment. Paterson (2000) also found, contrary to Single (1985), that the rate of long-term response was dependent on the frequency and magnitude of storms. Olson (2010) conducted a study looking at long-term response of the Wellington MSG beaches on a decadal scale following the 8.2  $M_w$  Wairarapa earthquake in 1855, which uplifted some coastal areas up to 6m. The study looked at an area which had a recent change in sediment supply, with gravel being introduced to a previously sandy system, and determining the stability of the coastline after both tectonic disturbance and introduction of gravel sediment. All three studies (Single, 1985; Paterson, 2000; Olson, 2010) concluded that

their respective sites were still responding to the earthquake, in which Olson (2010) stated that the MSG beach system was still adjusting to the introduction of large volume of fine grained sediment from nearshore areas uplifted in the 1855 earthquake. This long-term adjustment was not due to the pulses of sediment from earthquake induced landslides, but rather the erosion of nearshore sediment as base level changed over time (Olson et al., 2012).

There are only two known studies which investigate the short-term morphological response of MSG beaches following an earthquake (Stanley, 1968; Brown, 2017). Brown (2017) used historical data from the 1931 Napier earthquake, and modelled uplifted profiles in XBeach-G against different wave heights to simulate storm events. Brown (2017) found in her studies that beach response following tectonic uplift caused an increase in subaerial volume, with a widening of the beach face. Brown (2017) stated that the upper beach was abandoned after the uplift, as it was elevated out of the active beach system which was being reworked. The primary response following uplift was found to be ridge building, and there was a degree of erosion in the post-earthquake high water mark, in which sediment was eroding from the subaerial profile but accreting in the nearshore profile, suggesting the redistribution of sediment throughout the profile following a storm event (Brown, 2017).

Stanley's (1968) research was found to be the most relevant to this study, in which the observations were made in the field several months after varying degrees of uplift and subsidence affected the Alaskan coastline lined with MSG beaches following the 9.2  $M_w$  earthquake in 1964. Observations made by Stanley (1968), similar to observations by Brown (2017), included that swash aligned berms were a dominant morphological change. Stanley (1968) stated that new beaches developed below abandoned beaches to fit the new high water line, where material was transported and deposited on the upper beach. Beaches were not considered to be stable after a year, and it was believed that the new berms would take years to stabilise because of the lack of coarse sediment supply (Stanley, 1968). Lack of research surrounding the observations of MSG coastal systems following relative sea level fall after an earthquake is evident when reviewing coastal literature, especially in a three-dimensional sense when the sediment budget is considered.

Only one study (Stanley, 1968) has detailed short-term morphological changes following relative sea level change, whereas other studies have been dependent on historical data to develop conceptual models and interpret the coastal response on a decadal scale (Single, 1985; Paterson, 2000; Olson, 2010; Olson et al., 2012) or to use as the basis for a disturbance in order to model short-term response in various wave climate (Brown, 2017). There is a clear gap in literature in which the short-term response of beaches following significant fall in relative sea level due to tectonic uplift is very poorly documented, especially in New Zealand.

## 2.5 Surveying in a post-earthquake environment

The idea that surveyors play an important role following earthquakes was originally acknowledged in Hodgson (1927), where at the time, surveying was playing an important role in determining whether continents were still drifting. Hodgson (1927) stated that continuous monitoring of an area would be useful in the instance another earthquake was to occur, then the change in geomorphology could be determined. In terms of surveying the coastal environment, surveyors were used to determine whether the coast was ‘rising’ or ‘falling’, in which this information could inform the development of harbours (Hodgson, 1927). Since Hodgson (1927) first addressed the idea of earthquake displacement monitoring, which included locating three seismographs in a triangle to determine the epicentre of an earthquake; various methods of surveying have been used to record change following an earthquake. These techniques include geological mapping (Duffy et al., 2013), cadastral (property boundary) surveying (Lee et al., 2010; Duffy et al., 2013), using pre-existing monitoring devices, such as tidal gauges (Hyndman, 1995), remote sensing (Duffy et al., 2013), Global Positioning System (GPS) and Global Navigation Satellite System (GNSS) surveying as well as deformation modelling (Winefield et al., 2010).

The geodetic system is a coordinate system which uses a set of reference points to inform the location of places on earth. The World Geodetic System, known as WGS84, is a global standard coordinate system used for satellites and cartography, however countries often have their own systems in order to provide the highest accuracy and accommodate differences in tectonic environments (Donnelly et al., 2014). The current New Zealand geodetic system established in 2000 is known as NZGD2000, changing from the previously used fixed coordinate system known as NZGD1949 (Winefield et al., 2010). The system was upgraded as a result of the tectonic nature of New Zealand, meaning that a fixed coordinate system was not appropriate for a country which continuously undergoes slow tectonic change. In a physical sense, the NZGD system itself is a series of trig stations and geodetic marks which are distributed over the whole country as ‘known’ points, and surveys in a local area are tied to these marks. The NZGD2000 system is semi dynamic, however short-term rapid changes can only be accounted for by applying ‘patches’ to the National Horizontal Deformation Model (NDM) (Winefield et al., 2010).

Following a large earthquake, there are major disruptions to the geodetic system due to the horizontal and vertical displacement. Common surveying techniques immediately after an earthquake used to determine displacement and changes are primarily conducted using satellite data, as no on-land data is required to establish measurements of displacement if the satellite has

a built in GNSS system. For example, Massonnet et al. (1993) and Zebker et al. (1994) both used Synthetic Aperture Radar (SAR) interferometry from orbiting high resolution systems to capture displacement from the 7.3  $M_w$  Landers, California Earthquake in 1992. These studies highlighted the usefulness of satellite data to inform displacement and the convenience of not needing a re-established geodetic system to do so. Singh et al. (2002) used Indian Remote Sensing data to determine the changes in ocean parameters and land features affected by the 7.7  $M_w$  January 2001 earthquake in Gujarat, India. Light Detection and Ranging (LiDAR) data, collected using an built in GNSS positioning system, was used following the 2010 Christchurch earthquake to determine displacement, especially close to the surface rupture (Duffy et al., 2013). There is a large archive of satellite imagery for a site, and therefore a good source of pre-earthquake data is readily available for comparison following an earthquake. The use of Unmanned Aerial Vehicles (UAV) such as drones are now being used to obtain data soon after an earthquake, for both geomorphology surveying and to inform relief efforts (Xu et al., 2014), however non-commercial versions of these instruments are unlikely to have a built in GNSS positioning system, and will require ground truthing.

In order to conduct on ground surveying following an earthquake, the geodetic system must be re-established, to allow for surveys to be tied to accurate geodetic marks. This can be done through the addition of patches to the NDM, which adjust the geodetic coordinates, however due to the nature of earthquakes and associated aftershocks, the temporal matter in which these patches are applied is extremely variable (Winefield et al., 2010). The aftershocks create continuous displacement, which in some instances can accumulate to equal that of the event itself (Winefield et al., 2010). As shown in Figure 2.5, the frequency and magnitude of earthquakes decay over time, but in the Canterbury Earthquake Sequence, aftershocks larger than 3  $M_w$  were affecting the region more than 400 days after the event (Shcherbakov et al., 2012). Therefore, adjustments to the NDM following a tectonic event are not updated immediately following an event, as it is likely the area will undergo continuous change for at least months following an earthquake. The geodetic marks can be re-established using GNSS surveying equipment, as advised by Land Information New Zealand (LINZ), by resurveying a control framework, using static GNSS techniques (Land Information New Zealand, 2017). This involves occupying at least two benchmarks for 2–24 hours. Follow up surveying is required of additional marks in order to densify the geodetic network (Land Information New Zealand, 2017). Following the Kaikōura Earthquake, preliminary coordinates for geodetic marks were released for surveyors to use, of which these were further adjusted by up to 0.9m in some places by January 2018.

Various on-ground surveying techniques are used following an earthquake. Geological field

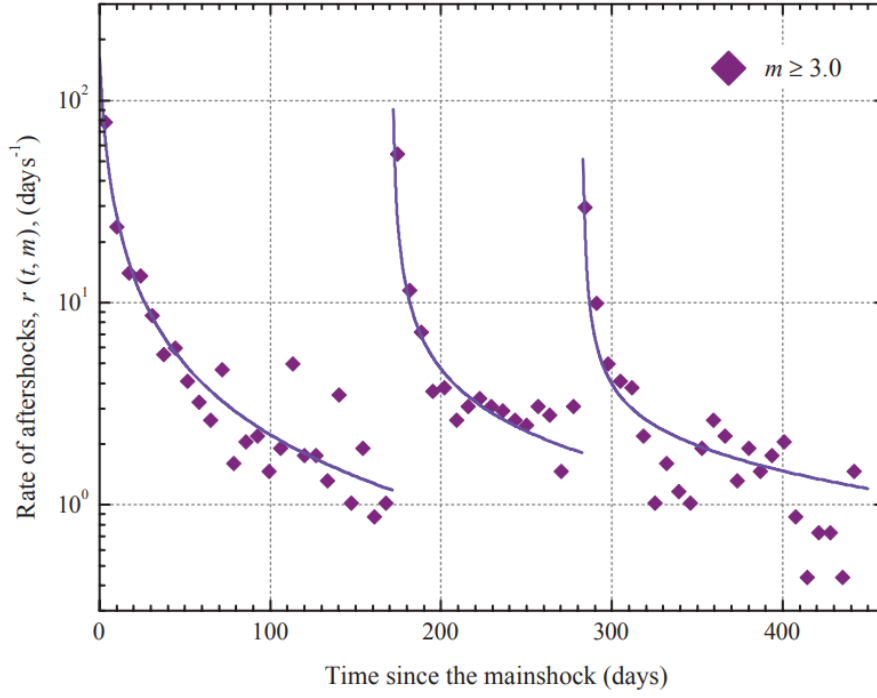


**Figure 2.5:** Aftershocks in the Canterbury Earthquake Sequence (CES) following three main earthquake events, which highlights the decay in frequency and magnitude of aftershocks following the event. Aftershocks were still occurring over 400 days after the initial earthquake in September 2010. Taken from Shcherbakov et al. (2012).

mapping is common around the direct surface rupture (Duffy et al., 2013). Cadastral surveying (the surveying of property boundaries) following an earthquake is also a common technique since it was first used in Taiwan to document displacement of the 7.3  $M_w$  Chi-Chi, Taiwan Earthquake in 1999, where the methods were used to accurately depict the displacement using building surveying data, down to 11 cm accuracy (Lee et al., 2006, 2010). The vested interest in property boundaries within society also means that there will be sufficient amounts of pre-earthquake data. This method was used following the September 2011 Darfield earthquake (Duffy et al., 2013), in which there was a cadastral survey conducted a month before the earthquake which could be used for comparison. Physical sites could be occupied following the earthquake using the 24 hour GPS on the base station to re-establish the site, and this could be used to determine changes following the earthquake as a comparative study (Duffy et al., 2013). This technique does not require the re-establishment of the geodetic system by LINZ, and can therefore be undertaken soon after the earthquake.

Literature surrounding surveying coastal environments largely focus on the use of marine species to detect large scale change, for example using surveys of uplifted brown algae in Kaikōura following the earthquake (Clark et al., 2017), or the use of monitoring tools such as tidal gauges which have long-term records to smooth affects of tidal changes and long-term changes such as El Nino (Hyndman, 1995). Beach surveying, and the methods involved following an earthquake

are largely undocumented. Studies have taken place to monitor beach profiles and the long-term effects of this following a large event, though no literature details this immediately after an event, or furthermore, no publication suggests a streamlined approach of how to survey a beach profile following an event. Following an earthquake, the geodetic system has been altered, therefore methods such as that used in Duffy et al. (2013) can be used to re-establish benchmark sites. This still leave the question as to what line to re-survey after an earthquake, the geospatial or the physical line. This will be explored further in Chapter 4. In cadastral surveying, the property boundaries are marked with physical markers, or features such as fences (Duffy et al., 2013), therefore giving the area a logical post-earthquake spot to reoccupy and use comparatively to determine displacement. The complexities in a coastal environment stem from the fact that the movement of physical markers in the field represent the movement of the piece of land which was previously monitored. Therein lies the problem of whether to continue to measure the geospatial line, in which the beach is a representation of the environmental conditions acting on that particular spot, or to continue to monitor the physical markers, which now represent a piece of beach affected by different environmental conditions. The approach to monitoring a coastal environment following an earthquake brings to light a lot of unanswered questions, in which surveyors have approached this issue before, but have not documented a streamlined approach for doing so. The lack of literature and publications addressing this issue creates an unsystematic error in the monitoring of beach systems and associated historical records, especially for routine monitoring performed by Regional Councils.

## 2.6 Conclusions

This chapter has highlighted the unique nature of MSG coastal environments, both beaches and hapuas, as well as the small amount of research surrounding these particular environments when compared to pure gravel or sand beach environments. The MSG environments are commonly associated with high energy coastal environments, and are highly dependent on sediment transport in the swash zone due to sediment being lost from the beach face part of the system when taken over the break point step. There is not a significant amount of literature on how a beach is expected to respond to relative sea level fall, especially in regards to short-term response. Studies have shown that beaches can take over 150 years to reach an equilibrium likened to their pre-earthquake state, especially with modern influences changing the environment. Brief observations of a post-earthquake environment, coupled with X-Beach-G modelling have shown that, in the short-term, the upper beach is stranded and continues to be unaffected, while changes occur in the nearshore and foreshore environment in response to

the change in the position of maximum wave effort translates landward over time. The limited literature surrounding post-earthquake, especially in terms of short-term observations, means that it is not known in its entirety how a MSG beach with different environmental conditions acting on them are expected to respond to an instantaneous drop in sea level. The methods used to survey in a post-earthquake environment are largely focused on cadastral surveying type techniques, however there is a large gap in literature where a best-approach method to surveying a post-earthquake coastal environment is yet to be developed. The low return period of a large earthquake event means that in a practical sense, the issues surrounding documenting post-earthquake coastal surveying it is rarely given the opportunity to be addressed.



# Chapter 3

## Study area: Kaikōura, New Zealand

### 3.1 Introduction

Kaikōura is located on the north eastern coast of the South Island, at the top of the Canterbury region, New Zealand. The area has a diverse landscape. The Kaikōura mountain ranges line the western boarder of the region, reaching over 2000 m in elevation. River catchments flow from the ranges across a large delta plain in the foreground of the mountains where the land has been developed for farming and a small, seasonally tourist driven, township. The coastline is fringed with MSG beaches, and limestone/ mudstone inter-tidal rock shore platforms directly surrounding the Peninsula (Stephenson, 1997). The narrow offshore shelf leads to the Kaikōura Canyon 6 km off the coast south of the peninsula. The Kaikōura Canyon joins the Hikurangi trough 15 km off the coast north of the Peninsula, with steep canyon physiography (Chandra, 1969). The unique coastal environment of Kaikōura is a result of its tectonically active history of the region, high energy coastal environment and close proximity to a large sediment source in the Kaikōura Seaward Ranges, in which the sediment only has to pass over a short distance to arrive at the coast. The following will look further in detail at different environments and processes present within the study area relevant to this research.

### 3.2 Field sites

The field sites are distributed along the 20 km stretch of coastline either side of the Peninsula, as shown in Figure 3.1. There are 18 MSG beach profiles in the study area, with 8 located south of the Peninsula, and 10 located north of the Peninsula.

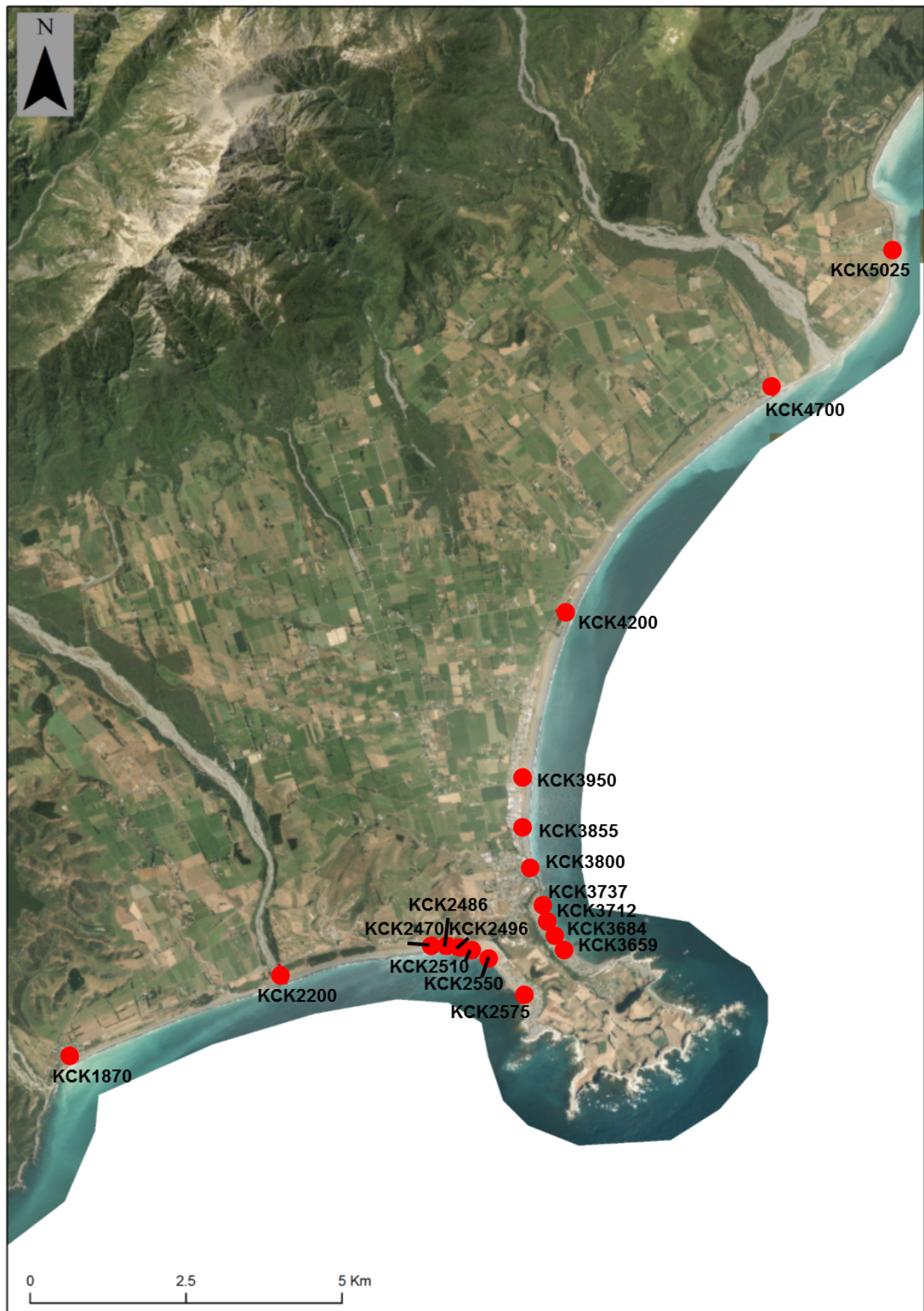


**Figure 3.1:** 18 Environment Canterbury beach profile sites, which have been surveyed annually from 1997–2015, and used for analysis in this study. Contains data sourced from the LINZ Data Service.

The sites comprise of MSG beach profiles ranging from 30 to 165 m in active beach across-shore distance. These profiles have been monitored annually by Environment Canterbury (ECan) from 1997 to 2015, and once after the earthquake in January 2017.

### 3.3 Fluvial environment

There are three main rivers in the Kaikōura study area, each with their catchments situated in the Seaward Kaikōura Ranges. These are the Kahutara River, the Kowhai River and the Hāpuku River (Chandra, 1969; Dawe, 1997). The Kahutara is the southern-most river of the three, which is a sediment source for the southern coast of Kaikōura (Berger, 2017). The Kowhai rivermouth is located approximately 6 km north of the Kahutara rivermouth. The Kowhai River is a small and steep braided river with a catchment area approximately 80 km<sup>2</sup> (Environment Canterbury, 2000). This river flows from the seaward Kaikōura Ranges across a gravel floodplain extending north and south of the Peninsula to the coastline (Environment Canterbury, 2000). The current position of the mouth is south of the Kaikōura Peninsula, however this is a result of human modification to stop flooding in the township, and its mouth was once north of the Peninsula as can be seen in Figure 3.2 (Chandra, 1969; Dawe, 1997). The Hāpuku and Puhi river catchment flows from its headwaters in the Kaikōura ranges to the coast approximately 15 km north of the Kaikōura Peninsula. The flow of the Hāpuku River increases 2.7 km from the coast as it joins with the Puhi River (Berger, 2017). This river is the main source of sediment for profiles north of the Peninsula. Smaller creeks, including Harnetts Creek, Swan Creek, Middle Creek and Lyell Creek, intersect the coastline and deposit sediment north of the Peninsula. Goldmine Creek, Floodgate Creek, Luke Creek and the Waimangarara River deposit sediment across the Kowhai and Waimangarara fans (Dawe, 1997; Boorer, 2002; Berger, 2017). Sediment supply and transport from these catchments to the coastline will be discussed in Section 3.4. The streams are mostly derived from the draining of rainfall and snow melt from Mt Fyffe. The streams transport sediment to the coastline, but at a smaller magnitude than the previously discussed large rivers. The rivermouth environments at the three main rivers in the study area all consist of small hapua environments (Creed, 2014; Hume et al., 2016). The rivermouths have large MSG barriers which migrate across the rivermouth, changing the outlet width, created through a wave dominated environment, forming the small hapua lagoons. The outlets of the hapua lagoons at the rivermouth migrate largely from south to north before being re-set occasionally by flood breaches opposite the main river channel (Hart, 1999).

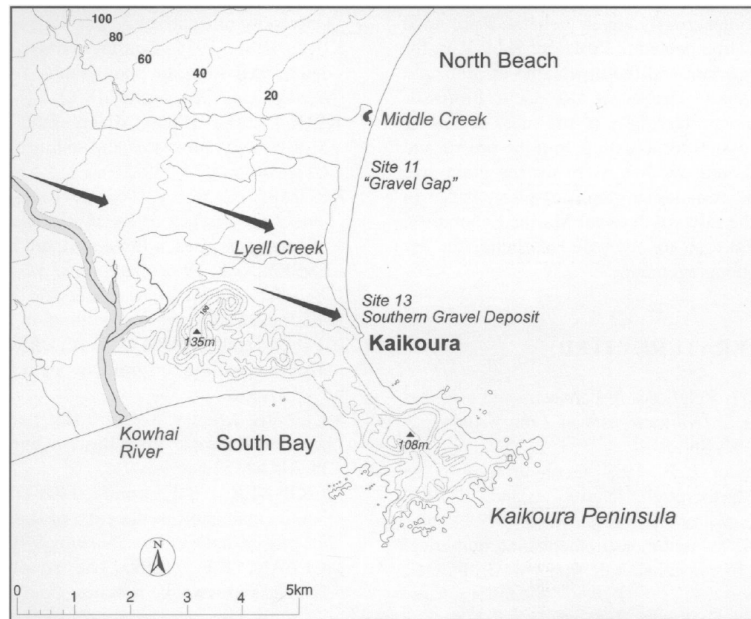


**Figure 3.2:** The Kowhai River historically flowed across the fan beneath the Mount Fyffe catchment. The mouth was once located on the northern side of the Peninsula near the Kaikōura Township. The Kowhai River currently flows south of the Kaikōura Peninsula, and is contained by stop banks, but after periods of heavy prolonged rainfall, the Kowhai River can flood old channel and exit the township at the Lyall Creek outflow which runs through the township. Taken from Dawe (2001).

### 3.4 Coastal environment

The coastline of Kaikōura is lined with MSG beaches north and south of the Peninsula (Chandra, 1969). The MSG beaches are present due to the high wave energy environment, and the coarse sediment source of quartzo-feldspathic metasediments (greywacke and argillites) from the basement rock eroding in the Kaikōura ranges. South Bay, Gooch's Beach and North Beach are all classified as MSG beaches by McLean (1970). Coastal cliffs, marine terraces and shore platforms are all uplifted features around the coastline which are a result of the high tectonic activity in the area (Chandra, 1969). Numerous studies have been undertaken looking at the geomorphology of the coastline (Chandra, 1969), the rock shore platforms (Kirk, 1977; Stephenson, 1997; Stephenson and Kirk, 1998), the sediment transport along the coastline (McLean, 1970; Dawe, 1997, 2001), the MSG beach morphology (Kirk, 1975, 1980), and a shoreline response to sea level rise (Berger, 2017). The combined literature surrounding the Kaikōura coastline has meant that processes and dynamics acting on the coastline are relatively well understood for the area. The following will look in detail at aspects of the coastal environment important to this study.

## Wind and wave climate

The major ocean current running along the east coast of the South Island is the Southland Current (Chiswell, 1996; Sutton, 2003). This current moves water in a northward direction in the offshore environment, however gets closer to the coastline around the Kaikōura area due to the water moving through the Mernoo Gap, an area of steep nearshore topography (Sutton, 2003). While the Southland Current is the predominant influence on the movement of water in the offshore environment, the nearshore sediment transport is influenced by the local wind and wave climate. Prevailing wind direction occurs from the south and south east around 40% of the time, and from the north east around 30% of the time (Boorer, 2002). Dominating southerly winds are a result of the passage of depressions and the associated cold fronts over the South Island (Stephenson, 1997). North westerly winds are usually a result of sea breeze conditions, or association cyclonic depressions from the north east of New Zealand which travel in a south direction (Stephenson, 1997).

The regional wind climate is a strong influence on the local Kaikōura wave climate. The wave climate in Kaikōura, as described in Stephenson (1997), is not continually monitored, however several studies have captured snapshots of the wave environment. Studies conducted by various coastal scientists in the late 1960s through to the mid 1970s, and described in Stephenson (1997), show that over this period, for 48% of the time waves were  $<0.5$  m. Wave heights between 0.5 and 1.25 m occurred 17% of the time, and wave in excess of 1.25 m occurred 4% of the time (Stephenson, 1997). Waves which exceeded heights of 1.5 m occurred 15% of the time on the southern coast of the Peninsula, and only 3% of the time on the northern side of the Peninsula (Stephenson, 1997). There is a strong presence of sub climates north and south of the Peninsula due to the sheltering of the Peninsula, as demonstrated in Figure 3.3. North-easterly driven waves create an environment with high swell energy north of the Peninsula, while the Peninsula buffers the swells creating a calm, low swell energy environment south of the Peninsula (Berger, 2017). When winds are prevailing from the south and south east, the opposite effect occurs, and the north of the Peninsula is sheltered from these swell conditions, while South Bay is exposed to a higher energy wave climate. Mclean (1972) used directional wave data offshore to determine that waves most often came from the north and north east (42%), while swells were observed most often coming from the south (43%). A characteristic of Kaikōura's wind and wave climate is the exposure of the coastline to the South Pacific Ocean, meaning that there is an unlimited amount of fetch, undisturbed by topography. The coastline therefore has a high wave energy environment, which Stephenson (1997, pg. 87) characterises as "where long periods of relatively calm seas are interrupted by high energy storms".





**Figure 3.3:** Wave conditions north and south of the Peninsula when a strong southerly is taking place. The left image is taken in South Bay, while the right image shows the contrasting calmer conditions at Gooches Beach, north of the Peninsula, demonstrating the buffering effect of the Peninsula. Image taken 24<sup>th</sup> August 2018. Photo credit: K MacDonald

Wave refraction occurs around the Kaikōura Peninsula, creating a wave shadow area when the prevalent wind direction is coming from the south (Pickrill and Mitchell, 1979). Changes in wave height and the angle of approach can influence the amount of wave energy that will arrive at the coastline, as well as long shore energy flux, currents, and sediment transport (López-Ruiz et al., 2015). As waves enter shallow water, refraction occurs as a result of friction between the wave and the nearshore bed. The wave interacts with the nearshore topography, affecting the distribution of wave heights and directions of wave approach along the shore (Pickrill and Mitchell, 1979). The more a wave bends around a headland, the more energy it loses, therefore influencing the amount of energy reaching the coastline. Waves are strongly refracted around the Kaikōura Peninsula, as waves coming from a dominating southerly direction bend around the headland due to interaction with the shallow nearshore topography. The refraction causes weaker wave energy north of the Peninsula, in the shadow of the Peninsula near the Kaikōura township. The refraction lessens further north, however wave refraction still affects wave direction near the Hāpuku rivermouth. Wave refraction and the less common prevailing north east wind direction influences the field sites north of the Peninsula shadowed by the headland topography close to the township, while the Southland Current is redeveloped and influences field sites further north of the Peninsula (Dawe, 1997).

## Tides

The tidal regime in Kaikōura is semi diurnal (Stephenson, 1997). The tidal range is predominantly microtidal (less than 2 m), as can be seen in annual tide extents taken from 2017, shown

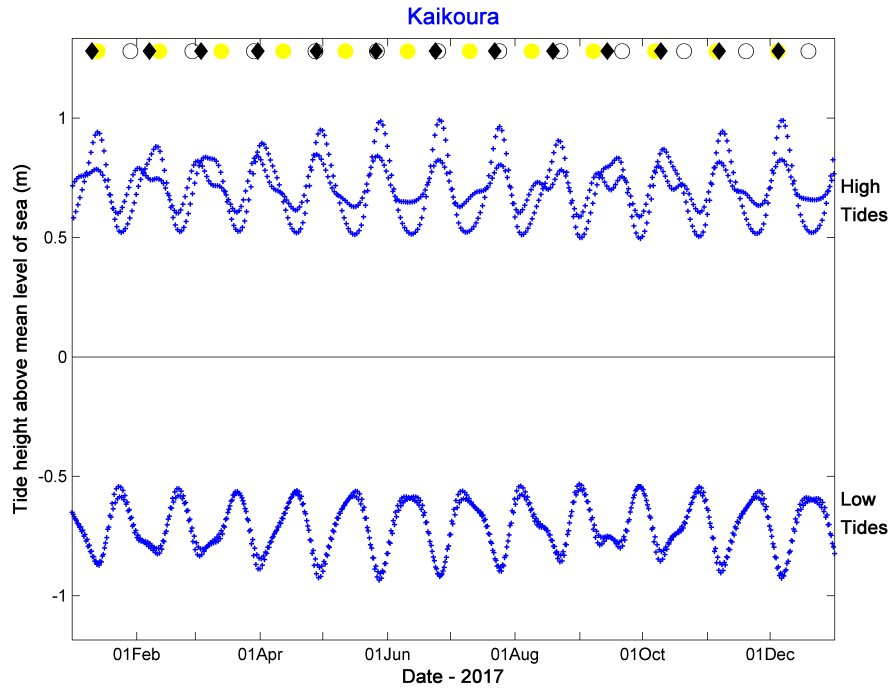


**Figure 3.4:** Tidal cycles measured in 2017, showing The high tide extents throughout the years (above MSL) and the low tide extents (below MSL), where MSL in Kaikōura is approximately 1.2 m. Data sourced from NIWA Tide forecaster.

in Figure 3.4. Kaikōura's tidal range is approximately 1.8 m between high and low tide. The mean sea level in Kaikōura is 1.2 m, while the hightide is around 2.1 m, and low tide is around 0.3 m. The spring-perigean range can exceed 2.5 m (Dawe, 1997). The microtidal nature of the coast means that the beaches have very narrow swash zones where wave energy is concentrated, due to the steep foreshores.

### Sediment supply to the coastline

The primary sediment source along the Kaikōura coastline is derived from the Seaward Kaikōura Ranges, in which the sediment is transported to the coast by the three main rivers, Figure 3.5; the Kahutara River, Kowhai River, and the Hāpuku River (Dawe, 1997; Boorer, 2002). It is thought that approximately 1000 t/km<sup>2</sup> is eroded annually from the Seaward Kaikōura Ranges (Hicks et al., 1996). There is a continuous supply of sediment available from the Kaikōura Seaward Ranges, and the delivery to coastal environments is increased under high river discharges during flooding and high rainfall events, due to the ability to move larger gravels downstream with high velocities in the waterways (Adams, 1980). Observations of relict greywacke deposits by Dawe (1997) show that erosion of torlesse from the mountain ranges is the main supplier of sediment to the coastline. Smaller streams and creeks which

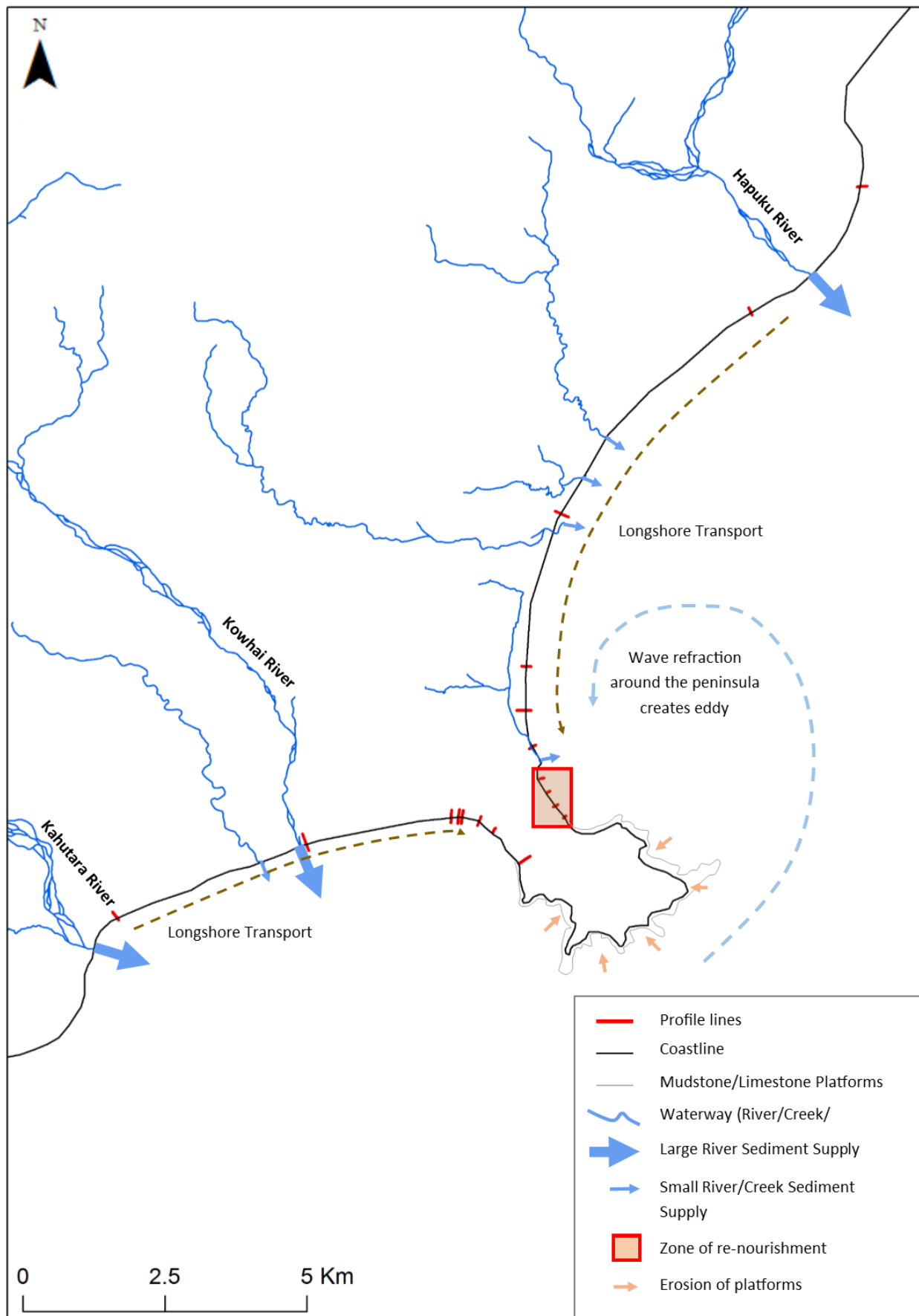


**Figure 3.5:** Schematic of the Kaikōura coastline showing the main sediment transport systems along rivers, creeks and tributaries. Longshore transport in the swash zone is the main process of moving sediment alongshore. Wave refraction around the Peninsula, as well as prevailing north-easterly winds, help drive longshore transport south from the Hāpuku River.



intersect the coastline also contribute to the sediment budget, as they carry sediment which is continuously eroded from the Kowhai, Waimangarara, and Hāpuku alluvial fans to the coast (Dawe, 1997; Boorer, 2002).

Limestone and mudstone platforms are present in the intertidal zone around the Peninsula. The erosion of the platforms is primarily due to the wetting and drying processes in the intertidal zone rather than wave abrasion (Stephenson and Kirk, 1996, 1998). The shore platforms are eroding at an average rate of 1.130 mm/yr, however the eroded material is so fine that it is mostly transported offshore rather than being reworked into the Kaikōura beaches (Stephenson and Kirk, 1998). Some eroded material does get reworked into the coastline, however this source is believed to contribute significantly less sediment compared to the scale of that supplied from the rivers.

Renourishment is a coastal hazard mitigation mechanism through which sediment is deposited at a point on the coastline to be reworked into the coastal system to help maintain an eroding coastline. Renourishment has been undertaken along the Kaikōura Esplanade, as shown in Figure 3.5, since 1997 to aid the long-term erosional trend along the shoreline adjacent to the Kaikōura township. The renourishment in Kaikōura was first proposed by Kirk (1986) who suggested renourishment would help maintain the foreshore and protect the infrastructure assets beyond the coastal zone. Initial renourishment efforts to slow erosion rates on the foreshore were taken by applying a volume of sediment to be reworked in the system. More recent renourishment is believed to be an effort to stop wave overtopping, by placing a sediment bund higher up the foreshore to protect the backshore an assets beyond the active beach.

Table 3.1 shows the recorded timing of renourishments, as well as the amount of sediment put into the coastal system at that time. OCEL Consultants NZ Ltd (2016) states in the consent application for the renewal of previous renourishment consents, that most of the material supplied to the beach has been placed south of Brighton Street, at the southern end of the Esplanade, with the intention of renourishing profiles KCK3659 to KCK3737, as shown in Figure 3.5. The material used for the renourishment was taken from South Bay as it was determined that the sediment in South Bay was similar to the relict sediment in the North Beach area. This is because the North Beach upper foreshore/ backshore sediment is relict sediment from when the Kowhai River used to intersect the coastline north of the Peninsula, as opposed to its current position south of the Peninsula (shown in Figure 3.2) (Dawe, 2001).

**Table 3.1:** Beach renourishment volumes which took place between 1997 and 2016 along the Kaikōura Esplanade by the Kaikōura District Council (KDC) to slow erosion rates in this area. Sediment was taken from South Bay and relocated to various locations along the Esplanade throughout the 19 year period. Information sourced from OCEL Consultants NZ Ltd (2016) and Bruce Gabites, ECan Coastal Scientist (Pers comm, 2018).

| Year          | Amount (m <sup>3</sup> ) |
|---------------|--------------------------|
| Early 1997    | 9,000—10,000             |
| October 2002  | 1265                     |
| December 2009 | 840                      |
| July 2011     | 500                      |
| April 2012    | 1000                     |
| January 2016  | 5000                     |

### Longshore sediment transport

Long shore transport is influenced by different mechanisms both north and south of the Peninsula, as seen in Figure 3.5. The Kahutara and Kowhai River supply sediment sites south of the Peninsula, where it is transported alongshore to South Bay by prevailing wind direction driving sediment transport in the swash zone, and influences from the Southland Current (Boorer, 2002). The dominating swash motions which drive longshore gravel transport, is cut off by the Peninsula as sediment is transported north by onshore swash processes. The Peninsula acts as a barrier to these swash transport processes, and traps the sediment at the South Bay sites, as there is no current or alongshore drift which drives transport of the sediment from South Bay around the Peninsula, especially heavy gravel material. Most beaches on the eastern edges are rocky or found in small pockets amongst intertidal platforms and cliff edges. Sediment can not transport around the peninsula because at a lot of the surrounding coast there is not a swash zone for the gravel to travel along.

The longshore transport mechanisms north of the Peninsula are influenced by the wave refraction around the Peninsula, as well as the southward drift caused by incoming north-easterly waves in the nearshore (Dawe, 1997; Berger, 2017). The Hāpuku River supplies sediment to sites north of the Peninsula, however the extent of the southern drift transportation only reaches as far south as Lyell Creek (Dawe, 1997). Sites south of Lyell Creek on the north side of the Peninsula exhibit erosional trends, suggesting that the sediment from the Hāpuku River does not reach the Esplanade area, hence for the need of renourishment in this area.

### 3.5 Tectonic history

The study area is located within the active Marlborough Fault system, where lies the boundary transition zone between the Australian and Pacific plates (Rattenbury et al., 2006), as seen in Figure 3.6 (left). The convergence rate of the boundary in this area is 41 mm/yr (Anderson and Webb, 1994), in which faulting associated with the convergence results in uplifting of the Kaikōura Seaward Ranges by 6–10 mm/year, a similar rate to the Southern Alps uplift caused by associated faulting from the convergence along the Alpine Fault (Van Dissen and Yeats, 1991). Most of the vertical and horizontal displacement in the river catchments in the study area have historically been related to the Hope and Jordan Thrust Faults located in the Marlborough Fault zone, whereas vertical displacement of the coastline has historically been associated with the offshore thrust faults within the Northern Canterbury Fold and Thrust Belt (Van Dissen, 1989). The inferred rate of long-term uplift along the Kaikōura Peninsula coastline is  $>1$  mm/yr, as evidenced by the 125,000 year old uplifted marine terraces (Ota et al., 1996; Beavan and Litchfield, 2012). As seen in 3.6, the Kaikōura region is bounded by several large faults, including the Alpine fault, Wairau Fault, Awatere Fault and the Clarence Fault, which all have single event displacement estimates of more than 5 m (Rattenbury et al., 2006). Smaller faults, inclusive of Hope Fault segments (Hope river - Taramakau; Conway - Kahutara; Mt Fyffe; and Seaward), Jordan Thrust, Kekerengu Fault and the Hundalee Fault are all shorter in length than the previously mentioned faults (10-110km) and have single event displacement estimates on 1–5 m.

Until the 2016 earthquake event, there had been no major coastal uplift in Kaikōura associated with any historically documented earthquake events in the Marlborough Fault System or the North Canterbury fold and thrust belt (Yetton and McCahon, 2009). On the 14th of November 2016, a significant  $M_w$  7.8 earthquake took place. As seen in 3.6 (right) a series of faults ruptured in a south west to north east direction during the event and subsequent aftershocks. The ruptures covered a 180 km length over the Kaikōura region, in the Marlborough Fault System. By August 2017, there had been over 18,500 aftershocks (GeoNet, 2017). The epicentre was located approximately 50 km south-west of the Peninsula, in which faults ruptured north from here all the way up to the Needles fault, which runs off the east coast towards the north into the offshore environment.

The earthquake significantly changed the coastal environment, with major changes being marked by the uplift and exposure of previously submerged wave cut platforms (Clark et al., 2017). The displacement ranging from  $-2.5$  m to  $6.5$  m along the coast north and south of the Peninsula (Clark et al., 2017),  $1.01$  m at the Peninsula (Stephenson et al., 2017), and a 12 m strike slip

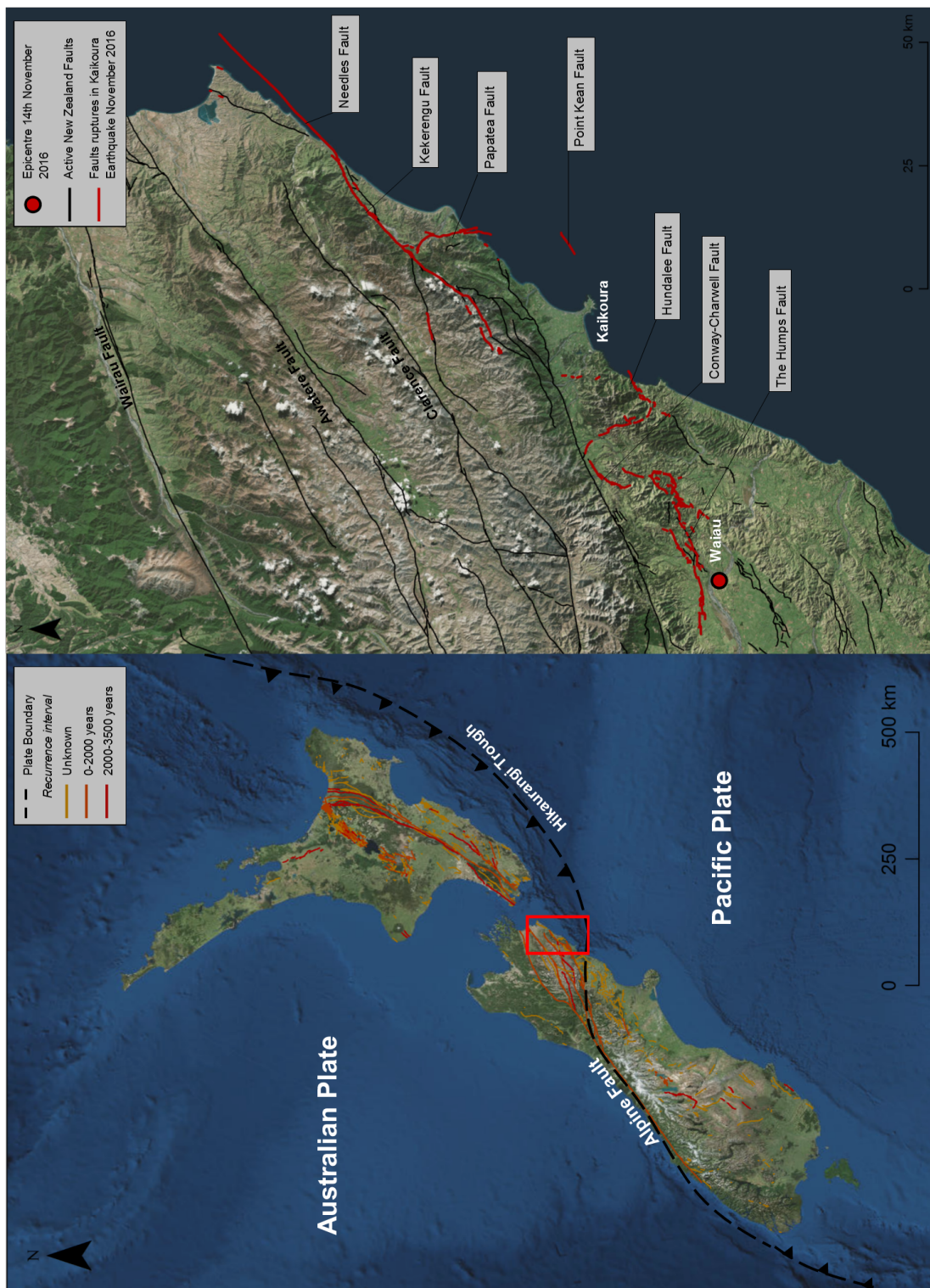


**Figure 3.6:** Distribution of fault lines across New Zealand, confined largely to the central North and South islands. (Left) New Zealand sits on the plate boundary of the Pacific and Australian Plates. (Right) Faults which affect Kaikoura, with the red faults detailing the faults which ruptured in the 2016 November earthquake. Data is provided from New Zealand GeoNet project and its sponsors EQC, GNS Science and LINZ. Basemaps are sourced from the LINZ Data Service.





**Figure 3.7:** Two of the estimated >10,000 landslides which occurred as a result of the 7.8 Kaikōura Earthquake. The left image shows a landslide which was located approximately 10 km south of the Peninsula. The landslide at Ohau Point (right), is located approximately 25 km north of the Peninsula. Seawalls have now been put at both locations to protect the recovery efforts from intense wave action. Images sourced from the LINZ Data Service.

displacement along the fault itself (Hollingsworth et al., 2017). More than 200 valley-blocking landslides were generated in the earthquake, a result also of the steep terrain in the Kaikōura Ranges, and many of these blocked large rivers causing dams to form (Dellow et al., 2017). The largest of these landslides to form was in the upper Hāpuku River catchment, where 12 million m<sup>3</sup> of debris blocked the river, forming a lake behind it (Dellow et al., 2017). The tens of thousands of landslides generated in the earthquake means that there is a surplus of sediment coming down the catchment, of which there would be an initial pulse of finer sediment at the coast, followed by the slower transport of gravel down the catchment over the years to decades following the earthquakes. The steep coastline backs the SH1 transport route along the coast to the southern end of the study, and further north of the study area. These transport routes were covered in landslide debris following the earthquake, as can be seen in Figure 3.7 where large land slides blocked SH1 south (left) and north (right) of the Peninsula. The inland route to access Kaikōura was also covered in landslide debris, however this was cleared quicker than SH1 and used as an access route to Kaikōura. The recovery efforts to re-establish the transport routes have had a further impact on the coastal system. Sediment from the coastal landslides entered into the coastal system, in some cases smothering species with fine sediment which live on the rock shore platforms. During the recovery efforts of SH1, it is likely that more sediment would have entered the system then also. Large seawalls have been built now in order to protect the new roads built which in most cases are confined to a steep cliff on its west and the ocean on its east. While these structures are necessary in order to protect the main transport route, the sea walls will have a lasting impact of the coastal processes occurring in the region for decades

to come.

In summary, it was likely that a large earthquake would affect the Kaikōura coastline eventually due to its location in an extremely tectonically active area. The effects of the earthquake have dramatically altered the coastal morphology, with significant uplift of the entire coastline. It is likely that the significant amount of inland and coastal landslides will have an impact on the coastal sediment budget over the coming years, however the affect of the seawalls now being built along the coast to protect SH1 recovery effects and re-establishment of transport routes will have an affect on coastal processes, and may have longer lasting affects on the coastline.

# Chapter 4

## Methodology

This chapter begins with an overview of the methodological approach to this research. It will then detail the data and methods used to answer the research objectives discussed in Chapter 1.

### 4.1 Introduction

The aim of this research is to further understand how MSG coastal environments respond to a large tectonic event when there is an earthquake-induced change in relative sea level. As can be seen in Figure 4.1, multiple steps were undertaken to firstly, establish the pre-earthquake state of the coastline; secondly, understand the changes and circumstantial complexities of re-collecting beach profile surveying data in a post-earthquake environment; and thirdly, determine how the MSG beaches were responding following the earthquake and develop conceptual response pathways to illustrate these responses. The study uses a mixed method approach, using a combination of desktop study, data analysis, and field data collection.

The study encompasses a 21 year time period with the November 2016 earthquake disturbance marking the change in environments from pre-earthquake to post-earthquake. The desktop study enables data collection for a coastal setting which has now been dramatically altered, where aspects of the beach profile such as grain size distribution and foreshore morphology are likely to have undergone significant changes. The desktop study reviewed and analysed research undertaken in the Kaikōura coastal setting prior to the earthquake in order to comprehensively understand the pre-earthquake coastal environment. Data analysis methods, such as statistical analysis, allowed for pre-earthquake data acquired in the desktop study to be quantified, which could then be used to later compare with field data collected in the post-earthquake

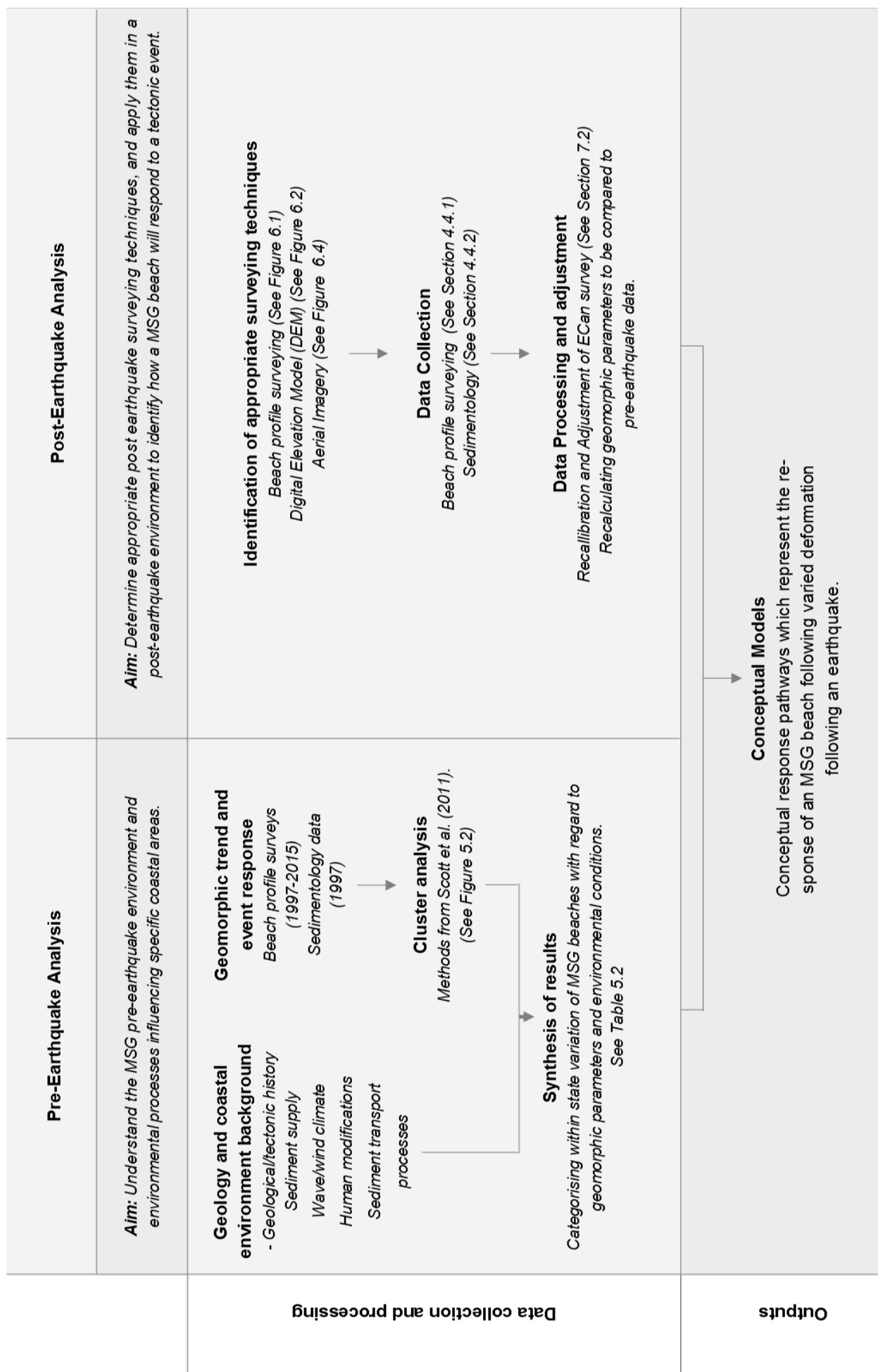


**Figure 4.1:** Research framework of the overall methodological approach. Two time periods are studied, pre-earthquake and post-earthquake. The pre-earthquake analysis uses both desktop analysis and data analysis to determine pre-earthquake beach trends, and the within-type variations of MSG beaches in the Kaikōura area. Post-earthquake beach response is determined through the collection of beach profile surveying and sedimentology data. An overall synthesis of results uses the pre-earthquake beach states to investigate the changes in the post-earthquake environment, and develop conceptual pathway models to illustrate how the MSG beaches responded post-earthquake.



environment in order to detect the effects of the earthquake and subsequent relative sea level fall. Field data methods, including beach surveying and sediment sampling were used in order to quantify the environment post-earthquake. Using a mixed method approach means that an accurate depiction of the Kaikōura coastal environment pre-earthquake and its response to the earthquake can be confidently determined. The following will describe the individual methods used in this study to determine the results presented in subsequent three chapters.

## 4.2 Data and methods: Pre-earthquake Kaikōura beaches analysis

In this section, methods used to address Objective 1: *To establish the pre-earthquake long-term trends of the unconsolidated coastal environments in Kaikōura, through the means of geomorphology and sedimentology* are presented.

### 4.2.1 Beach profile surveying data

A beach profile survey is a series of points taken using accurate GNSS surveying equipment to create a cross section of topographic changes across a beach (Morton et al., 1993). It provides a snapshot of the morphology of a beach along one cross section at one particular time, and geomorphic characteristics of the profile such as volume and shoreline extents can be calculated from these surveys. Beach profile data is the main source of data used throughout the course of this study to determine the long-term trends and morphology of the pre-earthquake Kaikōura coastal environment, as well as to inform the response of the coastline following an earthquake. The study area has an 18 year record (1997–2015) of 18 different beach profiles within the study area, as a result of an annual monitoring programme created by ECan in 1997. This means that the study area is well represented with beach profiles, and it would be fair to make assumptions about what was happening between profiles, as they are densely distributed where there is expected differences in the environmental conditions acting on the profile, such as wave climate and sediment supply. Beach profile surveys taken over a 18 year period allow for shoreline and volume trends over a long period to be determined, as well as being able to record and estimate the magnitude of coastal events and the effects on the coastline. The beach profiles also allow for highly accurate and detailed changes in beach shape to be monitored. The beach profile surveying data acquired from ECan was used to perform a cluster analysis of the 18 profiles to determine the different within-type variations of MSG beaches in the Kaikōura study area, which will be discussed in subsequent sections.

### 4.2.2 Classification of Kaikōura MSG beaches

A classification of the MSG beaches in Kaikōura was undertaken to determine the existence and significance of within-type variations existing amongst Kaikōura’s different coastal settings pre-earthquake, to then be used when analysing the response of the beaches in the post-earthquake environment. Framework for the MSG beach classification used in this study is outlined in Figure 4.2. The possible existence of within-type variations of MSG beaches was first mentioned in Jennings and Shulmeister (2002), however these within-type variations were not described. A series of geomorphic parameters were calculated for each of the 18 monitored profiles based on methods of beach classification schemes used in previous studies (Jennings and Shulmeister, 2002; Scott et al., 2011). Classification schemes in past studies have used a range of parameters to measure the variation in beach types, including environmental conditions such as wind and wave climate, as well as geomorphic parameters including sedimentology, beach slope and beach morphology (Short, 1979; Wright and Short, 1984; Carter and Orford, 1993). In more recent studies, Jennings and Shulmeister (2002) and Scott et al. (2011) focus largely on geomorphic parameters of gravel beach types, and wave climate, to establish classification within their selected sites. From these studies, the geomorphic parameters appropriate in a MSG beach setting were calculated for the 18 ECan monitored profiles using beach profile surveying data. Additional parameters such as long-term erosional or progradational trend helped to further classify the site specific MSG beaches from the broad term classified in Jennings and Shulmeister (2002). The parameters calculated for the classification of Kaikōura beaches are outlined in Figure 4.3, and include slope, volume, width, berm elevation and sedimentology in the mid tide zone and the upper foreshore. The parameters were calculated using a combination of literature, and analysis of 1997–2015 beach profile survey data and 1997 sedimentology data, provided by ECan. Specific details of calculations for individual parameters used for classification, both geomorphic and environmental can be found in Appendix B and Appendix C.

### 4.2.3 Cluster analysis of geomorphic parameters

A cluster analysis was undertaken using the statistical software *Statistica* by Statsoft, to cluster geomorphic parameters of each profile together in order to determine within-type variation groups, based on quantitative measurements (eg. beach volume) and arbitrary values (eg. long-term trend) given to each profile. Using the methods for cluster analysis of beach morphological parameters in Scott et al. (2011), a cluster analysis expressed in the form of a hierarchical tree was produced to identify different clusters of beach profiles. A range of amalgamation (linkage) rules were tested with this data, however due to the data being both categorical and

# Analysis and classification of Kaikoura Beach Profile Sites based on pre-earthquake data on geomorphic parameters in specific environmental settings

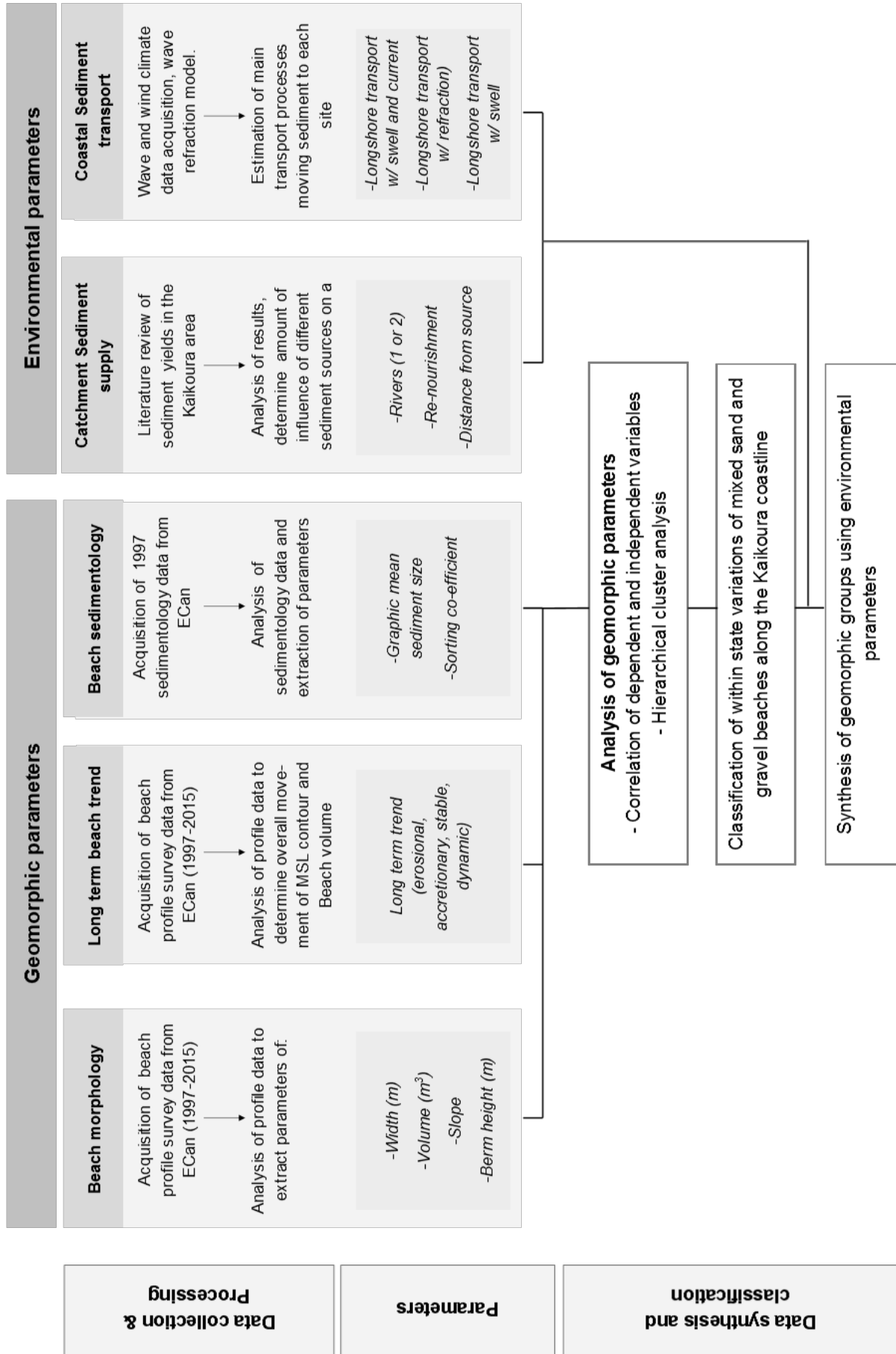


**Figure 4.2:** Framework of pre-earthquake classification of MSG beaches. The flow chart outlines the different methods and data used to calculate the different geomorphic and environmental parameters for the MSG classification component of this study. Adapted from Scott et al. (2011)

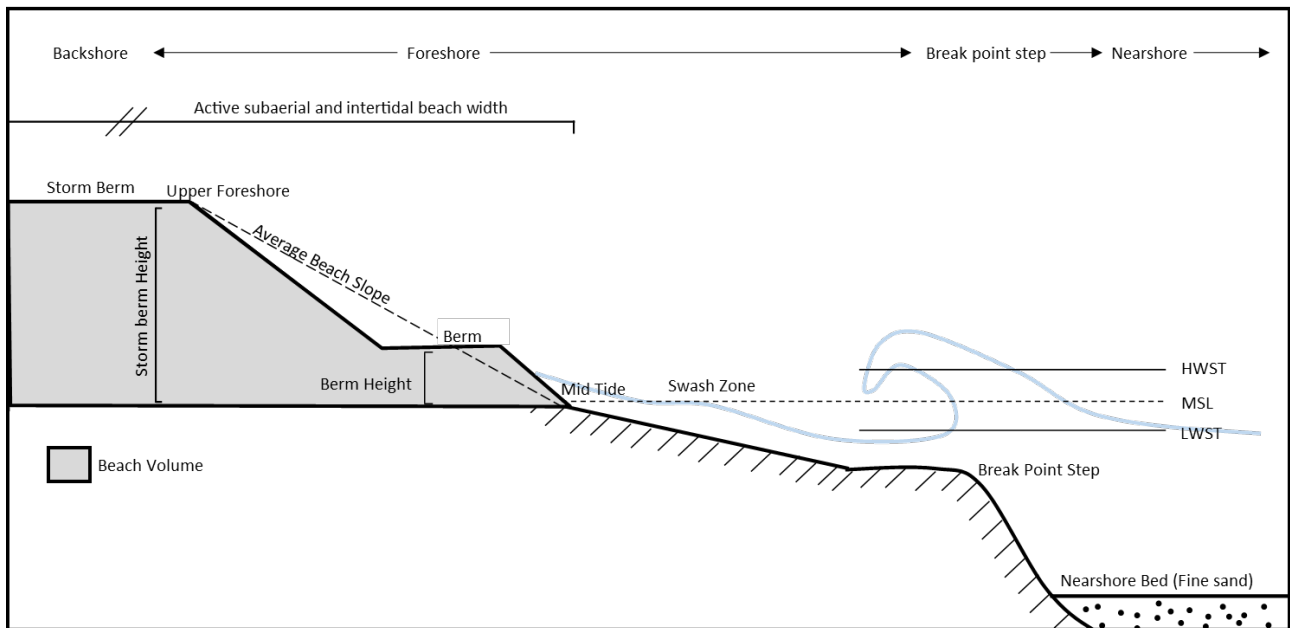


**Figure 4.3:** Schematic of a MSG beach profile showing the extent and occurrence of the geomorphic parameters calculated used in the classification component of this study in a simplified MSG environment. Adapted from Kirk (1980).

continuous, Unweighted Pair-Group Method with Arithmetic Mean (UPGMA) was deemed the appropriate method to use (Scott et al., 2011). In this method, the distance between all pairs is calculated, and the average of these distances determines the distance between two different clusters (Sneath and Sokal, 1973).

The method is successful when objects form natural distinct clumps, or have chain type clusters. The geomorphic groups were decided on based on the tree groupings, as well as knowledge and experience of the dataset used. Due to the size of the data set available in this study, applying a threshold of similarity, as done in Scott et al. (2011), would be less appropriate given that this study is dealing with profiles from a similar environment, and of the MSG variation, whereas Scott et al. (2011) was categorising beaches from across England and Wales where variations of beaches were more polarised and significant changes in environmental conditions were prominent.

A further confirmation of the hierarchical cluster analysis was done using Multi Dimensional Scaling (MDS), as per the methods used by Scott et al. (2011). The MDS takes the matrix of the Euclidean distances for dissimilarities between profiles determined in the hierarchical cluster analysis and places them on a two dimensional (2D) plot to visualise the clustering between groups. The close proximity of profiles on the 2D plot represents the closeness of similarity to another profile. The stress value is representative of a goodness of fit, where a value is given between 1 and 0. A 2D stress value of 0.1 represent excellent ordination (Clarke and Gorley, 2006). The technique is more effective with large group sizes, but is used here to visualise the

scattering of profiles relative to each other.

Interpretation of the results from this were synthesised with an analysis of environmental conditions acting on each profile, to determine the environmental settings of each cluster. These environmental conditions included sediment supply, sheltering and distances to sediment sources. It could be determined what common environmental parameters were strongly influencing the nature of the profiles, and this was later used to inform predictions of how different beach types might respond to the earthquake. The results produced from these methods are presented in Chapter 5.

### 4.3 Data and methods: Critiquing post-earthquake survey techniques

In this section, methods used to address Objective 2: *To evaluate post-earthquake surveying techniques and the data captured through the use of different methods* are presented. Methods for aerial imagery shore line analysis and DEM's generated from LiDAR data are presented here, with subsequent sections addressing GNSS beach profile surveying methods.

#### 4.3.1 Digital elevation model (DEM)

Two LiDAR data sets were used in this study, 2012 and June 2018. The two data sets were processed into digital elevation models, which could then be differenced (Figure 4.4) from one another to determine the change in elevation across a large area between 2012 and 2018.

LiDAR data is collected from an airborne platform, either by a helicopter or a satellite, and sends pulses to the ground surface and measures its return (Gigliano, 2010). This can allow for the ground elevation to be calculated, as thousands of points are collected and processed into a Digital Elevation Model (DEM). The airborne platform used in this study had a built in GNSS positioning system, which allowed for the position of points to be determined in real time. The resolution of a data set will vary, depending on the regularity of points being taken in a grid. The higher the resolution, the more defined characteristics of the landscape will become. For example, a 1 km by 1 km cell size may feature rolling hills, however these features will not be defined in the DEM, as only one elevation is assigned to each 1 km by 1 km cell. If LiDAR is collected where there are several points taken every 1 m, then a cell size of 1m by 1m can be developed and will be able to more clearly define the rolling hills in a DEM.

The 2012 LiDAR data set is freely obtained online from Land Information New Zealand. 2018 LiDAR data was collected by the North Canterbury Transport Infrastructure Recovery (NC-TIR) in June 2018 for recovery purposes. The datasets were cropped to the coastal study area in *ArcGIS*. The subtraction tool in *ArcGIS* was used, as can be demonstrated in Figure 4.4, to minus the 2012 data set from the 2018 data set, and to determine the amount of uplift/accretion and subsidence/erosion. The differential DEM generated in this study has attempted to separate these processes but classifying the output into subsidence ( $< -0.2$  m), the error associated with the method ( $-0.2$  m to  $0.2$  m), uplift ( $0.2$  m to  $1$  m) and additional accretion ( $> 1$  m). Both data sets are 1 m resolution, which has been documented in literature as having 0.15–0.25 m vertical accuracy (Aguilar et al., 2007; Giglierano, 2010), however the LiDAR metadata for the datasets used did not disclose the vertical accuracy. Cross sections of the profile lines were extracted from the DEM for comparison using the 3D analyst tool in *ArcGIS*, where one point every 1 m was extracted and could be processed into a beach profile in *Microsoft Excel*.

The period of time between the data sets (6 years) is not uncommon for analysis of LiDAR data due to the expenses involved in collecting it, and therefore is not as readily available as aerial imagery data or beach profile data. This should be acknowledged when analysing a coastal environment which is very dynamic, and therefore a 6 year time difference between data sets means that changes on the active beach can not all be directly attributed to the single uplift event. Similar to other forms of data collection, it is a snapshot of the coastal system, and the accuracy of interpretation of the processes and responses will increase with frequency of data collection. Interpolation of the results to determine long-term trends, needs to be done with caution.

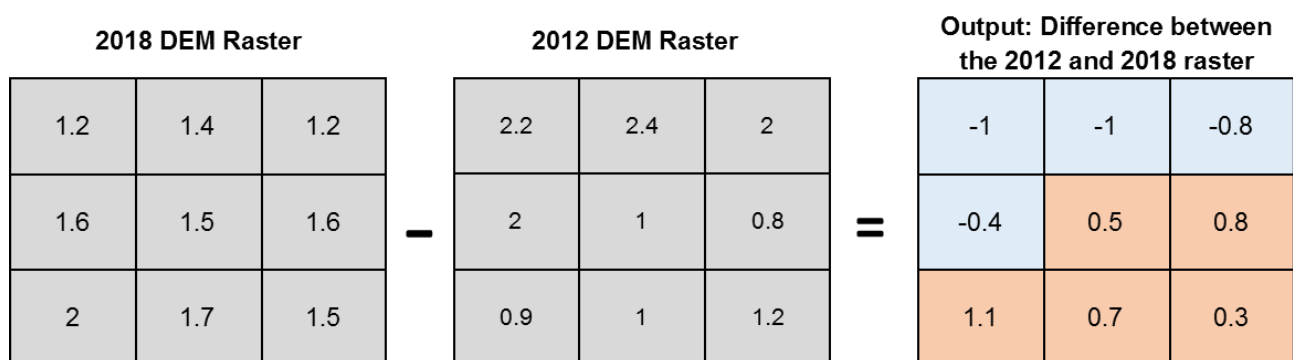


**Figure 4.4:** The subtraction tool in *ArcGIS* is used to determine the elevation differences between the 2012 and 2018 DEM. The tool subtracts one raster dataset from the other, and its output is the elevation difference between the two data sets. The red boxes represent an elevation fall from 2012–2018, which could be a result of subsidence, or in a coastal setting, erosion. The green boxes are calculated as a rise in elevation between 2012 and 2018, indicative of uplift or in a coastal setting, accretion.

### 4.3.2 Aerial imagery

Historical aerial imagery is collected from an airbourne platform, such as a plane or helicopter, however more recent aerial imagery can be collected from satellites or UAV's. Aerial imagery collected from an airborne platform with a built in GNSS positioning system means that the position of the imagery can be collected in real time. The images collected are orthorectified to remove image tilt, so that images are of a 'birds eye' view looking directly down on the landscape. The resolution of historical imagery, typically prior to 2000, is of a lower resolution than more modern imagery.

In this study, three aerial images are used to represent three different time periods. Available aerial imagery covering the Kaikōura study area which was of a resolution high enough to identify morphological features on a MSG beach was taken from 1999 (2.5 m resolution), 2014 (0.3 m resolution) and 2016 (0.2 m resolution). Two features were observed in each image to determine changes - the vegetation line and the wet water line. The measurement of the vegetation line is a common technique used on sand beach environments to measure the movement of the dune toe (Stafford and Langfelder, 1971). The vegetation line in sand beach environments is responsive to major storm events, and advances slowly over periods of low storm activity. In a sand beach environment, the vegetation line marks a defined zone of the beach. In MSG beaches, this is not the case, as the vegetation line is not representative of a beach zone, and is more representative of a hinterland environment. The plant species found at the vegetation zone on a MSG beach are not the same as the quick recovery, adaptable species found on a sand beach environment. Therefore, using vegetation line in a MSG beach environment should always be undertaken with caution of what the movements in vegetation line actually represent. Changes to the vegetation line are likely to be indicative of long-term, large storm events (or lack of) which will take a long time to recover. Caution must also be exercised using this feature in areas where the vegetation line is constrained in the backshore such as a parks, railways, and roads, where changes here are not representative of changes in the active beach.

The wet waterline is was the second feature identified on the images to identify shoreline changes along the coast. This feature is found where there is a change in shades of grey due to the saturation of the sand at the wave runoff (Stafford and Langfelder, 1971). Caution has to be exercised when looking at these results of the wet water line, as it can be significantly influenced by the tidal cycle, as well as variability in wave runoff along the coast. As seen in Figure 4.5, by using beach profile data taken at similar times of the capture of aerial imagery, estimates of slope length ( $x$ ) could be determined between the high tide and low tide marks. The variability of wave runoff was not calculated, but is considered as a factor which will affect the position of

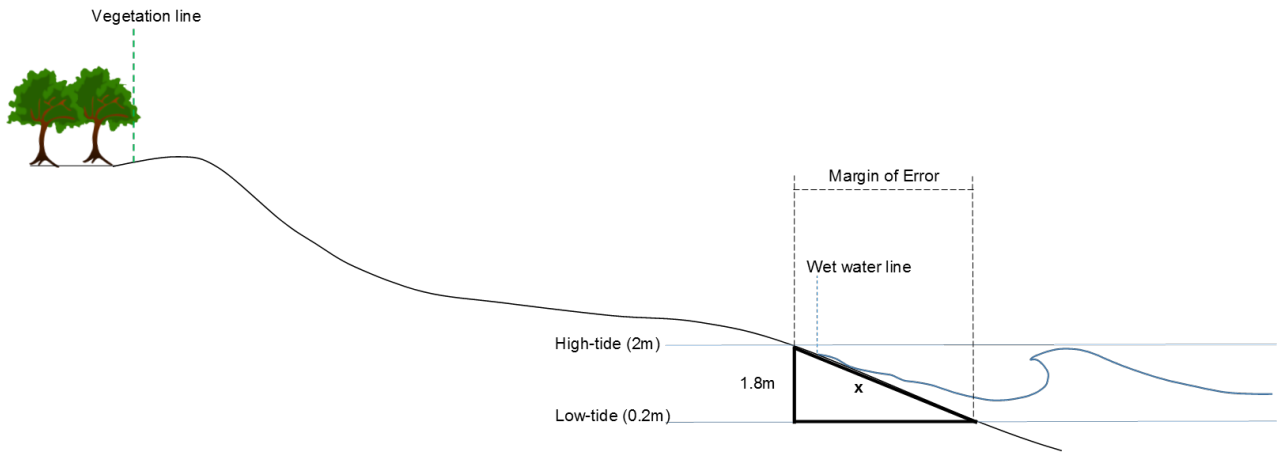


**Figure 4.5:** Two lines analysed on the aerial imagery are the vegetation line, marked where the last line of vegetation is before the beach turns into complete sediment. The second line is the wet water line, which is measured with consideration of a margin of error (MOE). The slope of the foreshore between the high tide and the low tide mark ( $x$ ) is measured as the MOE to account for the differences in tides when the images were captured. If the change in a shoreline is more than the MOE, then the change in shoreline is significant.

the wet water line. The distance between high and low tide on the beach profile was considered to be the margin of error (MOE). The MOE varied across profiles depending on the steepness of the foreshore, where KCK3800 is a steep profile, and therefore had a MOE of 6 m, whereas KCK2200 was very flat and wide, and therefore had a calculated MOE of 19 m. If changes from year to year exceeded the MOE at the profile, changes at the profile were deemed to be significant, however due to the large MOE at profiles, a more detailed shoreline analysis can not be undertaken using this technique.

The wet water line and the seaward vegetation line were traced along the coastlines of all three images and the difference at a profile from one image to another was determined using the measuring tool in *ArcGIS*. Caution is exercised in analysing the results, as variability in wave runup could not be accounted for within the MOE but may effect results, and different profile settings could have an influence on the migration of the vegetation line.

## 4.4 Data and methods: Post-earthquake Kaikōura beaches analysis

This section will present methods used to address Objective 3: *To identify what the short-term responses are in a MSG coastal environment following an earthquake-induced change in relative sea level.* This section will also introduce some method development in surveying in a post-earthquake environment.



#### 4.4.1 Beach profile surveying

Following the Kaikōura Earthquake, preliminary bench mark coordinates and ellipsoid heights were issued by Land Information New Zealand (LINZ), which identified that there were changes in the location of the bench mark positions due to the uplift in the coastal area. Initial reports of data collected 29<sup>th</sup> and 30<sup>th</sup> November 2016 by Christchurch City Council using RTK techniques and LINZ from 5<sup>th</sup> to the 9<sup>th</sup> of December 2016 using static techniques determined there was up to 0.98 m of vertical uplift and up to 1.97 m of horizontal movement around the Kaikōura township and Peninsula (LINZ, 2016). These benchmarks coordinates were reissued again in January 2018, when LINZ re-coordinated their control network in the area (A. Howes, ECan Surveyor, personal communication, 14 September 2018). ECan resurveyed the profiles in January 2017 after the earthquake using the preliminary bench mark coordinates and creating their own control framework, and have since recalibrated their results to fit with the 2018 re-coordinated control network.

The physical survey lines in the study area consist of two to four physical control points in the field, which mark the survey line in order for it to exist in the field physically and geospatially, as shown in Figure 4.6 where the orange triangles represent the control points at profiles in the South Bay area. ECan's control points for this survey area include nails in a fence, a bolt in the ground or a waratah in the ground. For the surveys conducted prior to the earthquake, there was no significant movement of the control points over the observed time period, and therefore the survey line consistently measured the same physical and spatial profile.

The earthquake caused large scale horizontal and vertical movement, which resulted in the movement of the physical control points. Following an event of such magnitude, there are two options when resurveying the beach profiles, as seen in Figure 4.7, which shows the movement of the beach profile, and the new geospatial and physical survey lines. The first option is to resurvey the physical survey line in the field using the new locations of the physical control points, and accept that the same piece of land is being measured but in a different geospatial location. The second option is to resurvey the geospatially correct line, which resurveys the profile using the pre-earthquake spatial line, but does not use the physical control points in the field. Using this method accepts that the ground that is being surveyed may be different to that previously surveyed, but the profile line location is geospatially consistent over time. Following an earthquake, a decision needs to be made whether to measure the physical or geospatial line herein. Each line will produce different results, but both will record a disturbance in the long-term data set. Disturbances recorded by measuring the physical survey line includes the physical deformation of the ground when the control points are not translated uniformly. The distance

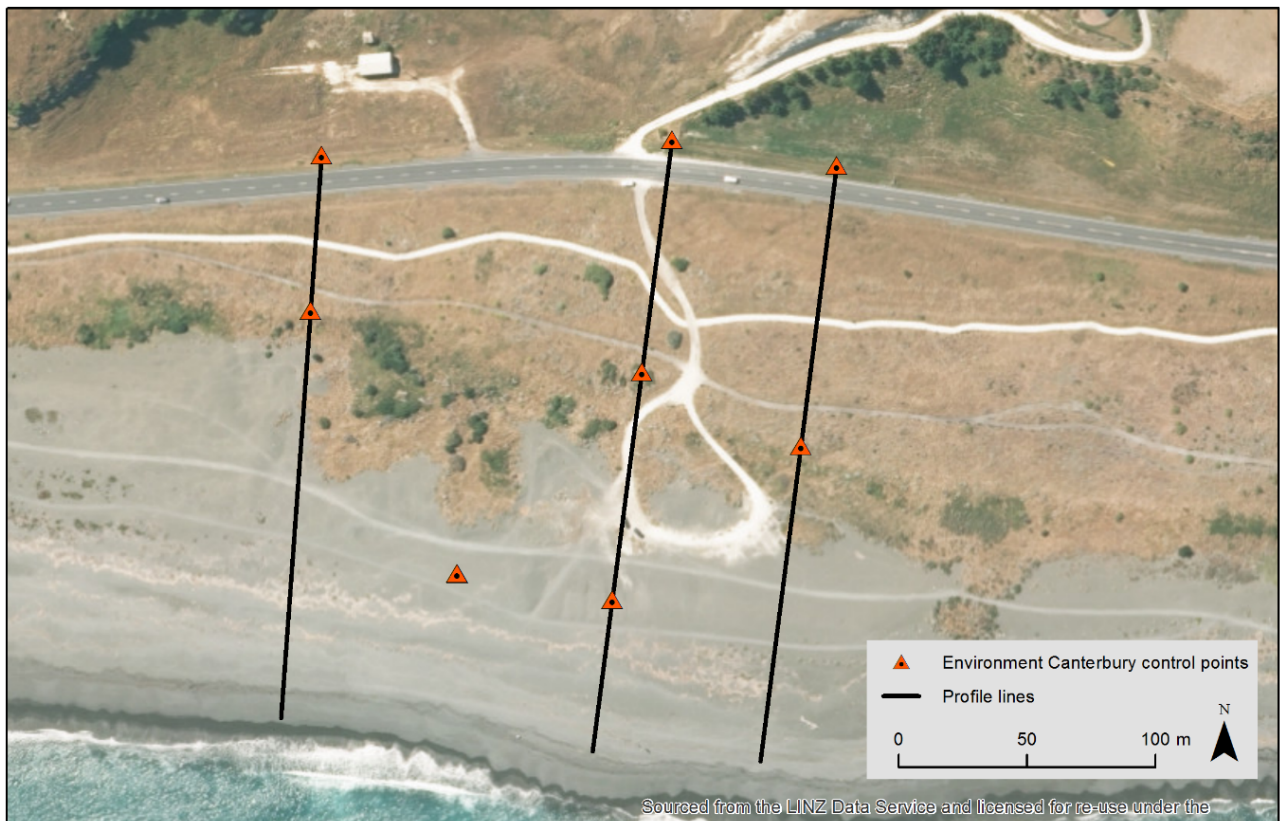


**Figure 4.6:** Profiles KCK2470 (left), KCK2486 (middle) and KCK2496 (right) profile lines, with control points intersecting the profile line in their pre-earthquake positions. Basemap sourced from the LINZ Data Service.

between the control points may change also with deformation, and therefore the across-shore position along the survey line will change also, as shown in Figure 4.7A. Disturbances recorded by measuring the geospatially correct line are inclusive of the surveying of a different piece of physical land, but is geospatially consistent with the pre-earthquake dataset, and therefore continues to measure the geomorphological change along the same plane as pre-earthquake. Land with previously relative lower elevation could move into the spatially correct plane, and the geomorphology of the beach profile could appear as if there was a loss of volume in sediment, as seen in Figure 4.7B. In terms of the geospatially correct survey line, there has been a loss of sediment, but it is not due to erosion or extraction, it is due to lateral movement of a different segment of land into the spatially correct plane.

The decision was made in this study to resurvey the geospatially correct line. This decision was made due to keeping consistency with ECan's decision to also measure the geospatially correct line, and therefore the 2018 survey results would be comparable to the 2017 survey. The measuring of the geospatially correct line is justified by the fact that the geomorphic features of the beach profile is a proxy for the environmental conditions acting on a profile, in which the environmental conditions change in a temporal and spatial sense (Short, 1996). By continuing to measure the geospatial line, the geomorphological change is continuously measured along

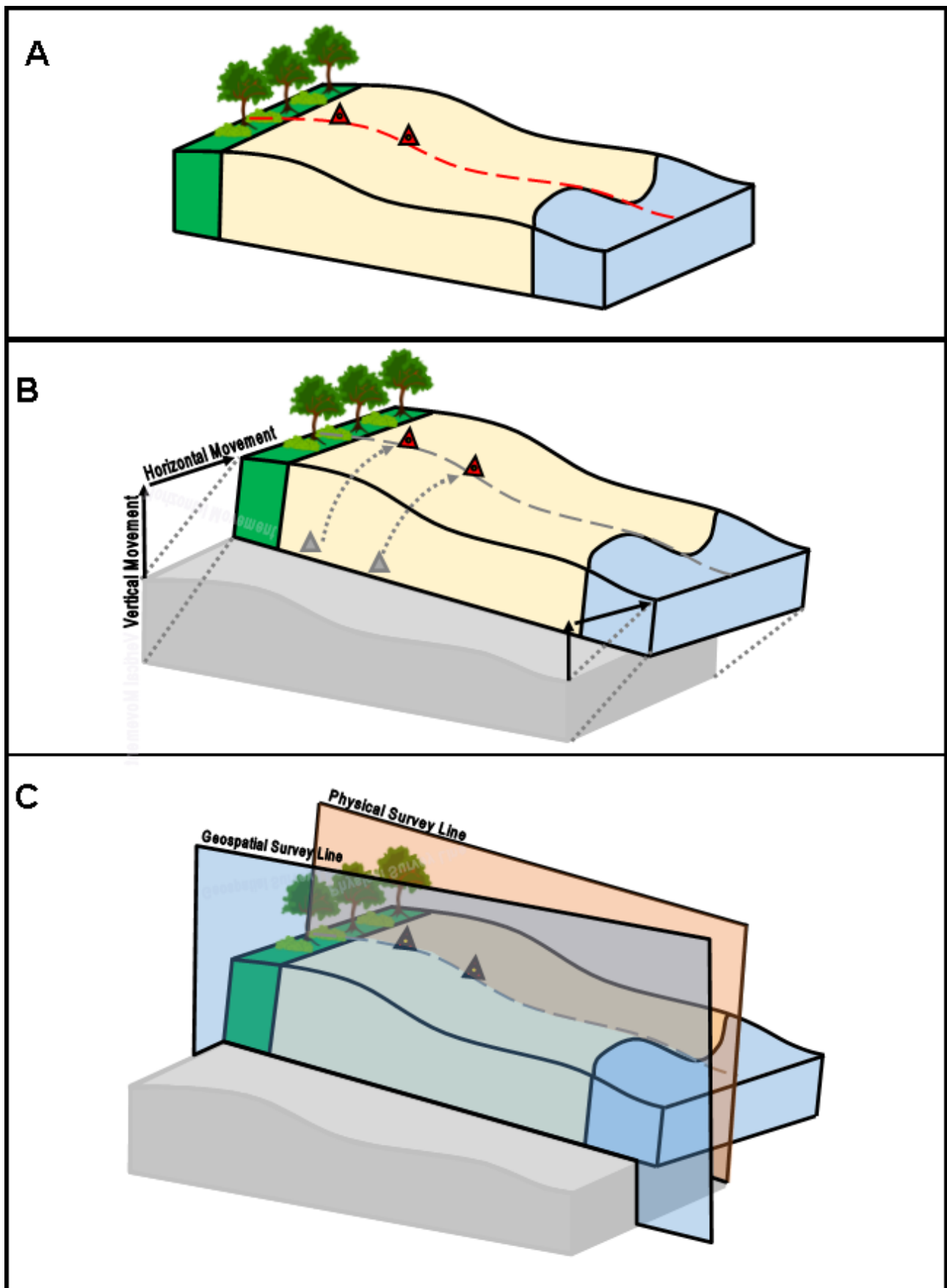


**Figure 4.7:** Sequence of diagrams showing the changing of survey planes following a major tectonic event. (A) Pre-earthquake survey line, which runs through two control points to the edge of the shoreline. (B) Uplift and horizontal translation moves the physical control points, which moves the physical survey line. (C) Two survey lines now exist following a large tectonic event. The geospatial line is the plane which is geospatially constant but is not physically marked in the field. The second plane is the physical survey plane which uses the physical control points, which acknowledges that the ground has moved but the same piece of ground is consistently being measured.

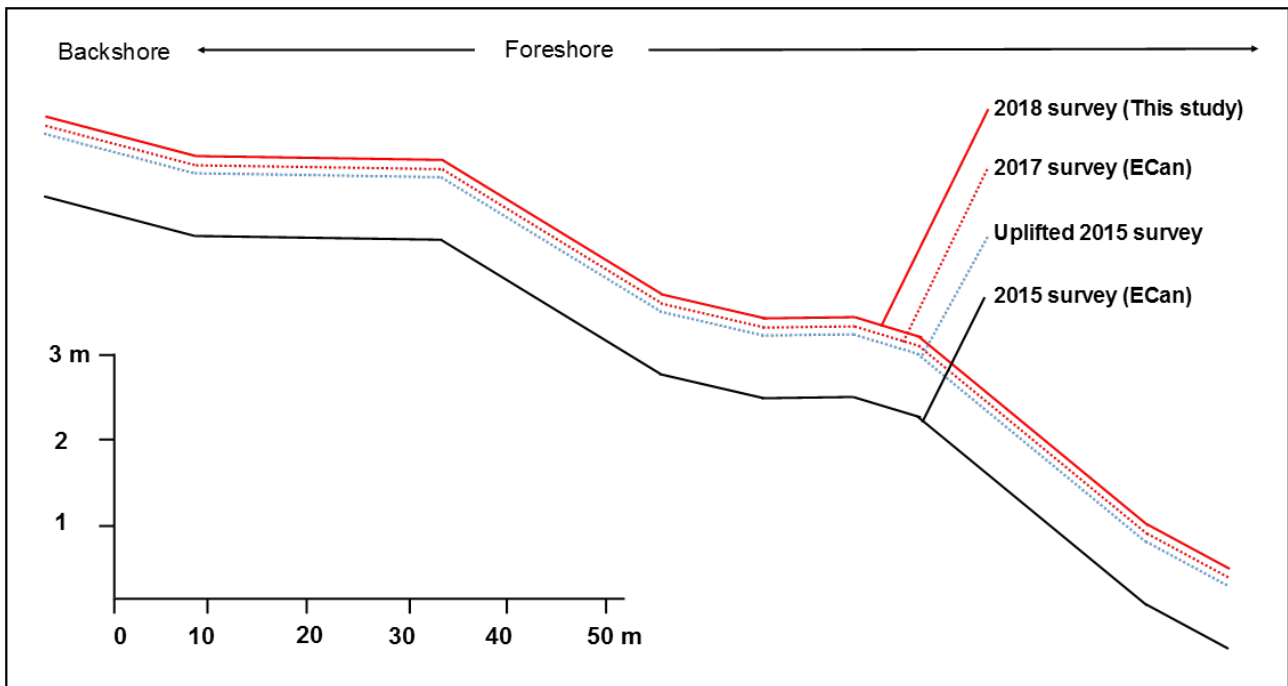


**Figure 4.8:** Four different profile lines are shown here on a simplified MSG beach profile, which are used for analysis in Chapter 7. The four lines are: pre-earthquake (2015), uplifted 2015 profile to represent an immediate uplifted profile after the earthquake, January 2017 survey profile, and September 2018 survey profile.

one plane, rather than switching to the physical plane which was adjusted by the earthquake. It is believed that the geomorphological change will be fairly represented along the geospatial plane, and this data collected can be compared to pre-earthquake profiles measured along this geospatial line also.

### Post-earthquake survey lines

There are three post-earthquake lines presented in the results section (or two survey lines when the profile was not resurveyed in 2017), as can be seen in Figure 4.8. In the January 2017 survey, KCK1870, KCK4220, KCK4700 and KCK5025 were not resurveyed. The three post-earthquake survey lines used in this study are:

1. Uplifted 2015 profile line
2. January 2017 Survey (collected by ECan)
3. September 2018 survey (collected in this study)

The following will detail the methods used to collect and process the data for each of these survey lines.

## **Uplifted 2015 profile line**

The uplifted 2015 profile line is representative of the beach profile immediately following the earthquake in November 2016. The the last survey taken before the earthquake (December 2015), was uplifted using to post-earthquake control point elevations, which were recalibrated to the January 2018 NDM update by ECan. When there was a 2017 survey of a profile, the 2015 survey was uplifted to the elevations of the control points for this profile. If there was no January 2017 survey, the 2015 profile was uplifted to the elevations of the control points taken in the September 2018 survey. The simulated uplift was applied to the 2015 profile in *Microsoft Excel* with the assumption that the land was uplifted uniformly across the whole profile. The rationale for this method is to simulate what the profile would have looked like immediately following uplift, in order for the potential short-term changes between the November 2016 earthquake and the January 2017 survey to be observed. The uplifted 2015 survey line must be analysed with caution, as there are limitations to this method, and multiple assumptions are made when using this data. Firstly, the uplifting of this profile assumes uniform uplift and no horizontal translation. It is known that there was horizontal translation following the earthquake, however data to translate the profile seaward/landward correctly is not currently available. The second assumption, is that the profile morphology remained the same from December 2015 until November 2016. For some profiles, this is a fair assumption, where only small changes were expected after analysing the long-term trend. For other profiles located on the open coast and ones near rivermouths, it is less likely that the profile experienced no changes in the 11 month period.

## **2017 Survey Data (Environment Canterbury)**

The 2017 survey was conducted by ECan in January 2017, just over two months after the main earthquake event. The survey was measured using a Trimble GPS system and the preliminary benchmark coordinates issued by LINZ shortly after the earthquake. ECan created their own control framework, by occupying several benchmarks for several hours at a time. The control framework was recalibrated in September 2018 by ECan to the January 2018 updated LINZ benchmark positions.

## **2018 Survey data collection**

Beach profile surveying was undertaken from the 19<sup>th</sup> of September to the 21<sup>st</sup> of September 2018. The 18 profiles are surveyed using the pre-earthquake coordinates for the control points

to measure the geospatially correct line. The beach profile surveys are retaken using GNSS surveying equipment, using LINZ benchmarks coordinates which were updated on January 2018. Base stations were set up over appropriate LINZ benchmarks which had been recorded as having been last maintained after the earthquake, and therefore had the most up to date coordinates following the earthquake. A repeater was used to increase the radio signal for an extra 10 km, for ease of not having to relocate the base station for surveys which were out of line of sight of the base station. The position of profiles, base stations and repeaters are shown in Figure 4.9. Profile lines and control points were loaded into the GNSS Trimble prior to surveying so the spatial points for the survey line and control points could be found in the field. The surveys were recorded using Real Time Kinematic (RTK) surveying, which recorded points measured within 2.3 cm. The profiles were surveyed as close to low tide as possible, but some profiles, due to time restrictions, were surveyed at high tide.

## 2018 Survey Data Processing

Survey data was extracted as a shapefile from the Trimble hand held unit and analysed in *ArcGIS*. The measuring tool was used to measure the distance between survey points, including the distance from the control point, in order to co-ordinate the same across-shore distance as the ECan profiles, as shown in Figure 4.10. Survey points were collected within 15 cm horizontally of the geospatial line in the field, and therefore parallel lines were created between survey points to maintain a consistent distance between points taken off the survey line. Data was extracted under the assumption that there were no significant elevation difference within 15 cm either side of the spatial survey line in the field. Across-shore distance and elevation were extracted from *ArcGIS*, and analysed in *Microsoft Excel*. The profiles plotted in *Microsoft Excel* were then analysed and parameters such as slope, volume, width and MSL contour were extracted using the same methods described in Appendix B. Data for the January 2017 survey was already processed by ECan, and the methods previously used to calculate profile statistics for the pre-earthquake data set were used to analyse the 2017 data set.

### 4.4.2 Sedimentology

Sediment sampling is a time consuming task for both collection and processing, however sedimentology data holds valuable information about sediment source and the amount of energy acting on a beachface. Sedimentology data was collected by ECan in 1997 at the upper fore-shore and the mid tide zone (locations of these points shown in Figure 4.3), and the data was processed using drying and sieving methods. A new technique was adopted for this study to





**Figure 4.9:** Location of base station set up and radio repeater set up over the 19<sup>th</sup> to 21<sup>st</sup> September 2018 fieldwork. Insets (left) shows the base station set up on the South Bay Wharf, and (right) the radio repeater set up at the northern end of Gooches Beach. Basemap sourced from the LINZ Data Service. Photo credit: K MacDonald.

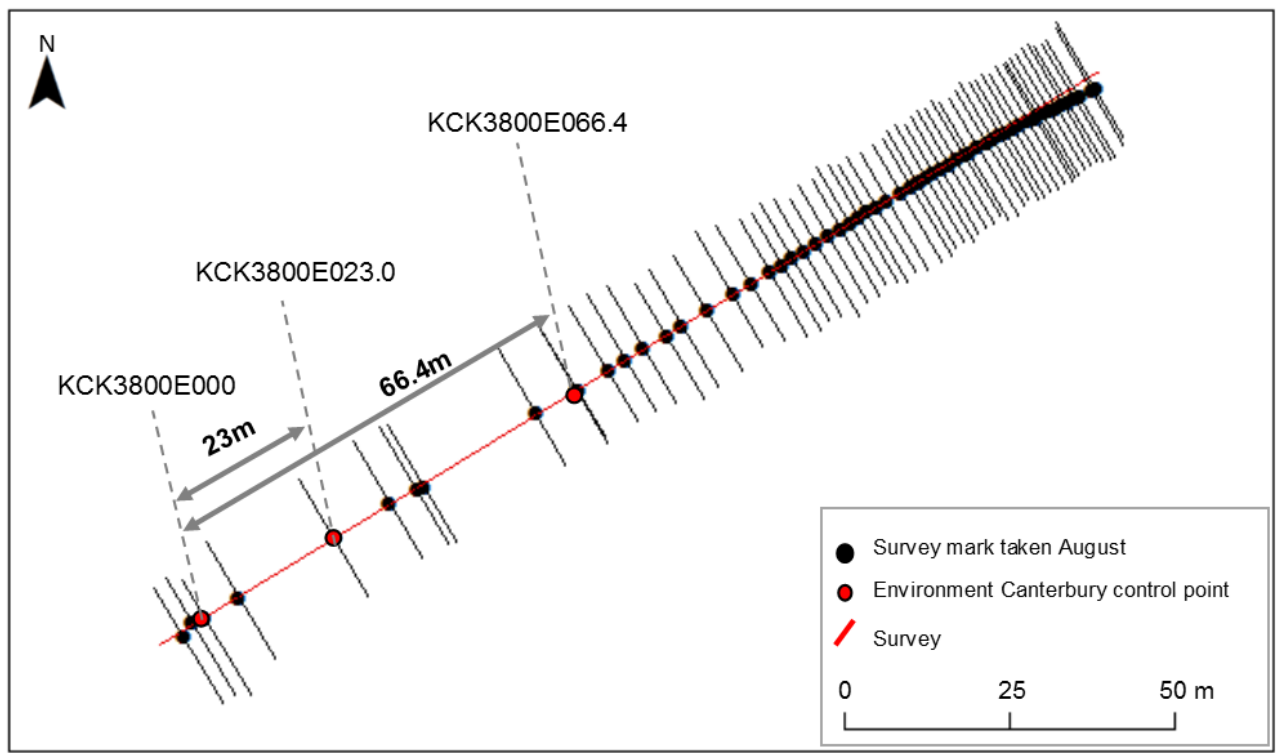


**Figure 4.10:** Annotated diagram of a screenshot of profile KCK3800 survey showing how the survey data was processed using *ArcGIS*. The geospatially correct location of the control points and known distance between control points meant that survey points collected along the geospatial plane could be comparable to 1997–2015 ECan surveys.

reduce collection and processing time. This method is known as Digital Grain Size (DGS) analysis, using the transferable wavelet method, as described in Buscombe (2013). DGS allows for researchers to use images of sediment to determine grain size distribution in a sample, as opposed to intrusive methods removing sediment from a site for analysis, while also reducing the time involved in collection and processing associated with this method. The transferable wavelet method used for this study is the most recent algorithm described in Buscombe (2013). This method takes a grey-scale (8-bit intensity) image, and analyses it based on energy fluctuations across the image, which can be representative of grain size. The algorithm identifies peaks and troughs of energy across the image, which is used to determine the location of individual grains, however does not measure individual grain sizes (Buscombe, 2013). The image of sediment is treated as a random field for analysis, similar to previous forms of this method (Buscombe et al., 2010; Buscombe and Rubin, 2012), however the Buscombe (2013) algorithm is better equipped for poorly sorted samples, and requires no calibration for different sediment types – consolidated, unconsolidated, sedimentary, and isotropic. Pentney and Dickson (2012) used version 2.2 of the DGS analysis software by Buscombe in a MSG beach field environment, and found that overall the version returned poor estimates of grain size distribution in MSG beach environments, but reasonable approximations of mean grain size. Pentney and Dickson



(2012) believed that taking multiple samples (50–100) would significantly improve the correlation between images and sieving results, but in doing so it would offset the time reduction benefit of this method in comparison to sieving methods.

## Data collection

Images of the sediment were collected at the same time as beach profile surveys were undertaken, from the 19<sup>th</sup> September to 21<sup>st</sup> September 2018. A hole for the camera lens and flash was cut in the top of a box 45 cm (w) x 30 cm (d) x 30 cm (h), and all images could be consistent in area and distance from the ground. Using a box meant that natural light was blocked out. A flash was used when taking the images, this gave a consistent light source for all of the sample images taken. Using a constant height and camera angle parallel to the ground surface meant that pixel to mm calibration was simple and consistent throughout samples.

As shown in Figure 4.11, the box was placed at the appropriate places along the beach profile (upper foreshore and mid tide zone), based on field observations as to where it was thought the storm berm was, and where the middle of the low and high tides were. Four images were taken at each profile, an image of the surface at both locations, and an image 10 cm deep. The purpose of this was to capture the differences in grainsize slightly deeper than the surface, as it was hypothesised that finer grains may have sunk deeper into the profile through the pore spaces created by the gravel on the MSG beach.

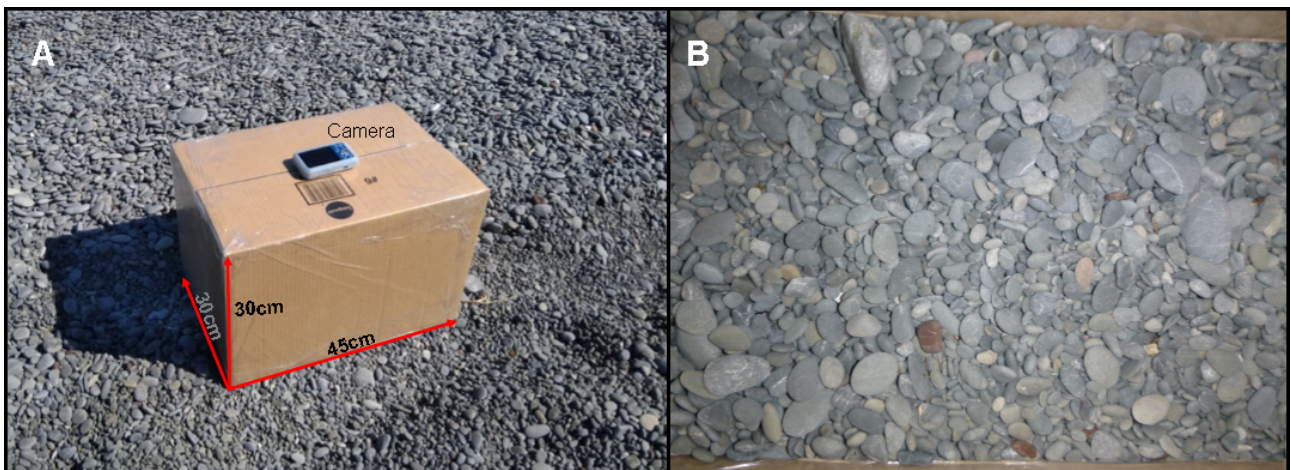


**Figure 4.11:** (A) Sediment sampling box in the field, showing dimensions and where the camera and flash is placed. (B) Example of a sediment sample image taken in the upper foreshore at profile KCK2510, showing that the box enables natural light to be excluded from the image, but the flash gives a consistent light source to the sample. Photo credit: K MacDonald.

## Data processing

The GUI for the algorithm described in Buscombe (2013) was obtained freely from <https://github.com/dbuscombe-usgs> and run in *MATLAB*. The algorithm is run through a user interface, where images are manually loaded in and settings can manually be adjusted as shown in Figure 4.12. Pixels per mm was calculated to calibrate the grain size statistics to be in mm and not pixels. For this study, the images were at a resolution of 12 pixels/mm. A region of interest (ROI) was applied to all images to ensure the outer image of the sediment sampler box is not included in the analysis. The filter and flatten options included in the user interface are used to improve the accuracy of the grainsize distribution (Buscombe, 2013), where the flatten function is used to subtract any linear trends, and the filter function is used to reduce noise (Prodger, 2017). These were tested, and did not create largely different results to a non-filtered/flattened image, therefore these filters were applied to each image. The statistical breakdown of the results was exported to *Microsoft Excel* for analysis using the save data function.

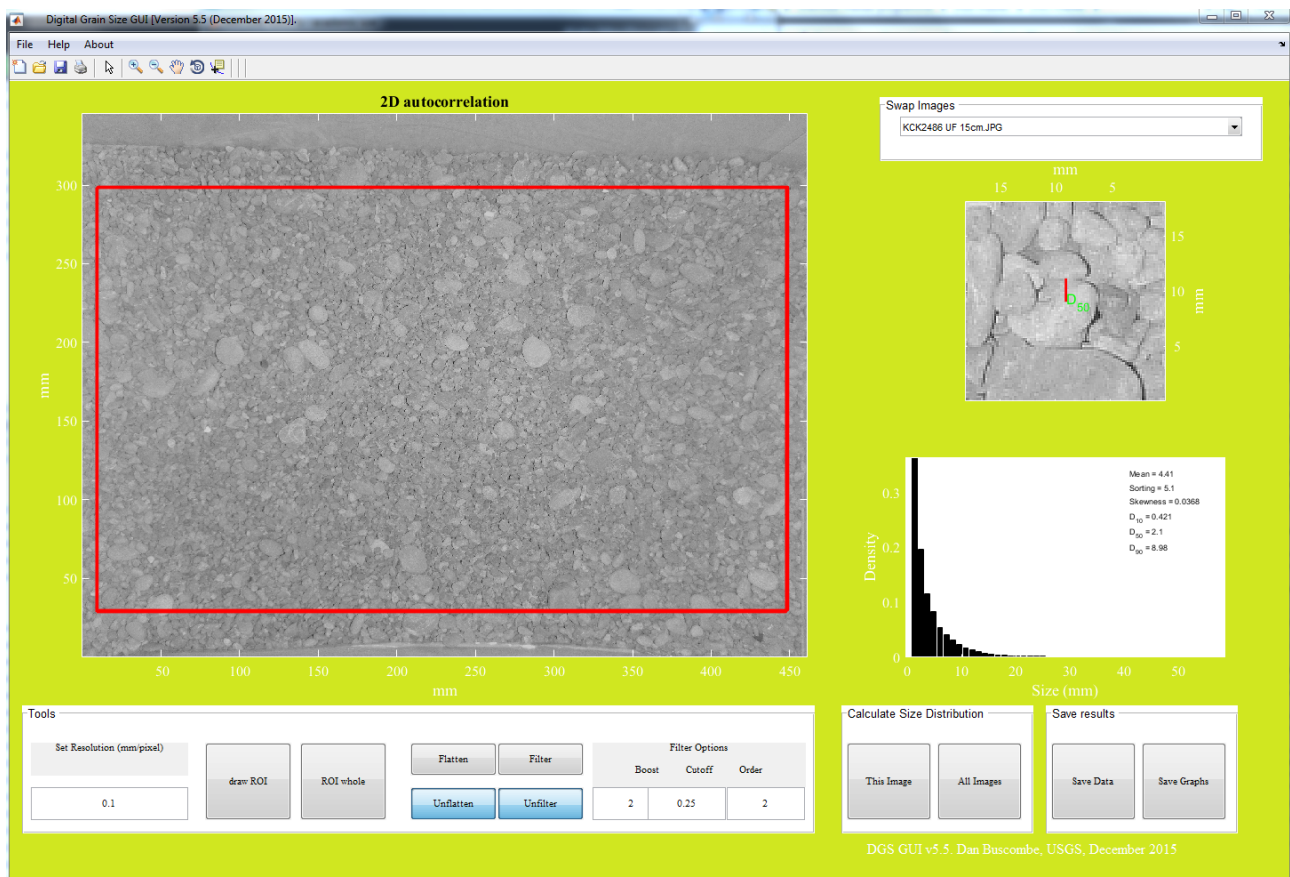


**Figure 4.12:** Screen capture of the DGS user interface, where images of sediment can be loaded into, a region of interest can be selected, filters can be applied, and a resolution can be set. Size distribution is then calculated, and a more extensive set of grainsize statistics is exported into *Microsoft Excel*.

The statistical breakdown gave both the arithmetic and the geometric means, sorting, skew and kurtosis; percent of sand, gravel and cobble in the sample; and the mm grain size at various percentiles. The graphic mean was calculated using the Folk and Ward (1957) equation:

$$M_z = \frac{\Phi_{16} + \Phi_{50} + \Phi_{84}}{3} \quad (4.1)$$

Grain size statistics calculated from this method were then compared to 1997 ECan sedimentology data to detect major changes across profiles over the 21 year period. Graphic mean and composition percentages were used to detect overall changes in the profiles.

# Chapter 5

## Kaikōura's Mixed Sand and Gravel Beaches

The following chapter presents results which contribute to achieving Objective 1: *To establish the pre-earthquake long-term trends of the unconsolidated coastal environments in Kaikōura, through the means of geomorphology and sedimentology.*

### 5.1 Introduction

Various beach classification schemes have been developed in past studies using key geomorphic parameters of a profile and environmental conditions acting on a site to classify different beach types, as shown in Table 5.1. Geomorphic parameters are considered to be dependent variables, which are the beaches physical characteristics that are influenced by environmental conditions. Environmental conditions are considered to be independent. They are processes which are variable both spatially and temporally, but influence basic coastal geomorphology (Wright and Thom, 1977). Variations of both geomorphic and environmental conditions are often used to classify different beach types.

Beach classification based on geomorphic parameters was first introduced by Wright and Thom (1977) with their broad morphodynamic approach to coastal depositional systems, highlighting the use of environmental conditions in determining the state of a coastline. Following this study, various physical classification schemes have been developed, with particular regard to classifying sand beach systems (Short, 1979; Wright and Short, 1984; Masselink and Short, 1993), using for the most part wave climates and sedimentology as key parameters to distinguish different

beach types. Coarse clastic beach classification schemes were developed alongside the timing of sand beach classification schemes, however held less of a focus in coastal science. Prior to the Jennings and Shulmeister (2002) study, coarse clastic beach classifications had been focused on sediment deprived gravel beaches in the northern hemisphere (Carter and Orford, 1988; Carter et al., 1990; Orford et al., 1996), of which they have very differing environmental processes acting on the sites than the study area at the focal point of this research, such as sediment supply (Jennings and Shulmeister, 2002). Jennings and Shulmeister (2002) was the first New Zealand specific coarse clastic beach classification scheme, and used primarily geomorphic parameters to determine the difference between pure gravel, composite and MSG beaches. A more recent study by Scott et al. (2011) used a combination of environmental conditions and geomorphic parameters to classify UK coarse clastic beaches through statistical analysis. A combination of methods from both Jennings and Shulmeister (2002) and Scott et al. (2011) are adapted for this study.

Jennings and Shulmeister (2002) suggest that coarse clastic beach types have within-type variations, and beaches will change within this spectrum following major events. These within-type variations of MSG beaches have not been acknowledged in literature, however field observations of the Kaikōura coastline indicate there is a spectrum of within-type variations of MSG beaches present within the study area. The parameters used in Jennings and Shulmeister (2002) only classified beaches down to the level of MSG, pure gravel and composite beach types, however the aim of this study is to further define the within-type variations of MSG beaches. If this study only selected the parameters from Jennings and Shulmeister (2002), it would only prove that the Kaikōura beaches in the study area are MSG beaches. There is no single set of parameters which will define a beach type. Often when singular parameters are analysed, as will be discussed in the subsequent sections, the expected range of the parameter will overlap with that of other beach types. It is therefore important to use a range of parameters in order to correctly classify beach types. Scott et al. (2011) most recent study used a combination of both geomorphic parameters and environmental conditions to create a gravel beach classification scheme. This Chapter aims to further classify the MSG beaches using a combination of geomorphic parameters listed in 5.1, then additionally synthesised the results using the various environmental conditions specific to the study area described in Chapter 3.

The following chapter presents research surrounding geomorphic parameters in gravel and sand beaches, with a specific focus on MSG beach types to determine how the parameters differ between beach types. These geomorphic parameters are then used to conduct a cluster analysis to identify and describe the within-type variations of MSG beaches on the Kaikōura coastline, of which the results are further synthesised by the calculated environmental conditions. Specific

methods for how these parameters were calculated can be found in Appendix B and C.

## 5.2 A review of geomorphic parameters

Geomorphic parameters are the dependent variables which measure the physical characteristics of the geomorphology of a beach. Various geomorphic parameters are used in this study to further define the within-type variations of MSG beaches. The following presents a review of literature of the geomorphic parameters used in this study, how they are used throughout previous classifications schemes, as well as what values are expected to be found at different beach types.

### Beach width

Beach width is not a common parameter distinctly used to classify beaches. It is acknowledged throughout literature, but is rarely used as a key parameter, mostly due to its correlation with other commonly used parameters such as beach slope (Scott et al., 2011). This parameter is highly variable across all beach types and environments. It is described in Wright and Short (1984) that dissipative (sandy) beaches are naturally much wider than reflective beaches, of which sand beaches can exist on a scale from a few metres to 1 km wide (Masselink and Kroon, 2009). Sand beaches have the ability to be very wide due to the low slope nature of a sand beach environment attributed to its small grain size. Jennings and Shulmeister (2002) found New Zealand pure gravel beaches to have widths from 18-50 m, while composite beaches can vary from <20 m to >60 m wide. MSG beaches typically range from 30 m to 200 m in width (Kirk, 1980; Shulmeister and Jennings, 2009). Beach width as a geomorphic parameter can not distinguish a beach type on its lonesome, due to the significant overlap of this parameter between gravel and sand beaches. Field observations in Kaikōura throughout this study noted that beach width was a dependent variable which was highly variable along the Kaikōura coastline, and therefore was used as a geomorphic parameter to further define these beaches within the MSG beach realm.

### Beach volume

Beach volume is calculated in this study as the amount of subaerial sediment beneath the active beach profile, above MSL. Various methods throughout literature are used to calculate the raw volume, but methods are also adopted as a proxy to identify changes in sediment volume. The

**Table 5.1:** Literature review of studies which have classified different beach types, and the parameters used in these study to classify the beach type and within-type variations.

| Source                          | Beach type classification scheme             | Key identified parameters   |
|---------------------------------|--|---|
| Bluck (1967)                    | Gravel Beaches<br>(High and low wave energy) | -Cross-shore sediment sorting<br>-Clast analysis<br>-Particle shape   |
| Short (1979)                    | Sand   | -Deep water and breaker wave height and period<br>-Wind direction and velocity<br>-Position and scale of all beach and surf zone forms<br>-Beach gradient<br>-Mean grain size |
| Wright and Short (1984)         | Micro-tidal sand beaches                     | -Surf zone morpho-dynamics<br>-Offshore surveying<br>-Beach surveying<br>-Sedimentology<br>-Nearshore dynamics<br>-Suspended sediment   |
| Caldwell and Williams (1985)    | Gravel beaches                               | Trigometric shape of beach profiles and berm location.  |
| Short (1991)                    | Macro-Meso tidal sand beaches                | -Wind and wave climate<br>-Beach forms<br>-Gradient<br>-Drainage patterns<br>-Sedimentology<br>-Beach length and scarping   |
| Masselink and Short (1993)      | Reflective dissipative sand beaches          | -Breaker height<br>-Wave period<br>-High tide sediment fall velocity<br>-Tide range   |
| Carter and Orford (1993)        | Gravel beaches                               | -Beach slope<br>-Crests<br>-Tidal zones   |
| Hegge et al. (1996)             | Sheltered beaches with low wave energy       | -Sedimentology<br>-Dimensions of geomorphic features<br>-Slope<br>-Curvature<br>-Wave and long shore wave climate   |
| Jennings and Shulmeister (2002) | Gravel beaches in New Zealand                | -Slope<br>-Sedimentology<br>-Wave climate<br>-Iribarren number<br>-Width  |
| Scott et al. (2011)             | Various beach types across England and Wales | -Wave climate<br>-Bar morphology<br>-Slope.   |

position of the MSL contour can be used as a proxy for volume change in equilibrium sand beach environments (Farris and List, 2007), however this proxy is not accurate for sand beaches with high seasonal (or storm/swell) variation (Quartel et al., 2008). No literature suggests using this as a proxy in a MSG beach environment, however it should be noted that this study found that MSL contour and volume mostly followed similar long-term trends and showed distinct spikes in sediment change in the subaerial environment at sites which were not very dynamic in nature. It could not confidently be used as a proxy in all MSG beach environments, as shown in Figure 5.1, where a very dynamic profile (KCK2200) underwent significant volume loss, but experienced shoreline progradation at the same time. Therefore both the MSL contours (or 1 m contour when necessary) and the raw sediment volume were calculated and analysed separately to identify long-term trends.

Literature surrounding beach volume in coastal science is often discussed as volume change. Volume as a raw value is not indicative of a beach type, however there is distinct variability in trends of volume change across different beach types. It must be acknowledged that volume change does not always indicate erosion or accretion, as often a change in volume is indicative of sediment redistribution across a profile, from the subaerial environment to the nearshore environment, and therefore the sediment still remains in the beach system. An example of this is a sandy beach response to a storm event by forming a bar in the nearshore in order to dissipate incoming wave energy, suppressing further onshore erosion (Sallenger Jr et al., 1985). Volume change in a MSG beach environment can also be indicative of redistribution of sediment (Single, 1985), however lots of energy is required to push gravel onshore once it travels seaward of the break point step. Once sediment is transported off the breakpoint step it is often lost from the system (Kirk, 1980).

MSG beaches are made up of coarse material which has the ability to absorb more wave energy, and therefore undergo a smaller amount of volume change in storm events when compared to sand beach response (Dingler, 1981). In previous literature, sand beaches are the focal point of beach volume analysis, with particular regard to storm response and the movement of the sediment across a beach profile into the nearshore. Changes in sediment volume on sandy, seasonally variant beaches have been recorded in the order of  $100 \text{ m}^3\text{m}^{-1}$  in response to a storm (Aubrey, 1979),  $50 \text{ m}^3\text{m}^{-1}$  variation over several months (Dubious, 1988), to  $19 \text{ m}^3\text{m}^{-1}$  change in the total volume of a sandy beach in a micro tidal environment over a season (Quartel et al., 2008). There is large variation when discussing the expected sediment volume changes in a sand beach environment, and the results are highly dependent on the scale of the event disturbing the beach profile. Literature surrounding MSG volume change in a beach has been more recently addressed by Brown (2017). Brown (2017) used *XBeach-G* to run different wave



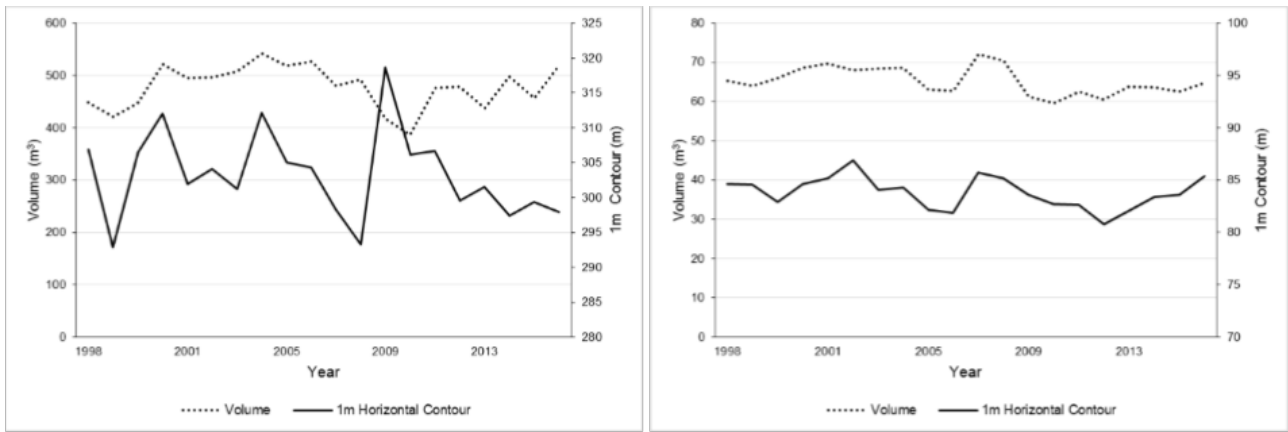


**Figure 5.1:** Volume and 1m horizontal contour changes over the 1997–2015 period for profile KCK2200 (left) and KCK3684 (right). The figures show that the 1m contour and the volume track very similarly at profiles which are less dynamic, however at profile KCK2200, the 1 m contour can vary significantly, while its volume is undergoes much less significant year to year changes.

heights against tectonically disturbed beaches, and found that volumes in an uplifted beach with various wave heights acting on it suffered subaerial volume loss, but sub aqueous volume gain. Under large waves, the subaerial beach profile was seen to erode  $50 \text{ m}^3\text{m}^{-1}$ .

OCEL Consultants NZ Ltd (2016) conducted a beach volume analysis of profiles located near the Kaikōura township to aid the consent application for renourishment by Kaikōura District Council. In the report, and matched by the results calculated in this study, over the 18 year analysis, the beach profiles considered to be erosional and require renourishment, had a net rate of change between  $-1.2 \text{ m}^3$  to  $+1.1 \text{ m}^3$  per year (inclusive of years where renourishment was undertaken), with year to year changes never reaching more than  $+/- 10 \text{ m}^3$ . This shows that MSG beaches only require small amounts of net change to be considered in an erosional state when compared to the previously discussed response of sand beach environments. The MSG beaches at the focus of the OCEL Consultants NZ Ltd (2016) research were also small in volume, and there for what would be considered to be a small loss of volume in a large sand beach environment, is relatively large in a narrow MSG high energy environment. Beach volume was used in this study as a raw value, as a geomorphic parameter to establish the size of the beach profile, and also to determine the long-term trend of the profile by assessing the beach volume change from year to year.

## Beach slope

Beach slope, aside from sedimentology, is the most common geomorphic parameter used in existing classification schemes. In previous literature it has been measured as a beach gradient across the whole beach width, or as a gradient for separate sections of the beach. The common

use of this parameter is likely due the information that can be drawn from beach slope, such as grain size, hydraulic conductivity and wave energy. In the Wright and Short (1984) model, wide dissipative beaches have low slopes, whereas narrow reflective beaches have steeper slopes. Sand beaches typically have flatter beach slopes than gravel beaches due to the relationship between beach slope and increasing grainsize in the foreshore (McLean and Kirk, 1969). Beach slope is also influenced by permeability of sediment in the foreshore and the wave energy acting on it (Bascom, 1951; Masselink and Li, 2001). Beach face slopes (measured from highest berm to low tide) of pure gravel beaches are found to be from 0.1–0.25, composite beaches slopes from 0.03–0.1, and MSG beaches are thought to be from 0.04–0.12 (Jennings and Shulmeister, 2002). Like beach width, this parameter overlaps between different beach types and therefore can not be used by itself to classify beaches, however the parameter is indicative of other information relating to the geomorphology of the profile.

### **Berm height**

Elevation of the storm berm was a key parameter employed in the Jennings and Shulmeister (2002) study which helped to distinguish gravel, MSG and composite beaches. The elevation of the storm berm varies between sites as a result of exposure to wave action, grain size, and beach slope (Hanslow et al., 2000). Berms are formed by deposition at the wave run-up limit, and the height of the wave runup is a result of wave conditions approaching the coast (Hunt, 1959). As noted by Hanslow et al. (2000), exposed beaches are expected to have higher average berms than protected beaches due to the higher wave runup. Steeper beaches have higher berm heights than flatter beaches, as steeper beaches tend to have a higher runup, and the coarser sediment has the ability to be piled up into a steeper angle of repose. Both the average heights of the berm and the storm berm were used in this study as a geomorphic parameter.

### **Long-term trend**

Long-term trend is not a common parameter used for classifying beach types, however it encompasses multiple environmental conditions, including the balance between sediment supply, transport and wave energy. Kirk (1980) stated that MSG beaches tend to occur on high energy coasts with a long-term erosional trend, while other studies have detailed coastlines which have variable long-term trends on MSG beaches (Berger, 2017; Carruth, 2017). High wave energy is a common setting where MSG beaches occur which may suggest that the coastline would be eroding in a high energy environment, however the long-term trend is also strongly effected by coarse sediment supply and its transport to the profile, and therefore long-term trend is site

dependent. While it is not a common parameter used throughout literature for beach classification, it was used in this study as an additional parameter to define further within-type variations of MSG beaches, as beaches which exhibited similar long-term trends were expected to have similar geomorphic properties as a result.

## **Sedimentology**

Various aspects of sedimentology, including particle shape, mean grain size and sorting, are identified throughout beach classification literature as a key parameter to use when distinguishing a beach type. Most studies listed in Table 5.1 use some form of sedimentology in their beach classification scheme. Mean grain size is the most widely used sedimentology measure (Masselink and Hughes, 2014). MSG beaches typically exhibit grain sizes between coarse sand and pebbles, whereas pure gravel beaches mainly comprise of pebble sized sediment (Jennings and Shulmeister, 2002). Sand beaches have sand sized sediment, however there can be variability of this from fine to coarse grained sand (Short, 1979, 1991). Sedimentology is the key parameter in beach classification, which on the broadest scale can be used solely to classify a beach type, however it is a dependent variable which is influenced by its environmental conditions, including wave climate and sediment supply. The parameter can be difficult to enforce in a MSG beach environment where sediment patterns across-shore are unknown, and extremely variable. It is difficult to get a sediment sample on a MSG beach which is representative of the whole profile.

Sorting of the beach sediment is influenced by wave energy, sediment supply and sediment size. In pure gravel and pure sand beaches, grain size decreases away from the sediment source and sorting increases (Sunamura and Horikawa, 1972), however the processes surrounding MSG beaches are thought to be more complicated (Pickrill and Mitchell, 1979). McLean (1970) found no strong trends suggesting sorting increased with distance away from rivermouths in Kaikōura. Dawe (2001) came to similar conclusions as McLean (1970), in which the sediment source for some beaches were relict deposits which existed from old sediment sources, as there was no direct relationship between sorting/grain size and distance from the river source in Kaikōura.

Sorting, particle shape and packing are all sedimentology parameters which play an important part in gravel beach geomorphology where the hydraulic conductivity heavily influences beach slope. Hydraulic conductivity is the ability for water to transmit through sediment. Buscombe and Masselink (2006) state that hydraulic conductivity is sensitive to grain size, the distribution of sediment on the surface, and the variation of sediment size with depth. In a pure

gravel environment, Buscombe and Masselink (2006) suggests that there is a linear relationship between hydraulic conductivity and mean grain size, however this relationship is different for mixed sized distributions which have poorer sorting (Horn, 2002). Sand beaches tend to have poorer hydraulic conductivity due to the small grain size and tight sediment packing, whereas gravel beaches have higher hydraulic conductivity (Horn et al., 2003).

### 5.3 Classification of Kaikōura MSG beaches

Using the geomorphic parameters described in Section 5.2, a cluster analysis was undertaken to determine whether there were distinct within-type geomorphic variations of the MSG beaches along the Kaikōura coastline. The cluster analysis showed that while there was a gradient of change between the groups, there are predominantly three main groups which represent the different within-type variations in the study area, as shown in Figure 5.2.

The three dominating groups are: (1) accretionary South Bay beaches; (2) wide and flat open coast and rivermouth beaches; and (3) steep and narrow beaches. The distribution of these groups shows a geographical trend in location, as seen in Figure 5.3, where Group 1 is located in South Bay, Group 2 is located on the open coast and near rivermouths, and Group 3 is predominantly located close to the Kaikōura Peninsula. The images, as shown in Figure 5.4, show that there is physical variability throughout all profiles, showing Group 1 profiles have developed berms, are steep, wide and have a lot of sediment. Group 2 appears to have a smaller grain size, and are significantly wider and flatter relative to the other groups. Group 3 profiles have less volume of sediment and are much smaller beaches than Group 1 and 2. Principal Component Analysis showed that volume, slope and beach width were the components which contained the most variability between the within-type variations. Sorting was shown to have the lowest variability in the data set, which is likely due to the MSG beach nature being poorly sorted, as it comprises of a wide range of sediment sizes, and therefore most profiles would share this characteristic.

MDS ordination, as shown in Figure 5.5, shows the 2D distribution of clusters for 6 of the 10 tested parameters. This analysis shows that Group 1 and Group 3 are tightly clustered with similar parameters measured, whereas Group 2 is more sparsely clustered, and there is more variability of individual parameters within the group than seen in the other two clusters. Group 2 consists of the outliers of the profiles analysed, as seen in both Figure 5.2 and 5.5, where profile KCK4200 and KCK4700 are distanced from the central cluster. While this cluster is sparse in distribution, it is grouped together due to its relative similarity in parameters when compared to other groupings, with particular regard to width, volume and slope. Between three groups

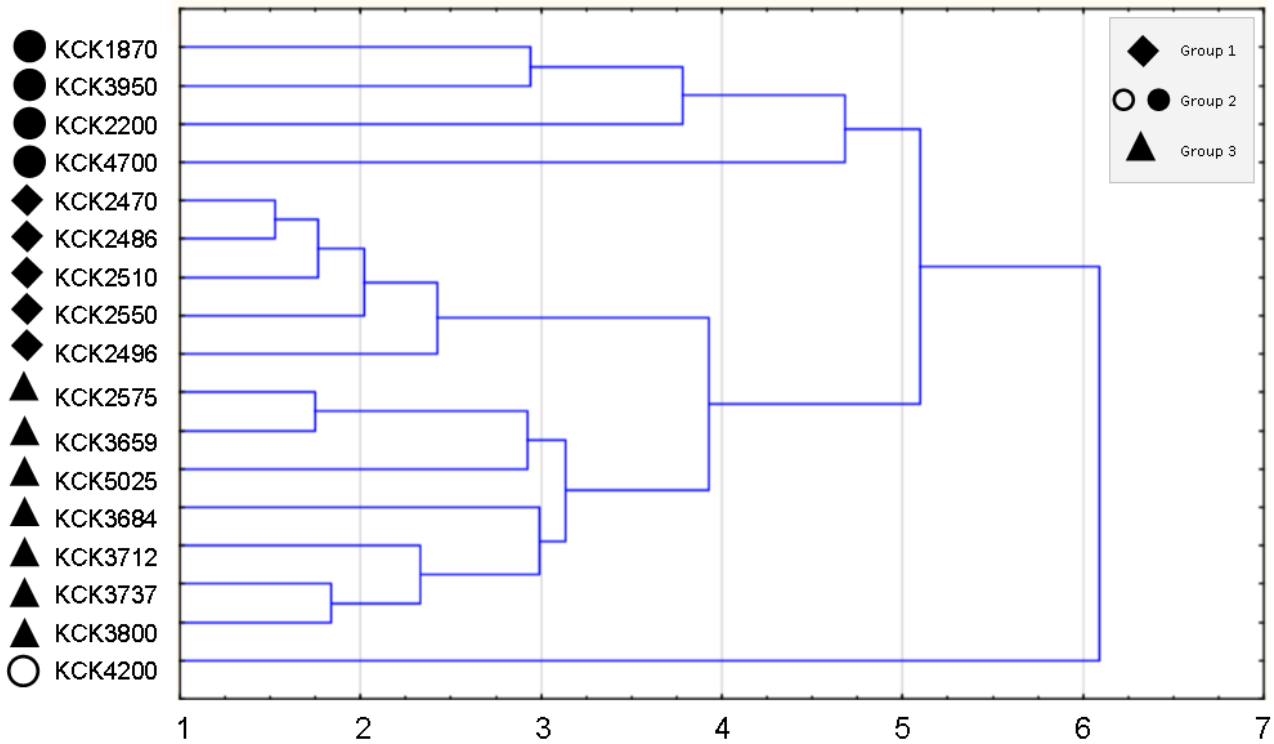


**Figure 5.2:** Results of Hierarchical Cluster analysis showing three main clusters, and profile KCK4200 as an outlier. Group 1 consists of profiles which are located in South Bay which have a strong accretionary trend. Group 2 profiles are predominantly located in open coast and rivermouth environments. Group 3 consists of profiles which are steep and narrow, and distributed widely throughout the study area.

identified, there are distinct characteristics which, while existing on a gradient of MSG beach characteristics, are distinctive enough to be considered a within-type variation. The following will describe each within-type variation of an MSG beach determined from the cluster analysis, well as how environmental factors discussed in Chapter 3 which also influence the profiles and can create further variations of the MSG beach state.

### 5.3.1 Group 1: Accretionary South Bay beaches

This category of beach has an active width range of 55 m to 100 m, and exhibit intermediate to steep profiles of 0.09 to 0.15. These beaches have strong accretionary trends, proven through continued subaerial volume increase and progradation of the MSL contour throughout the analysed period. These profiles have a wide range of mean clast size of granule ( $-1.76\Phi$ ) to small pebble ( $-3.74\Phi$ ) on their upper foreshore, and the material is all moderately (0.85) to well sorted (0.37). In the mid tide zone, the graphic mean clast size is granule ( $-1.5\Phi$ ) to small pebble ( $-3.25\Phi$ ), of which the material is moderately well sorted (0.59) to very well sorted (0.33) in this zone, of which the sorting promotes good permeability in the foreshore. Profiles in this group have high storm berm elevations (6 m) indicating moderate to high exposure to



**Figure 5.3:** Distribution of groups based on the cluster analysis using geomorphic parameters. The cluster analysis results showed that there were 3 main variations of MSG beaches found in the study area, and they are predominantly distributed in geographically similar areas with common environmental conditions acting on the profiles. Basemap sourced from the LINZ Data Service.





**Figure 5.4:** Images taken August 2018 of the three different beach groups: (Top) Group 1 accretionary South Bay beaches, taken at KCK2486 and KCK2550; (middle) Group 2 wide and flat open coast and rivermouth beaches, taken at KCK2200 by the Kowhai rivermouth and KCK4220 by the oxidation ponds; and (bottom) Group 3 steep and narrow beaches, taken at KCK3737 and KCK5025. Photo credit: K MacDonald

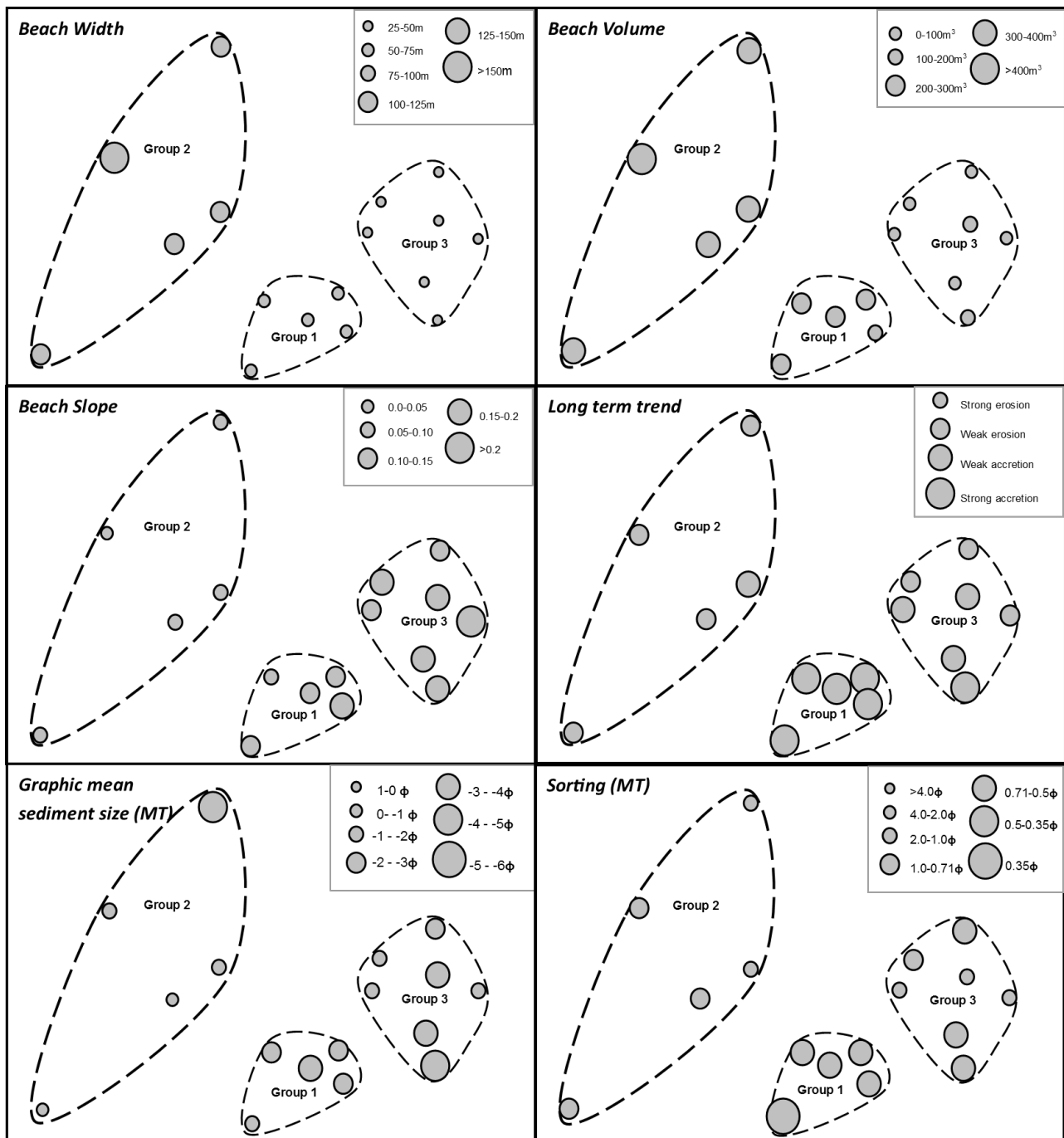


**Figure 5.5:** MSD ordinations of beach profiles from the similarities matrix, showing the variation of each parameter for each group, as per the scale at the top right of each graph. The dashed lines represent the grouping of profiles as per the MSD ordinations and hierarchical cluster analysis.



wave energy at these profiles. These profiles have variability in their berm elevations of 2.5 m to 4 m. All of these profiles are located in the South Bay area of the study area.

When considering environmental conditions acting on this group, no sub categories are required, as seen in Table 5.2. The profiles are located in South Bay, in which the Peninsula acts as a sediment trap, in which sediment is transported a short distance along shore from the Kahutara and the Kowhai Rivers, and build up in South Bay. Wave and wind climate conditions favour the accretionary trends at these profiles. The constant sediment supply has allowed these profiles to sustain a large volume of sediment over a long period. A prevailing wind direction from the south influences the alongshore transport in a north direction, using swash zone processes to transport gravel from the main rivers. Limestone rock shore platforms in the nearshore environment, especially east of profile KCK2550 shows that long shore transport ceases at this point, as the gravel can not transport itself in the swash zone around the miniature headland, and therefore builds up sediment. The nearshore limestone platforms may play a role in dissipating wave energy as it approaches the coast, and therefore minimising the effects of large wave events on these profiles.

### **5.3.2 Group 2: Wide and flat open coast and rivermouth beaches**

The cluster analysis created the sub group of wide and flat open coast and rivermouth beaches from the outliers of the profiles, of which the profiles were sparsely distributed in the 2D MDS ordination plot (Figure 5.5). This category of beach is very wide (100–165 m) and is very flat with low gradient slopes ( $<0.08$ ). These beaches have very dynamic trends overall. The MSL excursion data shows that these beaches prograde and transgress significant amounts from year to year, exhibiting cyclical behaviour with the recovery of lost subaerial sediment volumes often by the following annual survey. The graphic mean clast size of Group 2 profiles ranges from coarse sand ( $0.33\Phi$ ) to very small pebbles ( $-2.6\Phi$ ) in their upper foreshore, with most profiles in this area having poorly sorted (1.25) textures. In the mid tide zone, the graphic mean clast size ranges from very coarse sand ( $-0.4\Phi$ ) to medium pebble ( $-4.79\Phi$ ), in which the sorting in this zone is from poorly (1.52) to moderately sorted (0.81), which may promote less permeability in the foreshore. The storm berm elevations at these profiles are the same or higher than profiles described in Group 1 (5.5–7.5 m), meaning that these beaches are exposed to the same or higher amounts of wave energy. The exception to this is KCK2200, which storm berm elevation is 4 m, however this is likely related to the much larger width that this beach profile exhibits.

Based on environmental conditions acting on the sites, Group 2 profiles can be further divided

based on the distance to a sediment source, and the features at the profile, as seen in Table 5.2. Profile KCK2200 is located at the mouth of the Kowhai River, where it often has a Hapua lagoon outlet running through the bottom of the profile. This profile can therefore be grouped by itself, as its close proximity to the rivermouth offers an immediate sediment supply to the profile, and its responses to fluctuations in the outflow of the rivermouth. The remaining profiles in this group are still located closer to sediment supplies than other groups, but rely in long shore swash zone transport for sediment. The profiles in this group are all located at a distance from the Peninsula, and undergo more exposure to the high energy wave climate as they are not sheltered from north easterlies and southerlies to the extent profiles in Group 1 and 3 are. There are no limestone reef sections at these profiles, and therefore no dissipation of incoming wave energy, leaving the beaches exposed to large wave and storm events, and causing the large fluctuations in subaerial volume and shoreline extents.

### 5.3.3 Group 3: Steep and narrow beaches

This category of beach is narrow in width (30–60 m) and steep (0.11–0.20). These beaches have weak trends, both erosional and accretionary, except for profiles KCK3800 and KCK3855 which have strong accretionary trends similar to those in Group 1. The MSL excursion plots of these profiles show that they exhibit cyclical behaviour showing both accretion and erosion responses to previous years changes, but the MSL contour does not change position significantly from year to year as it does with the profiles from Group 2. There is a lot of variability in the mean clast size and sorting texture between the profiles in this group. The graphic mean clast size on the upper foreshore ranges from granule ( $-1.54\Phi$ ) to large pebble ( $-5.52\Phi$ ), and varies from poorly sorted (1.63) to well sorted (0.47). The mid tide zone also has variability, with its medium clast size ranging from granule ( $-1.39\Phi$ ) to medium pebble ( $-4.03\Phi$ ), and ranging from poorly sorted (1.09) to moderately well sorted (0.56). The storm berm elevations at these profiles are at or less than 5.5 m, and berm elevations are between 2.5–3 m.

Based on the environmental conditions acting on the profiles in this group, the group can be further divided into 4 subgroups, primarily based on the sediment source supplying the profile and how it is transported to the profile. As detailed in Table 5.2, this group is inclusive of many different environmental settings, where 3 out of 4 of these sub groupings are sediment starved. Profile KCK2575 is classed as a narrow and steep swash effected beach, as it is located too far around the Peninsula to trap sediment from the long shore drift which nourishes the Group 1 profiles, due to the minature headland and limestone platforms blocking swash zone processes being able to transport gravel to this profile. This profile has good sheltering from

**Table 5.2:** A summary of the environmental conditions measured and acting on the different beach groups. This shows the break down of the three main within-type variations, describing the contributing factors to their geomorphic states. Within-type variations can be sub-categorised again based on environmental conditions, and refining groups based on their geographic distribution within the study area.

| Geomorphic Group | Environmental Sub Category | Sites   | Description   | Hinterland   | Sediment supply                               | Sediment transport  | Sheltering from Southerlies and North Easterlies  | Distance to natural sediment source | Distance from central peninsula |
|------------------|----------------------------|---------|---|--|---|---|---|-------------------------------------|---------------------------------|
| Group 1          | 1A                         | KCK2470 | Intertidal, accretionary beaches which trap sediment coming from longshore drift processes. Located in South Bay with favourable environmental parameters.  | Fluvial plain/<br>Fluvial plain with urban development | Rivers and creeks<br>(Two main rivers)        | Sediment transport from main current direction, and predominant wind direction, southern side of peninsula traps sediment | Exposed to southerlies, protected from north easterlies   | 2500 - 3460m                        | 5640 – 6410m                    |
|                  |                            | KCK2486 |   |  |   |   |   |                                     |                                 |
|                  |                            | KCK2496 |   |  |   |   |   |                                     |                                 |
|                  |                            | KCK2510 |   |  |   |   |   |                                     |                                 |
|                  |                            | KCK2550 |   |  |   |   |   |                                     |                                 |
| Group 2          | 2A                         | KCK1870 | Wide and flat beaches which have long term very dynamic trends with the ability to erode and accrete significant amounts. Located closer to sediment sources than other sites on corresponding side of peninsula.   | Fluvial plain and Urban development on fluvial plain   | Rivers and creeks<br>(One or two main rivers) | Long shore transport with currents and swells, and some wave refraction   | Exposure to both north easterlies and southerlies, some protection depending on location around peninsula | 700 to 8980m                        | 7625-15245m                     |
|                  |                            | KCK3950 |   |  |   |   |   |                                     |                                 |
|                  |                            | KCK4220 |   |  |   |   |   |                                     |                                 |
|                  |                            | KCK4700 |   |  |   |   |   |                                     |                                 |
|                  |                            | KCK2200 |   |  |   |   |   |                                     |                                 |
| Group 3          | 2B                         | KCK2575 | Narrow and steep, stable beaches which is located close to a sediment source but nearshore swash processes affect the distribution of sediment to this site.  | Limestone/mudstone peninsula                           | Rivers and creeks<br>(Two main rivers)        | Longshore transport and swash processes   | Sheltered from north easterlies, exposed to southerlies   | 4260m                               | 4920m                           |
|                  |                            | KCK3659 |   |  |   |   |   |                                     |                                 |
|                  | 3A                         | KCK3684 | Narrow and steep beaches with a naturally eroding trend, however have been renourished to maintain a more stable trend. Sediment from the main source does not reach these sites due to being too distant from the source.  | Limestone/mudstone peninsula                           | Renourishment                                 | No natural sediment supply reaching these sites   | Exposed to north easterlies, sheltered from southerlies   | 11640 to 11025m                     | 4880-5635m                      |
|                  |                            | KCK3712 |   |  |   |   |   |                                     |                                 |
|                  |                            | KCK3737 |   |  |   |   |   |                                     |                                 |
|                  | 3B                         | KCK3800 | Strong accretionary trend beaches where sediment is supplied from a distant sediment source, transported by prevailing wind direction and wave refraction. Beach widths and volumes larger than 3B.   | Fluvial Plain  | Rivers and creeks<br>(One main river)         | Sediment supply from Longshore drift caused by wave refraction and prevailing wind, weaker transport                      | Exposed to north easterlies, protected from southerlies.  | 9750- 10375m                        | 6235-6850m                      |
|                  |                            | KCK3855 |   |  |   |   |   |                                     |                                 |
|                  | 3C                         | KCK5025 | Narrow and steep beaches with a long term steady erosional trend. Located close to a sediment source but surrounding environmental conditions such as eddying from wave refraction and prevailing wind direction do not favour sediment transport north from the river. | Fluvial plain  | Rivers and creeks<br>(One main river)         | Long shore transport (with swell direction)   | Exposed to north easterlies, some sheltering from southerlies   | 1840m                               | 18450m                          |
|                  |                            |         |   |  |   |   |   |                                     |                                 |
|                  |                            |         |   |  |   |   |   |                                     |                                 |

north easterlies which impact the profiles located north of the Peninsula. Profiles KCK3659 to KCK3737 have long-term erosional trends, and significant amounts of sediment have been used to artificially renourish these profiles in the past in order to stabilise them. These profiles are located close to the Peninsula along the Esplanade, and therefore are very distant from the main sediment source of the Peninsula (From the Hāpuku River). A small headland by the Lyell Creek, paired with the distal sediment source, is likely to be the cause of sediment starvation at these profiles. Sub-groups 3A and 3B are similar in that barriers interrupt swashzone sediment transport, through geographically these two sub-groups differ. Profiles KCK3800 and KCK3855, located near the I-site and the Railway station, are geomorphically most similar to Group 3 profiles, however a big difference between these profiles from the rest of the Group 3 profiles is its strong accretionary trends, similar to Group 1 profiles. The profiles are located just north of the Lyell Creek, which is likely the extent of sediment transport south from the Hāpuku River, highly influenced by wave refraction around the Kaikōura Peninsula. These two profiles are the only Group 3 profiles which have a constant sediment supply. KCK5025 is categorised as being a narrow and steep eroding beach, as it is the only profile out of the four in this group that is strongly eroding. It is not known whether the profile is not supplied with enough sediment as majority of sediment moves south from the Hāpuku River, or if the small bay just north of the profile is a sheltered area in which the sediment is settling and moving past profile KCK5025 where the profile is quite exposed to wave energy.

## 5.4 Conclusions

This chapter comprises a unique review of beach classification techniques and literature from the perspective of usefulness in MSG beach analysis, as the basis for developing a classification scheme to determine the different within-type variations of MSG beaches there are in the Kaikōura study area. The results of this analysis showed that there are three main geomorphic groups which exist as within-type variations, of which within the three groups, there are smaller clusters which exist due to the different environmental conditions acting on each profile. Profiles south of the Peninsula have more favourable wind and wave climate conditions for transporting sediment, as well as two large river systems supplying sediment. Profiles north of the Peninsula are supplied with sediment from one main source, which is double the distance away from profiles than those located south of the Peninsula. Wave refraction helps transport some sediment to profiles north of the Peninsula, however profiles south of the Hāpuku River are dependent on the prevailing NE wind direction to drive a southward swell direction to transport river from the sediment. Swash zone processes which transport gravel alongshore proves

to be a main factor in which determines sediment starvation at a profile, in which profiles in Group 3 (KCK2575–KCK3737) are affected due to sediment not being able to be transported to the profiles by swash zone processes, and therefore exhibit weak erosional trends. Sediment supply to a profile was apparent in being a strong driver in long-term trends at a profile, and consequently had an affect on its within-type classification. A later chapter will discuss the implications of this finding in the context of a post-earthquake environment.

# Chapter 6

## Surveying in a Post-Earthquake Environment

The following chapter presents results which contribute to achieving Objective 2: *To evaluate post-earthquake surveying techniques and the data captured through the use of different methods.*

### 6.1 Introduction

The use of data acquired from UAV's and satellites is favourable in a post-earthquake environment because it does not require the restoration of the geodetic system, and it does not require people to enter the affected area (unless using a remote aircraft such as a drone). Captured LiDAR data to generate digital elevation models (DEM) and aerial imagery can be a quick way to determine areas of significant change following an event (Singh et al., 2002; Duffy et al., 2013; Xu et al., 2014). Surveying on the ground using GNSS equipment is a technique used to determine more detailed post-earthquake changes, especially for cadastral surveying and monitoring geomorphic changes (Morton et al., 1993). For the purpose of this study, to further understand the response of a MSG beach following an earthquake, a high level of detail is required. This chapter will explore and critique three commonly used surveying techniques: (1) GNSS beach profile surveying; (2) DEM differential maps generated from LiDAR data; and (3) Historical shoreline analysis using aerial imagery. The data extracted using these three techniques will be examined for its usefulness in informing the response of MSG beaches after an earthquake. The methods used for the results presented in this chapter are described in Chapter 4.

## 6.2 Results

This section will detail the data which can be extracted from three popular surveying techniques, the level of accuracy involved in the technique and the data resolution which could inform the conceptual response model of MSG beaches.

### 6.2.1 Beach profile surveying

Beach profile surveying is a prominent and common technique used to infer long-term trends of a coastline, as well as to inform coastal management decisions and engineering applications in a coastal area (Morton et al., 1993). GNSS beach profile surveying is a high accuracy and resolution technique used to continuously monitor beach profiles over a long period of time, in which can track both beach shape, volume and shoreline trends across a period. The data collected using this technique is of a high enough resolution to show long-term trends over a long time period and inform a conceptual response model. Aerial imagery and LiDAR can be used to compliment beach profile surveying, however will never be able to compete with the small margin of errors involved with the surveying equipment used (2 cm for GNSS survey equipment used, 15–25 cm for LiDAR DEM). As previously mentioned in Chapter 4, the downfall of using GNSS survey equipment in a post-earthquake environment is that it is most commonly used with the geodetic system. Following an earthquake, the geodetic system is warped and needs to be re-established, which can take months to years after the event to be done accurately (Winefield et al., 2010).

Beach profile surveying has the ability to collect a point at each change in slope, as per the judgment of the operator. This can mean that clear and easily accessible areas, such as an open beach environment, change be accurately surveyed. As shown in Figure 6.1, profile KCK3855 has very small berms that can be measured in great detail, and from this, changes in volume and foreshore extents can also be derived in comparison to previous years records. Beach profile surveying is the only method in which beach shape change can be analysed with accuracy and great detail. In Figure 6.1, the uplift of the 2015 profile could simulate what the profile would look like immediately following the earthquake, and therefore could help inform movement of sediment in the across-shore environment following the earthquake, and whether there was progradation and/or volume gain beyond the initial uplift. The post-earthquake red lines in Figure 6.1 show that after the earthquake there was progradation of the shoreline and a berm re-established at an elevation similar to the berm in the 2015 profile. These results, when validated through various other beach profile responses, can be used to inform a conceptual model. As

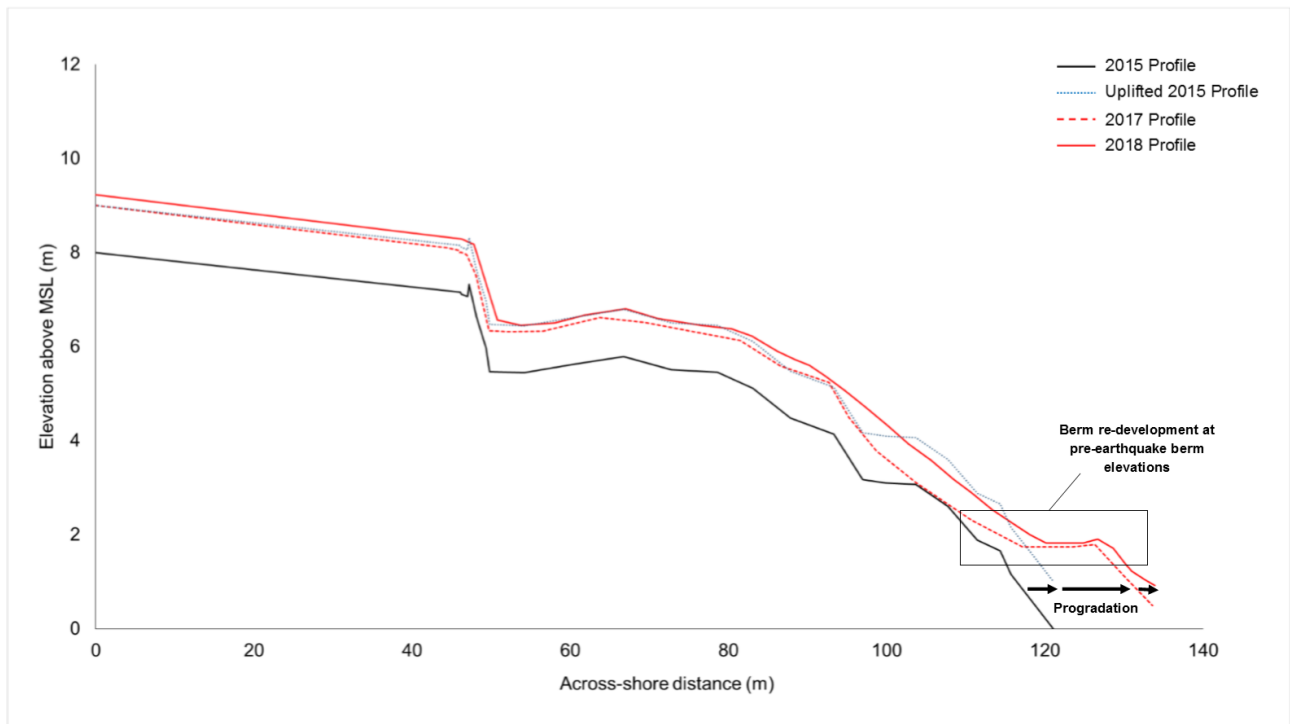


**Figure 6.1:** Beach profile survey collected using GNSS surveying equipment at profile KCK3855 near the railway station. The four different lines represent different time periods: 2015, immediately after the earthquake, January 2017, and September 2018.

the beach profile represents only a small portion of the coastline, multiple profiles need to be monitored and compared in order to be able to establish an idea of what is happening in the coastal environment as a whole, and the small detailed profile responses need to be validated by other within-type profiles to ensure the response is common and not a result of the small section being monitored.

### 6.2.2 Digital Elevation Model

LiDAR data can be used to develop a DEM, and a differential DEM can be developed by subtracting the 2012 DEM from the 2018 DEM (Figure 4.4) to determine the elevation changes after an event over a large area. It is an attractive surveying technique in a post-earthquake environment for many reasons, including spatial coverage, it can operate independently of the geodetic system, and it has a quick processing time (Hart et al., 2015; Clark et al., 2017). It requires no on ground contact, minimising risk to people entering a tectonically active area. It also requires no adjustment of the geodetic system, and therefore is a reliable source of data to determine change from immediately after an earthquake. Depending on the scale of the area being surveyed, data collection can be costly, though processing the data can be done at low cost. After the 2016 Kaikōura Earthquake, LiDAR data was collected immediately after the



earthquake to help inform recovery efforts, by determining where landslides had fallen blocking main transport routes such as SH1, and where train tracks had been displaced. The 1 m resolution LiDAR is appropriate for measuring landslides which have displaced thousands of tonnes of sediment. The 1 m resolution LiDAR is not sufficient for accurately determining changes on a scale less than 1 m, such as small berm changes on a beach. An issue with using LiDAR is due to the costs involved, as there is usually an event which prompts the collection of this data, and therefore it is not frequently collected as is done with the GNSS beach profile surveying. This also means that the changes in the coastal environment, due to the 6 year time gap between the LiDAR data used in this study, can be attributed to the earthquake, and therefore red areas (in Figure 6.2) are deemed to have eroded/subsided and therefore there is a decrease in sediment volume, while green areas have accreted/uplifted, and therefore there is an increase in sediment volume over the analysed period.

The differential DEM, shown in Figure 6.2, details that areas close to rivermouths have undergone an increase in subaerial sediment between 2012 and 2018, and shows sediment build up at land features which interrupt swash zone sediment transport. This is seen in Figure 6.2, where profiles KCK3800 and KCK3855 have undergone elevation changes of over 1 m in their coastal environment, and profiles located south of the Lyell Creek mouth, where there is a feature interrupting sediment swash zone transport, show patches of erosion and/or subsidence in the foreshore along the Esplanade at profiles KCK3737 and KCK3712. This same trend is apparent in the right image of Figure 6.2, where profiles in South Bay are collecting sediment, and a seaward extended features stops sediment from reaching KCK2575 through long shore transport in the swash zone, creating an different trend to the Group 1 accretionary South Bay beaches. When the differential DEM is compared to the elevation and beach shape change derived from beach profile survey data, the results are very similar. The DEM shows erosion/subsidence in the upper foreshore of profiles along the Esplanade (Figure 6.2), in which the beach profile data can confirm that this is erosion.

Cross sections can be extracted from a DEM to replicate a beach profile survey. Figure 6.3 shows a 2018 GNSS beach profile survey at KCK3684 compared to the cross section extracted from the DEM along the same geospatial survey line. Cross sections extracted from DEM's can be used in place of a beach profile survey, however features smaller than 1 m can not be as accurately depicted using this method as in GNSS beach profile surveying. Figure 6.3 shows the errors involved in extracting cross sections from a DEM are much larger than the GNSS beach profile survey. The extracted profile uses more points (every 1 m) to create the profile than the profile generated using GNSS equipment, and therefore it may generate some small berm like features which are not indicative of the real profile, and are just caused by error, or the method

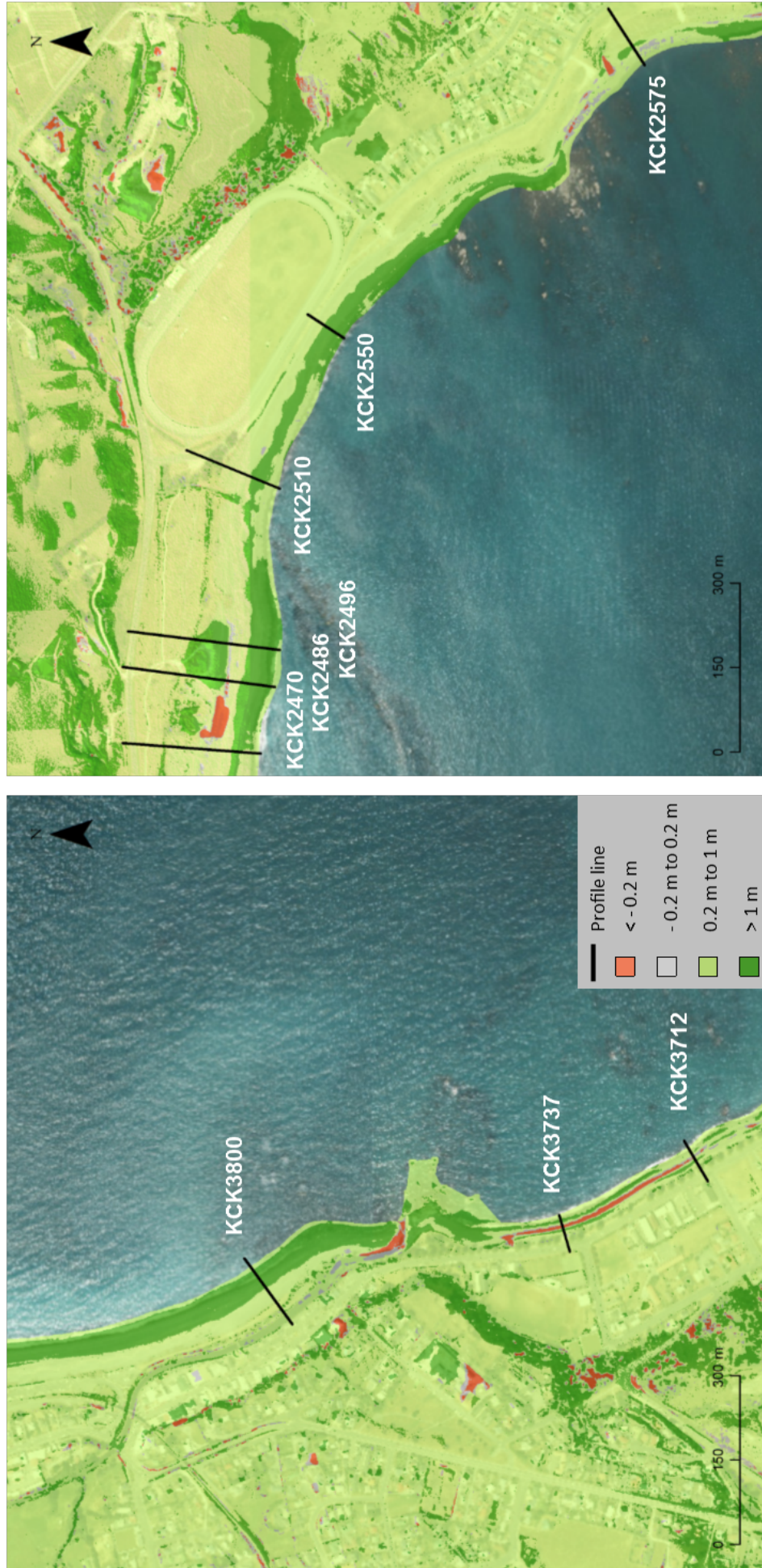


**Figure 6.2:** Two differential DEM's showing the difference in elevation from 2012 to 2018 by the Kaikōura township (left) and the South Bay area (right). Green indicates uplift/accretion of sediment on the beach over the 4 year period, and red represents the subsidence/erosion. Grey represents the error margin of 1 m resolution LiDAR which is 0.15-0.25 m. Light green represents what may be considered as a direct result of the uplift as over these two areas, they were uplifted approximately 1 m. Beyond the 1 m uplift (dark green) may be a result of accretion, human modification or translation of land in steep areas.

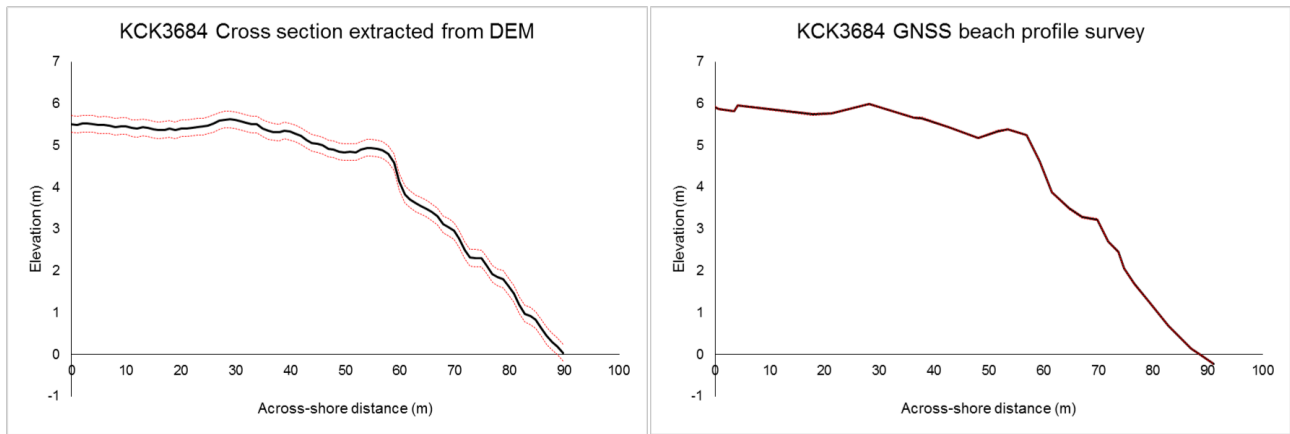


**Figure 6.3:** Profiles from profile KCK3684 extracted from the 2018 DEM using the 3D analyst tool in *ArcGIS* (left) and beach profile survey collected using GNSS surveying equipment (right). The raw data is represented with a black solid line. Red dotted lines account for the error in the technique, where DEM will have a 0.2 m (0.15 to 0.25 m) vertical accuracy, and GNSS beach profile surveys will have 0.02 m vertical accuracy.

may miss small berms all together. Generally the cross sections extracted from DEM's can be used to generate reasonably accurate volumes and shoreline changes, however the accuracy and detail required for depicting changes in beach shape is not obtainable from DEM's.

### 6.2.3 Aerial imagery

Aerial imagery is used to determine the historical shoreline change by measuring consistent morphological features on a coastline and tracking its migration over time. Aerial imagery is available for well populated areas over a historical time scale (dating back to the 1930's), however is less often captured in rural areas, such as Kaikōura, where the historical record is much smaller than the nearby city of Christchurch. The use of aerial imagery to determine shoreline change is a particularly common technique used in sand beach environments where morphological features such as dune toes can be easily identified and are representative of changes in the shoreline. MSG beaches are much steeper environments than sand beaches, and typically do not harbour as easily identifiable features. The steep nature of the beaches also means that shoreline changes may be large in terms of removing volumes of sediment from the shoreline, but these changes may not be as obvious in aerial imagery.

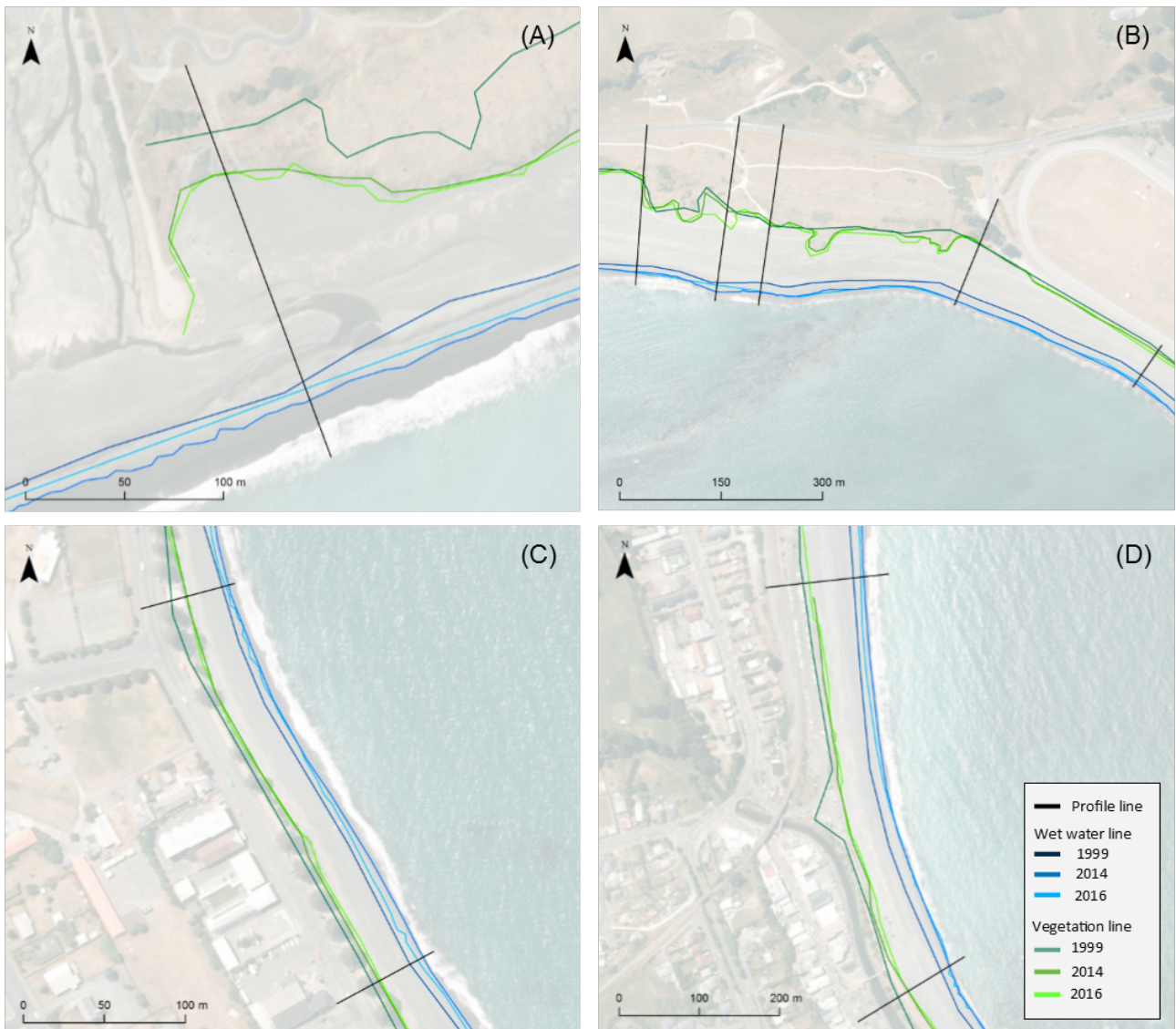
The results of the shoreline analysis showed that there was generally a progradational trend along the coastline between 1999 and 2014, in which the extent of the wet water line and the vegetation line moved seaward, as seen in Figure 6.4. Profiles were deemed to have undergone significant change when the measured change between two images was more than the calculated MOE (Section 4.3.2). When these year to year changes were compared to the calculated margin of error, 50% of profiles were considered to have changed significantly between 1999 and 2014.

Figure 6.4, shows that the shoreline retreated between 2014 and 2016 following the earthquake when it is taken at face value. Between 2014 and 2016, only 2 profiles (KCK1870 and KCK2486) underwent what would be considered as significant change along the shoreline, of which these significant changes were transgressive following the earthquake, not the progradation from instantaneous uplift, expected from literature (Stanley, 1968; Paterson, 2000; Brown, 2017). Profiles along the Esplanade showed shoreline retreat following the earthquake (Figure 6.4C), as is the same with profiles KCK2200 (Figure 6.4A), and KCK3800 and KCK3855 (Figure 6.4D). Profiles in South Bay looked to have maintained similar wet water line extents between 2012 and 2016 (Figure 6.4B). All of these profiles, except for KCK2486 (Figure 6.4B), were deemed as having undergone change which was not significant as it not exceed its calculated MOE.

The vegetation line was analysed to see if the movement was relative to the shoreline change, and could be indicative of progradation or transgression along the coast. There was not a consistent relationship along the coast between vegetation line change and wet water line change, as demonstrated in Figure 6.4 where vegetation line change was significant at profile KCK2200 (A), while the wet water line changes were much smaller. As described in Section 4.3.2, landward of the vegetation line on a MSG beach contains species that are more representative of a hinterland zone, rather than a defined beach zone as seen on a sand beach environment. Some profiles also have heavily maintained and developed backshores, where the migration of vegetation would not be indicative of shoreline development, as it is significantly impacted by humans. For example, profiles located at the Esplanade 6.4 have heavily maintained backshores where there are picnic areas and a skate park along the immediate backshore, and therefore there would be no expected relationship between changes in vegetation line and wet water line due to the human modification present in the area. This trend dominates the study area, as most profiles are backed by some form of maintained infrastructure such as roads, parks, and buildings. For profiles which were not backed by hard structures or had maintained backshores, there was a general progradational trend from 1999 to 2016.

The results in the aerial imagery shoreline analysis show that vegetation is a feature which could be used to reflect the correct progradational trend in the coastline south of the Peninsula, however it can not accurately represent change when it is constricted in its backshore environment and therefore is not indicative of changes in the active beach. The changes in the vegetation line also have only represented a trend, and distance in which the shoreline has prograded over this time could not be accurately determined numerically. The results of the wet water line do not reflect the changes seen in the beach profile survey data and discussed in previous literature due to the large MOE involved when taking into account tidal cycles and consideration of wave





**Figure 6.4:** Four different areas of shoreline analysis using aerial photography are shown here. (A) KCK2200; (B) KCK2470 to KCK2550; (C) KCK3712 and KCK3737; and (D) KCK3800 and KCK3855. Each image has 6 lines present, 3 representing the wet water line extent for 1999, 2014 and 2016; and 3 representing the vegetation line extent for 1999, 2014 and 2016. Basemaps sourced from the LINZ Data Service.

runup. The accuracy of the shoreline analysis technique at these beaches is very low, given that at most profiles the vegetation line could not be used to represent shoreline change due to the human modification in the back shore, whilst when the errors in using the wet water line are accounted for, changes between the chosen imagery were not large enough to exceed the MOE and be deemed significant. These results have shown that it is difficult to use aerial imagery as an accurate surveying technique on a MSG beach, not just in a post-earthquake environment, but in monitoring year to year changes also when there has not been significant changes to the environment. Even when the area did undergo significant geomorphic changes, aerial imagery analysis can not be used to accurately depict the changes in the MSG coastal system. This method of surveying can not produce data accurate and detailed enough to inform a short term

conceptual response model.

## 6.3 Discussion

The analysis of the data produced from three different surveying techniques has detailed the usefulness of each method in a post-earthquake environment, and furthermore the level of detail produced from each technique to inform a conceptual response model. A summary table outlining the benefits and drawbacks of the previously discussed techniques is presented in Table 6.1. One limitation of using beach profile data is that it is only a small snapshot of a bigger environment, and lots of interpolation is used between profiles to inform a big picture of trends and response. While LiDAR and aerial imagery techniques are lower in resolution and accuracy than beach profile surveying, they provide a larger spatial coverage, and can offer more detail in a broad brush sense of what changes have occurred in the study area. Multiple beach profile surveys are required spatially along the coastline, and frequently re-surveyed, to establish an accurate idea of trends along a coastline. Fortunately, in this study there is an 18 year record of profiles distributed throughout the study area to be able to determine long-term trends with confidence. In circumstances where there was no long-term historical data, determining response through beach profile surveying is much more difficult, and will require strategic planning of where to take profiles, as well as a mixed method approach to confirm that trends seen in beach profile surveying are occurring on a larger scale.

There are many limitations to using a differential DEM to detect morphological change in a coastal system, and even more so in a tectonically active environment. The first being that there is interpolation of data in a DEM on a cell size scale means that often coastal features smaller than 1 m will not be identifiable in the DEM. In comparison to beach profile surveying, LiDAR data is lower in resolution on both a spatial, and often also a temporal scale due to the costs involved in collecting large data sets. The second, and most prominent, is that the because the coastal system is dynamic and consistently changing, the process of uplift can not be separated from coastal accretion; nor can subsidence be separated from erosion. Therefore, the data is not high enough resolution to detect changes that are  $<1$  m horizontally, nor is it able to determine the main cause of change, as it could with a hard structure, for example, a building where all of the vertical change could be attributed to tectonics. The differential DEM is useful for determining broadscale changes, such as areas of uplift and subsidence. It can help determine if sediment may be being trapped and built up along the coast in relation to other coastal features, such as small outlying features in the coastal zone, or the build up of sediment alongshore of a rivermouth.

**Table 6.1:** A summary table of the benefits, drawbacks, and accuracy/errors of each method analysed in Chapter 6.

| Surveying technique                                | Benefits  | Drawbacks   | Accuracy/Errors   |
|--|---|---|---|
| <b>GNSS Beach profile surveying</b>                | <ul style="list-style-type: none"> <li>• Highly accurate technique</li> <li>• Low cost</li> <li>• Produces detailed results</li> <li>• Low processing time</li> </ul>   | <ul style="list-style-type: none"> <li>• Requires operation on ground</li> <li>• Used in conjunction with the geodetic system</li> <li>• Only captures small portion of coastline</li> </ul>  | <ul style="list-style-type: none"> <li>• 2 cm accuracy</li> <li>• Errors can occur when using in post-earthquake environment</li> </ul> |
| <b>Differential DEM generated using LiDAR data</b> | <ul style="list-style-type: none"> <li>• Covers a large spatial area</li> <li>• Can have good resolution</li> <li>• Built in GNSS positioning system so can act independently of the geodetic system</li> </ul>                         | <ul style="list-style-type: none"> <li>• Large costs involved</li> <li>• Low temporal resolution</li> <li>• Resolution generally not high enough to monitor beach shape changes</li> <li>• Difficult to distinguish changes caused by tectonics from changes caused by coastal processes (erosion/accretion)</li> </ul> | <ul style="list-style-type: none"> <li>• Vertical accuracy 15-25cm</li> </ul>   |
| <b>Aerial imagery shoreline analysis</b>           | <ul style="list-style-type: none"> <li>• Covers a large spatial area</li> <li>• Built in GNSS positioning system so can act independently of the geodetic system</li> <li>• Can have good temporal resolution in urban areas</li> </ul> | <ul style="list-style-type: none"> <li>• Can have high costs</li> <li>• Historical data is usually low resolution</li> <li>• Difficulties tracing common feature along steep coastal zones</li> <li>• Can not capture tidal range and run up differences</li> </ul>   | <ul style="list-style-type: none"> <li>• Tidal range differences can generate upwards of 10 m of error</li> </ul>                       |

The topographic profiles extracted from the DEM's are a useful technique following an earthquake to determine volume changes, shoreline changes, and the extent of the uplift. These profiles should not be compared with the pre-earthquake beach profiles collected using GNSS survey equipment, as the different methods include different errors and levels of accuracy. This method can be used post-earthquake as a quick-fix method to quickly determine broad changes, however the results should be analysed with a level of skepticism, and not used to inform beach shape change analysis.

Likened to the DEM differential analysis, aerial imagery is useful for seeing significant changes, however the steep nature of MSG beaches paired with the lack of identifiable features in low resolution imagery means that the amount of detail to inform small scale morphological change can not be derived from this technique. The large margins of error and steep slopes mean that in aerial view, smaller scale changes are difficult to determine. There is currently no commonly accepted approach to analysing MSG beach change using aerial imagery techniques, and this reflects the complex MSG environments. Single (1985) traced the line of the storm berm along the Napier beaches, however aerial imagery in Kaikōura in 1999 was not of a high enough

resolution to be able to identify this feature consistently along the coastline.

The results of beach profile survey data have shown the expected progradation of shoreline and volume growth as recorded in literature (Stanley, 1968), though these results were not mirrored in the aerial imagery analysis. Beach profile surveys could be used to compare with the results of the aerial imagery shoreline analysis to determine how accurate the analysis could be. A major issue with using aerial imagery is the tidal range and how this affects the beach. Due to the steepness of MSG beaches, the tidal range horizontally is significantly less than that on a flat sand beach. When the tidal range is considered, it can be determined that the images taken in 1999 and 2014 were taken at similar tide times, given that if the images were taken at low tide, the shoreline change largely matches shoreline change at low tide seen in the beach profile surveys, as can be seen in Figure 6.5. When comparing shoreline extents for the 2014–2016 period, it becomes clear that the images taken in 2016 are taken at a different tidal extent as the images show a transgression between 2014–2016 when there is an expected progradation due to uplift, and therefore using aerial imagery creates results which may not be truly indicative of the real trend occurring.

Figure 6.5 is an example of how the time that the tidal cycle to image is collected will affect the perceived results of the analysis. The figure shows the three beach profile surveys taken using GNSS survey equipment at similar times to the aerial imagery being captured. The aerial imagery results showed that KCK2550 prograded from 1999 to 2014 by 14 m, and transgressed from 2014 to 2016 by 3 m. The change in shoreline was regarded as significant for the period of 1999–2014, as the change exceeded the 8 m MOE for the profile. The change between 2014 and 2016 was not regarded as significant as retreating 3 m did not exceed the MOE. As seen in Figure 6.5, the timing of the capture of the aerial imagery in regards to tidal range will change the narrative as to how beach response is perceived over period of time. If the 1999 and 2014 images are captured at low tide, the foreshores are shown to have changed 14 m on both the beach profile survey and the aerial imagery. The beach profile data for this profile shows that at the low tide extent, the beach has prograded 10 m between 2014–2016, whilst the aerial imagery determined that the wet water line had retreated by 3 m. Figure 6.5 demonstrates that if the 2016 image is captured when the beach is at high tide, then when compared to the low tide image captured in 2014, the beach would be seen to be retreating by 3 m, matching the aerial imagery analysis.

The results produced by using aerial imagery for shoreline analysis produce realistic results which, when caution is exercised, can be used to determine if there are significant changes along a shoreline over a large area. Due to the MOE considered in the results, which must be considered when analysing shoreline change using the wet water line, detailed results could not



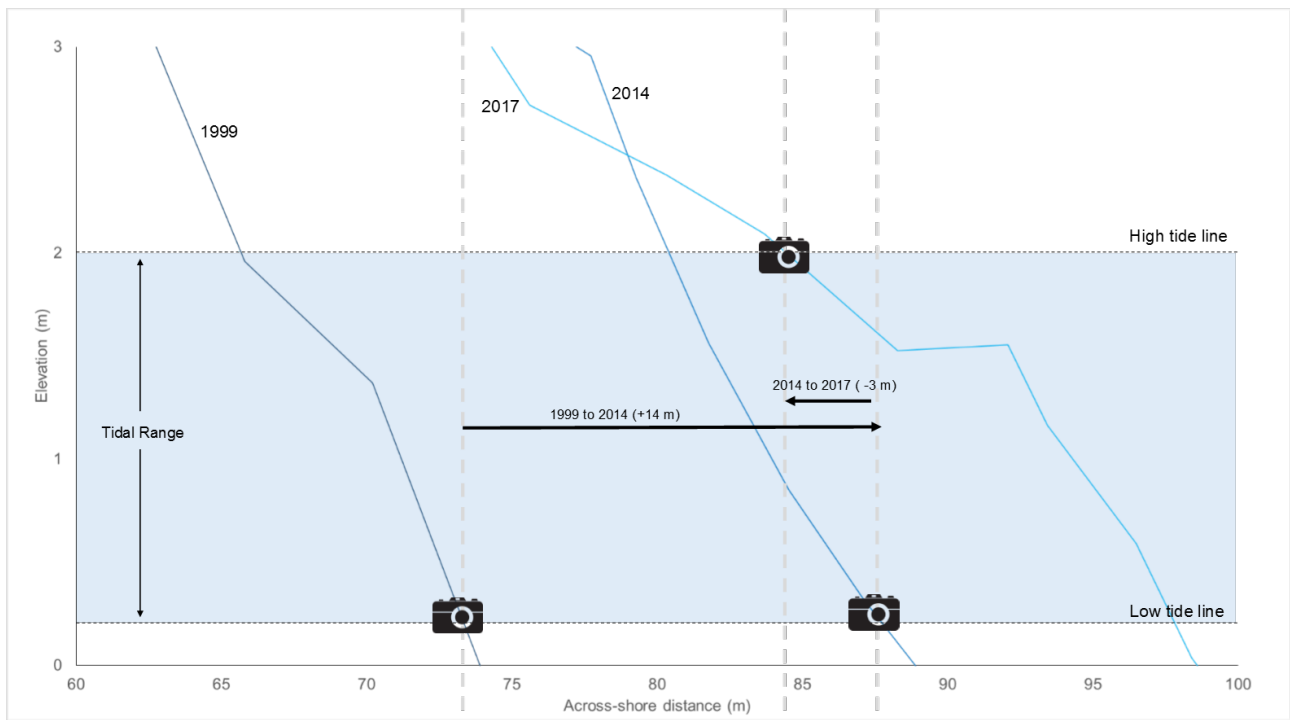


**Figure 6.5:** Explanatory diagram showing the effect tides have on the interpretation of shoreline analysis using aerial imagery. This diagram shows the foreshore profile lines of profile KCK2550 for 1999, 2014 and 2017, the profiles closest to the time of capture of aerial imagery. The shaded blue area represents the tidal range. If the images in 1999 and 2014 were captured at low tide, the beach profile data shows the same wet water line change as the aerial imagery results. The 2016 aerial imagery must have been therefore taken at high tide in order for aerial imagery to have shown a retreat of 3 m. If the 2016 image was taken at low tide, aerial imagery would have shown progradation of 10 m between 2014 and 2016.

be produced, unless information about the time of capture in relation to the tidal cycle can be obtained and paired with some form of beach profile survey. This issue rarely effects LiDAR and beach profile surveying, as long as the high tide does not affect access to a profile. Typically, a mixed methods approach using both LiDAR and beach profile surveying would generate a high resolution survey to accurately depict post-earthquake changes, as well as inform a conceptual response model.

## 6.4 Conclusions

The results from this chapter have highlighted the uses and limitations for various common post-earthquake surveying techniques. Beach profile surveying is the most accurate and detailed technique due to the high accuracy equipment used, and the ability to man the equipment in the field to determine slope change. Difficulties do arise with this method in a post-earthquake environment due to the dependence on the geodetic system. Both LiDAR data and aerial imagery are commonly used techniques to assess large scale changes over a large area, however

can not be relied on to acquire detailed data to inform beach shape change, and in the instance of aerial imagery, accurate shoreline analysis. Subsequent chapters will use the GNSS beach profile surveying data to analyse geomorphological changes in the beach systems and inform the conceptual response model, while LiDAR data will help complement these results and validate a broader scale picture of the coastal processes acting along areas of the coast which have not been directly surveyed using beach profile surveying.

# Chapter 7

## Post-earthquake geomorphological response

The following chapter presents results which contribute to achieving Objective 3: *To identify what the short-term responses are in a MSG coastal environment following an earthquake-induced change in relative sea level.*

### 7.1 Introduction

The instantaneous transformation of the coastline following the 2016 Kaikōura Earthquake event was well illustrated by the uplift of the rock shore platforms, which distinctly showed the magnitude of change in the coastal environment. Changes of the unconsolidated coastline following the earthquake have been left largely undocumented. Previous chapters of this thesis have focused on the pre-earthquake environment, including describing the environmental conditions which influence the morphology of the coastline throughout the study area, as well as determining the within-type variations of MSG beaches along the Kaikōura coastline. This chapter will now focus on how the subaerial environment of the MSG beaches responded to varying degrees of uplift throughout the study area (Figure 7.1), in order to better understand how a MSG beach responds to an environmental disturbance of such a large magnitude, using the techniques discussed in Chapter 6. The post-earthquake geomorphic response has been informed primarily by beach profile surveys and sedimentology data.

The collection of survey data, as explored in previous chapters, is a difficult task due to the different methods used post-earthquake to collect the data in January 2017 and September

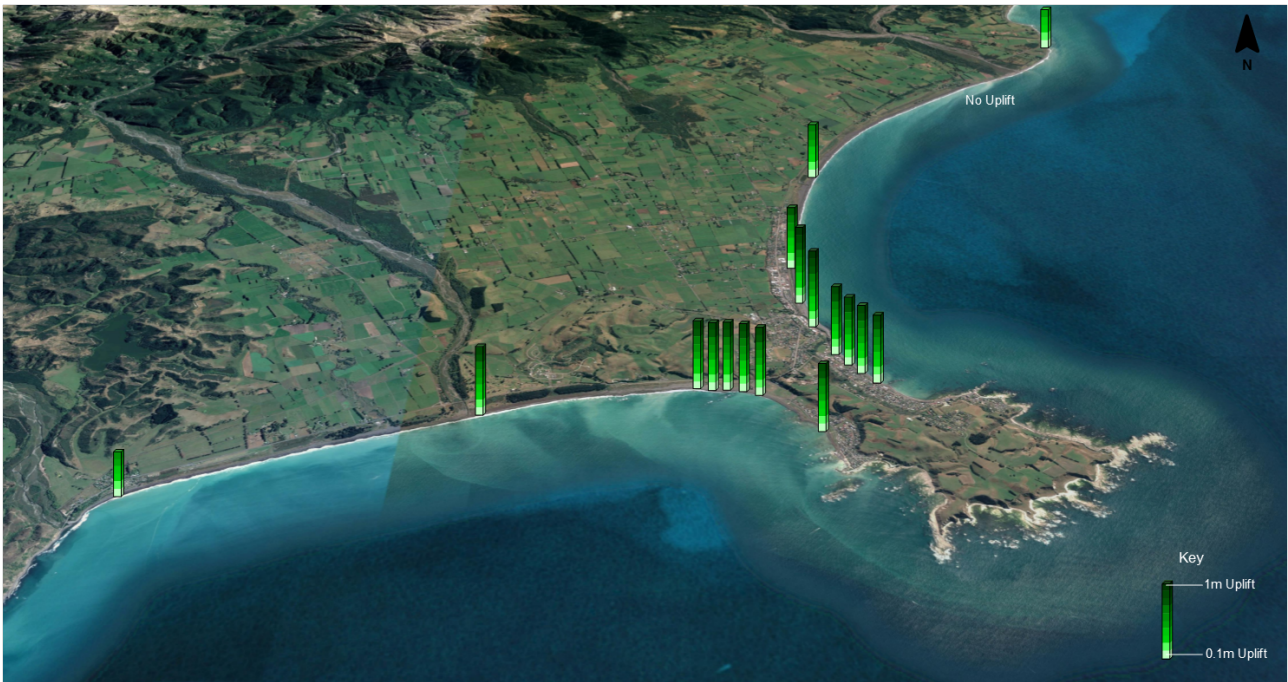


**Figure 7.1:** Differential uplift in the study area predominantly caused by the 14<sup>th</sup> of November 2016 earthquake, showing that areas closer to the Peninsula uplifted between 0.8-1m, matching the Clark et al. (2017) study, whereas profiles further away from the Peninsula, both north and south, experienced different degrees of uplift. Both profile KCK1870 and KCK5025 experienced 0.5-0.6m of uplift, while profile KCK4700 experienced no change in elevation of control points. Imagery from Google, Digital Globe.

2018. When re-surveying the beach profiles in January 2017, ECan created their own control framework using preliminary geodetic benchmarks issued within a month of the earthquake, and recalibrated their results at a later date to fit their control framework with corrected geodetic mark elevations issued in January 2018. This study collected survey data in September 2018, when the geodetic system had been corrected in accordance with the January 2018 update. The beginning of this chapter will investigate the differences between the two collected surveys and how they may affect the results.

There are various ways to measure the post-earthquake response of the beach using the type of surveying data collected in this study and presented in this chapter. Previous studies using similar data have observed changes to volume, shoreline change, and change in berm elevation (Stanley, 1968; Single, 1985; Brown, 2017). These three parameters have been expressed throughout literature through the means of quantitative modelling (Single, 1985; Brown, 2017) or through the means of qualitative descriptions (Stanley, 1968). The parameters discussed in the subsequent sections were calculated using the methods discussed in Chapter 4, in order to produce comparable post-earthquake data. Observations are made in relation to the volume, shoreline change, berm redevelopment, and sedimentology. The results are a combination of qualitative descriptions and numerical analysis of the relationship between the uplifted 2015

profile line, the ECan 2017 survey and the 2018 survey conducted in this study.

This chapter will begin with an investigation into the adjustment of the 2017 ECan survey to match the backshore elevations of the 2018 survey, in order to determine the significance of adjustment when determining patterns of response between the two surveys. The chapter will then present the results of the post-earthquake investigation, with particular regard to beach volume, shoreline change, berm redevelopment and sedimentology. An interpretation of these results to identify how MSG beaches respond following a large tectonic event, in a broader regional context will conclude the chapter.

## **7.2 Investigating differences in post-earthquake surveying data**

The results presented in this chapter use the January 2017 ECan beach profile survey data which has been re-calibrated to the January 2018 NDM update, and the September 2018 survey data collected in this study. When these two surveys are overlapped to represent the change over the 22 month period, there is a difference in elevation in the backshore environment of the profile, with some profiles having a difference of up to 35 cm. This difference was explored to determine the potential causes of this difference, and the impact it could have on the interpretation of the results.

The ECan 2017 data set was manually adjusted to best of fit the backshore environment to the September 2018 survey, as can be seen in Figure 7.2 where the backshore of the 2017 profile (2017 ‘raw’) is manually uplifted (2017 ‘adjusted’) to visually match the backshore of the 2018 (2018 ‘raw’). A difference between the two survey data sets was expected due to the human error involved in collecting the data and the complications which come with collecting this survey data before the geodetic system is adjusted to account for deformation from the earthquake event. The differences between both of the datasets may be a result of (1) continued uplift from aftershocks between 2017 and 2018; (2) different post-earthquake surveying approaches, as ECan made their own control framework in 2017 when the benchmarks were not re-established, while the 2018 survey was taken almost 2 years after the event and could use the updated geodetic marks; (3) continuous adjustment in the NDM, in which different benchmarks are adjusted differently with new patches; or (4) human modification of the backshore environment.

As discussed in Chapter 4, pre-earthquake beach profile surveys were annually conducted between 1997 and 2015. These surveys were collected using GNSS surveying equipment, and were relative to LINZ benchmarks distributed along the coastline in the study area. The earthquake

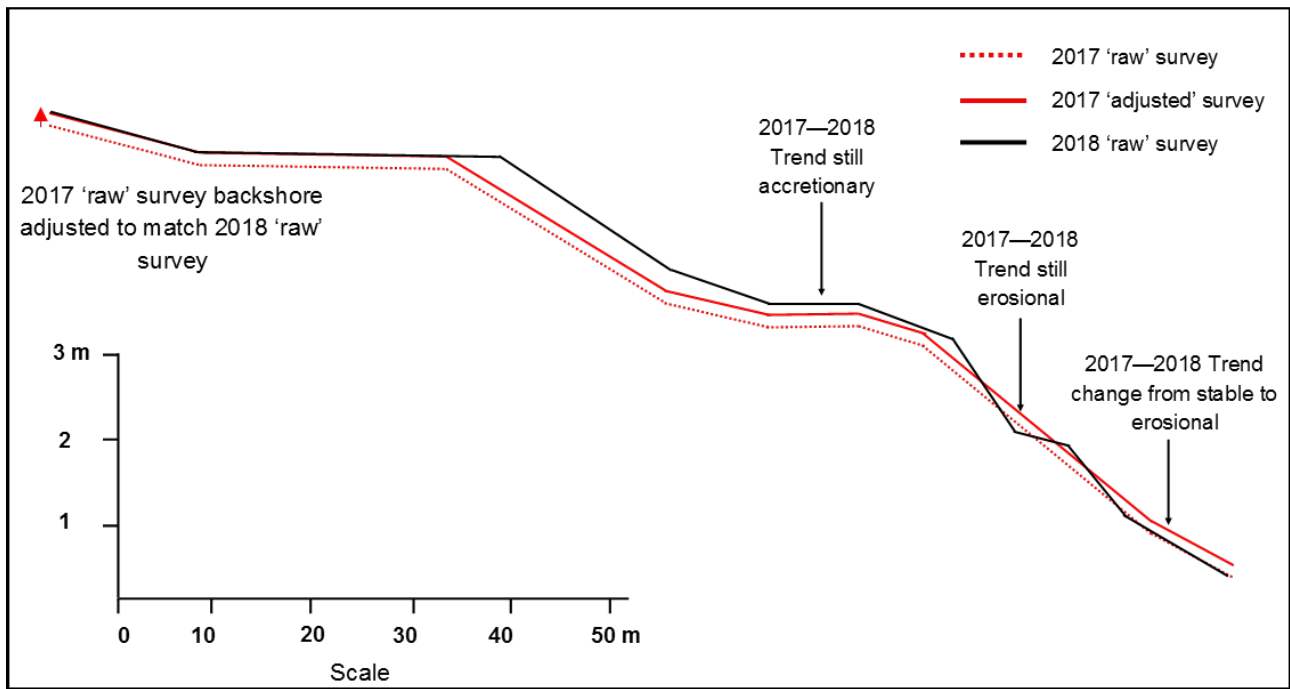


**Figure 7.2:** Manual adjustment in *Microsoft Excel* to match the ‘raw’ 2017 survey to the backshore of the 2018 survey taken in this study. This figure shows how the uplifting of the backshore can affect perceived trends between 2017–2018 on the beach profile. Where the dotted red (raw 2017) and the solid red (adjusted 2017) appear on the same side of the black solid line (2018), there was no change in trend from year to year between the two surveys when the 2017 survey is manually adjusted. The lower foreshore shows a change in trend where the raw data shows a stable trend from 2017–2018 where both profiles stay the same, whereas the adjusted 2017 profile shows erosion in this area from 2017 to 2018.

in 2016 warped the stretch of coastline, and changed the position of the benchmarks previously used to conduct the beach profile surveys. The warping changed the position and elevation of the benchmarks to different extents along the coastline (Figure 7.1). When ECan conducted their post-earthquake survey in January 2017, they re-established a control framework using preliminary benchmark elevations and position which were issued immediately after the earthquake, and created a pseudo-corrected sea level relative plane. The preliminary benchmarks issued after the earthquake have since been corrected in the NDM in January 2018 and December 2018, meaning that the control framework created by ECan needed to be recalibrated in order to be correctly aligned with the reissued benchmark positions. ECan used a series of benchmarks across the Kaikōura area to create the control framework, however these benchmarks were different to the ones used to conduct the September 2018 survey in this study. The ECan data was recalibrated to match the January 2018 issued benchmark positions, and the September 2018 survey was conducted using these benchmark positions also. Further development of the NDM resulted in the reissuing of these benchmark coordinates in December 2018 which showed that some benchmarks moved more than others when compared to the January 2018 positions. The changes across the benchmarks seen in the December 2018 update could

explain the difference in the backshore environment elevations. The December 2018 update of benchmark positions and elevations used to create the control framework by ECan in 2017 may be (1) different between the benchmarks used, and therefore recalibration is not the simple task of elevating the whole plane by the changes in elevation between January 2018 and December 2018 benchmark positions; and (2) different to the changes in the benchmarks used to collect the September 2018 survey, and therefore could explain the differences in the backshore environment elevations. Due to the time restrictions of this project, the recalibration of the ECan data to the December 2018 update could not be undertaken to test this theory, and therefore the September 2018 survey was not recalibrated either in order for the two surveys to still be comparable.

The difference between the datasets may be attributable to the aftershocks following the 2016 earthquake, as can be seen in Figure 7.3, where aftershocks with epicentres in the study area are shown in periods of six months following the earthquake. In the six months following the earthquake, 1453 aftershocks had epicentres in the study area. The amount of aftershocks in this area decreased in the subsequent analysed six month periods following the earthquake. From May 2017 to November 2017 there were 167 aftershocks; from November 2017 to May 2018 there were 107 aftershocks; and from May 2018 to November 2018 there were 79 aftershocks with epicentres in the study area (GeoNet, 2018). Figure 7.3 shows that there is a decline in aftershocks with time following the earthquake, where over 50% occurred within the first three months after the earthquake. In the 20 month period between the two beach profile surveys used in this study, there was over 3000 aftershocks attributed to the original rupture, however only one of these was  $>5 M_w$ . Between 10–20 of these aftershocks were between  $M_w$  4 and 5, and the rest were below a  $M_w$  4. Of the 620 aftershocks which occurred between the January 2017 and September 2018 and were centred directly within the study area, only one was a  $M_w$  5.1, and only four were  $M_w$  4–5. Although there was a significant number of aftershocks in the period between the January 2017 and September 2018 surveys, there were few which were capable of causing a 35 cm uplift. Figure 7.3 shows that in the wider region the amount of aftershocks  $> 3 M_w$  was 261 between the January 2017 survey and the September 2018 survey, and there was a significant decrease within the study area of aftershocks of this magnitude also. Majority of the earthquake activity which could cause this change occurred before the January 2017 survey was taken, rather than in the time period between the two discussed surveys. While the large frequency of small magnitude aftershocks, as well as the smaller frequency of larger aftershocks could cumulative cause the elevation differences between the two surveys, it is more likely that the difference is due to either (1) the error discussed in the previous section due to the differences in survey techniques and updates to the NDM; or (2) a result of reconfiguration works undertaken in backshore environments as a result of recovery efforts.



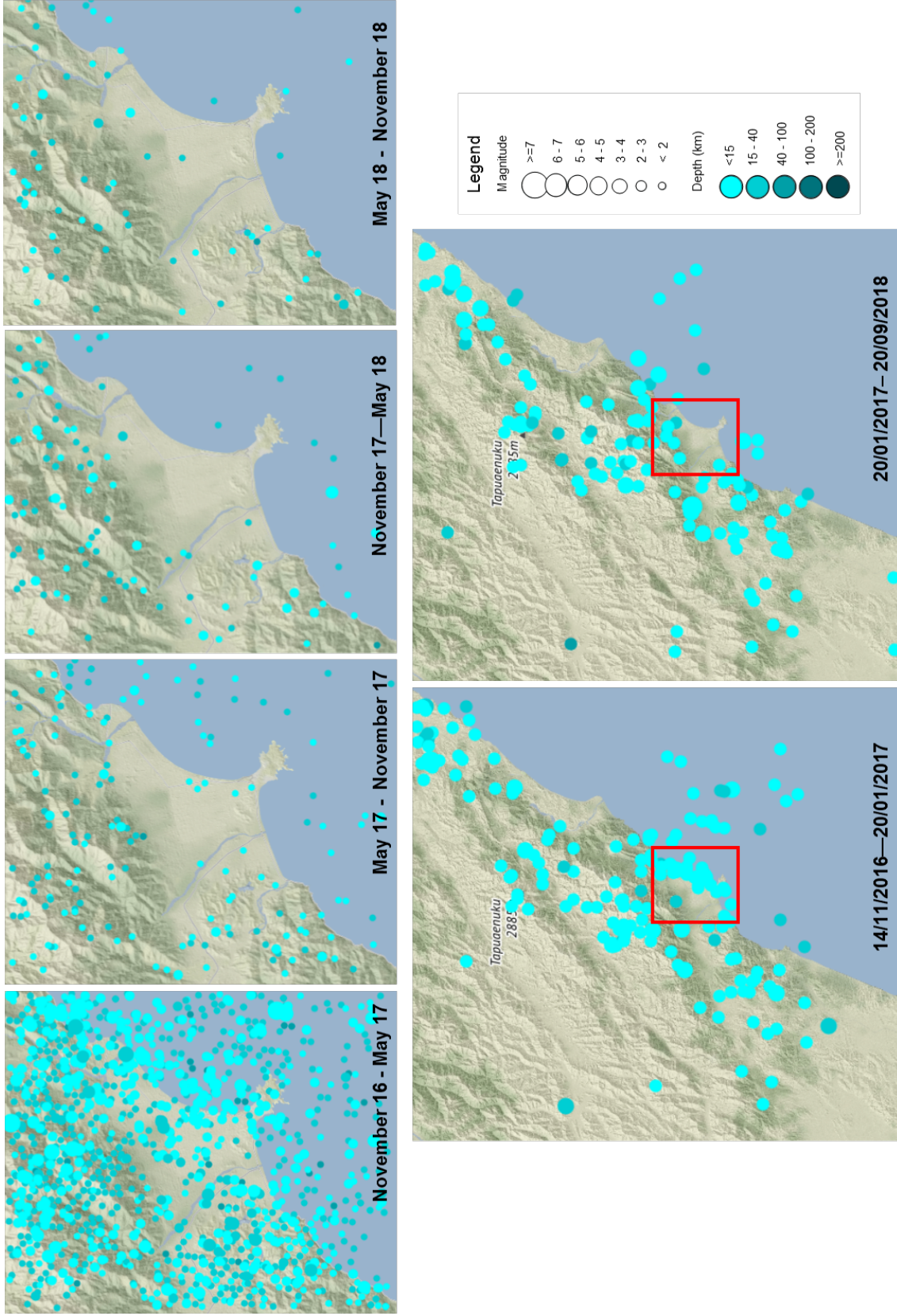


**Figure 7.3:** Magnitude, depth and location of earthquakes and aftershocks with epicentres in the study area (top) and larger rupture region (bottom) following the November 2016 earthquake. (Top row) the occurrence of aftershocks and earthquakes in the six months following the earthquake, and subsequent images show the 6 month periods in sequence. The images show that most aftershocks are  $<3 M_w$ , and the frequency of aftershocks drops from 1453 in the six months after the earthquake, to 167 between May 2017 and November 2017, to 107 between November 2017 and May 2018; and 79 between May 2018 and November 2018. (Bottom row) the occurrence of aftershocks  $> 3 M_w$  in the larger region from the November earthquake to the January 2017 survey (bottom left), compared with aftershocks between the January 2017 survey and the September 2018 survey (bottom right). The red box highlights the study area, showing most aftershocks in the study area occurred before the first survey. Data is provided from New Zealand GeoNet project and its sponsors EQC, GNS Science and LINZ. Basemap is sourced from OpenStreetMap.



The main issue which would arise if the difference between the dataset is infact an ‘error’, meaning that the difference in dataset elevations was not a result of recovery works in the backshore or aftershocks, is that it may alter how the beach is perceived to be responding after the earthquake. As can be seen in the example shown in Figure 7.2, the adjustment of the 2017 survey to match the 2018 survey can change some of the trends occurring between the two surveys. For example, the 2017 ‘raw’ data may allude to the beach having a stable trend from 2017 to 2018, however if the ‘error’ is removed and the backshore elevations are matched, it might show the 2017-2018 relationship to be erosional, as seen in the lower foreshore in Figure 7.2.

In order to see if this would be an issue when developing a conceptual model for coastal response, the data was manually adjusted in *Microsoft Excel*, so that all 2017 and 2018 surveys had matching backshore elevations, with the assumption that no further uplift happened from January 2017 to September 2018 from subsequent aftershocks. As seen in Table 7.1, there is variation in the amount of vertical adjustment needed for each profile, ranging from  $-0.1$  to  $+0.35$ . When the new volumes and 1 m contours are calculated using the adjusted profiles, Table 7.1 shows there is a variability in the amount of change, though for most profiles, volumes changed by  $10\text{--}15\text{ m}^3$ , and 1 m contour changed less than 5 m.

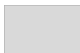
Two profiles (KCK2470 and KCK3659) in Table 7.1 are shaded light grey, indicating that when their relationship between 2017 and 2018 surveys was analysed using the adjusted 2017 data, there was a change in trend. All other profiles continued to show the same 2017–2018 trend in volume and 1 m contour response when the data was adjusted. It was therefore deemed that although it is unknown whether the differences in elevation is real, a result of human error, or could be explained by the recent NDM update, when the data is adjusted to account for an elimination of an ‘error’, the overall trend of the geomorphic response at a profile is not affected. The two profiles which were affected by an adjustment will be cautiously analysed, with the knowledge that adjusting the data will affect the perception of how the beach profile is responding.

### 7.3 Geomorphological response

The following section will detail the geomorphological response of the subaerial MSG coastal environment, determined from GNSS beach profile surveying methods, as well as sedimentology data collected using DGS analysis techniques described in Chapter 4. The beach profile morphology results are determined using the September 2018 survey collected in this study, and the ‘raw’ January 2017 survey collected by ECan.

**Table 7.1:** Adjustment of the ECan January 2017 survey to match the backshore elevations of the 2018 survey taken in this study to minimise the unexplained differential ‘error’. Calculations of volume and 1 m horizontal contour were recalculated for the adjusted surveys and are shown here compared as ‘raw’ (ECan survey) and ‘adjusted’ (ECan survey backshore adjusted to September 2018 survey backshore) to identify significant differences which would affect the perception of the results. Shaded numbers are the figures which their adjusted value did not have the same relationship (Progradation or Transgression) with the 2018 survey as the raw 2017 survey.

| Site    | Vertical Adjustment | Raw Volume (m <sup>3</sup> ) | Adjusted Volume (m <sup>3</sup> ) | Raw 1m Contour (m) | Adjusted 1m Contour (m) |
|---------|---------------------|------------------------------|-----------------------------------|--------------------|-------------------------|
| KCK1870 | No 2017 Survey      |                              |                                   |                    |                         |
| KCK2200 | +0.35               | 607                          | 661                               | 306                | 311                     |
| KCK2470 | +0.20               | 336                          | 352                               | 231                | 233                     |
| KCK2486 | +0.25               | 342                          | 363                               | 269                | 270                     |
| KCK2496 | +0.15               | 341                          | 353                               | 262                | 263                     |
| KCK2510 | +0.15               | 326                          | 337                               | 170                | 170                     |
| KCK2550 | +0.15               | 267                          | 277                               | 94                 | 95                      |
| KCK2575 | +0.10               | 102                          | 106                               | 100                | 101                     |
| KCK3659 | -0.10               | 107                          | 103                               | 59                 | 59                      |
| KCK3684 | -0.05               | 94                           | 92                                | 92                 | 92                      |
| KCK3712 | No Adjustment       | 151                          |                                   | 63                 |                         |
| KCK3737 | No Adjustment       | 92                           |                                   | 59                 |                         |
| KCK3800 | +0.10               | 259                          | 265                               | 143                | 144                     |
| KCK3855 | +0.20               | 268                          | 282                               | 131                | 132                     |
| KCK3950 | +0.30               | 417                          | 446                               | 191                | 196                     |
| KCK4220 | No 2017 Survey      |                              |                                   |                    |                         |
| KCK4700 | No 2017 Survey      |                              |                                   |                    |                         |
| KCK5025 | No 2017 Survey      |                              |                                   |                    |                         |

 Trend relationship to 2018 survey data is changed with an adjustment of data

### 7.3.1 Differential coastal uplift

The entirety of the study area was located within one region of the fault, meaning that no profiles cross the fault boundary, as was seen in Single (1985). Due to the study area being located on one side of the fault, similar degrees of uplift would be expected. As can be seen in Figure 7.1, there is some variability in the amount of uplift throughout the study area, and in particular, profiles located further away from the Peninsula. South of the Peninsula, profile KCK1870 experienced 0.6 m of uplift. North of the Peninsula, profile KCK4700, located just south of the Hāpuku River did not experience any uplift. Profile KCK5025, north of the Hāpuku River, experienced 0.5 m of uplift. Profiles close to the Peninsula, including South Bay and the township experienced uplift of approximately 1 m.

The amount of uplift at a profile, in conjunction with beach slope, can pre-determine the extent of initial shoreline progradation. Group 2 beaches, which are classed as wide and flat (Figure 5.2), only need a small amount of uplift to induce a large amount of shoreline progradation. Group 3 beaches which are narrow and steep (Figure 5.2) would require significantly more uplift to achieve a similar amount of instantaneous progradation.

### 7.3.2 Volume change

Beach profile surveying allowed for the calculation of volume change from year to year. The data acquired only allowed for calculation of subaerial volume change, so therefore interpretations must accept that loss of subaerial volume can be indicative of the erosion of sediment from the system into the offshore environment, or a result of redistribution of sediment into the nearshore. As shown in Figure 7.4, all profiles surveyed in 2017 were shown to have increased in subaerial volume post-earthquake. Between the 2017 and 2018, some profiles began to show a loss of subaerial volume, however despite this, still maintained a net gain in volume change since the earthquake.

The sediment volume in the active beach environment increased following the earthquake for all five profiles in Group 1. All profiles have maintained a net overall gain of volume since the 2015 pre-earthquake profile, however profile KCK2510 is the only profile demonstrates signs of retreating back to its pre-earthquake volume, of which it gained  $54 \text{ m}^3$  between 2015–2017, then lost  $17 \text{ m}^3$  between 2017–2018. The other four profiles appeared to undergo a rapid increase in volume between 2015–2017, but since the 2017 survey their rate of subaerial accretion has decreased. There is still a net continuation of their pre-earthquake accretionary trends. As shown in Table 7.2, post-earthquake volume change rates are still significantly larger over the observed post-earthquake period than pre-earthquake. The high rate of positive change seen in the 2017–2018 survey shows that the volume increase is more than just the volume acquired from the uplift of the profile into the subaerial zone, and that there is an additional source of sediment driving continuous accretion at these profiles.

The only profile which has shown an overall net loss since the earthquake is profile KCK4700, which has lost  $212 \text{ m}^3$  since the 2015 survey. This profile was not surveyed in 2017, and therefore it is hard to determine if there has been constant erosion since the earthquake, or this is just a snapshot of dynamic nature of the profile, as the extent of the erosion is not outside of the envelope of change for this profile. This profile was not uplifted in the earthquake, and therefore did not experience the instantaneous volume gain that other profiles did. The results here show that an expected increase in sediment budget coming from the Hāpuku River has not had an



**Figure 7.4:** Summary of post-earthquake volume changes between each survey following the earthquake. All profiles surveyed in 2017 experienced an increase in subaerial volume. The 2018 survey showed some profiles had begun to erode, but profiles still maintained an overall net gain of subaerial sediment volume. Profile KCK4700 was not surveyed in 2017, however the overall volume change from 2015-2018 shows a significant loss of subaerial volume. This profile also experienced no uplift. No profiles showed volume loss between 2015-2017.

**Table 7.2:** Rates of volume change per year, from 1997–2015 (Pre-Earthquake), compared with 2015–2018 (Post-Earthquake), demonstrating the changes in volume at most profiles being excessively more over the 3 year period since the 2015 survey. The rate of change at most profiles was more extreme during the 2015–2017 stage, however most profiles demonstrated continued growth at a rate higher than pre-earthquake during the 2017–2018 period. It is important to note that the pre-earthquake columns is averaged over a 17 year period, whilst the post-earthquake columns is only representative of a 2 year period.

| Profile | Pre-earthquake<br>(m <sup>3</sup> / year) | Post-earthquake<br>(m <sup>3</sup> / year) | Profile | Pre-earthquake<br>(m <sup>3</sup> / year) | Post-earthquake<br>(m <sup>3</sup> / year) |
|---------|---|--|---------|---|--|
| KCK1870 | - 8                                       | + 30                                       | KCK3684 | 0   | + 11                                       |
| KCK2200 | + 4                                       | + 72                                       | KCK3712 | + 1                                       | + 10                                       |
| KCK2470 | + 5                                       | + 21                                       | KCK3737 | + 0.6                                     | + 3  |
| KCK2486 | + 6                                       | + 29                                       | KCK3800 | + 6                                       | + 30                                       |
| KCK2496 | + 4                                       | + 39                                       | KCK3855 | + 8                                       | + 27                                       |
| KCK2510 | + 5                                       | +12  | KCK3950 | + 3                                       | + 28                                       |
| KCK2550 | + 6                                       | + 20                                       | KCK4220 | - 1                                       | + 37                                       |
| KCK2575 | + 0.7                                     | + 6  | KCK4700 | + 5                                       | - 71                                       |
| KCK3659 | - 1                                       | + 15                                       | KCK5025 | - 2                                       | + 7  |

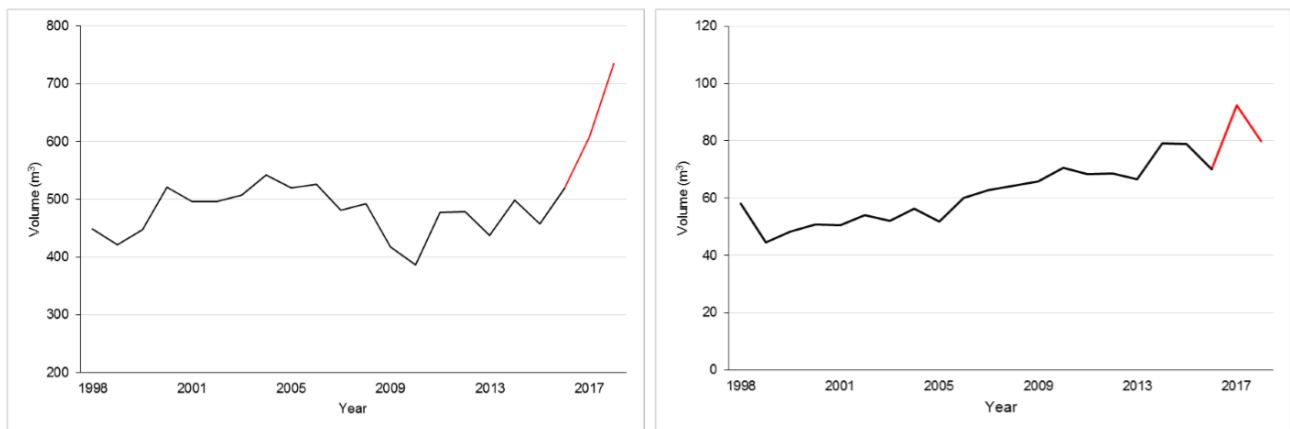


**Figure 7.5:** Two graphs showing the rate of volume change following the earthquake (red) in relation to its pre-earthquake trend. Profile KCK2200 (left) showed a strong accretionary trend following the earthquake, as the volume of sediment at the profile has far exceeded any volume previously seen at the profile. Profile KCK3737 (right) shows that initially the volume increased beyond any volume seen at the profile pre-earthquake, however from January 2017 to September 2018 volume has begun to decline back to pre-earthquake figures.

overriding positive impact at this profile, however there is also no geomorphic barrier to trap sediment at this profile, and therefore sediment may have been reworked through the system, southward down the coast. A human influence which may be hindering growth at this profile may be the mining of alluvial gravels taking place in the Hāpuku River, which will be discussed further in Chapter 8. The dynamic nature of this profile and limited monitoring, means there is no evidence to suggest there were not other large fluctuations of accretion or erosion between 2015 and 2018.

All Group 2 profiles which experienced uplift have increased in volume since the earthquake as shown in Figure 7.4. Profiles KCK1870 and KCK4220 have increased in volume since the earthquake, though the 2018 survey showed that the amount of volume increase did not extend beyond the envelope of change at these profiles. Profiles KCK3950 and KCK2200 (Figure 7.5) have seen continuous volume increase since the earthquake, showing growth beyond any volume previously measured at these profiles. These two profiles are the most uplifted profiles out of the five discussed Group 2 profiles (uplifted 1 m). Profile KCK2200, located at the mouth of the Kowhai River, has significantly increased in volume since it has been uplifted, gaining over 200 m<sup>3</sup> in volume since the 2015 survey, as seen in Figure 7.5. Most of this volume increase has occurred between the 2017-2018 surveys, following the trends of profiles further north in South Bay, where there is a nearby sediment source promoting further subaerial increase beyond what has been uplifted.

All Group 3 profiles which were resurveyed in 2017 showed a volume increase which exceeds any previous maximum volume found at the profile. Sub-groups (Table 5.2) 3A and 3B both experienced a significant amount of volume increase relative to their pre-earthquake profile, increasing 22-48 m<sup>3</sup> in volume between its 2015 and 2017 surveys. This is shown in Figure 7.5 where profile KCK3737 is shown as having a volume increase from 2015–2017, then decrease from 2017–2018. Between 2017-2018, all profiles in sub-group 3A and 3B (Table 5.2) lost subaerial volume, except for KCK3684, however all profiles still maintained an overall net gain. The loss of subaerial volume here is indicative that there is no nearby sediment source to maintain the volume gained through uplift. Sub-group 3C (Table 5.2) increased significantly in volume between 2015 and 2017, and continued to increase in subaerial volume between 2017 and 2018 surveys at a slower rate. Sub-group 3D (Table 5.2) was only resurveyed in 2018, and showed it had increased 20 m<sup>3</sup> between 2015 and 2018, though had not exceeded its maximum volume extent as seen at other profiles within Group 3. The results from the volume analysis of Group 3 show that profiles with a pre-earthquake erosional trend are struggling to maintain the volume increase from the uplift, and seen in Figure 7.5, while profiles which had an accretionary trend pre-earthquake have been able to maintain the volume increase from the uplift.

### 7.3.3 Progradation and transgression

Progradation and transgression have been measured through the movement of the 1 m horizontal contour in the post-earthquake surveys, which is approximately at the MSL contour (1.2 m). As seen in Figure 7.6, similar to volume, all profiles which experienced progradation as a result of uplift, and have maintained a net seaward movement of the shoreline. The only profile which has experienced significant transgression since 2015 is profile KCK4700 (46 m), which as described in Section 7.3.2, also has experienced significant volume loss.

Since the 2017 survey, all Group 1 profiles, except for profile KCK2496, have transgressed at their 1 m contour. KCK2510 has undergone shoreline transgression since the 2017 survey back to its pre-earthquake shoreline extent, in which as of the 2018 survey, the profile only had a net shoreline gain of 1.4 m. Other Group 1 profiles which have undergone transgression have still been able to maintain a positive net gain of shoreline progradation since the uplift. Profiles in this group have shown that they can undergo shoreline transgression but still be increasing in volume. This may be indicative of berm reformation at elevations above the 1 m contour.

Similar to the trends shown in Section 7.3.2, Group 2 profiles have undergone the greatest magnitude of shoreline changes. As described above, KCK4700 underwent severe shoreline retreat, whilst other profiles have experienced progradation from 2015 through to 2018. KCK2200 has prograded 31.5 m at its 1 m horizontal contour from 2015–2018. Other Group 2 profiles have experienced a net overall change between 13.5–21.2 m. Rates of progradation at these profiles slowed between the 2017–2018, however at KCK2200 the rate of progradation significantly increased between 2017–2018. This may be a result of its close proximity to its sediment source. It should be recalled that this profile is also extremely dynamic, and although its shoreline extent and volume growth is now outside of the envelope of change, large fluctuations in shoreline position are not uncommon at this profile.

Group 3 profiles which were surveyed in both 2017 and 2018 have shown that their 1 m contour is beginning to retreat back to the pre-earthquake extents, or progradation rates have slowed down significantly (KCK3684 and KCK3712), as seen in Figure 7.6. Profiles KCK3800 and KCK3855 continue to prograde between 2017–2018, suggesting that there is a sediment supply reaching these two profiles. All profiles in this group have managed to maintain a net gain of seaward horizontal movement since the earthquake, however the more or less stable trends of these profiles and the survey data presented suggests that shoreline retreat is occurring at most of these profiles (KCK2575–KCK3737) two years on from the earthquake event, and the positive impact of coastal uplift is not being retained in these areas.

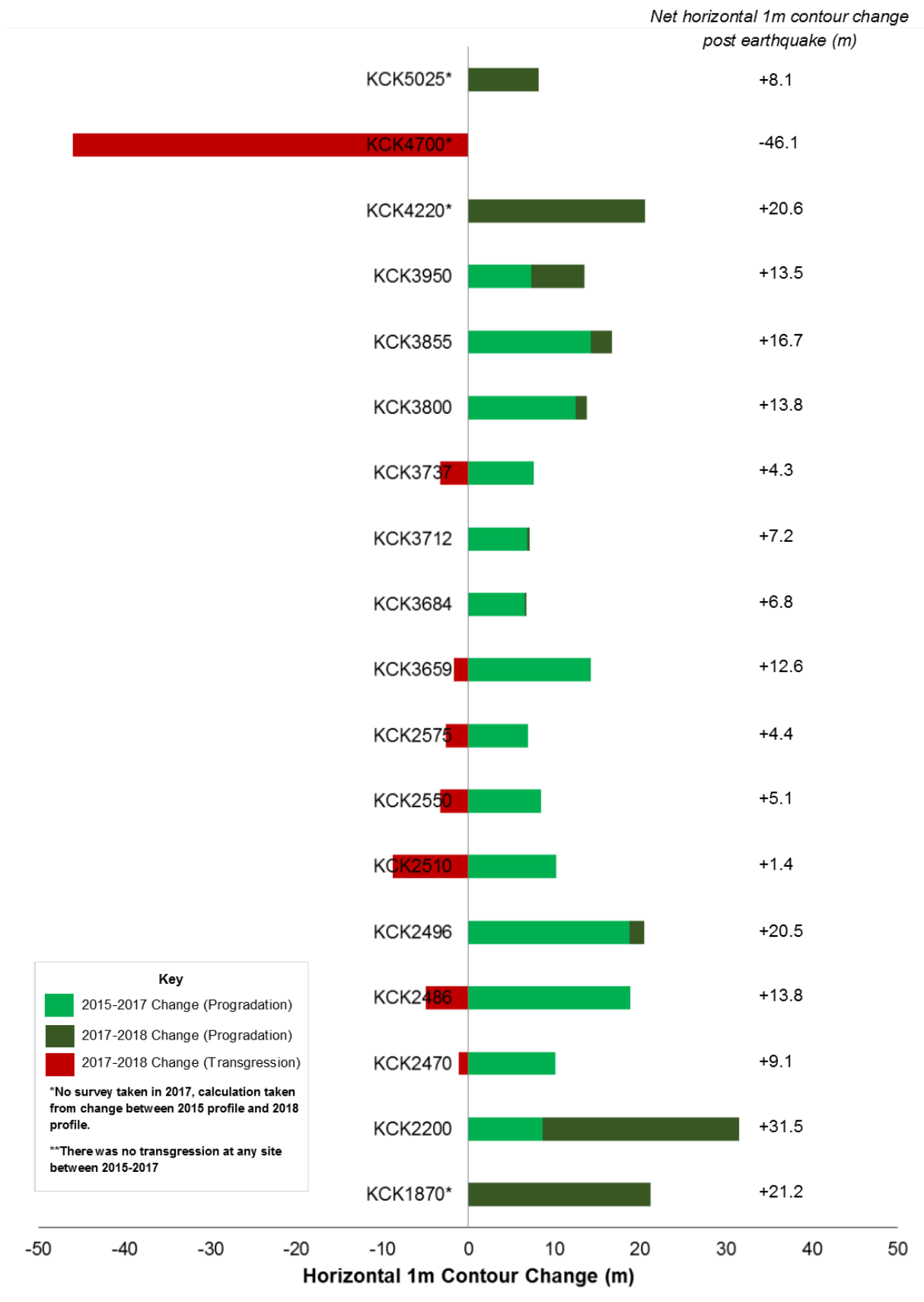


**Figure 7.6:** A summary of horizontal 1 m contour changes following the earthquake. The 2017 survey showed progradation at all profiles following the earthquake. 50% of profiles surveyed in both 2017 and 2018 showed shoreline transgression from 2017 to 2018. Profile KCK2200 showed continued progradation at a high rate in 2018, while profile KCK4700 has undergone a substantial amount of shoreline transgression. No profiles that were surveyed in 2017 showed transgression between 2015–2017.



### 7.3.4 Berm redevelopment

Berms are formed at the swash runup limit, and storm berms are formed at the top of the storm runup limit. It was expected that berm redevelopment would occur relative to the new sea level and wave runup elevations. The results show that this is a trend which has occurred at different rates throughout the study area, with most berm redevelopment occurring in similar patterns for each within-type variation group. The 2017 survey showed that at most profiles there was more berm development at elevations lower than where pre-earthquake berms were formed relative to sea level. By the 2018 survey, the sediment had been reworked into the system and the berms had eroded, and the beaches are starting to reform berms at heights relative to sea level, in line with the elevations pre-earthquake berms, but now at a more seaward extent due to the instant progradation discussed in Section 7.3.3.

As seen in Figure 7.7, Group 1 profile KCK2550 exhibits this trend. Sediment from the uplifted 2015 profile looks to redistribute into the lower foreshore between 2015–2017, then the 2017–2018 illustrates that movement of that sediment back up the profile to reform a berm at the same elevation as pre-earthquake, but at a more seaward extent. Some of the other Group 1 profiles have not yet redeveloped their berm, and their foreshores have flattened between the 2017–2018 surveys after a short stint of minor berm development at a lower elevation. While these profiles have not yet redeveloped their berms, they have begun to develop storm berms at elevations similar to their pre-earthquake elevations (between 5–6 m). Areas landward of the pre-earthquake storm berm position have been uplifted and remain largely unchanged, and are now considered to be out of the active beach face system.

Group 2 profiles have shown similar results to Group 1 profiles, with the re-establishment of pre-earthquake storm berm elevations. These profiles showed no real development of a berm at a low elevation, however most of these profiles did not exhibit this feature pre-earthquake, likely due to the smaller grain size and the low slope not allowing for a build up of swash zone sediment. Figure 7.7 shows KCK2200 having redeveloped its pre-earthquake storm berm at the same elevation, with its uplifted active beach landward of this having undergone minimal changes since the earthquake. The lower foreshore shows no development of a berm, despite it having a developed berm in its 2015 survey. Profiles in this group are largely dominated by continuous growth of the foreshore, and therefore is not developing berms as it undergoes continuous growth and change adjusting to the post-earthquake environment.

Group 3 profiles appear to be the group which has undergone the most stable berm redevelopment, with profiles initially re-establishing the berm and storm berm by the 2017 survey, then undergoing narrowing and steepening of these features between the 2017–2018 surveys.

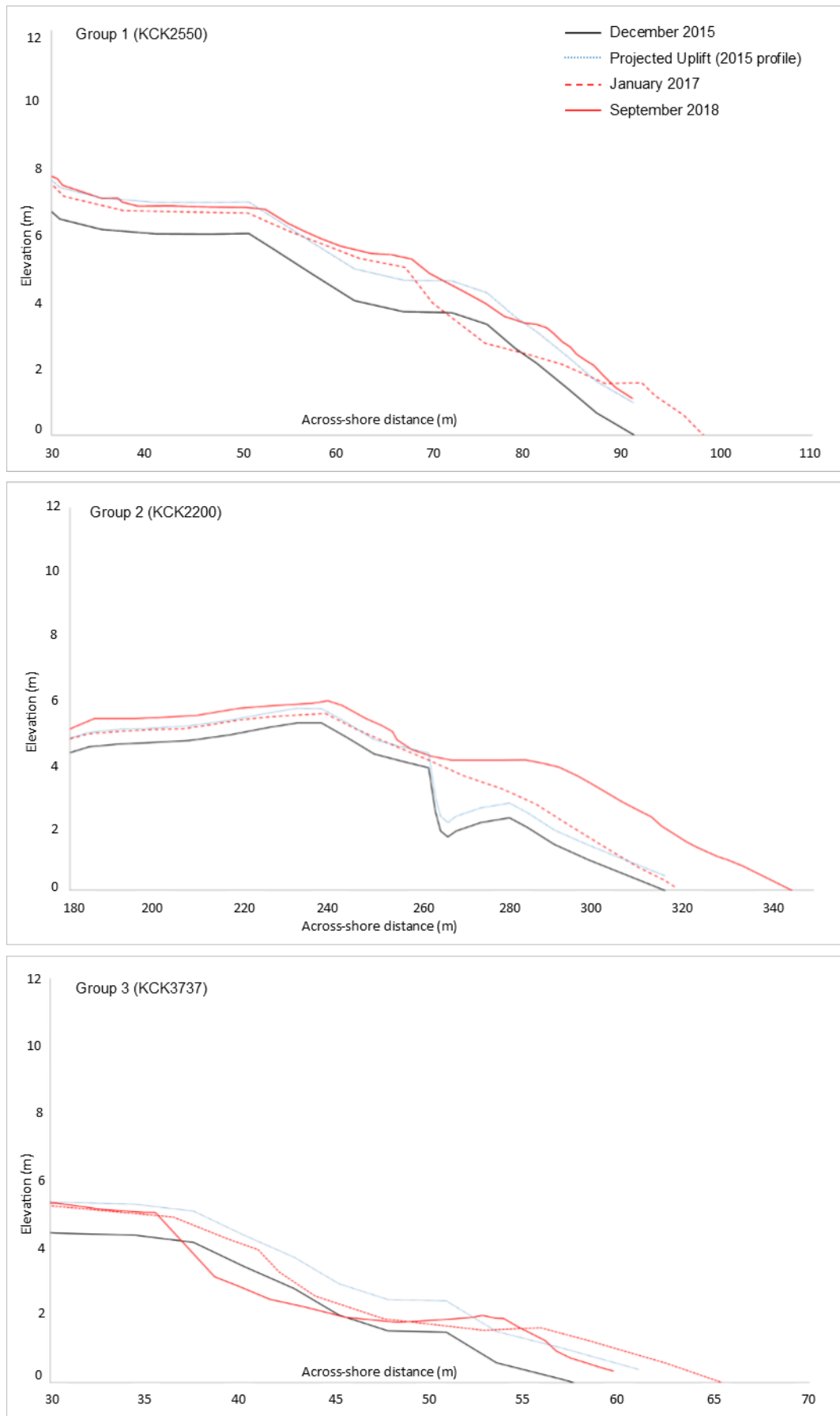


**Figure 7.7:** Berm morphology changes seen in post-earthquake surveys, representative of the three different geomorphic groups. Group 1 and 3 show the berms redevelopment at pre-earthquake elevations, while Group 2 profiles have redeveloped the storm berm but the lower foreshore continues to grow and flatten out.

Profiles KCK3659 through to KCK3737 all exhibit this trend strongly, paired with the data presented in Sections 7.3.2 and 7.3.3 that most of these profiles had begun to transgress and lose volume. As seen in Figure 7.7, KCK3737 appears to be eroding throughout the whole profile, and is eroding into the uplifted backshore, where in other groups, this area remained untouched landward of the storm berm following the uplift. Profile KCK3737 appears to have redeveloped its berm quickly however the erosive nature of the beach has eaten into the backshore, not allowing for a redevelopment of the storm berm at the same elevation as prior to the earthquake. Other profiles located along the Esplanade appear to follow this trend, or have developed very small storm berms. Profiles KCK3800 and KCK3855 have redeveloped storm berms at the same pre-earthquake elevations, however these beaches continue to grow, and the berms are therefore developing at a more seaward position. The contrast between these two sub-groups being that Esplanade profiles redevelop berms while the beach retreats back to pre-earthquake states, whereas the township profiles (KCK3800 and KCK3855) redevelop their berms as they continue to grow, much like Group 1 profiles.

### 7.3.5 Sedimentology

The difficulty of analysing MSG beach sedimentology data largely stems from the very diverse and varied sediment patterns that occur across a MSG beach profile. This results in difficulties in sediment sampling in a MSG environment where the across shore sediment patterns are extremely variable, and therefore it is impossible to get a sample representative of the entirety of the profile, especially with consideration of the vertical mixing of the sediment within the profile. The absence of a long-term data set for the Kaikōura MSG these beaches means that it is difficult to attribute changes in sedimentology between profiles directly to the earthquake event. The following will present the sedimentology results with these limitations in mind, and will be discussed further in Section 7.4.

As shown in Table 7.3 and Figure 7.8, graphic mean size and composition percentages are two of the parameters analysed in the 2018 results to compare to the 1997 sedimentology results. The table shows that most profiles throughout the study area have experienced some degree of change in sedimentology since 1997.

Group 1 profiles continued to have very similar mean grain sizes, in which the changes of grain sizes were no more than one class size (eg. small pebble to very small pebble) as seen in Figure 7.8. The sand/gravel compositions of these profiles however were noted as having largely changed, due to their 1997 results measuring 100% gravel in both the MT and UF zones. The results showed that there was over a 20% textural change in both the UF and MT zones at all

**Table 7.3:** Comparison of sand/gravel composition percentages between 1997 and 2018 for both the upper foreshore (UF) and the mid tide zone (MT).

| Profile        | Zone | Composition 2018<br>(Sand %/ Gravel %) | Composition 1997<br>(Sand % / Gravel %) | Profile        | Zone | Composition 2018<br>(Sand %/ Gravel %) | Composition 1997<br>(Sand %/ Gravel %) |
|----------------|------|--|---|----------------|------|--|--|
| <b>KCK1870</b> | MT   | 33 / 66                                | 74 / 26                                 | <b>KCK3684</b> | MT   | 15 / 85                                | 0 / 100                                |
|                | UF   | 44 / 56                                | 74 / 26                                 |                | UF   | 20 / 80                                | 0 / 100                                |
| <b>KCK2200</b> | MT   | 37 / 63                                | 15 / 85                                 | <b>KCK3712</b> | MT   | 15 / 85                                | 0 / 100                                |
|                | UF   | 37 / 63                                | 86 / 14                                 |                | UF   | 11 / 89                                | 0 / 100                                |
| <b>KCK2470</b> | MT   | 19 / 80                                | 0 / 100                                 | <b>KCK3737</b> | MT   | 11 / 89                                | 0 / 100                                |
|                | UF   | 21 / 79                                | 0 / 100                                 |                | UF   | 14 / 86                                | 0 / 100                                |
| <b>KCK2486</b> | MT   | 24 / 76                                | 0 / 100                                 | <b>KCK3800</b> | MT   | 25 / 75                                | 0 / 100                                |
|                | UF   | 30 / 70                                | 0 / 100                                 |                | UF   | 26 / 74                                | 0 / 100                                |
| <b>KCK2496</b> | MT   | 46 / 54                                | 3 / 97                                  | <b>KCK3855</b> | MT   | 11 / 89                                |  |
|                | UF   | 28 / 72                                | 0 / 100                                 |                | UF   | 30 / 70                                |  |
| <b>KCK2510</b> | MT   | 44 / 56                                | 0 / 100                                 | <b>KCK3950</b> | MT   | 10 / 90                                | 43 / 57                                |
|                | UF   | 27 / 73                                | 0 / 100                                 |                | UF   | 33 / 67                                | 12 / 88                                |
| <b>KCK2550</b> | MT   | 16 / 84                                | 0 / 100                                 | <b>KCK4220</b> | MT   | 18 / 82                                | 74 / 26                                |
|                | UF   | 26 / 74                                | 0 / 100                                 |                | UF   | 46 / 54                                | 98 / 2                                 |
| <b>KCK2575</b> | MT   | 21 / 79                                | 11 / 89                                 | <b>KCK4700</b> | MT   | 13 / 87                                | 0 / 100                                |
|                | UF   | 31 / 69                                | 4 / 96                                  |                | UF   | 24 / 76                                | 63 / 37                                |
| <b>KCK3659</b> | MT   | 30 / 70                                | 31 / 69                                 | <b>KCK5025</b> | MT   | 25 / 75                                | 16 / 84                                |
|                | UF   | 27 / 73                                | 2 / 98                                  |                | UF   | 30 / 70                                | 1 / 99                                 |

profiles in this group, where profiles had an increase in sand composition since 1997.

Group 2 profiles have undergone some amount of composition change at each profile, with most profiles changing textural composition of more than 25% (Table 7.3), and have undergone an increase in gravel composition from their 1997 readings. Changes in mean grain size of more than 2 class were common in Group 2 profiles, where most profiles increased in mean grain size, as seen in Figure 7.8. The changes found across all profiles of increase/decrease in grainsize did not follow a clear trend.

Group 3 profiles appear to have undergone the smallest degree of changes relative to other groups, with the majority of mean grain sizes and compositions revealing similar textures. As seen in Figure 7.8, profiles KCK3800 and KCK5025 have undergone the most change out of all profiles in their UF zone. KCK3800 has changed from having a mean grain size of 45.7 mm to 4.05 mm, and KCK5025 having changed from 36 mm to 3.92 mm. Most of the Group 3 profiles were measured as having no sand in 1997 (KCK3684 to KCK3800), whereas measurements from this study show that sand now makes up a small portion of the beach composition (11–26%).

The 1997 sedimentology data showed that primarily open coast profiles were the only profiles which contained surface sand in both their MT and UF zones (over 50% of profiles), however DGS analysis has shown that all of the profiles now have sand present on the beach surface in these zones. The most pronounced changes in sand/ gravel composition were in open coast

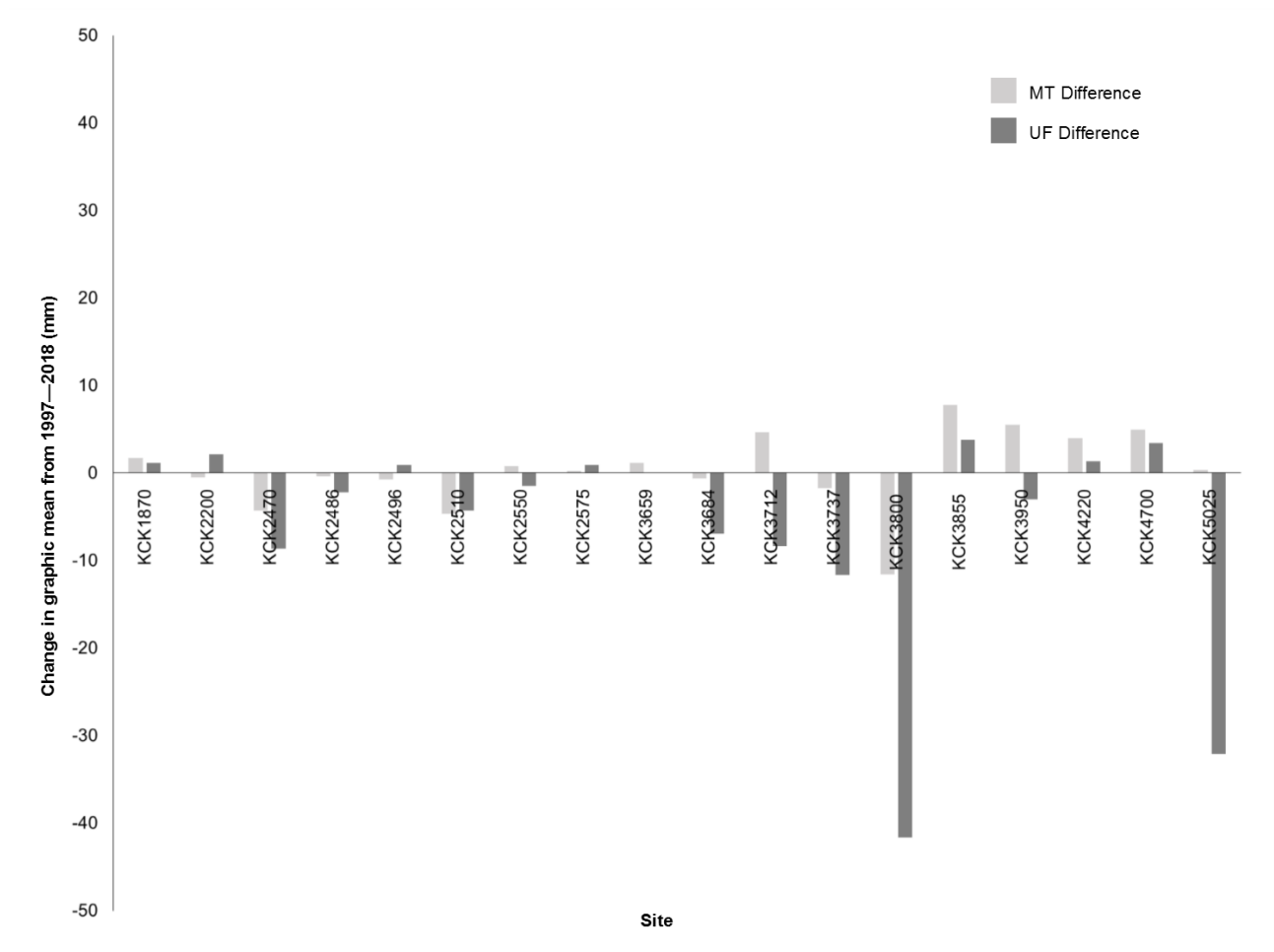


**Figure 7.8:** Differences in 1997 and 2018 graphic mean beach sediment sizes (mm), shown from south to north along the horizontal axis. A negative value implies that the mean grain size has decreased since 1997, and a positive grain size change implies that the mean grain size has increased since 1997. Most profiles have undergone change to some degree. The raw graphic mean results are found in Appendix D.

profiles, however there was no trend in whether the textural change was an increase in sand or gravel at the profile. There was no significant overall trend (increase or decrease) of mean grain size across all profiles. All profiles measured experienced some degree of change, which was expected due to the large time period between sampling (21 years). Large changes across all profiles could indicate that there was an impact from the earthquake itself. The small fluctuations found at most profiles here can likely be attributed to the evolution of the profile itself over the long period, and the change in local environmental conditions influencing profile. For example, changing conditions which could attribute to the sedimentology changes could include dredging of South Bay Harbour, renourishment of the Esplanade, or mining of gravel from the Hāpuku River.

Conclusively, the data confirms that there is no significant trend occurring indicating that the earthquake has altered sedimentology significantly, or that the earthquake has thus far had lasting effect on the mean grain size and texture of the coastline. Previous studies have shown

that sedimentology following an earthquake can be altered but recover quickly in a coastal environment (Hart et al., 2015). Gravel sediment is larger and heavier, and therefore may take decades to work its way down a catchment. Sand is much finer and lighter and will therefore make its way down a catchment much quicker, and therefore increase in sand and fines at profiles may be a result of this. The occurrence of sand at all profiles now may be indicative of a higher amount of fine sediment in the budget coming down from rivers following the earthquake, or likely it may be from a development of the profile over the 21 year period. There may have been a drastic change following the earthquake, where the relative MT and UF zones have shifted and new ones are being developed, but these zones have been re-established as a result of the environmental conditions acting on the profile, promoting similar grain sizes in the zones which are surveyed.

## **7.4 Discussion**

### **7.4.1 Geomorphological response**

The results presented in this chapter found very similar results as the few other studies which have investigated the changes in MSG beaches following an earthquake event. The results found in this study largely support the findings of Stanley (1968) in terms of initial progradation of shorelines, as well as weak berm development in the initial year following the earthquake. Stanley (1968) believed berms would take more than two years to stabilise because of the fine sediment moving through the system, and the lag of gravel coming from the catchments to build up stable berms in the MSG environment. Single (1985) proposed that long-term response of an uplifted beach involved erosion of the nearshore profile until wave energy returned to its pre-earthquake position of maximum wave effect, which was then followed by erosion in the subaerial environment. Some results found in this study, such as Group 3 beaches which suffered subaerial volume loss between 2017-2018 surveys, have indicated trends similar to those discussed in the Single (1985) model, where profiles have initially gained volume immediately after the earthquake, then began to erode the subaerial environment as the beach responds. The short term erosive response at these sites however may be more indicative of poor sediment supply to the profiles, as opposed to the quick erosion of the nearshore environment.

Paterson (2000) believed that the uplift of the beach profile would promote initial progradation and accretion due to the dissipation of wave energy further out from the beach, and reduce erosional wave energy acting onshore and removing sediment. All sites in the study that were uplifted underwent initial progradation and volume gain, and some continued to do so between

the 2017-2018 surveys. Group 1 profiles had varying response where some continued to accrete between the 2017-2018 survey, while others stabilised or began to erode. The rate at which the Kaikōura beaches fully recover from the earthquake may be dependent on a number of variables that were not fully understood in Single's (1985) and Paterson's (2000) studies, such as the pre-earthquake state of the beaches, and an understanding of the environmental conditions acting on the beaches immediately prior to and following the earthquake.

There are several possible environmental conditions which may influence the rate at which the beach profiles respond to the earthquake event. The first main influence to consider is the sediment supply to a profile, as identified in Chapter 5. Following an earthquake, there will be pulses of fine sediment down a catchment, followed by some delayed pulses of coarser sand and gravel, as the heavier gravel material will take longer to move down a catchment to the beach system (Stanley, 1968). An additional source of sediment to the profiles is the fine sediment being eroded from the nearshore as the post-earthquake position of maximum wave effort reworks the nearshore environment in order for it to return to its pre-earthquake position. These additional sources of sediment to the system create the assumption that along with the additional sediment from uplift, an accretional trend would occur across all profiles due to more sediment being reworked into the system. At some profiles in this study, when the uplifted 2015 profile is used to simulate the immediate uplift following the earthquake, profiles are seen to have gained additional sediment beyond the initial uplift between 2015 and 2017. These initial additional volume gains could be a temporary change as the beaches adjust to the change in sediment budget with increased fines following the earthquake. This initial gain then loss of sediment is recorded at several Group 3 sites located along the Esplanade, while Group 1 and 2 profiles were more inclined to redistribute sediment relative to berm forming, whilst also continuing to gain in sediment volume from 2017–2018.

MSG beaches have high energy wave climates, and therefore while fine pulses of sediment may be added to the system by eroding nearshore beds or from pulses down the catchment, they may not last in the beach profile long, as fine sediment that is not reworked into the beach profile will likely move offshore. The addition of sediment to the system will only result in accretion at a profile if it is the right material. The addition of material to profiles beyond what was uplifted suggests that there is some addition of sediment of the right texture in the nearby area which causes some short term accretion. There is an initial spike in volume gain following the uplift which could be a result of the additional fine sediment which quickly moved down the catchment working its way through the beach system, following this the rate of accretion at a profile slows as the pulses of sediment reduce in frequency and size as time passes following the earthquake, and the sediment source returns to producing pre-earthquake volumes down

the catchment. In the initial years following the earthquake, trends will be altered due to these changes to the sediment budget, but eventually the environmental conditions will return to pre-earthquake conditions and the long-term response of the MSG beach will begin.

Sediment supply was determined to be an important factor which influenced the classification of MSG within-type variations, where Group 1 profiles were sediment traps which had a clear path alongshore from a sediment source to where sediment could accumulate. Group 2 profiles had good sediment supplies due to close proximities to sediment sources but would fluctuate due to their exposure on the open coast, and sediment coming down from the catchment moving through the profiles. Group 3 profiles were typically sediment deprived due to barriers blocking sediment from moving alongshore in the swash zone, or due to distance from a sediment supply meaning that sediment would not be transported that far along the coastline. There is a clear underlying theme in the geomorphological beach response: beaches which had accretional and dynamic trends pre-earthquake will resume accretional trends post-earthquake due to the continuation of environmental conditions in a post-earthquake environment, as well as the changes such as nearshore wave dissipation and increase in sediment supply. These profiles will likely take longer to return to their pre-earthquake profile as they continue to grow in the initial years following the earthquake. Beaches with erosional trends pre-earthquake were eroding because of the sediment deprivation at the profile. These trends continue at the profiles post-earthquake, where even if there is an increase in sediment budget to the whole coastline, these sites are not likely to receive any of it. These beaches will retreat to their pre-earthquake profile extents significantly faster than profiles which exhibited pre-earthquake accretional trends.

A Kaikōura-specific environmental condition which could change the rate of response for MSG beaches is the fact that many profiles are located with rock shore platforms in the nearshore environment, especially profiles located on the eastern edges of the Kaikōura Peninsula. In Single (1985) model, the position of maximum wave effect steps out seaward as the profile is uplifted, and the response of the beach is dependent on the erosion of the uplifted nearshore until the position of maximum wave effect transgresses and begins to act on the subaerial environment as it did pre-earthquake. The rate at which the nearshore will erode is indicative of how long it will take until the subaerial beach will respond. This could be influenced in Kaikōura if the position of maximum wave effect steps off the rock shore platform, or if the nearshore environment is composed of consolidated limestone. The response rate when eroding the nearshore bed of fines is relatively slow and on a decadal scale in accordance with Singles (1985) model; however this could be slowed even further if the position of maximum wave effect needs to erode through consolidated limestone rock. Studies on the rates of limestone inter-tidal platforms erosion show that the rate at which these platforms erode is very slow ( $1.48 \text{ mma}^{-1}$



(Stephenson and Kirk, 1996) to  $1.53 \text{ mma}^{-1}$  (Kirk, 1977)) and the erosional process is largely driven by the wetting and drying processes in the inter-tidal zone (Stephenson and Kirk, 1998). The rate of response, therefore, would be slowed significantly by this process. This process does not appear to affect the beach profiles used in this study, but it may have a pronounced effect on beaches near the more eastern edges of the Kaikōura Peninsula. Pieces of rock shore platforms were uplifted out of the water and above the inter-tidal zone after the earthquake, especially in the South Bay and Esplanade areas, and these may also be having an impact on wave dissipation and longshore sediment transport. This concept will be discussed further in the subsequent chapter.

### 7.4.2 Sedimentological response

The sedimentology results presented in this chapter are the first sedimentology results produced since Dawe (1997) in the study area, despite numerous consents being granted for renourishment of the Esplanade. The DGS technique used is designed to create grain size distributions on many different surface types, including MSG beaches (Buscombe, 2013). The field notes and images taken at the profile along with the images collected for the analysis in the DGS software all produced similar results, and therefore the results produced were not largely different to what was predicted with the human eye.

The difficulties analysing the results of the MSG sedimentology data largely lies with the across-shore and vertical mixing of sediment, meaning that a small sample is not a fair representation of what is occurring in the system. There are significantly varied sediment patterns across-shore and alongshore on MSG beaches which are not fully understood. McLean (1970) and Dawe (1997) have conducted research to investigate the sediment patterns along the Kaikōura coastline, however these two studies were 27 years apart, similar to the 21 year period between this study and Dawe (1997) data set. The lack of long-term data means that unless there is a large and uniform identifiable change in the sedimentology across a larger area, it is difficult to determine what changes are a direct result of the earthquake, and what changes are just due to the natural evolution of the beach itself over the 21 year period. An increase in fine grained sediment would be expected in the beaches in the months following the earthquake, as lighter sediment would move down the catchment quickly, whilst gravel may take up to decades to move down the catchment.

Following the September 4th 2010 earthquake in Christchurch, there was an increase of fine sediment in the beaches from 3% to 40% only 4 months after the earthquake (Taylor, 2013; Hart et al., 2015). The increase in fines contributed to beach erosion and scarping along the

beach. In the subsequent 3 years after the earthquake, the fines winnowed out of the system. If there was an increase in fine sediment along the Kaikōura coast following the earthquake, the high energy environment along the coastline would likely winnow out the fine sediments from the beach profiles quickly, and therefore it is difficult to attribute the increase of sand at a profile directly to the earthquake. The coastline is situated close to the Kaikōura ranges, and is well connected, and therefore the fine sediment would likely make its way to the coastline within weeks to months following the earthquake, then winnow out quickly as the sediment is reworked in the high energy environment. Therefore, the changes to sedimentology caused by the earthquake are likely to be reworked by the high energy environment, and are more indicative of longer term changes in the environmental conditions acting on the profile, especially wave climate and sediment supply, rather than a direct result of the earthquake.

The lack of data collected over this region to track sedimentology changes is the biggest barrier to interpreting these results correctly. As stated above, the poor representation of one sample at a site is off putting for many people conducting research on MSG beaches, as well as the time consuming and laborious techniques involved in sieving and sorting the sediment. The DGS analysis method is a quick technique to collect and process sedimentology, and what may be sacrificed in small detail, is made up for with the seamless nature of the technique. While little is known about the sedimentology patterns in MSG beaches, a larger, annual data set would be a first step in addressing this issue. DGS analysis is an attractive option for future collection of sedimentology data.

## 7.5 Conclusions

The beach profiles analysed in this study have undergone significant changes following the 2016 earthquake, and the morphology of the beach continues to change in response to the tectonic disturbance. The beach profiles responded relatively similarly within their within-type groups. The main trends were discovered in volume change, in which all groups gained volume as a result of the uplift of sediment into the subaerial zone of the profile, however the rate of which these profiles continued to accrete or erode between the 2017–2018 profiles differed depending on their geomorphic groups. Shoreline progradation and transgression followed very similar trends shown through volume change analysis. Berm redevelopment was occurring relative to the new sea level at most profiles, however the rate at which these berms redeveloped differed also between geomorphic groups, with Group 3 profiles having redeveloped the most stable berms post-earthquake, with Group 1 profiles only redeveloping stable storm berms. Sedimentology data suggested that there was now more sand present at the profiles than seen in 1997, however

it is not conclusive as to whether this was a result of the earthquake or the development of the profile over the 21 years since the data was last collected. These results will be discussed in the following chapter, and will be used to inform a broader conceptual response model.

# Chapter 8

## Discussion

### 8.1 Introduction

As first stated in Chapter 1, the overall aim of this research is to further our understanding of how MSG coastal environments respond to a large tectonic events where there is an earthquake-induced change in relative sea level. Following an earthquake, beaches respond to significant changes to environmental conditions, including the change in relative sea level and sediment supply. This chapter will broadly discuss the results presented in Chapters 5, 6 and 7 to inform conceptual response pathway models for the different variations of MSG beaches found on the Kaikōura coastline, as well as discuss the implications of seismic activity in coastal resource management in New Zealand herein.

### 8.2 Conceptual response pathways

Four conceptual response pathway models have been developed using the results found in this study, combined with findings of various other authors (Single, 1985; Paterson, 2000; Brown, 2017). The results from this study were able to inform the shorter term response, whilst previous studies provided details for the longer term response. The results in Chapter 5 showed that there are three main within-type variations of MSG beaches on the Kaikōura coastline. These groups, classified based on a variation of geomorphic parameters, represented the different environments along the coastline, as well as the variations of MSG beach types existing within the study area. Sediment supply and sediment transport to each profile were primary factors which polarised the three groups. Prior to the earthquake, Group 1 profiles had a long-term

accretionary trend, and geographically the profiles in this group were located in an area which would be considered a sediment trap. Group 2 profiles had different geomorphic properties to Group 1, however these profiles had long-term stable/accretionary trends, in which the profile varied significantly from year to year due to sediment pulses moving alongshore and passing through the profile. Group 3 profiles primarily had erosional trends, and were narrow profiles with little sediment supply.

As identified in Chapter 7, the response of the beach profiles followed similar patterns in terms of volume and shoreline change, as well as beach shape change within their group. As a result of these findings, there were two predominant trends in which the beaches were responding in the short-term post-earthquake environment: accretionary profiles and erosional profiles. The difference between these two profile responses was primarily that pre-earthquake erosional profiles were found to be retreating back to pre-earthquake extents 22 months after the earthquake, whilst pre-earthquake accretional and dynamic beaches had a increased/stable sediment supply which promoted growth or maintaining of the increased volume caused by the earthquake uplift. From herein, Group 3 profiles will be referred to as erosional profiles, while Group 1 and 2 profiles will be referred to as accretional profiles.

The conceptual response pathway models presented in this chapter use Single's (1985) response model to inform the longer term response of the conceptual model. There are several limitations and differences between Single's (1985) model to this conceptual model which need to be acknowledged, due to the lack of data availability following the Napier earthquake, of which the models presented in this chapter have attempted to address. The first is the time period which this research has informed is for the first 1-2 year response of a MSG beach, while Single (1985) addressed the response on a decadal, long-term scale. Data availability could not inform the pre-earthquake environment or the immediate post-earthquake environment in Napier in his study, and therefore the response was produced looking at long-term, historical scale responses.

Single (1985) addresses a response model using profiles as a 2D approach, and 3-Dimensional (3D) approach which is inclusive of volume. The increase in sediment volume to the profile in Single (1985) is primarily attributed to the increase from the uplift of the 2D profile, and no longshore transport is assumed. The conceptual models presented in this chapter acknowledge the important role longshore sediment transport plays in these systems, as well as the increase in sediment budget following an earthquake due to the influx of sediment from landslide debris up the nearby catchments. The conceptual models acknowledge the changes in sediment budgets across the different profiles following the earthquake, where there is an expected increase in fines in the sediment budget following the earthquake, then pulses of gravel in the years following.

Single (1985) also believed that pre-earthquake the Napier beaches were in or near a quasi-

equilibrium state, and after the earthquake, these beaches were evolving back to an equilibrium steady state. His model, however, assumes that the beaches were in an equilibrium state prior to the earthquake, in which the beach response will be complete when the beach is of the same form as it was pre-earthquake in terms of profile shape. In this research, the 18 year pre-earthquake data set was used to determine trends of the different beach profiles prior to the earthquake in Kaikōura, where most profiles were proven to have accretionary or erosional profile states prior to the earthquake. While these beaches could be equilibrium in plan view, most are not in profile, and therefore these beaches are likely to be classified as quasi-equilibrium, working towards a steady state equilibrium in which there is no net sediment change in both planar and profile form. The difference in pre-earthquake beach state means that the long-term response may differ from Single's (1985) model. For example, if prior to the earthquake beaches had strong erosional trends, following the earthquake these trends may resume and could erode beyond the pre-earthquake profile. However, Single's (1985) model is the most commonly accepted long-term response model for this beach type to an earthquake event, and therefore the response model is applied here with caution to represent the long-term response in the conceptual models produced in this chapter.

The following will present the four different MSG profile responses to a 1 m fall in relative sea level. Two profiles represent the erosional and accretional profile response in a typical MSG beach environment found in Kaikōura. Two profiles represent the erosional and accretional MSG beach response in a Kaikōura specific scenario where limestone rock shore platforms are present in the nearshore. Estimated conceptual sediment budgets are aligned alongside the response profile to acknowledge the 3D component of the models.

### **8.2.1 Accretional profile response pathway**

The accretionary profile response pathway is presented in Figure 8.1. The first three stages of the model are informed by the results presented in Chapter 7, while stages four and five are informed by Single's (1985) model. The conceptual model (Figure 8.1) begins with the uplift of a pre-earthquake accretionary beach profile. Following the uplift, there is instantaneous progradation and an increase in volume due to sediment being uplifted into the subaerial zone. The position of maximum wave effect, the seaward extent in the nearshore where wave energy is moving sediment, is 'stepped' out in a seaward direction.

In Stage 2 of the conceptual model, months following the earthquake, storm berms will develop at lower elevations than the pre-earthquake storm berm, and there is unstable development of small berms at lower elevations than pre-earthquake elevations. In Stage 3 of the conceptual

model, 2 years after the earthquake, the initial berm redevelopment in Stage 2 has moved further up the beach profile, at elevations similar to pre-earthquake elevations. In addition to this there is growth and stabilisation of the storm berm, which builds up at an elevation similar to pre-earthquake elevations. Over this time period, the beach has maintained its volume and progradational changes following the earthquake, and some beaches with good sediment supplies will continue to accrete.

Stages 4 and 5 of Figure 8.1 represent the longer term response, as modeled by Single (1985). These stages are ‘faded’ out in the figure to represent the uncertainty in the long-term response at these profiles due to the knowledge of pre-earthquake trends at these profiles. The two stages show the nearshore is subject to slow erosion as the position of maximum wave effect erodes the nearshore, retreating landward back to its pre-earthquake position. In Stage 5, the nearshore has eroded, and the subaerial environment erodes back to a pre-earthquake profile form, with the position of maximum wave effect also returning to its pre-earthquake position. During this whole response period, the pre-earthquake storm berm has been uplifted out of the active beach environment, and experienced no changes. The old storm berm becomes a perched, relict part of the beach system in its backshore. These two stages are uncertain as the pre-earthquake conditions of the Kaikōura beaches do not equate to the assumed equilibrium beaches in Napier used to develop this model. Therefore, there is a possibility that this response will occur, however there is also a chance that the beach may continue to accrete.

The conceptual model shows that the responses in an accretional beach largely surround berm re-development relative to sea level, and slow eroding of the nearshore. The continued accretional trends of the profile are likely due to several factors, including a large and possibly increased sediment supply nourishing the area, as well as the dissipation of wave energy in the nearshore environment from the position of maximum wave effect stepping in a seaward direction following the uplift. A degree of dissipation of wave energy in the nearshore, comparative to pre-earthquake conditions, will last as long as the nearshore is eroding and the position of maximum wave effect is seaward of its pre-earthquake position. This process is consistent with the research of Paterson (2000) who found that uplift and wave dissipation in the nearshore promoted onshore accretion as a result of the lower energy environment acting on the subaerial beach in the post-earthquake Napier environment. Single (1985) found that the subaerial environment began to respond in full to the earthquake after the nearshore had eroded, and following this the subaerial environment eroded back to its pre-earthquake profile extent and shape. The conceptual model long-term response for accretionary beach shows the erosion back to pre-earthquake extents, however it is possible that if the beaches continue to have wave energy dissipated in the nearshore and a good sediment supply, these beaches

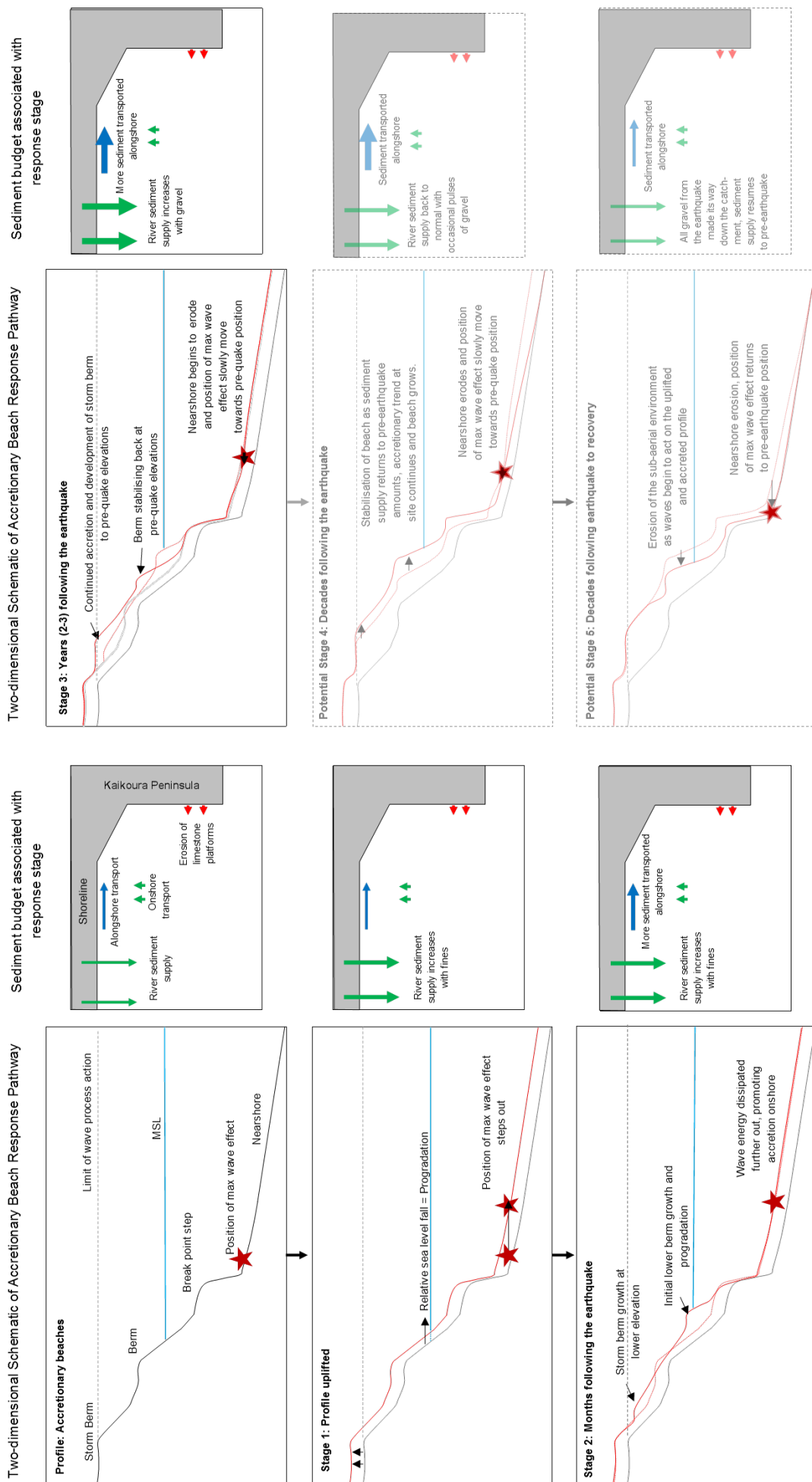


**Figure 8.1:** Conceptual model showing accretional beach response following an earthquake with their associated sediment budget on the right. This model indicates that when uplift occurs, the position of maximum wave effect steps out, there is an increase in sediment supply as fines move down the catchment. Over the subsequent months, berms build with the increased sediment budget at elevations lower than pre-earthquake berm elevations. In the years following the earthquake (Stage 3), there is still an increase in gravel sediment moving down the catchment and promoting further accretion of the beach. Stages 4 and 5 are faded out to represent the uncertainty of these model outcomes, due to the knowledge of pre-earthquake accretional trends. Single's (1985) model informs these two stages, however its unknown how accurate the fully response will be in this setting. Slowly, the nearshore will erode from the concentration of the wave energy in a seaward position, and the point of maximum wave effect will move landward. The old storm berm becomes a paleo beach, and undergoes no further changes.



may not erode back to their pre-earthquake profile extents, and the beaches could continue to accrete.

Following the earthquake there was also redevelopment of berms and storm berms at elevations lower than their pre-earthquake positions, and over a year later these berms had migrated to positions in alignment with pre-earthquake elevations relative to sea level and were deemed to be more stable. This process is consistent with Stanley's (1968) research which observed MSG beach changes following the 1964 Great Alaskan earthquake. Stanley (1968) found that weak berms developed following the earthquake due to the influx of fine sediment making its way down the catchment and to the profiles alongshore. He believed it would take over two years to develop stable berms as there was not enough gravel sediment to build these immediately after the earthquake, due to the lag in gravel transport to the coast. The conceptual model shows storm berms reforming at lower elevations in the initial few months post-earthquake, then migrating up the profile by Stage 2 back to pre-earthquake elevations. This is possibly a result of short time period between the event and the survey, where there may not have been enough high wave energy events to re-develop a berm at the elevations seen pre-earthquake, which developed over a series of storm events (Roberts et al., 2013).

The response will be severely influenced by the fact that these beaches had strong accretionary trends prior to the earthquake, and therefore this trend would be expected to continue after the beach profile had been uplifted. Additional sediment added to the sediment budget of these profiles needs to be of the right size, otherwise it will filter through the beach system and not stay within the profile. For example, the fine sands eroding in the nearshore are additional to the sediment budget, however it is unlikely they will make their way permanently into the beach profile due to their ability to being easily transported offshore (Stanley, 1968; Paterson, 2000).

The Group 2 profiles represented by this conceptual profile have less consistent pre-earthquake trends when compared to Group 1, as these profiles proved to be very dynamic and had the ability to accrete and erode by significant amounts from year to year. Since the earthquakes these profiles have rapidly increased in sediment volume and continue to prograde. The rate that these profiles are growing is higher than Group 1 profiles, and therefore based on these two short-term observations, Group 2 beach types are more likely to take longer to return to a pre-earthquake profile.

Two profiles which were originally considered to be Group 3 profiles based on geomorphic parameters, KCK3800 and KCK3855, shared a response path in common with other accretional profiles, as opposed to responding in a similar way to other Group 3 erosional profiles. Another anomaly was KCK4700, which significantly eroded following the earthquake, however there

was no tectonic component to this profile as it did not undergo any uplift, and therefore was not considered for interpretation in the conceptual model. The post-earthquake response of KCK4700 will be discussed in a later section.

### 8.2.2 Erosional profile response pathway

The erosional conceptual response pathway is shown in Figure 8.2, and is representative of profiles from Group 3, which did not have a sufficient sediment supply due to physical barriers preventing alongshore swash zone sediment transport to these profiles. Stage 1 of the conceptual response pathway shows there was an initial gain in volume, as the profile is uplifted, as well as progradation of the shoreline. Similar to the accretional response pathway model, the position of maximum wave effect steps out seaward as a result of the uplift. Stage 2 shows the profile response in the months following the earthquake, where both the storm berm and the berm are reformed at elevations similar to pre-earthquake berm elevations, relative to sea level, and the change in position of maximum wave effect is beginning to affect the nearshore bed.

In Stage 3, the first years following the earthquake, the storm berm has eroded, and the berm has continued to develop at an elevation relative to sea level and its pre-earthquake position. The erosion in the subaerial environment may be indicative of erosion in the nearshore, as suggested by Single (1985) in his post-earthquake model, however it is also likely due to the lack of sediment supply in the area not being able to supply the subaerial profile, and therefore the subaerial environment is being effected before the nearshore has eroded back to pre-earthquake extents. The position of maximum wave effect moves landward as the nearshore begins to erode. As the wave energy begins to act on the subaerial environment, the profile begin to erode back to its pre-earthquake shape and extent. This was demonstrated in the results of the 2018 survey, where erosional trends were found at these profiles, and most of these profiles had berm development in the lower profile, and erosion of the storm berm.

Stage 4 and 5, in the same fashion as the accretional response pathway model, are faded in Figure 8.2 to represent the uncertainty of the long-term response in beaches with long-term erosional trends. The long-term response modeled by Single (1985) would be more likely to take place in an erosional beach setting, as the profile will naturally erode back to its pre-earthquake beach extents. However, in this scenario it is likely that the beach will continue to erode past its pre-earthquake extents and create scarping at the back of the active beach. This profile response differs from the accretional profile, where the nearshore has mostly eroded back to a pre-earthquake position, and a limited sediment supply at the profiles mean that there is nothing slowing down this process. In Stage 5, the beach has responded in full, and the position

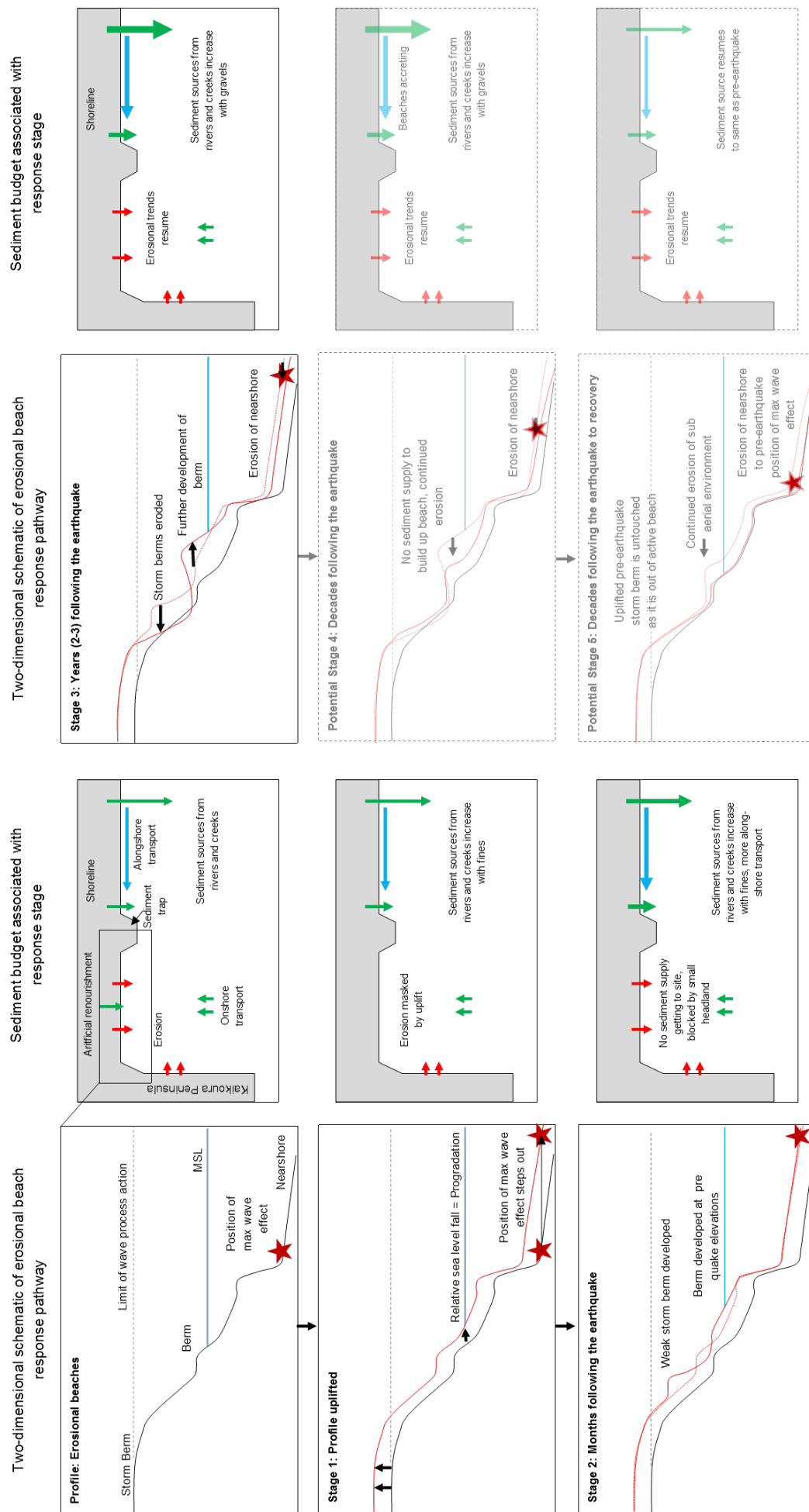


**Figure 8.2:** Conceptual response pathway for erosional beach profiles, which had poor sediment supplies and erosional trends pre-earthquake. Stages 1–2 demonstrate the immediate and short-term effects of the earthquake, where the old storm berm is lifted out of the wave action zone, and the foreshore is reworked to form berms relative to sea level, at elevations similar to pre-earthquake. Stage 3 shows the response in the years following the earthquake, where the uplifted profile is eroding back to the pre-earthquake position, where it will still continue to erode due to the lack of sediment reaching the profiles, and the pre-earthquake trends resuming. Stages 4 and 5 are informed by the Single (1985) model, however due to the knowledge that these beaches were eroding pre-earthquake, it is uncertain whether they will respond in the same way as Single's (1985) model. The continued erosion may erode away at the beach below the limit of wave process action, and cause scarping.

of maximum wave effect is back at the pre-earthquake position, the profile has eroded back to match the pre-earthquake profile shape. The backshore still maintained its elevation gain, as this part of the profile was not reworked by the wave energy acting on the beach system.

The erosional conceptual response pathway predominantly demonstrates erosional trends following the earthquake, which was an expected response given that these profiles already showed long-term erosional trends pre-earthquake. Despite the sediment pulses of sand and gravel from the catchment contributing to the sediment budget following the earthquake, the distance from the river sediment source, combined with the lag in time it will take for gravels to travel down the catchment and alongshore to these profiles means that it is likely the only increase in sediment budget for these profiles will be from the erosion of uplifted fine sands in the nearshore. MSG beaches are predominantly fueled by alongshore transport, not onshore–offshore transport (Kirk, 1980). Therefore, even if there was fine sediment that had made its way into the nearshore of these profiles, it is unlikely to make it onshore into the subaerial environment and stay in the gravel dominated, high energy foreshore. It is likely that the long-term movement of gravel pulses of sediment down the coast will not make it to these profiles, as alongshore transport it is stopped by barriers (Figure 6.2), and therefore the profiles will still continue to erode without a stable sediment source. The results of this study suggest that the rate at which these profiles will erode back to their pre-earthquake profile will be much quicker than an accretionary profile. Once the beach has reached its pre-earthquake profile extent, it is likely that the profile will continue to erode based on its pre-earthquake trend. Single (1985) believed that the erosion scarp at the storm wave runup limit could continue to erode until the wave energy can be totally dissipated on the foreshore, and erosion of the scarp will then only occur during significant high wave periods. The only influence which would change the erosional response pattern would be the introduction of a new sediment source to these profiles, for example by renourishment on the Esplanade, or movement of the Kowhai River back to its original outlet north of the Peninsula.

### **8.2.3 Rock shore platform accretionary response pathway**

Rock shore platforms are an unusual feature of the Kaikōura MSG beach study area, which are not considered in the Single’s (1985) model due to their absence from his Napier study area. The rock shore platforms are located around the Kaikōura Peninsula, and are made of consolidated mudstone and limestone, and can promote perched beaches upon these platforms, as can be described in various forms in Gallop (2012). These platforms can provide protection for the beaches in erosive events, and promote sand transport onshore (Gallop, 2012). Little

is understood about the state of the perched beaches in Kaikōura specifically, and the geomorphology surrounding these settings. None of the profiles used in this study fall into this category, however it is an important concept to introduce into this conceptual model, to be further expanded on in future research, as many beaches on eastern sections of the Peninsula in the study area are likely to have been affected by this. It should be emphasised that the following is a conceptual model which was not directly examined in this study, however it highlights the slow response period which is likely to occur should the nearshore bed of an uplifted beach consist of consolidated limestone.

Figure 8.3 shows that during the initial earthquake induced uplift (Stage 1), the limestone platform is uplifted into the pre-earthquake nearshore environment, and the position of maximum wave effect is stepped out seaward, as seen in the previous two conceptual response models. The position of maximum wave effect needs to erode the nearshore in order to return to its pre-earthquake position, and subsequently the beach can return to its pre-earthquake extents as described the previous two conceptual models. The erosion of the nearshore in this conceptual pathway will take a lot longer than the erosion of the nearshore in the previously discussed erosion and accretion pathway responses, as instead of eroding unconsolidated fines, the position of maximum wave effect has to erode through the limestone platform to return to its pre-earthquake position. While the position of maximum wave effect slowly (century scale) erodes away the nearshore, wave energy continues to be dissipated further seaward than pre-earthquake, and promotes further accretion of the perched profile if there is a strong sediment supply, with berms developing at pre-earthquake elevations (Stage 2).

Stages 4 and 5 of Figure 8.3 are faded to represent the uncertainty of long-term response in these specific environments, given that the both the pre and post-earthquake environments have proven to be very different to Single's (1985) model and assumptions. The significant difference between this conceptual model to the previous two is that following the uplift, the nearshore is consolidated, and therefore erosion of the nearshore environment will take significantly longer than the erosion of unconsolidated fine sediment in the previous two models. The erosion of the nearshore will likely take hundreds of years. Studies have shown that the limestone platforms erode in an intertidal environment at 1.130 mm/yr in Kaikōura, of which the erosion is mostly a result of wetting and drying (Stephenson and Kirk, 1998). Therefore, the rate at which the consolidated and submerged platform will erode is likely to be thousands of years. When this process is completed and the wave energy can act as it did pre-earthquake on the subaerial beach, and the subaerial environment will be reworked slowly landward towards its pre-earthquake profile, or with sufficient sediment supply, may continue to accrete.

The location of the beaches around the more eastern edges of the Peninsula means they are

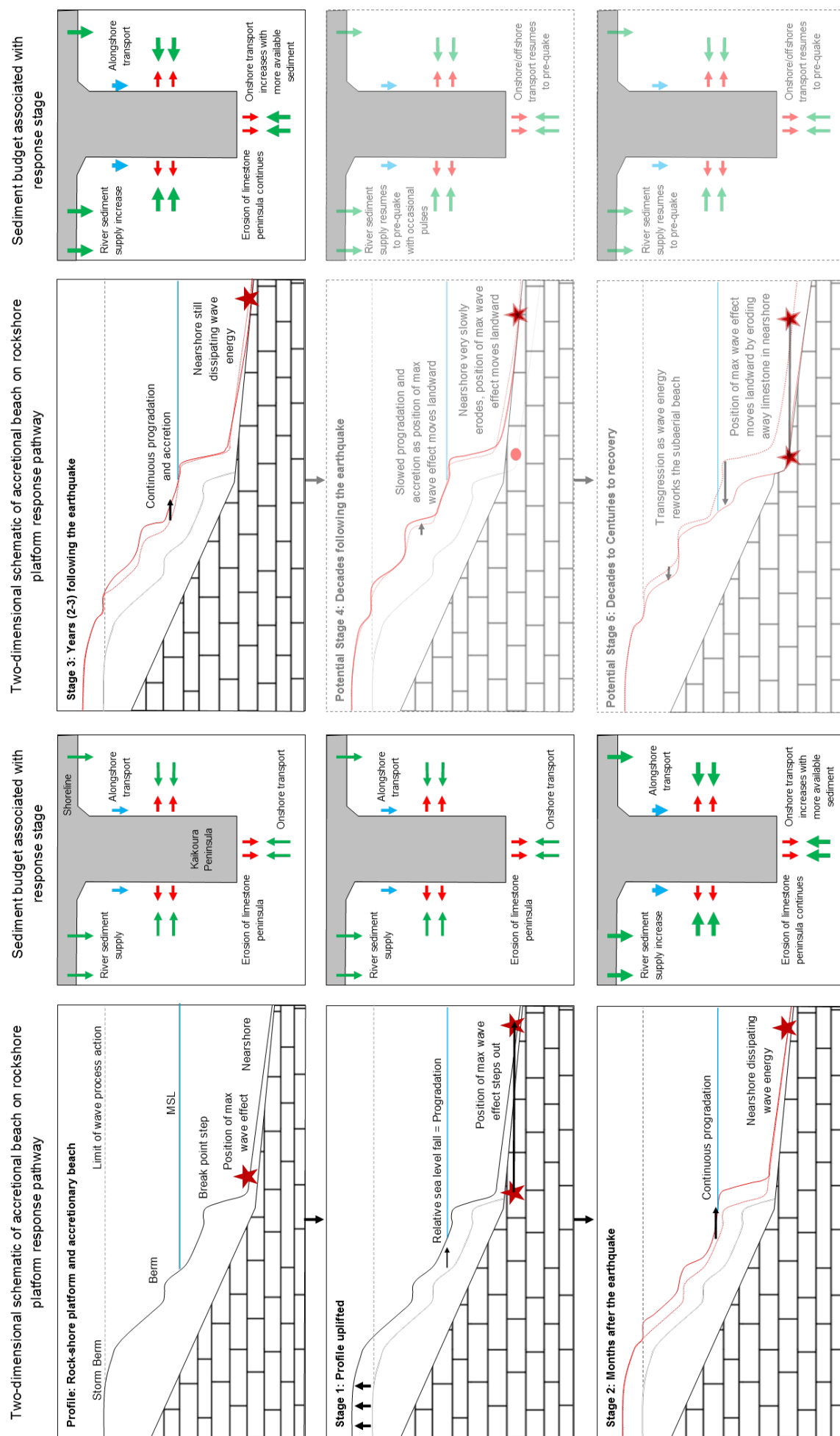


**Figure 8.3:** Conceptual response pathway for accretional beaches which are located on top of limestone platforms. The position of maximum wave effect is stepped out into the nearshore, and the rate of response is dependent on the rate at which the nearshore can be eroded, which is very long due to the nearshore being consolidated limestone. The erosion of the nearshore profile takes a long time because of slow erosion rate of consolidated rock. The max wave effect position slowly moves seaward, and in doing so wave energy reaches closer to the beach, and as this happens, the profile slowly retreats to the pre-earthquake profile extent. This response is likely to be on a several decades to century scale. Stages 4 and 5 are based on Single's (1985) model, and are faded out to represent the uncertainty that these responses will occur due to the differences in circumstances between the Kaikōura and Napier coastal environments.

largely dependent on onshore-offshore movement of sediment, as opposed to the alongshore transport which drives sediment movement seen in Figures 8.1 and 8.2. Low energy environments, enhanced by the dissipation of wave energy further away from the break point step, promotes onshore movement of sediment (Ciavola and Castiglione, 2009), which if there is a good sediment supply to the profile, there will be accretionary trends at the beaches. Following an earthquake, there may be an additional finer sediment availability in the nearshore environment which could be moved onshore, however additional gravel to the sediment supply following the earthquake would be unlikely to affect these beaches, due to the distance from the sediment sources, barriers blocking this alongshore transport, as well as the energy required to push gravel onshore in these environments. During the whole 5 stages, the uplifted pre-earthquake storm berm remains untouched, and creates a relict beach, unless wave washover occurs at the profile.

#### **8.2.4 Rock shore platform erosional response pathway**

The erosional response pathway for beaches located on the rock shore platforms is seen in Figure 8.4. The model shows that the predominant sediment characteristics of the profiles are onshore-offshore transport of sediment from the erosion of the limestone platforms, and the profiles are not reliant on the sediment supply from rivers, as other response models have demonstrated. This lack of alongshore transport and sediment availability means that there is erosion of sediment from the subaerial environment, as seen also in Figure 8.2. The uplifted profile steps out the position of maximum wave action, and over time, the limestone in the nearshore will erode away in order for the position of maximum wave effect to move back to its pre-earthquake position, as seen in the previous models. Similar to Figure 8.3, the rate at which the nearshore will erode is significantly longer in the consolidated nearshore environment than the unconsolidated nearshore environment demonstrated in Figures 8.1 and 8.2. Initially, as shown in Stage 1, there is some progradation after the uplift, from additional suspended sediment supply in the nearshore, and wave energy being dissipated further away from the beach, promoting onshore movement of the sediment, however this trend will likely change to erosional within the first few years of the earthquake, as seen in Figure 8.2.

In the years following the earthquake, the erosional processes which were occurring pre-earthquake will resume, and although the nearshore has not eroded back to pre-earthquake position due to the slow erosion of the consolidated limestone platform, the subaerial beach will erode back to its pre-earthquake profile, due to the lack of sediment supply to the profile. The only addition to the sediment budget at these profiles is the small amount of eroded nearshore consolidated

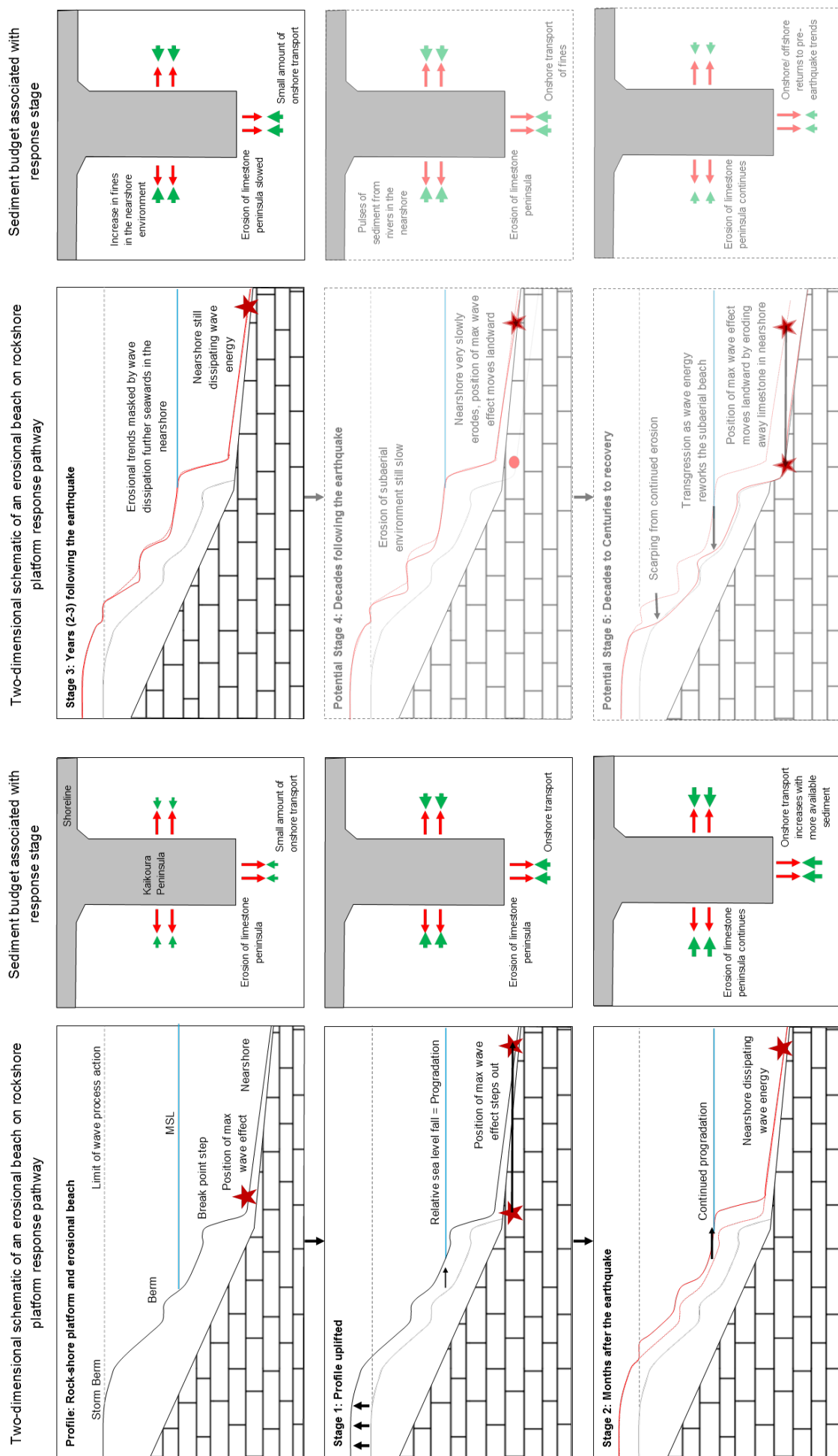


**Figure 8.4:** Conceptual response model for erosional beaches on limestone platforms. Uplift makes the position of max wave effect step out, and has to erode the limestone platform to return back to its pre-earthquake position. Progradation and accretion occurs in the initial months after the earthquake because there is more suspended sediment in the nearshore from distant sediment sources, and wave energy is dissipated further seaward than before the earthquake. The position of maximum wave energy very slowly begins to move landward. Over time, the lack of sediment supply to the profiles and the increased wave energy acting on the subaerial environment leads to erosion of the profile back to the pre-earthquake profile extents, potentially creating a scarp as it continues to erode back into the sediment below the limit of wave process action.



limestone and the position of maximum wave effect slowly moves landward, however as stated in Stephenson and Kirk (1998), the eroded sediment is so fine it is unlikely to rework into the beach system and is more likely to be transported offshore. The uplifted storm berm does not undergo any changes in the months to decades following the earthquake, and creates a relict beach in the backshore. As the subaerial environment erodes over time, the upper foreshore may erode away beneath the limit of wave process action, and a steep scarp may occur, eroding into the backshore environment if there is no washover. In terms of a long-term response which encompasses the erosion of the nearshore environment, both models described in Figures 8.4 and 8.3 will take centuries to recover their nearshore to pre-earthquake extents given the slow erosion rates of the consolidated and submerged limestone. Beaches with unconsolidated nearshores will have a significantly quicker recovery period in comparison.

### **8.2.5 Environmental conditions influencing response rate**

As addressed throughout Section 8.2, Single's (1985) model for beach response was not able to consider some factors which this study was able to address. The main difference between this study and Single (1985) was that it was determined in this study that prior to the earthquake a lot of the profiles were not in equilibrium or stable. Single (1985) could identify using aerial imagery some sites which he suspected were not planar equilibrium prior to the earthquake, based on the shape of the coastline and surrounding features. A limitation of the conceptual models presented in Section 8.2 was that the long-term response of beaches which are not in equilibrium is yet to be determined. However, this is a difficult task given the amount of variables which would act and change on a profile over a decadal scale response time period. When sediment supply and changes to the sediment budget are taken into consideration, the rate at which a beach will return to its pre-earthquake profile extent is affected. The conceptual response models presented demonstrate that the long-term response is likely to be influenced by the sediment available to the profile. In order to return to the pre-earthquake profile following an earthquake which has uplifted a beach profile, erosion will take place. Profiles with pre-earthquake erosional trends will continue to erode after the uplift, and will therefore return to their pre-earthquake profile extent quicker than accretionary profiles. The rate at which accretionary profiles return to their pre-earthquake form will be significantly slower than erosional profiles, and furthermore, sites with consolidated nearshore environments will take centuries to fully respond, due to the slow rate at which the nearshore can erode.

Another main factor which will affect the rate of response is climate change, and its associated effects with increase in storm intensities and sea level rise (Kay et al., 2015; Mullan et al.,

2016). An increase in storm intensity could lead to more significant erosional events acting on the coastline. This could impact the recovery of the beaches, as the erosion of the beaches will speed up the rate in which the profile returns to the pre-earthquake extents. Sea level is expected to rise by 0.5–1 m as a result of climate change by 2100 depending on the Representative concentration pathway (RCP) being modelled (Cazenave et al., 2014; Horton et al., 2014). The 1 m uplift of the coastline means that going forward, the backshore environment is in a more resilient position than prior to the earthquake. However, as stated above, the erosional beaches are still eroding post-earthquake, and therefore the uplift should be utilised as a ‘buffer’ for sea level rise, rather than a coastal development opportunity, as seen in Napier where uplifted land was utilised for a development opportunity, followed by ensuing erosion problems decades later (Single, 1985). The accretionary beaches, if not significantly impacted by the increase in storm intensities, will continue to thrive and the 1 m elevation gain will likely continue to have a positive effect on the beach. The erosional beaches, as seen in Figure 8.2, will maintain the elevation in the backshore, however any shoreline advances made as a result of the uplift will be lost in the response, and therefore the erosional beach types are only slightly better off in the face of sea level rise relative to pre-earthquake conditions, as the effects will still be of that predicted before the earthquake, however the elevated backshore will have slightly more protection now from events such as storm surges based on elevation alone.

In summary, beaches which exhibited accretionary trends prior to the earthquake, are likely to continue to do so in the long-term following the earthquake, and are more resilient now against sea level rise and events associated with climate change. Beaches exhibiting erosional trends prior to an earthquake are likely to retreat back to their pre-earthquake profiles quicker than accretional beaches, and are not as resilient against sea level rise and associated climate change events as accretional beaches. The uplift should, in both instances, be treated as a ‘temporary buffer’ for sea level rise, and the beaches should continue to be monitored to determine the further changes that these beaches will undergo in the medium-term response period, as well as how they respond to sea level rise.

### **8.3 Consideration of seismic hazards in coastal environments**

Typically, seismic hazards in coastal environments are largely focused on the tsunami impacts, a subsequent hazard occurring after an earthquake. Little consideration is had for the long-term impacts which result from coasts undergoing significant uplift, as the effects are usually

interpreted as a positive impact where beaches have more available sediment, both from increased sediment supply from landslide debris in catchments, as well as increased beach volume from more sediment being uplifted into the subaerial environment. Public misconception of the recovery of uplifted beaches is very prominent, especially due to the long-term response which is often longer than the average human coastal residence or lifetime (Single, 1985; Olson, 2010). Reports on areas currently affected by significant coastal erosion refer to the erosion being largely caused by the lack of earthquakes resulting in less sediment coming down the catchment to renourish the beaches (Allis, 2016). An example of this is the Granity, Hector and Ngakawau area on the West Coast, New Zealand, which is experiencing significant erosion that is suspected to be a part of the long-term trends at the site. Several reports investigating the erosion issue states that the beaches are dependent on the sediment input from catchments generated by slips and landslides in earthquakes, bringing sediment to the coastline to renourish the beaches (Ramsey, 2007; Allis, 2016). The report does not mention that the nearshore may be recovering from the 1929 Buller (Murchison) earthquake which was  $M_w$  7.8 and promoted 4.5 m of uplift in the nearby town of Westport, or furthermore the 1717 Alpine Fault earthquake (Yetton, 2000). The response of the nearshore in the decadal to century time scale following the earthquake, as demonstrated in Section 8.2, shows that once the nearshore has responded, the subaerial environment will likely erode due to the position of maximum wave effect moving landward (Single, 1985). Usually the time gap between the event and the erosional response is quite significant, leaving a lot of time for the societal impacts of the event to resolve and the community to move on. Furthermore, in a dynamic coastal environment, it could be perceived that these systems would respond in a much quicker time frame, and therefore effects 80 years on may not be attributed to such event. However, the long-term response of the nearshore and its associated effects with subaerial erosion years on from the earthquake should be considered in a tectonically active country. Coastal erosion is a modern day issue along the Napier coastline, where erosional trends along the coastline are largely attributed to the deformation of the coastline following the 1931 Napier earthquake, where the effects of this tectonic event are acknowledged as a possible cause for modern erosion despite the historical nature of the event (Komar, 2010).

The infrequent nature of these large tectonic events means that the importance of them in a coastal setting can often be overlooked, or forgotten. In a tectonically active country, such as New Zealand, the beaches are significantly influenced and shaped by seismic activity. This can be by the instant uplift causing relict beaches in the backshore, to river aggradation affecting the sediment budget, to the slow long-term recovery of the nearshore. Tectonics are not acknowledged as a coastal process effect in many conceptualisations of coastal geomorphology (eg. Cowell and Thom, 1994). Many theories have been largely developed in countries which

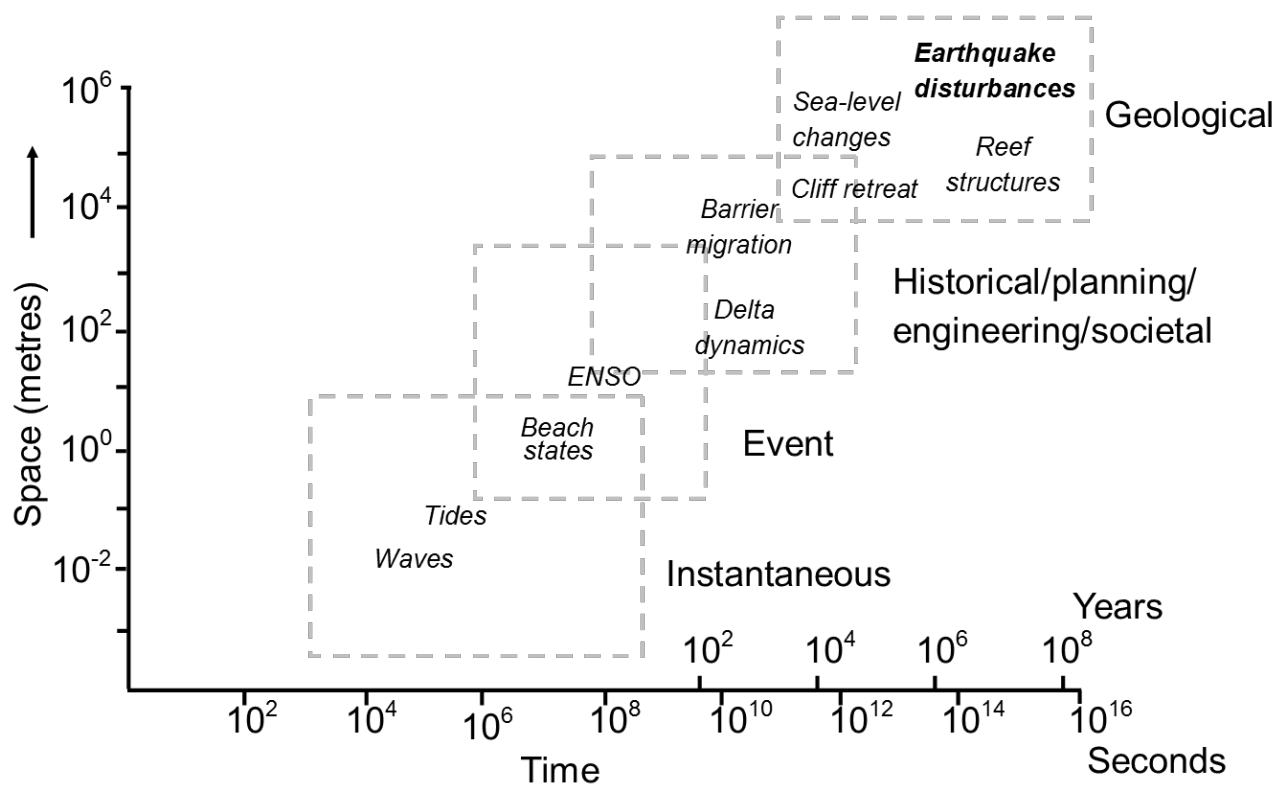


**Figure 8.5:** A temporal and spatial representation of coastal processes which affect the coastal morphology. Earthquake disturbances has been added to the conceptual diagram in the geological section due to the long return interval of earthquakes, and the response period of its sub-sequential hazards and impacts. Earthquake disturbances encompasses all short and long-term effects of the earthquake, including tsunami inundation to river aggradation, to long-term nearshore adjustments. Adapted from Woodroffe (2003) after Cowell and Thom (1994).

are not as tectonically active, and therefore tectonics do not have such a distinctive presence in coastal morphology, such as in Australia and Britain. New Zealand is very tectonically active, and therefore consideration of seismic activity needs to be acknowledged as a prominent process affecting the geomorphology of the coastline. Figure 8.5 shows how tectonic activity would be incorporated into the Cowell and Thom (1994) conceptual model, later adapted by Woodroffe (2002).

Figure 8.5 shows that tectonics as a process encompasses a large range of spatial and temporal components of the model, and affect the coastline on a geological scale due to the long return intervals. On a short-term temporal scale, tectonics cause instantaneous change over a large area. Subsequently, tsunamis can occur in the hours following an earthquake, which can have a detrimental impact on the sediment supply directly on the beach, as described in Paris et al. (2009), where 275,000 m<sup>3</sup> of sediment was eroded along a 9 km stretch of coastline in Sumatra, Indonesia. Impacts from the earthquake continue to shape the coastline throughout the entirety of the time scale, with different environmental disturbances continuing to effect the recovery period of the coastline until the next earthquake occurs, over the long return interval between

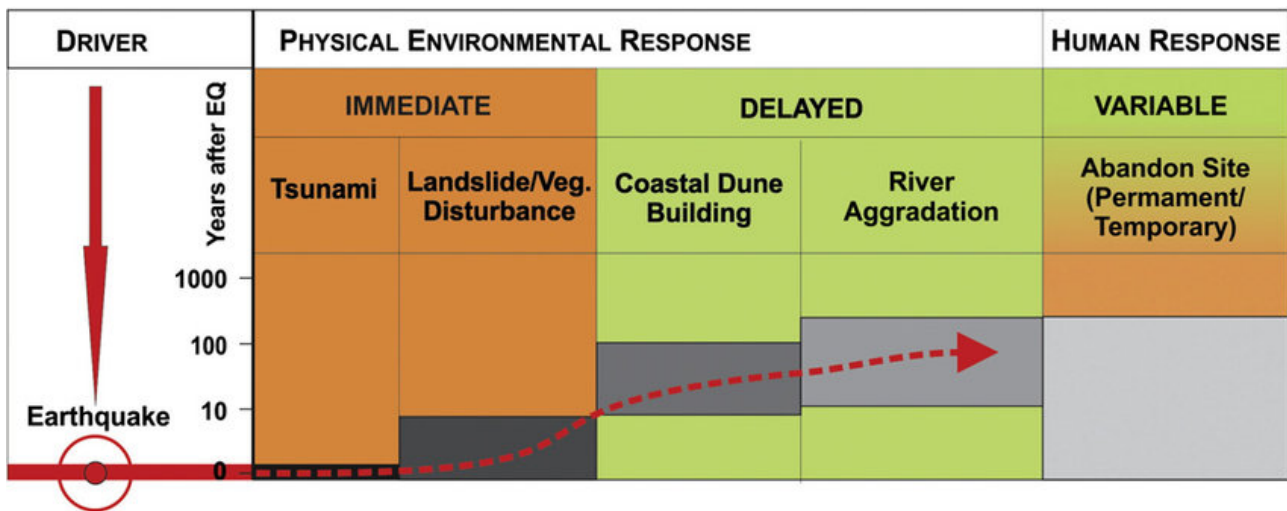


**Figure 8.6:** Seismic Staircase model that shows that immediate and delayed responses of the sand beach environment following an earthquake. The responses of humans are variable, but can be both immediate and delayed (Taken from Goff and McFadgen, 2002)

events. As seen Goff and McFadgen (2002) seismic staircase model (Figure 8.6), progress from the tsunami to the landslide and vegetation disturbance between between 0–10 years after the earthquake. Following this, in a sand beach environment, there is coastal dune building between 10–100 years, with river aggradation happening from 10–200 years following the earthquake. Paleo-beaches occur with the abandonment of the storm berm as it is uplifted out of the limit of wave process action, and will historically mark the amount of uplift which occurred if not destroyed by washover, erosion or a tsunami after the event.

In summary, tectonics play a significant role in shaping New Zealand beaches, over various spatial and temporal scales. Most New Zealand beaches are reliant on ‘injections’ of sediment through tectonic events, caused by the landslides and associated sediment travelling down the catchment as a result. Tectonic activity reintroduces sediment to the coastline, and when uplift occurs erosional trends can be masked for a period of time. The infrequency of large events means that the long-term response component of these events are often forgotten. A large amount of research in regards to coastal processes comes from continents which do not experience seismic activity on the same significant scale. The inclusion of tectonics in these models, and the acknowledgement of these processes in coastal geomorphology is necessary for global applicability in future iterations to ensure that the consideration of historical events is accounted for when assessing the erosion hazard on coastlines which will experience sea level rise in the future.

## 8.4 Implications for Kaikōura coastal resource management

The Kaikōura coastline is significant to the local community and tourism industry, in terms of the natural beauty of the landscape features, the opportunities for recreational use and the unique biodiversity which resides there, which are all utilised to create economic opportunities to drive tourism and other coast dependent industries within the local area. The results from this study have shown that following significant uplift in a coastal environment, erosional trends at a profile can be initially masked, but eventually a lack of sediment supply to a profile will result in the continuation of erosional trends. The uplift essentially acts as a ‘buffer’ for coastal events following uplift, however the buffer should not be perceived as a permanent change to the coast. Prior to the earthquake, Group 3 profiles located along the Esplanade were renourished using sediment extracted from South Bay for 18 years 3.5. The consent for the renourishment was renewed in 2016 (OCEL Consultants NZ Ltd, 2016). The long-term trend analysis for these profiles (presented in Chapter 5 and seen in more detail in Appendix A) showed that the renourishment was effective in masking erosional long-term trends, however there were still periods of erosion following renourishment. The uplift of around 1 m in this area masked initial erosional trends and provided more sediment in the subaerial environment between the November 2016 earthquake and the January 2017 survey. The results then showed erosion was occurring between 2017 and 2018. An implication for resource management in this area is that these sites need to continue to be continuously monitored over the coming years to ensure that the uplift is not misconcieved as being a long-term solution to the erosional problems along the Esplanade. Renourishment may need to be undertaken at these beaches again in the near future, as these beaches are likely to erode quickly to their pre-earthquake profile, and continue to erode if not renourished.

Another resource management issue which has drawn attention in this study is the mining of alluvial gravels in the Hāpuku River, and the direct implications south of the rivermouth at profile KCK4700 where the profile has undergone significant erosion since the earthquake. At the time the survey was taken, gravel extraction from the Hāpuku River was taking place, as per the consent granted in May 2017 to extract gravel until May 2019 (Environment Canterbury, 2017). The significant erosional trend following the earthquake recorded at this profile (Figure 7.4) was not outside of its long-term envelope, and the profile was also not recorded to have uplifted by anything following the earthquake. The consent states that the during excavation, all efforts should be undertaken to minimise erosion of the Hāpuku River bed, and to minimise the discharge of sediment to the Hāpuku River (Environment Canterbury, 2017). The consent

does not state a total limit of how much gravel can be extracted, only that stockpiles must not exceed 10,000 cubic metres. There is no mention in the consent about the implications on the coastal systems with the extraction of its sediment supply. A delayed response of the earthquake will be river aggradation (Figure 8.6), and management of this will eventually need to be undertaken to ensure the water levels of the rivers do not exceed the river banks. If the extraction of alluvial gravel at the Hāpuku River was for this purpose rather than commercial reasons, steps could be taken to introduce this sediment to the coastal environment, as opposed to removing the sediment from the catchment supply, which will have an effect on the sediment budget of the coastline. The coastline between the north of the Peninsula and the Hāpuku River is heavily reliant on the sediment from the Hāpuku River. If the mining is the cause or a contributor to the erosion at KCK4700, then this may have a flow on effect to sites further south if the mining continues as the beaches nearshores begin to erode and the subaerial environments begin to be reworked to their pre-earthquake extents. Caution should be exercised when granting these consents in the future, and part of the consent application should require a detailed coastline impact assessment on how the amount of gravel extraction will effect the Kaikōura coast.

The South Bay area recently underwent changes in the backshore of profiles KCK2470 to KCK2496, where the area has been infilled with gravel and limestone chip and converted to a freedom camping site. The profiles here are accretionary beaches, which are likely to continue to thrive following the earthquake, however this knowledge was not available to the Kaikōura District council when the decision was made to change this site. There was also no coastal consent granted by ECan to infill the coastal site, and there was also no coastal impact assessment undertaken. Fortunately, this research showed that the South Bay sites predominantly have an accretionary trend after the earthquake, however this may not be the case in a few decades when the nearshore begins to retreat. More consideration needs to be taken when developing coastal land after the earthquake. The uplift should be merely considered a buffer for the time being, as eventually the additional beach gained from the earthquake may erode away.

In the face of sea level rise over the next 100 years and beyond, it can not be expected that a predicted 1 m sea level rise by 2100 has been cancelled out by 1 m of uplift. While the backshores will remain 1 m higher than prior to the earthquake, the reworking of the beach sediment over time will result in most instances with the retreat of the beach profile and the shoreline back to pre-earthquake profile extents. The rise of sea level will therefore still have an impact on the beach, and any increased storm frequency and intensity associated with climate change could continue to further impact the coastline. The impact of the uplift is positive, and the Kaikōura coastline will be more resilient than it was previously, however the coastline

should continue to be monitored to determine the rate of the retreat of the beaches as sediment gets reworked through the coastal system, and it should not be a given that areas which were uplifted are in the clear from sea level rise. Coastal hazards will be evolving over the coming years as the beaches respond to the earthquake, changes in sediment, and the associated effects of climate change and sea level rise. Consideration of these current and future issues needs to be accounted for in the Kaikōura District Plan, as well as the Regional Coastal Environment Plan. This will ensure that development near the coast (eg. South Bay freedom camp site), or activities which will have an effect on the coast (eg. gravel extraction at the Hāpuku River) will have to consider the current and future state of the coastline as it responds to the earthquake and climate change, of which hazard considerations which are alluded to in Objective 5 of the New Zealand Coastal Policy Statement (NZCPS, 2010).

## 8.5 Surveying in post-earthquake environments

This study has highlighted the difficulties with collecting and analysing data that relies on the geodetic system following an earthquake. The lack of research and protocol available means that there is potential for earthquake disturbances to be recorded differently after event ( eg. re-measuring using the geospatially correct line vs re-measuring using the physical line). A distinction between the two lines needs to be understood, and going forward, protocol for this type of event needs to be created so that nationwide, the methods used to record disturbances are consistent. This research used the geospatially correct line, as explained in Chapter 4. It would be proposed that from herein, the re-surveying of Kaikōura beach profiles uses the geospatial line, and physical benchmarks are realigned to this geospatial line. Furthermore, in future tectonic events in New Zealand, it would be suggested that the geospatial line method is also used, so the recorded disturbance in the historical data set is uniform across the country, and there is no confusion over what has actually been measured.

An apparent issue prominent in this research was the slow recovery of the geodetic system after the earthquake, as a result of the accessibility to the area, and the timely nature to remodel the NDM due to the area being continuously affected by aftershocks in the years following the earthquake. There is the option of creating a control framework to conduct the surveys, which is recommended by LINZ following an earthquake, however in the instance of the Kaikōura Earthquake, the control framework created was still vertically out by about 1 m when adjusted to the finalised NDM patches applied to the geodetic system.

The collection of LiDAR and aerial imagery after an earthquake is popular because if collected with a built in GNSS positioning system, data can be collected without the need for the geodetic



system to be re-established, and change from the earthquake can be accurately determined on a local or regional scale. As presented in Chapter 6, in order to obtain data to inform the conceptual models and the level of detail required for this research, beach profile surveying is the only technique explored in this study which could provide this level of detail. LiDAR data is useful in the sense that it can be used to determine the change in the area at a metre resolution scale (as seen in Kaikōura case study), where vertical accuracy is within 15–25 cm. The resolution of this data is not high enough, however, to obtain detailed information about beach shape change, where berm shape change and movement can not be accurately depicted. Aerial imagery can often be higher resolution than LiDAR, however lacks the vertical component required to determine the changes in elevation following the earthquake.

When addressing the issue of what is the correct way to survey following an earthquake, it is difficult to suggest a robust procedure which can be used following an earthquake to determine changes in such detail required for this study. In the interest of coastal geomorphology, beach profile surveying should be undertaken as soon as possible following an earthquake, within the constraints of avoiding hazard exposure and gaining access to the sites. ECan's approach of creating their own control framework following the earthquake is the most viable option available in order to be able to collect data in the interim period between the earthquake and re-establishment of the geodetic system. By measuring the geospatially correct line in the field, it means that it is a seamless to compare collected field data with spatially accurate LiDAR data to refine the accuracy of the survey data taken using a created control framework. The data collected can be compared to LiDAR to see how vertically accurate the survey was, with 15–25 cm being an acceptable error between the two due to the difference between LiDAR and beach profile survey techniques' error margins. The data can be recalibrated to the re-established geodetic system in the years following the earthquake to ensure greater accuracy. This research highlights the need for survey data to be collected in the initial months and years following the earthquake to ensure these recovery periods are captured in detailed surveys.

## 8.6 Conclusions

This chapter has presented the conceptual models developed through the collection and analysis of beach profile surveys and LiDAR imagery, and presented them in both erosional and accretional environments following an earthquake. More specifically, the models showed what beach response may look like around the limestone peninsula environment, where the response time would increase as the nearshore would have to erode away limestone platforms in order for the position of maximum wave effect to return to a pre-earthquake position. The rate at which

the profile returns to a pre-earthquake position and beach shape is dependent on the sediment supply to the profile, the changes in the sediment budget as a result of sediment coming down the catchment from landslides, and the dissipation of wave energy seaward due to the uplift of the profile. The conceptual models highlight vital role of tectonic activity acting on New Zealand beaches, giving boosts of sediment to the budget, and uplifted profiles to create relict beaches in the backshore. Here, earthquakes largely shape the continuous changes to coastal geomorphology, and show that the temporal scale at which these beaches respond is large enough to interfere with other processes acting on the coastline, such as relative sea level change. The importance of acknowledging the lasting impacts of earthquakes on the coastline means that there are implications for resource management, and misconceptions of how beaches fare in the wake of these events can often be detrimental to resilient long-term planning, as seen in Napier. Despite the positive impacts of the uplift on the Esplanade, the previously eroding part of the Kaikōura coastline should continue to be monitored to ensure it can be managed as it quickly retreats back to its pre-earthquake profile state. In order to collect this information to be able to monitor the changes of the profiles following the earthquake, the geospatially correct line should be measured, for ease of comparison with LiDAR data when the geodetic system has not yet been re-established. A control framework in the area should be generated, however caution should be exercised when interpreting the initial results of the surveys, as the control framework will need to be recalibrated as the NDM is updated.

# Chapter 9

## Conclusions

The aim of this research was to further our understanding of how MSG coastal environments respond to a large tectonic events where there is an earthquake-induced change in relative sea level, and three main objectives were used to do this.

### 9.1 Key findings

Objective one of this research was: *To establish the previous long-term trends of the unconsolidated coastal environments in Kaikōura, through the means of geomorphology and sedimentology.*

This objective was accomplished by determining the within-type variations of the Kaikōura coastline using both geomorphic and sedimentological parameters of the 18 Kaikōura beach profiles monitored from 1997–2015. The existence of within-type variations of MSG beaches on the Kaikōura coastline was determined using a hierarchical cluster analysis of pre-determined geomorphic parameters and environmental conditions attributed to each profile. The classification showed that there were predominantly three within-type variations of MSG beaches on the Kaikōura coastline: (1) South Bay accretionary beaches, (2) wide and flat rivermouth and open coast beaches, and (3) narrow and steep beaches. It was determined that the groups were distributed geographically, and therefore the environmental conditions acting on the profiles were influencing the geomorphic parameters being classified.

These results are significant in the context of MSG beach research, due to the fact that previously within-type variations of sand beach types had been established (Short, 1974), and on a broader scale, gravel type beaches have been classified by geomorphic parameters to determine

the difference between pure gravel, MSG and composite (Jennings and Shulmeister, 2002). This study has taken Jennings and Shulmeister's (2002) classification scheme one step further and used attributes from previous classification schemes to produce an initial classification scheme for within-type variations of MSG beaches in the Kaikōura region. This is a significant contribution to MSG beach research in order to validate Jennings and Shulmeister (2002) predictions, as well as observations, that within-type variations of these beach types exist in the field. It has provided framework that could be further refined in a more extensive study of these within-type MSG variations in a country where MSG beaches are commonly found and widely distributed, where there is greater variation in environmental conditions.

The second objective of this study was: *To evaluate post-earthquake surveying techniques and the data captured through the use of different methods.*

This objective was achieved by determining what post-earthquake surveying techniques and coastal monitoring techniques are commonly used, and applying these techniques to the Kaikōura region using pre and post-earthquake data. The methods analysed were LiDAR generated DEM's, aerial imagery for shoreline analysis, and beach profile surveying. These techniques were then critiqued on what information could be obtained when applied to the Kaikōura coastline, and how this information could inform a short-term conceptual response model. The results of this analysis showed that LiDAR generated DEM used to determine changes in the coastal environment gave relatively accurate results, however the errors in the technique were much higher than that of beach profile surveying. Beach profile surveying was the most effective method to inform a conceptual model, as it was able to capture a high level of detail with great accuracy, though it could only capture a small snapshot of the coastline. The high number of profiles monitored following the earthquake means that assumptions between profiles could be depicted with reasonable accuracy, and DEM complimented this technique as it could capture a large spatial area, but in lower resolution. The aerial imagery results showed that the technique was difficult to use in a MSG environment due to the steep beaches, and a lack of consistent identifiable features along a shoreline with various within-type beaches. The wet water line and the vegetation line were used, however the errors calculated and considered when using this method meant that detailed shoreline change could not be obtained from this method to help inform a conceptual response model.

These results are significant because there is currently no protocol following an earthquake informing what is the most effective surveying technique to obtain quick and accurate data in a coastal environment. These results show that the common collection of LiDAR following an earthquake can still be used to help inform coastal changes, however for a detailed and accurate analysis of beach shape change, beach profile surveying needs to be undertaken. The

importance of this technique has been highlighted, and going forward it may be more of a priority to continuously monitor these profiles using beach profile surveying in order to continue bridging the gap of knowledge between short-term and decadal beach response.

The third objective of this research was: *To identify what the short-term responses are in a MSG coastal environment following an earthquake-induced change in relative sea level.*

This objective was achieved by collecting beach profile surveying data using GNSS surveying equipment, and analysing beach profile volume, shoreline, and beach shape changes following the earthquake, using surveys from January 2017 and September 2018. The results from the beach profile surveying showed that there was variation in how a beach responded following an earthquake, but predominantly beach profiles exhibited similar trends within their within-type group established in Objective 1. There were two main response pathways established, which represented the short-term response of the profiles monitored: accretionary beaches and erosional beaches. These responses were largely driven by the pre-earthquake state determined in Objective 1, and the sediment supply to the profile. If a profile had a pre-earthquake erosional trend and a poor sediment supply, it showed a post-earthquake erosional trend in which the profile was seen to be rebuilding berms relative to sea level and eroding back to its pre-earthquake profile extents. Alternatively, profiles which exhibited accretional or dynamic trends pre-earthquake with good sediment supplies have continued to grow since the earthquake and re-establish berms relative to sea level. If these profiles eventually retreat to pre-earthquake profile extents due to retreat landwards of the position of max wave effort, then the rate at which this occurs will be slower than the rate at which erosional beaches respond. Additionally, two conceptual models were also considered which included limestone rock shore platforms, which highlight that if the uplift steps the position of maximum wave effort steps out beyond the limestone platform, the rate at which it will respond will likely be on a century scale due to the nearshore response having to erode consolidated material in order for the position of maximum wave effort to retreat inland.

These results are significant because they are the first directly observed and documented short-term responses following an earthquake-induced fall in relative sea level on a New Zealand MSG beach. Prior to these results, MSG beach response to an earthquake in New Zealand had only been observed on a historical time scale. These results contribute to the greater response model of MSG beaches, in which now the main response trends following an earthquake have been measured and recorded, as well as decadal response detailed by Single (1985). A continuation of this research by measuring the Kaikōura coastline annually will mean that the interim gap of knowledge between short-term response and long-term response can be determined.

## 9.2 Limitations

There are several limitations when considering the scope of this research. One main limitation of this research is that the results produced through the form of conceptual response models can only be attributed to a MSG beach model, not gravel or sand. The application of the conceptual response model to different beach types would not represent beach response in that environment due to the model being based on MSG beach morphology and sedimentology. Studies which directly address this issue in a sand or gravel beach need to be undertaken to further understand those response dynamics.

Furthermore, an additional limitation to this research is the inference of the nearshore environment. Due to the dangerous, high energy wave climate on a MSG beach, nearshore and break point step survey data is rarely collected, and therefore the model has been informed with theory rather than field data. The research largely focused on the subaerial response, while seaward features of this environment were inferred for the purpose of the conceptual model. The nearshore response was out of scope for this research as it largely responds on a longer term scale, however the collection of this data could further refine the conceptual model presented in this study.

Another limitation of this research is that research was carried out comprehensively in a large area, however the response is only valid in a regional context where similar environmental conditions and settings influence the profiles studied, and consequently the response following an earthquake. Coastal response was found to be dependent on the environmental conditions at the profile, and therefore significant differences in environmental conditions would also effect the response of the MSG beach.

Finally, the time frame of which this study was conducted over was limited, and therefore the collection of data was also limited. The two year period following the earthquake could only be represented in this study through the means of two different beach profile surveys, however a more detailed short-term response model could be developed with a greater number of surveys. The time constraints on this project means that the beach responses between 2–50 years using detailed surveying data has not yet been investigated. A continuation of this research or the coastal monitoring programme by ECan could collect the data which could inform the response during this period.

## 9.3 Future research

Future research stemming from this study could venture into many different fields. The first being, the continual development of the conceptual response model, through the means of being able to incorporate nearshore and offshore bathymetry data into the model, and being able to determine the exact position of the maximum wave effect, to then be able to calculate the rate at which the nearshore responds in these environments. A continuation of this study could be carried out to further define the conceptual model presented in this study over the coming years.

A detailed sediment budget study for Kaikōura also needs to be undertaken to better inform the conceptual model. It is assumed during this study that the earthquake has increased the available sediment due to increased sediment coming down the catchment due to landslides inland, but it not know by how much the sediment budget has increased, or when pulses of sediment make their way down, how long this will effect the coastline for.

Another area of this study which highlighted the need for further research is the need for more research on sediment patterns and dynamics on MSG beaches. As detailed in Section 9.2, the lack of sedimentology data on these beaches meant that normal sediment distributions at each profile could not be established, and changes from the 1997 sedimentology data could not be attributed directly to the earthquake or evolution of the profile itself. Further research needs to be conducted to determine these trends across MSG profiles. Using the DGS analysis methods detailed in this study could provide a quick collection and processing method to carry this out and create a long-term data set.

Lastly, an issue encountered in this study was the re-surveying of post-earthquake environments when the geodetic system had been destroyed. Future research should look into how the geodetic system can be re-established quickly and accurately after an earthquake, by decreasing the amount of time between the development and application of NDM patches to the geodetic system.

# References

- Adams, J. (1978). Data for New Zealand pebble abrasion studies. *New Zealand Journal of Science*, 21, 607–610.
- Adams, J. (1980). Contemporary uplift and erosion of the Southern Alps, New Zealand. *Geological Society of America Bulletin*, 91, 1–114.
- Aguilar, F. J., Aguilar, M. A., and Aguera, F. (2007). Accuracy assessment of digital elevation models using a non-parametric approach. *International Journal of Geographical Information Science*, 21(6), 667–686.
- Allis, M. (2016). *Managing and adapting to coastal erosion at Granity, Ngakawau and Hector*. Prepared for West Coast Regional Council by NIWA. Client Report Number HAM2016-009.
- Anderson, H., and Webb, T. (1994). New Zealand seismicity: Patterns revealed by the upgraded National Seismograph Network. *New Zealand Journal of Geology and Geophysics*, 37(4), 477–493.
- Anthony, E. J. (2009). Shore processes and their palaeoenvironmental applications. In H. Chamley (Ed.), *Developments in Marine Geology* (Vol. 4, p. 445-448). Amsterdam: Elsevier Science.
- Athukorala, P., and Resosudarmo, B. P. (2005). The Indian Ocean tsunami: Economic impact, disaster management, and lessons. *Asian Economic Papers*, 4(1), 1–39.
- Aubrey, D. G. (1979). Seasonal patterns of onshore/offshore sediment movement. *Journal of Geophysical Research: Oceans*, 84(10), 6347–6354.
- Bascom, W. (1951). The relationship between sand size and beachface slope. *EOS, Transactions American Geophysical Union*, 32(6), 866–874.
- Beavan, R. J., and Litchfield, N. J. (2012). *Vertical land movement around the New Zealand coastline: Implications for sea-level rise*. Lower Hutt, New Zealand: GNS Science Report 2012/29. 41 p.



- Berger, H. V. (2017). *Characterising landscape and sea level dynamics to predict shoreline responses over the next 100+ years in a high energy tectonic setting, Kaikoura, New Zealand* (Unpublished master's thesis). University of Canterbury.
- Bluck, B. J. (1967). Sedimentation of beach gravels; examples from South Wales. *Journal of Sedimentary Research*, 37(1), 128–156.
- Boorer, S. (2002). *Geomorphic evolution of the South Bay coast, Kaikoura* (Unpublished master's thesis). University of Canterbury.
- Borja, Á., Dauer, D. M., Elliott, M., and Simenstad, C. A. (2010). Medium-and long-term recovery of estuarine and coastal ecosystems: Patterns, rates and restoration effectiveness. *Estuaries and Coasts*, 33(6), 1249–1260.
- Brown, S. (2017). *Modelling storm behaviour and relative sea level change on mixed sand and gravel barrier beaches in South Hawke's Bay, New Zealand* (Unpublished master's thesis). University of Auckland.
- Bruun, P. (1954). Coast erosion and the development of beach profiles. *U.S. Army Beach Erosion Board Technical Memorandum*, 44.
- Bruun, P. (1962). Sea-level rise as a cause of shore erosion. *Journal of the Waterways and Harbors division*, 88(1), 117–132.
- Bruun, P. (1983). Review of conditions for uses of the Bruun Rule of erosion. *Coastal Engineering*, 7(1), 77–89.
- Bruun, P. (1988). The Bruun Rule of erosion by sea-level rise: A discussion on large-scale two-and three-dimensional usages. *Journal of Coastal Research*, 4, 627–648.
- Buscombe, D. (2013). Transferable wavelet method for grainsize distribution from images of sediment surfaces and thin sections, and other natural granular patterns. *Sedimentology*, 60(7), 1709–1732.
- Buscombe, D., and Masselink, G. (2006). Concepts in gravel beach dynamics. *Earth-Science Reviews*, 79(1-2), 33–52.
- Buscombe, D., and Rubin, D. M. (2012). Advances in the simulation and automated measurement of wellsorted granular material: 2. Direct measures of particle properties. *Journal of Geophysical Research: Earth Surface*, 117, 1–18.

- Buscombe, D., Rubin, D. M., and Warrick, J. A. (2010). A universal approximation of grain size from images of noncohesive sediment. *Journal of Geophysical Research: Earth Surface*, 115, 1–17.
- Caldwell, N. E., and Williams, A. T. (1985). The role of beach profile configuration in the discrimination between differing depositional environments affecting coarse clastic beaches. *Journal of Coastal Research*, 1(2), 129–139.
- Carruth, D. (2017). *Hawke’s Bay Coastal Monitoring 2017*. Prepared for Hawke’s Bay Regional Council, ISSN 1174 3085.
- Carter, R., Jennings, S. C., and Orford, J. D. (1990). Headland erosion by waves. *Journal of Coastal Research*, 6(3), 517–529.
- Carter, R., and Orford, J. D. (1988). Conceptual model of coarse clastic barrier formation from multiple sediment sources. *Geographical Review*, 78(2), 221–239.
- Carter, R., and Orford, J. D. (1993). The morphodynamics of coarse clastic beaches and barriers: A short-and long-term perspective. *Journal of Coastal Research, Special Issue*(15), 158–179.
- Cazenave, A., Dieng, H. B., Meyssignac, B., von Schuckmann, K., Decharme, B., and Berthier, E. (2014). The rate of sea level rise. *Nature Climate Change*, 4, 358–361.
- Chandra, S. (1969). *Geomorphology of the Kaikoura area* (Unpublished master’s thesis). The University of Waikato.
- Chiswell, S. M. (1996). Variability in the Southland Current, New Zealand. *New Zealand Journal of Marine and Freshwater Research*, 30(1), 1–17.
- Ciavola, P., and Castiglione, E. (2009). Sediment dynamics of mixed sand and gravel beaches at short time-scales. *Journal of Coastal Research, Special Issue*(56), 1751–1755.
- Clark, K. J., Nissen, E. K., Howarth, J. D., Hamling, I. J., Mountjoy, J. J., Ries, W. F., ... Villamor, P. (2017). Highly variable coastal deformation in the 2016  $M_w$  7.8 Kaikoura earthquake reflects rupture complexity along a transpressional plate boundary. *Earth and Planetary Science Letters*, 474, 334–344.
- Clarke, K., and Gorley, R. (2006). Primer v6. 1.10: user manual/tutorial PRIMER-E [Computer software manual]. Plymouth Routines in Multivariate Ecological Research.

- Coburn, A. W., Spence, R. J. S., and Pomonis, A. (1992). Factors determining human casualty levels in earthquakes: Mortality prediction in building collapse. In *Proceedings of the First International Forum on Earthquake related Casualties. Madrid, Spain, July 1992*.
- Cooper, J. A. G., and Pilkey, O. H. (2004). Sea-level rise and shoreline retreat: Time to abandon the Bruun Rule. *Global and Planetary Change*, 43(3-4), 157–171.
- Cowell, P. J., Roy, P. S., and Jones, R. A. (1992). Shoreface translation model: Computer simulation of coastal-sand-body response to sea level rise. *Mathematics and Computers in Simulation*, 33(5-6), 603–608.
- Cowell, P. J., and Thom, B. G. (1994). *Morphodynamics of coastal evolution*. Cambridge, United Kingdom and New York, USA: Cambridge University Press.
- Creed, S. (2014). *A classification of small hapua-type river mouths on the mixed sand and gravel coasts of Canterbury, New Zealand* (Unpublished honour’s dissertation). University of Canterbury.
- Darwin, C. (1851). *Geological observations on coral reefs, volcanic islands, and on South America: Being the geology of the voyage of the Beagle, under the command of Captain Fitzroy, RN, during the years 1832 to 1836*. Smith, Elder.
- Dawe, I. N. (1997). *Sediment patterns on a Mixed Sand and Gravel Beach, Kaikoura, New Zealand* (Unpublished master’s thesis). University of Canterbury.
- Dawe, I. N. (2001). Sediment patterns on a mixed sand and gravel beach, Kaikoura, New Zealand. *Journal of Coastal Research, Special Issue*(34), 267–277.
- Dellow, S., Massey, C., Cox, S., Archibald, G., Begg, J., Bruce, Z., ... Glassey, P. (2017). Landslides caused by the m<sub>w</sub>7.8 Kaikōura earthquake and the immediate response. *Bulletin of the New Zealand Society for Earthquake Engineering*, 50(2).
- Dickson, M. E., Kench, P. S., and Kantor, M. S. (2011). Longshore transport of cobbles on a mixed sand and gravel beach, southern Hawke’s Bay, New Zealand. *Marine Geology*, 287(1-4), 31–42.
- Dingler, J. (1981). Stability of a very coarse-grained beach at Carmel, California. *Marine Geology*, 44(3-4), 241–252.
- Donnelly, N., Crook, C., Haasdyk, J., Harrison, C., Rizos, C., Roberts, C., and Stanaway, R. (2014). Dynamic datum transformations in Australia and New Zealand. In *Proceedings of research at locate14* (pp. 48–59).

- Doocy, S., Cherewick, M., and Kirsch, T. (2013). Mortality following the Haitian earthquake of 2010: A stratified cluster survey. *Population Health Metrics*, 11(1), 5.
- Dubious, R. (1988). Seasonal changes in beach topography and beach volume in Delaware. *Marine Geology*, 81, 79–96.
- Duffy, B., Quigley, M., Barrell, D. J., Van Dissen, R., Stahl, T., Leprince, S., ... Bilderback, E. (2013). Fault kinematics and surface deformation across a releasing bend during the 2010  $m_w$  7.1 Darfield, New Zealand, earthquake revealed by differential LiDAR and cadastral surveying. *Bulletin*, 125(3-4), 420–431.
- Environment Canterbury. (2000). *Kaikoura Floodplain: A strategy for reducing the impacts of flooding and flood sediment deposition*. Christchurch, New Zealand: Record Number: C16C/178578.
- Environment Canterbury. (2005). *A summary of monitoring and investigations on the Canterbury Bight Coastline*. Christchurch, New Zealand: Record Number: U05/77.
- Environment Canterbury. (2017). *Resource Consent CRC174216*. Christchurch, New Zealand.
- Everts, C. H. (1985). Sea level rise effects on shoreline position. *Journal of Waterway, Port, Coastal, and Ocean Engineering*, 111(6), 985–999.
- Farris, A. S., and List, J. H. (2007). Shoreline change as a proxy for subaerial beach volume change. *Journal of Coastal Research*, 23(3), 740–748.
- FitzGerald, D. M., Fenster, M. S., Argow, B. A., and Buynevich, I. V. (2008). Coastal impacts due to sea-level rise. *Annual Review of Earth and Planetary Sciences*, 36, 601–647.
- Folk, R. L. (1980). *Petrology of sedimentary rocks*. Austin, Texas: Hemphill Publishing Company.
- Gallop, S. L. (2012). *Classification and morphodynamics of perched beaches* (Unpublished doctoral dissertation). The University of Western Australia.
- GeoNet. (2017). *M 7.8 Kaikoura Mon, Nov 14 2016*. <https://www.geonet.org.nz/earthquake/story/2016p858000>. (Accessed: 2018-12-19)
- Giglierano, J. D. (2010). Lidar basics for natural resource mapping applications. *Geological Society, London, Special Publications*, 345(1), 103–115.
- Goff, J. R., and McFadgen, B. G. (2002). Seismic driving of nationwide changes in geomorphology and prehistoric settlement: A 15<sup>th</sup> century New Zealand example. *Quaternary Science Reviews*, 21(20-22), 2229–2236.

- Goto, K., Takahashi, J., Oie, T., and Imamura, F. (2011). Remarkable bathymetric change in the nearshore zone by the 2004 Indian Ocean tsunami: Kirinda Harbor, Sri Lanka. *Geomorphology*, 127(1-2), 107–116.
- Hanslow, D. J., Davis, G. A., You, B. Z., and Zastawny, J. (2000). Berm height at coastal lagoon entrances. *In 10th annual NSW Coastal conference, 2000*.
- Hart, D. E. (1999). *Dynamics of mixed sand and gravel river mouth lagoons: hapua* (Unpublished master's thesis). University of Canterbury.
- Hart, D. E. (2007). River-mouth lagoon dynamics on mixed sand and gravel barrier coasts. *Journal of Coastal Research, Special Issue*(50), 927–931.
- Hart, D. E. (2009). Morphodynamics of non-estuarine rivermouth lagoons on high-energy coasts. *Journal of Coastal Research*, 56(2), 1355–1359.
- Hart, D. E., Byun, D. S., Giovinazzi, S., Hughes, M. W., Gomez, C., et al. (2015). Relative sea level changes on a seismically active urban coast: Observations from laboratory Christchurch. *In Australasian coasts and ports conference 2015: 22<sup>nd</sup> Australasian Coastal and Ocean Engineering Conference and the 15<sup>th</sup> Australasian Port and Harbour Conference* (p. 384).
- Hegge, B., Eliot, I., and Hsu, J. (1996). Sheltered sandy beaches of Southwestern Australia. *Journal of Coastal Research*, 12(3), 748–760.
- Hicks, M., Hill, J., and Shankar, U. (1996). Variation of suspended sediment yields around New Zealand: The relative importance of rainfall and geology. *IAHS publication*(236), 149–156.
- Hodgson, E. A. (1927). The Relation of the Surveyor to Earthquakes. *Journal of the Royal Astronomical Society of Canada*, 21, 155.
- Hollingsworth, J., Ye, L., and Avouac, J. (2017). Dynamically triggered slip on a splay fault in the  $M_w$  7.8, 2016 Kaikoura (New Zealand) earthquake. *Geophysical Research Letters*, 44(8), 3517–3525.
- Horn, D. (2002). Beach groundwater dynamics. *Geomorphology*, 48(1-3), 121–146.
- Horn, D., Li, L., and Holmes, P. (2003). Measurement and modelling of gravel beach groundwater response to wave run-up. *In Coastal sediments* (Vol. 3).
- Horton, B. P., Rahmstorf, S., Engelhart, S. E., and Kemp, A. C. (2014). Expert assessment of sea-level rise by AD 2100 and AD 2300. *Quaternary Science Reviews*, 84, 1–6.

- Hume, T. M., Gerbeaux, P., Hart, D. E., Kettles, H., and Neale, D. (2016). *A classification of New Zealand's coastal hydrosystems*. Prepared for Ministry for the Environment, HAM2016-062 NIWA Client Report.
- Hume, T. M., and Herdendorf, C. E. (1988). A geomorphic classification of estuaries and its application to coastal resource management a New Zealand example. *Ocean and Shoreline Management*, 11(3), 249–274.
- Hunt, I. (1959). Design of sea-walls and breakwaters. *Transactions of the American Society of Civil Engineers*, 126(4), 542–570.
- Hyndman, R. D. (1995). Giant earthquakes of the Pacific Northwest. *Scientific American*, 273(6), 68–75.
- Ivamy, M. C., and Kench, P. S. (2006). Hydrodynamics and morphological adjustment of a mixed sand and gravel beach, Torere, Bay of Plenty, New Zealand. *Marine Geology*, 228(1-4), 137–152.
- Jennings, R., and Shulmeister, J. (2002). A field based classification scheme for gravel beaches. *Marine Geology*, 186(3-4), 211–228.
- Karunaratna, H., Horrillo-Caraballo, J. M., Ranasinghe, R., Short, A. D., and Reeve, D. E. (2012). An analysis of the cross-shore beach morphodynamics of a sandy and a composite gravel beach. *Marine Geology*, 299, 33–42.
- Kay, S., Caesar, J., Wolf, J., Bricheno, L., Nicholls, R. J., Islam, S., ... Lowe, J. A. (2015). Modelling the increased frequency of extreme sea levels in the Ganges–Brahmaputra–Meghna delta due to sea level rise and other effects of climate change. *Environmental Science: Processes and Impacts*, 17(7), 1311–1322.
- Kazama, M., and Noda, T. (2012). Damage statistics (Summary of the 2011 off the Pacific Coast of Tohoku Earthquake damage). *Soils and Foundations*, 52(5), 780–792.
- Kelk, J. G. (1974). *A Morphological Approach to Process Interaction on the Mid-Canterbury Coastline* (Unpublished doctoral dissertation). University of Canterbury.
- Kirk, R. M. (1969). Beach erosion and coastal development in the Canterbury Bight. *New Zealand Geographer*, 25(1), 23–35.
- Kirk, R. M. (1975). Aspects of surf and runup processes on mixed sand and gravel beaches. *Geografiska Annaler: Series A, Physical Geography*, 57(1-2), 117–133.

- Kirk, R. M. (1977). Rates and forms of erosion on intertidal platforms at Kaikoura Peninsula, South Island, New Zealand. *New Zealand Journal of Geology and Geophysics*, 20(3), 571–613.
- Kirk, R. M. (1980). MSG beaches: Morphology, processes and sediments. *Progress in Physical Geography*, 4(2), 189–210.
- Kirk, R. M. (1986). *Beach erosion along the Esplanade*. Unpublished report to Kaikoura District Council.
- Kirk, R. M. (1991). River-beach interaction on mixed sand and gravel coasts: A geomorphic model for water resource planning. *Applied Geography*, 11(4), 267–287.
- Kirk, R. M., and Lauder, G. A. (1994). *Guidelines for managing lagoon mouth closures on significant coastal/wetland lagoon systems-coastal processes investigation*. Report to Department of Conservation, Science and Research Division (Draft).
- Komar, P. D. (2010). Shoreline evolution and management of Hawke’s Bay, New Zealand: Tectonics, coastal processes, and human impacts. *Journal of Coastal Research*, 26(1), 143–156.
- Land Information New Zealand. (2017). *Surveys for post-earthquake geodetic control*. <https://www.linz.govt.nz/land/surveying/earthquakes/kaikoura-earthquakes/surveys-for-post-earthquake-geodetic-control>. (Accessed: 2018-11-27)
- Leatherman, S. P., Zhang, K., and Douglas, B. C. (2000). Sea level rise shown to drive coastal erosion. *EOS, Transactions American Geophysical Union*, 81(6), 55–57.
- Lee, Y. H., Chen, H. S., Rau, R. J., Chen, C. L., and Hung, P. S. (2006). Revealing surface deformation of the 1999 Chi-Chi earthquake using high-density cadastral control points in the Taichung area, central Taiwan. *Bulletin of the Seismological Society of America*, 96(6), 2431–2440.
- Lee, Y. H., Wu, K. C., Rau, R. J., Chen, H. C., Lo, W., and Cheng, K. (2010). Revealing coseismic displacements and the deformation zones of the 1999 Chi-Chi earthquake in the Tsaotung area, central Taiwan, using digital cadastral data. *Journal of Geophysical Research: Solid Earth*, 115(B3).
- López-Ruiz, A., Solari, S., Ortega-Sánchez, M., and Losada, M. (2015). A simple approximation for wave refraction—application to the assessment of the nearshore wave directionality. *Ocean Modelling*, 96, 324–333.

- Marsden, I. D., Hart, D. E., Reid, C. M., and Gomez, C. (2015). Earthquake disturbances. In M. J. Kennish (Ed.), *Encyclopedia of estuaries* (pp. 207–214). Dordrecht: Springer.
- Mason, T., and Coates, T. (2001). Sediment transport processes on mixed beaches: A review for shoreline management. *Journal of Coastal Research*, 17(3), 645–657.
- Masselink, G., and Hughes, M. G. (2014). *An introduction to coastal processes and geomorphology*. London, United Kingdom: Routledge.
- Masselink, G., and Kroon, A. (2009). Morphology and morphodynamics of sandy beaches. In F. Isla and O. Iribarne (Eds.), *Coastal zones and estuaries* (pp. 221–243). Oxford, United Kingdom: Encyclopedia of Life Support Systems Publishers Co. Ltd.
- Masselink, G., and Li, L. (2001). The role of swash infiltration in determining the beachface gradient: A numerical study. *Marine Geology*, 176, 139–156.
- Masselink, G., and Short, A. D. (1993). The effect of tide range on beach morphodynamics and morphology: A conceptual beach model. *Journal of Coastal Research*, 9(3), 785–800.
- Massonnet, D., Rossi, M., Carmona, C., Adragna, F., Peltzer, G., Feigl, K., and Rabaute, T. (1993). The displacement field of the Landers earthquake mapped by radar interferometry. *Nature*, 364, 138–142.
- McLean, R. F. (1970). Variations in grain size and sorting on two Kaikoura beaches. *Journal of Marine and Freshwater Research*, 4(2), 141–164.
- McLean, R. F., and Kirk, R. M. (1969). Relationships between grain size, size-sorting, and fore-shore slope on mixed sand–shingle beaches. *New Zealand Journal of Geology and Geophysics*, 12(1), 138–155.
- Morton, R. A., Leach, M. P., Paine, J. G., and Cardoza, M. A. (1993). Monitoring beach changes using GPS surveying techniques. *Journal of Coastal Research*, 9(3), 702–720.
- Mullan, A. B., Sood, A., and Stuart, S. (2016). *Climate Change Projections for New Zealand: Atmospheric Projections based on Simulations undertaken for the IPCC Fifth Assessment*. Prepared for the Ministry for the Environment, NIWA Client Report WLG2015-31,.
- OCEL Consultants NZ Ltd. (2016). *Resource consent application renewal of consents to enable ongoing beach renourishment The Esplanade Kaikoura*. Unpublished consent application prepared by OCEL for the Kaikoura District Council.
- Olson, D. (2010). *Decadal shoreline stability in Eastbourne, Wellington Harbour* (Unpublished master’s thesis). Victoria University of Wellington.



- Olson, D., Kennedy, D. M., Dawe, I., and Calder, M. (2012). Decadal-scale gravel beach evolution on a tectonically-uplifting coast: Wellington, New Zealand. *Earth Surface Processes and Landforms*, 37(11), 1133–1141.
- Orford, J., Carter, R., and Jennings, S. (1996). Control domains and morphological phases in gravel-dominated coastal barriers of Nova Scotia. *Journal of Coastal Research*, 12(3), 589–604.
- Ota, Y., Pillans, B., Berryman, K., Beu, A., Fujimori, T., Miyauchi, T., . . . Climo, F. M. (1996). Pleistocene coastal terraces of Kaikoura Peninsula and the Marlborough coast, South Island, New Zealand. *New Zealand Journal of Geology and Geophysics*, 39(1), 51–73.
- Pari, Y., Murthy, M. R., Subramanian, B., Ramachandran, S., et al. (2008). Morphological changes at Vellar estuary, India – Impact of the December 2004 tsunami. *Journal of Environmental Management*, 89(1), 45–57.
- Paris, R., Wassmer, P., Sartohadi, J., Lavigne, F., Barthomeuf, B., Desgages, E., . . . Brunstein, D. (2009). Tsunamis as geomorphic crises: Lessons from the December 26, 2004 tsunami in Lhok Nga, west Banda Aceh (Sumatra, Indonesia). *Geomorphology*, 104(1-2), 59–72.
- Paterson, M. (2000). *The Effect of Earthquake Induced Relative Sea Level Change on a Gravel Beach: Hawke’s Bay, New Zealand* (Unpublished master’s thesis). Victoria University of Wellington.
- Pentney, R. M., and Dickson, M. E. (2012). Digital grain size analysis of a mixed sand and gravel beach. *Journal of Coastal Research*, 28(1), 196–201.
- Pickrill, R. A., and Mitchell, J. S. (1979). Ocean wave characteristics around New Zealand. *New Zealand Journal of Marine and Freshwater Research*, 13(4), 501–520.
- Pilkey, O. H., and Davis, T. W. (1987). An analysis of coastal recession models: North Carolina coast. In D. Nummedal, O. H. Pilkey, and J. D. Howard (Eds.), *Sea-level fluctuation and coastal evolution* (p. 59-68). Tulsa, OK: Society of Economic Paleontologists and Mineralogists.
- Pontee, N. I., Pye, K., and Blott, S. J. (2004). Morphodynamic behaviour and sedimentary variation of mixed sand and gravel beaches, Suffolk, UK. *Journal of Coastal Research*, 20(1), 256–276.
- Prodger, S. (2017). *Spatial and temporal variability of sandy beach sediment grain size and sorting* (Unpublished doctoral dissertation). University of Plymouth.

- Quartel, S., Kroon, A., and Ruessink, B. G. (2008). Seasonal accretion and erosion patterns of a microtidal sandy beach. *Marine Geology*, 250(1-2), 19–33.
- Ramsey, D. K. (2007). *Managing and adapting to coastal erosion on the West Coast: Ngakawau and Hector*. Prepared for West Coast Regional Council, NIWA Client Report: HAM2007-007.
- Rattenbury, M. S., Townsend, D. B., and Johnston, M. R. (2006). *Geology of the Kaikoura area* (Vol. 1). Lower Hutt, New Zealand: Institute of Geological and Nuclear Sciences.
- Roberts, T. M., Wang, P., and Puleo, J. A. (2013). Storm-driven cyclic beach morphodynamics of a mixed sand and gravel beach along the Mid-Atlantic Coast, USA. *Marine Geology*, 346, 403–421.
- Rosati, J. D., Dean, R. G., and Walton, T. L. (2013). The modified Bruun Rule extended for landward transport. *Marine Geology*, 340, 71–81.
- Rosen, P. S. (1978). A regional test of the Bruun Rule on shoreline erosion. *Marine Geology*, 26(1-2), 7–16.
- Rovere, A., Stocchi, P., and Vacchi, M. (2016). Eustatic and relative sea level changes. *Current Climate Change Reports*, 2(4), 221–231.
- Sallenger Jr, A. H., Holman, R. A., and Birkemeier, W. A. (1985). Storm-induced response of a nearshore-bar system. *Marine Geology*, 64(3-4), 237–257.
- Saville, T., and Watts, G. M. (1969). Coastal regime, recent U.S. experience. In *22nd international navigation congress* (p. 249-271).
- Schwartz, M. L. (1967). The Bruun theory of sea-level rise as a cause of shore erosion. *The Journal of Geology*, 75(1), 76–92.
- Scott, T., Masselink, G., and Russell, P. (2011). Morphodynamic characteristics and classification of beaches in England and Wales. *Marine Geology*, 286(1-4), 1–20.
- Shcherbakov, R., Nguyen, M., and Quigley, M. (2012). Statistical analysis of the 2010  $M_w$  7.1 Darfield earthquake aftershock sequence. *New Zealand Journal of Geology and Geophysics*, 55(3), 305–311.
- Short, A. D. (1979). Three dimensional beach-stage model. *The Journal of Geology*, 87(5), 553–571.

- Short, A. D. (1991). Macro-meso tidal beach morphodynamics: An overview. *Journal of Coastal Research*, 7(2), 417–436.
- Short, A. D. (1996). The role of wave height, period, slope, tide range and embaymentisation in beach classifications: A review. *Revista chilena de historia natural*, 69(4), 589–604.
- Shulmeister, J., and Jennings, R. (2009). Morphology and morphodynamics of gravel beaches. In F. Isla and O. Iribarne (Eds.), *Coastal Zones and Estuaries* (pp. 244–261). Encyclopedia of Life Support Systems.
- Singh, R. P., Bhoi, S., and Sahoo, A. K. (2002). Changes observed in land and ocean after Gujarat earthquake of 26 January 2001 using IRS data. *International Journal of Remote Sensing*, 23(16), 3123–3128.
- Single, M. B. (1985). *Post-earthquake beach response, Napier, New Zealand* (Unpublished master’s thesis). University of Canterbury.
- Sneath, P. H., and Sokal, R. R. (1973). *Numerical taxonomy. The principles and practice of numerical classification*. San Francisco: W. H. Freeman.
- Stafford, D. B., and Langfelder, J. (1971). Air photo survey of coastal erosion. *Photogrammetric Engineering*, 37(6), 565–575.
- Stanley, K. W. (1968). *Effects of the Alaska earthquake of March 27, 1964, on shore processes and beach morphology*. U.S. Geological Survey Professional Paper 543J, 21 p.
- Stephenson, W. J. (1997). *Development of shore platforms on Kaikoura Peninsula, South Island, New Zealand* (Unpublished doctoral dissertation). University of Canterbury.
- Stephenson, W. J., Dickson, M. E., and Denys, P. H. (2017). New insights on the relative contributions of coastal processes and tectonics to shore platform development following the Kaikōura earthquake. *Earth Surface Processes and Landforms*, 42(13), 2214–2220.
- Stephenson, W. J., and Kirk, R. M. (1996). Measuring erosion rates using the micro-erosion meter: 20 years of data from shore platforms, Kaikoura Peninsula, South Island, New Zealand. *Marine Geology*, 131(3-4), 209–218.
- Stephenson, W. J., and Kirk, R. M. (1998). Rates and patterns of erosion on inter-tidal shore platforms, Kaikoura Peninsula, South Island, New Zealand. *Earth Surface Processes and Landforms: The Journal of the British Geomorphological Group*, 23(12), 1071–1085.
- Sunamura, T., and Horikawa, K. (1972). A study using aerial photographs of the effect of protective structures on coastal cliff erosion. *Coastal Engineering in Japan*, 15(1), 105–111.

- Sutton, P. J. (2003). The Southland Current: A subantarctic current. *New Zealand Journal of Marine and Freshwater Research*, 37(3), 645–652.
- Tanaka, H., Ishino, K., Nawarathna, B., Nakagawa, H., and Yano, S. (2007). Coastal and river mouth morphology change in Sri Lanka due to the 2004 Indian Ocean Tsunami. In *Coastal sediments' 07* (pp. 842–855).
- Tanaka, H., Tinh, N. X., Umeda, M., Hirao, R., Pradjoko, E., Mano, A., and Udo, K. (2012). Coastal and estuarine morphology changes induced by the 2011 Great East Japan Earthquake Tsunami. *Coastal Engineering Journal*, 54(01), 1250010-1–1250010-25.
- Taylor, G. (2013). *Management of Sand Beaches for the Protection of Shellfish Resources* (Unpublished doctoral dissertation). University of Canterbury.
- Todd, D. J. (1992). River mouth and coastal processes of the Ashburton river mouth. In T. Dons and D. Stringer (Eds.), *Natural Resources of the Ashburton River and Catchment* (pp. 208–234). Canterbury Regional Council Report 92(36).
- Udo, K., Sugawara, D., Tanaka, H., Imai, K., and Mano, A. (2012). Impact of the 2011 Tohoku earthquake and tsunami on beach morphology along the northern Sendai coast. *Coastal Engineering Journal*, 54(01), 1250009.
- Van Dissen, R. J. (1989). *Late Quaternary faulting in the Kaikoura region, southeastern Marlborough, New Zealand* (Unpublished master's thesis). Oregon State University.
- Van Dissen, R. J., and Yeats, R. S. (1991). Hope fault, Jordan thrust, and uplift of the seaward Kaikoura Range, New Zealand. *Geology*, 19(4), 393–396.
- Villagran, M., Cienfuegos, R., Catalán, P., and Almar, R. (2013). Morphological response of central Chile sandy beaches to the 8.8  $M_w$  2010 earthquake and tsunami. In *Proceeding of Coastal Dynamics* (pp. 24–28).
- Wentworth, C. K. (1922). A scale of grade and class terms for clastic sediments. *The Journal of Geology*, 30(5), 377–392.
- Winefield, R., Crook, C., and Beavan, J. (2010). The application of a localised deformation model after an earthquake. In *Proceedings of XXIV FIG Congress 2010* (pp. 11–16).
- Woodroffe, C. D. (2002). *Coasts: Form, process and evolution*. Cambridge, UK: Cambridge University Press.
- Wright, L. D., and Short, A. D. (1984). Morphodynamic variability of surf zones and beaches: A synthesis. *Marine Geology*, 56(1-4), 93–118.

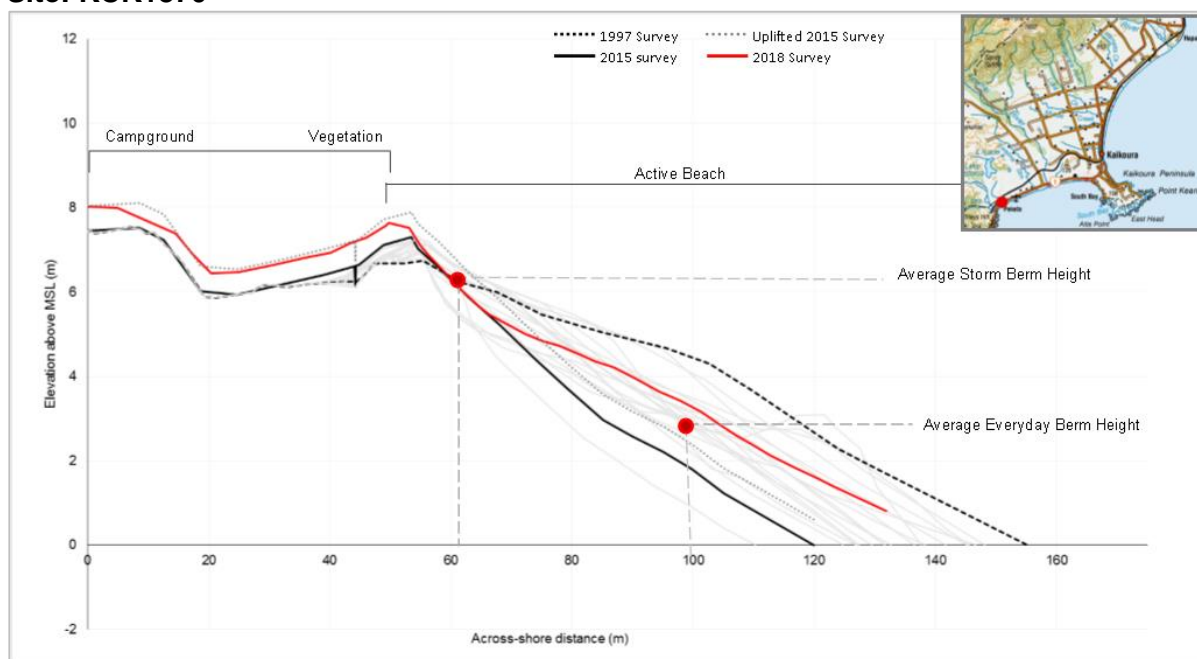
- Wright, L. D., and Thom, B. G. (1977). Coastal depositional landforms: A morphodynamic approach. *Progress in Physical Geography*, 1(3), 412–459.
- Xu, Z., Yang, J., Peng, C., Wu, X., Li, R., Zheng, Y., ... Tian, B. (2014). Development of an UAS for post-earthquake disaster surveying and its application in Ms 7. 0 Lushan Earthquake, Sichuan, China. *Computers and Geosciences*, 68, 22–30.
- Yetton, M. D. (2000). *The probability and consequences of the next Alpine Fault earthquake, South Island, New Zealand* (Unpublished doctoral dissertation). University of Canterbury.
- Yetton, M. D., and McCahon, I. F. (2009). *Earthquake Hazard Assessment for Kaikoura District*. Report prepared by Geotech Consulting Ltd. Environment Canterbury Report: R 09/31.
- Zebker, H. A., Rosen, P. A., Goldstein, R. M., Gabriel, A., and Werner, C. L. (1994). On the derivation of coseismic displacement fields using differential radar interferometry: The Landers earthquake. *Journal of Geophysical Research: Solid Earth*, 99(B10), 19617–19634.



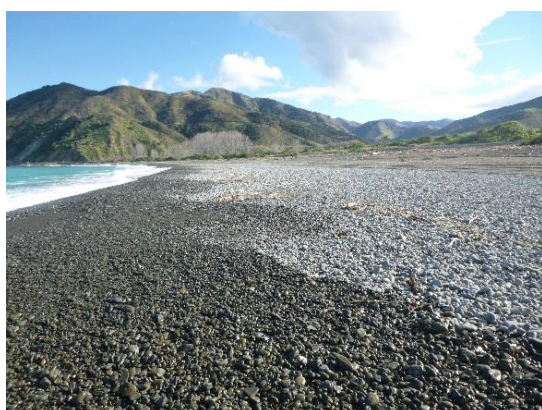
# Appendices

## A Site descriptions for Environment Canterbury beach profiles

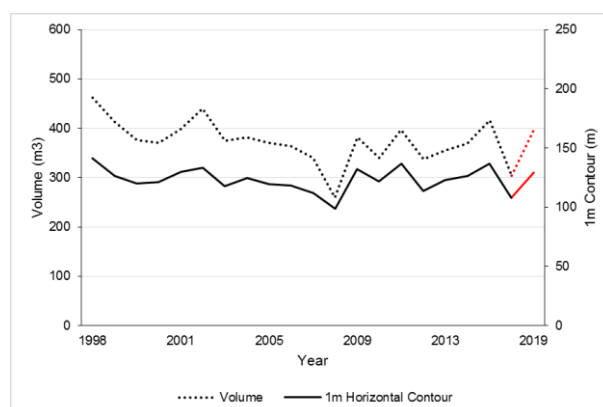
## Site: KCK1870



A: Annotated cross-sectional beach profile for Environment Canterbury site KCK1870, in Peketa, Kaikōura. Profile lines include 1997 Survey (Black dashed line); 2015 Survey (Solid black line); 2015 elevation profile (Grey dashed line); and 2018 Survey (Solid red line). Inset (top right) shows location within the study area.



B: Picture of KCK1870 facing South towards the Kahutara River. Taken August 22<sup>nd</sup> 2018.



C: Beach profile horizontal width change at the MSL contour between 1997 and 2015 for Environment Canterbury site KCK1870.

### Site description:

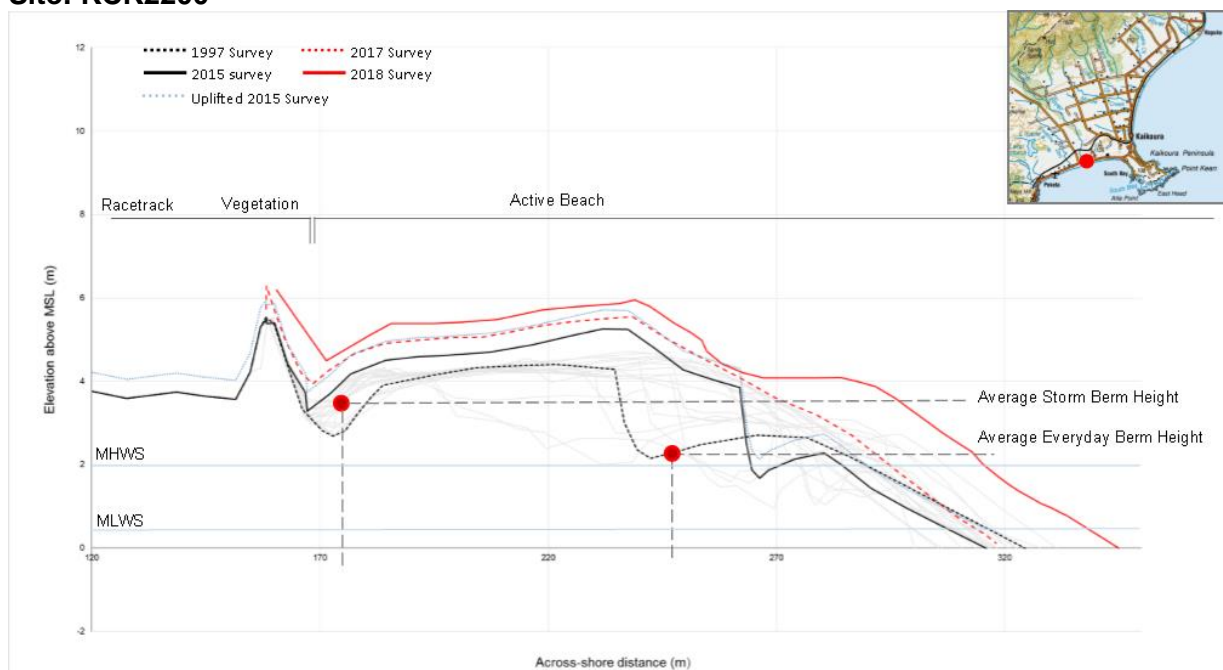
Site KCK1870 is the most southern site of those analysed. It is located approximately 700m north of the Kahutara River mouth, on the beach alongside the Peketa Holiday Park. It has an active beach width of approximately 100 m, in which the foreshore is extremely dynamic, and in some events has eroded and rebuilt 30 m between annual surveys. The MSL excursion plot (C) has shown there is a long term slight erosional trend. The profile is aligned in a SE to NW orientation. Wave energy coming from the south may be dissipated at this site as there is a small headland just south of the Kahutara River which causes waves to refract around it.

### Site Statistics (Pre Quake):

|                                  |                    |                              |                         |
|----------------------------------|--------------------|------------------------------|-------------------------|
| <b>Active beach width</b>        | 100 m              | <b>Beach Slope</b>           | 0.085                   |
| <b>Average berm height</b>       | 3 m                | <b>Overall profile trend</b> | Dynamic/ weak erosional |
| <b>Average storm berm height</b> | 6 m                | <b>Geomorphic group:</b>     | Wide and Flat           |
| <b>Average beach volume</b>      | 372 m <sup>3</sup> | <b>Subcategory:</b>          | Open Coast              |



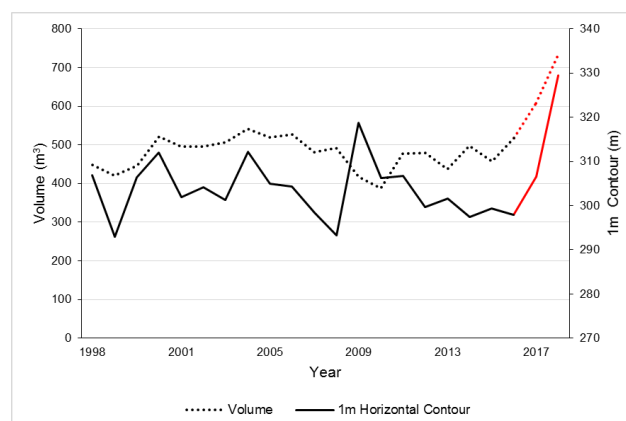
## Site: KCK2200



A: Annotated cross-sectional beach profile for Environment Canterbury site KCK2200 near the Kowhai River mouth. Profile lines include 1997 Survey (Black dashed line); 2015 Survey (Solid black line); 2015 elevated post quake profile (Grey dashed line); 2017 Survey (Dashed red line) and 2018 Survey (Solid red line). Inset (top right) shows the location in the study area.



B: Picture of site KCK2200 facing north. Image Taken 22<sup>nd</sup> August 2018.



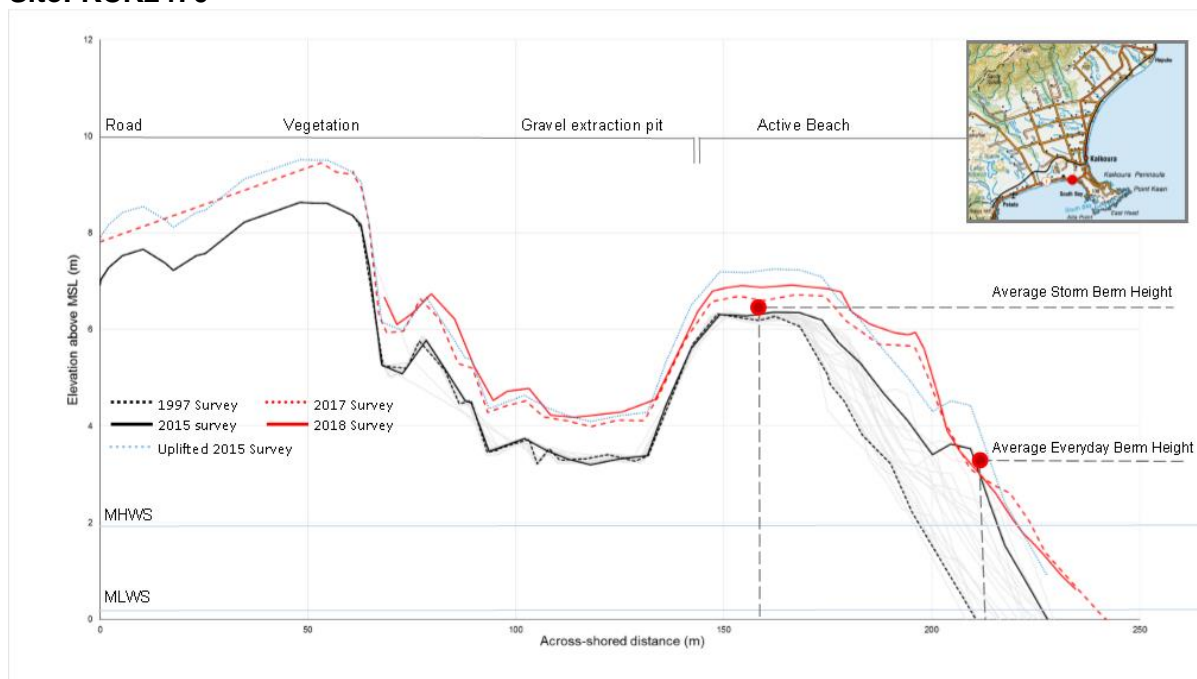
C: Beach profile horizontal width change at the MSL contour between 1997 and 2015 for Environment Canterbury site KCK2200.

### Site description:

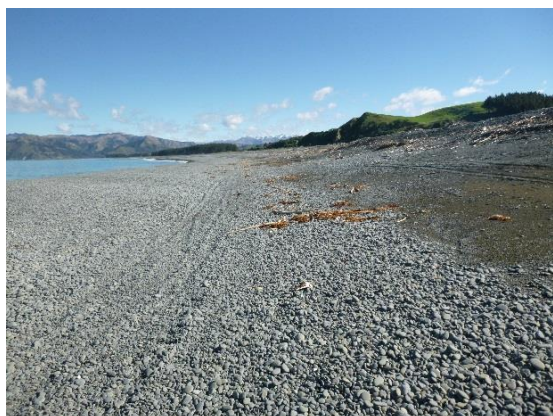
KCK2200 is located directly north of the Kowhai River mouth, where a hapua lagoon often intersects the profile as the outlet migrates north. The profile is aligned in a SE to NW orientation, but is located at the middle/north section of an uninterrupted 5.5 km stretch of the coastline. The location of the profile in close proximity to the Kowhai River mouth, which leads to the profile being very dynamic due to sediment fluxes coming from the catchment. The active beach profile is 160 m wide, the largest of all of the profiles analysed. The foreshore is very dynamic and responsive to large storm events, and changes in sediment supply, as shown in the annotated diagram (A). Overall the MSL excursion plot (C) shows a slightly eroding profile.

| Site Statistics (Pre Quake): |                    |                       |                        |
|------------------------------|--------------------|-----------------------|------------------------|
| Active beach width           | 165 m              | Beach Slope           | 0.027                  |
| Average berm height          | 2.5 m              | Overall profile trend | Dynamic/weak erosional |
| Average storm berm height    | 4 m                | Geomorphic group:     | Wide and flat          |
| Average beach volume         | 478 m <sup>3</sup> | Subcategory:          | Hapua/ Rivermouth      |

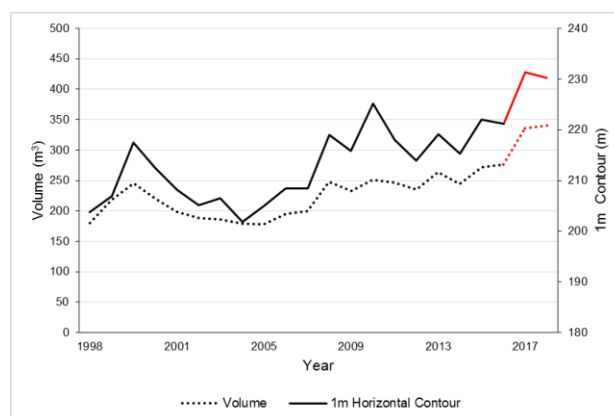
## Site: KCK2470



A: Annotated cross-sectional beach profile for Environment Canterbury site KCK2470 in South Bay, Kaikōura. Profile lines include 1997 Survey (Black dashed line); 2015 Survey (Solid black line); 2015 elevation profile (Grey dashed line); 2017 Survey (Dashed red line) and 2018 Survey (Solid red line).



B: Picture of KCK2470 facing South. Picture taken 22<sup>nd</sup> August 2018.



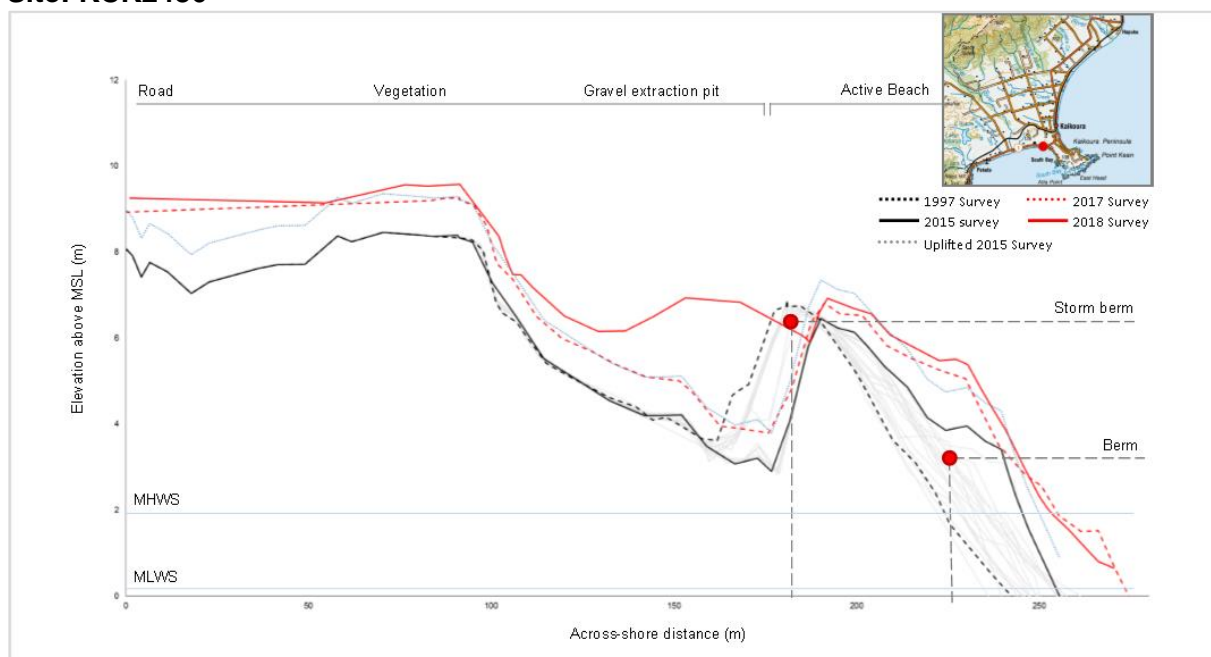
C: Beach profile horizontal width change at the MSL contour between 1997 and 2015 for Environment Canterbury site KCK2470.

### Site description:

KCK2470 is located as the coastline begins to bend around to the meet the Kaikōura Peninsula. It is approximately 500 m south of the turn off to South Bay Road. The site has an active beach width of 80 m, of which the sediment making up the beach profile is well sorted and rounded clasts, due to the longshore transport of the sediment coming from the south. Wave energy becomes lower in north easterlies at this site due to the shelter from the peninsula. The profile is aligned in a North to South orientation. The annotated diagram (A) shows an overall trend of accretion across the profile, as shown in Figure C, which also shows a strong accretionary trend at the MSL contour.

| Site Statistics (Pre Quake):     |                    |                              |                          |
|----------------------------------|--------------------|------------------------------|--------------------------|
| <b>Active beach width</b>        | 70 m               | <b>Beach Slope</b>           | 0.107                    |
| <b>Average berm height</b>       | 3.5 m              | <b>Overall profile trend</b> | Accretionary             |
| <b>Average storm berm height</b> | 6 m                | <b>Geomorphic group:</b>     | Medium accreting beaches |
| <b>Average beach volume</b>      | 222 m <sup>3</sup> | <b>Subcategory:</b>          | Sediment trapping        |

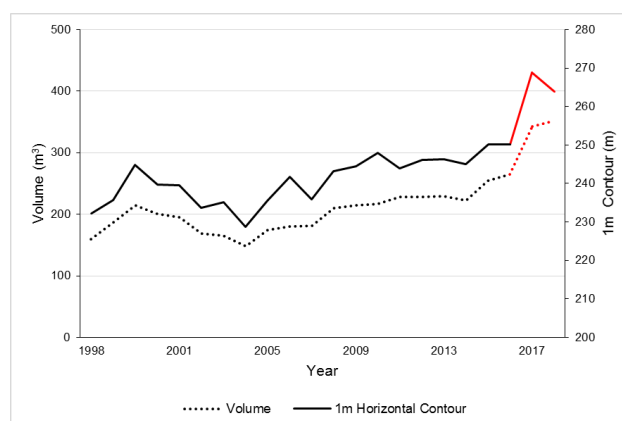
## Site: KCK2486



A: Annotated cross-sectional beach profile for Environment Canterbury site KCK2486 in South Bay, Kaikōura. Profile lines include 1997 Survey (Black dashed line); 2015 Survey (Solid black line); 2015 elevation profile (Grey dashed line); 2017 Survey (Dashed red line) and 2018 Survey (Solid red line). Inset (top right) shows location of the site in the study area.



B: Picture of KCK2486 facing north. Picture taken 22<sup>nd</sup> August 2018.



C: Beach profile horizontal width change at the MSL contour between 1997 and 2015 for Environment Canterbury site KCK2486.

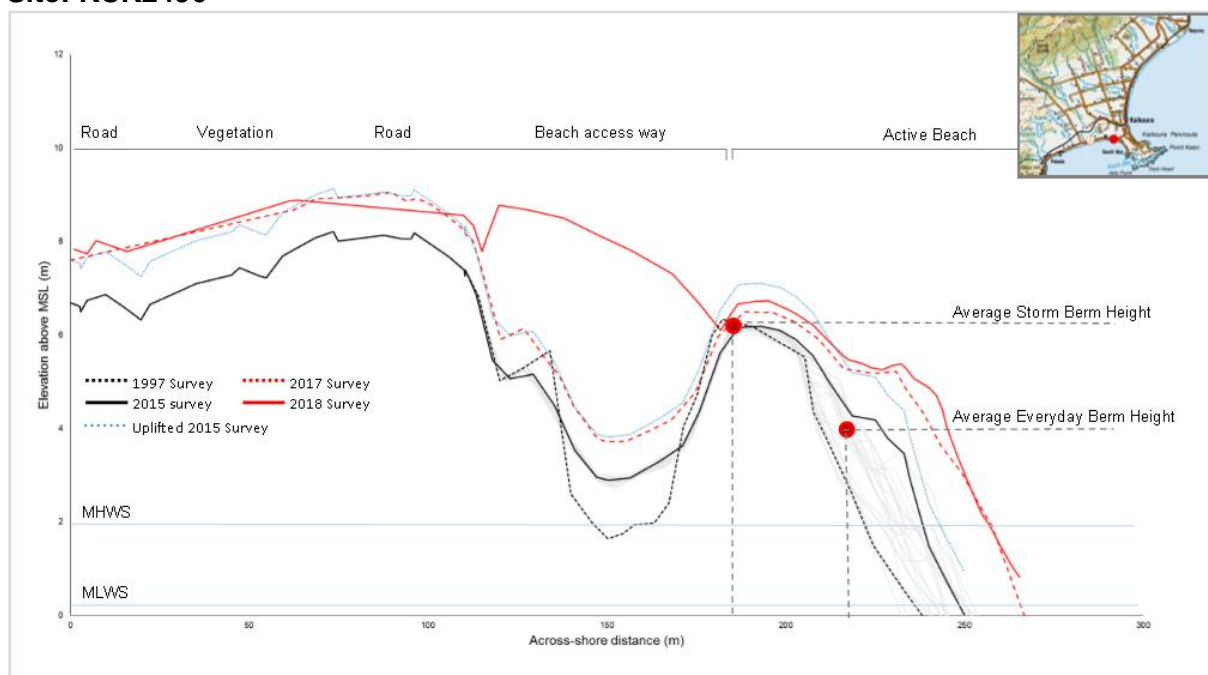
### Site description:

KCK2486 is aligned in a SW to NE orientation, and is 125 m north of KCK2470. The site is at the northern end of a long stretch of uninterrupted coastline, where the coastline begins to bend around to the Kaikōura Peninsula. It has a wide active beach width of 100 m. The site is sheltered from wave and wind coming from the north. The beach at this site is made up of well sorted, rounded clasts, as the sediment has been transported from sources south of the site. The annotated diagram (A) shows the profile has accreted and moved seaward over time, matched by the excursion plot (C) showing there is a long term accretionary trend at the MSL contour.

| Site Statistics (Pre Quake): |                    |                       |                           |
|------------------------------|--------------------|-----------------------|---------------------------|
| Active beach width           | 65 m               | Beach Slope           | 0.098                     |
| Average berm height          | 3 m                | Overall profile trend | Accretionary              |
| Average storm berm height    | 6 m                | Geomorphic group:     | Medium, accreting beaches |
| Average beach volume         | 202 m <sup>3</sup> | Subcategory:          | Sediment trapping         |



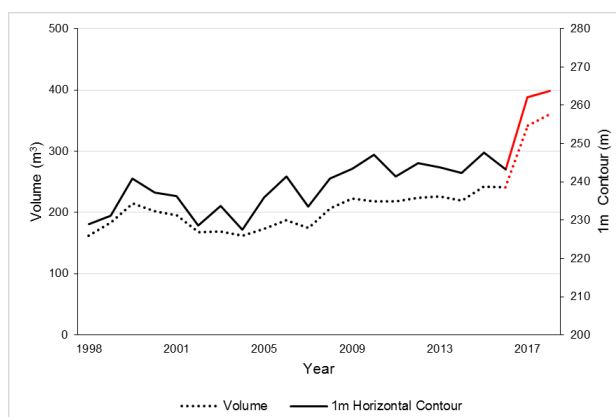
## Site: KCK2496



A: Annotated cross-sectional beach profile for Environment Canterbury site KCK2496 in South Bay, Kaikōura. Profile lines include 1997 Survey (Black dashed line); 2015 Survey (Solid black line); 2015 elevation profile (Grey dashed line); 2017 Survey (Dashed red line) and 2018 Survey (Solid red line). Inset (top right) shows location of site in the study area.



B: Picture of KCK2496 facing South. Picture taken 22<sup>nd</sup> August 2018.



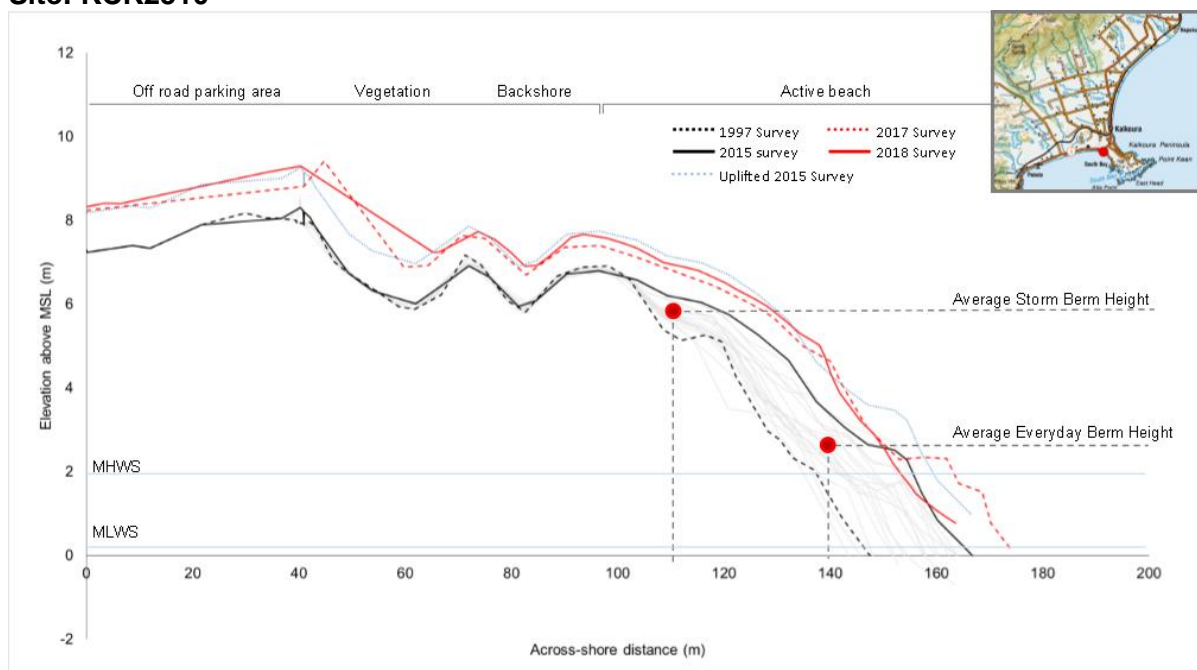
C: Beach profile horizontal width change at the MSL contour between 1997 and 2015 for Environment Canterbury site KCK2496.

### Site description:

KCK2496 is located 70 m north of KCK2486, just south of the South bay turn off. The site is at the end of a long stretch of straight coastline, and is aligned in SW to NE orientation, as the coastline begins to bend around to the Kaikōura Peninsula. As shown in the annotated diagram (A), the site has an 85 m wide active beach profile, which over time has accreted and developed a more defined berm features. The MSL excursion plot (C) shows a long term accretionary trend at the MSL contour, which follows cyclical behaviour, showing responses to eroding and accretionary events.

| Site Statistics (Pre Quake):     |                    |                              |                           |
|----------------------------------|--------------------|------------------------------|---------------------------|
| <b>Active beach width</b>        | 60 m               | <b>Beach Slope</b>           | 0.103                     |
| <b>Average berm height</b>       | 4 m                | <b>Overall profile trend</b> | Accretionary              |
| <b>Average storm berm height</b> | 6 m                | <b>Geomorphic group:</b>     | Medium, accreting beaches |
| <b>Average beach volume</b>      | 200 m <sup>3</sup> | <b>Subcategory:</b>          | Sediment trapping beaches |

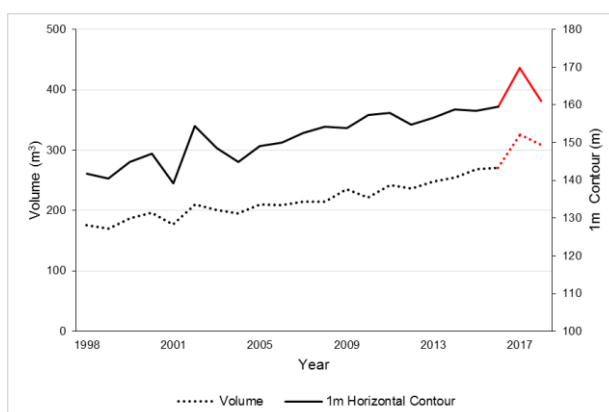
## Site: KCK2510



A: Annotated cross-sectional beach profile for Environment Canterbury site KCK2510 in South Bay, Kaikōura. Profile lines include 1997 Survey (Black dashed line); 2015 Survey (Solid black line); 2015 elevation profile (Grey dashed line); 2017 Survey (Dashed red line) and 2018 Survey (Solid red line). Inset (top right) shows location of the profile in the study area.



B: Picture of KCK2510 facing south. Picture taken April 19<sup>th</sup> 2018.



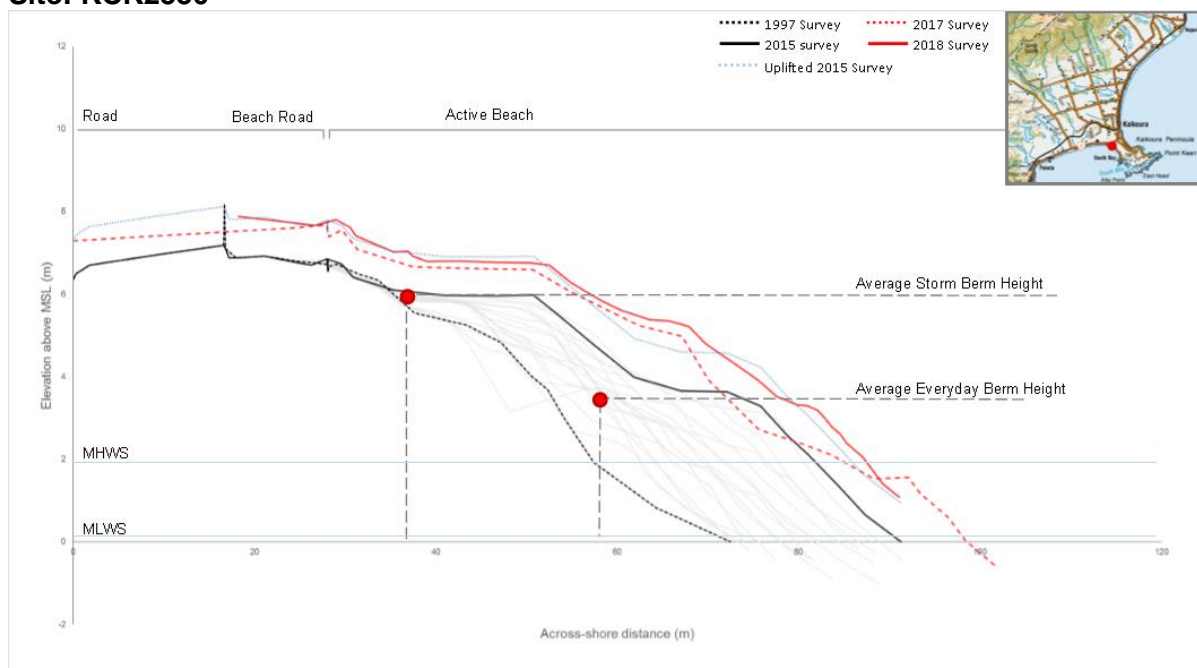
C: Beach profile horizontal width change at the MSL contour between 1997 and 2015 for Environment Canterbury site KCK2510.

### Site description:

KCK2510 is located at the South Bay turnoff, and is aligned in a SW to NE orientation. The site is protected from storm events coming from the north, and is an accumulation of sediment coming from the south. The sediment at this site is very well sorted and well rounded, as it is transported along shore from the Kowhai River and the Kahutara River. The profile, as shown in the annotated diagram (A), has an active beach width of approximately 70 m, and has followed a long term accretionary trend, as shown in both Figures A and C. While the active beach profile is similar to the sites surrounding it, this site has a sparse amount of sediment in its backshore where the beach road and parking area is.

| Site Statistics (Pre-Quake):     |                    |                              |                           |
|----------------------------------|--------------------|------------------------------|---------------------------|
| <b>Active beach width</b>        | 60 m               | <b>Beach Slope</b>           | 0.134                     |
| <b>Average berm height</b>       | 2.5 m              | <b>Overall profile trend</b> | Accretionary              |
| <b>Average storm berm height</b> | 6 m                | <b>Geomorphic group:</b>     | Medium, accreting beaches |
| <b>Average beach volume</b>      | 216 m <sup>3</sup> | <b>Subcategory:</b>          | Sediment trapping         |

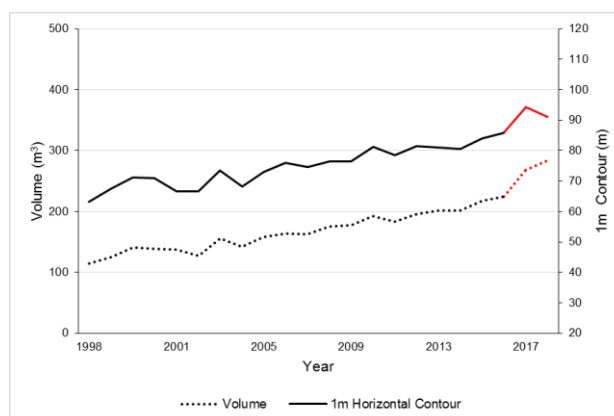
## Site: KCK2550



A: Annotated cross-sectional beach profile for Environment Canterbury site KCK2550 in South Bay, Kaikōura. Profile lines include 1997 Survey (Black dashed line); 2015 Survey (Solid black line); 2015 elevation profile (Grey dashed line); 2017 Survey (Dashed red line) and 2018 Survey (Solid red line). Inset (top right) shows the location of the profile in the study area.



B: Picture of KCK2550 facing South. Picture taken 21<sup>st</sup> August 2018.



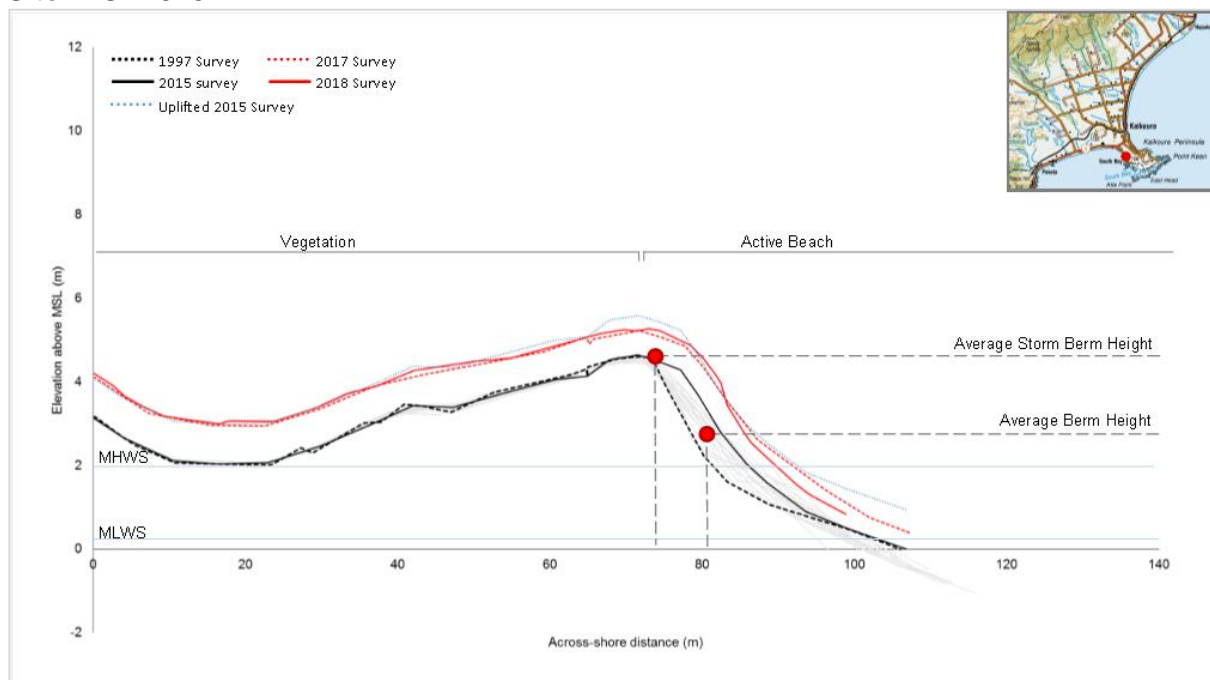
C: Beach profile horizontal width change at the MSL contour between 1997 and 2015 for Environment Canterbury site KCK2550.

### Site description:

KCK2550 is located at the beach across from the racetrack in South Bay, approximately 300m alongshore from KCK2510. The beach is aligned in a SW to NE orientation, and protected from storm events coming from the north by the Kaikōura Peninsula. As shown in the annotated diagram (A), the foreshore follows a strong accretionary trend, where, similar to KCK2510, the site is a trap from sediment moving north from the Kowhai River and the Kahutara River, by longshore transport. The active beach profile width is 55 m. Nearby offshore to this site, rock shore platforms are visible.

| Site Statistics (Pre Quake):     |                    |                              |                           |
|----------------------------------|--------------------|------------------------------|---------------------------|
| <b>Active beach width</b>        | 50 m               | <b>Beach Slope</b>           | 0.152                     |
| <b>Average berm height</b>       | 3.5 m              | <b>Overall profile trend</b> | Accretionary              |
| <b>Average storm berm height</b> | 6 m                | <b>Geomorphic group:</b>     | Medium, accreting beaches |
| <b>Average beach volume</b>      | 166 m <sup>3</sup> | <b>Subcategory:</b>          | Sediment trapping         |

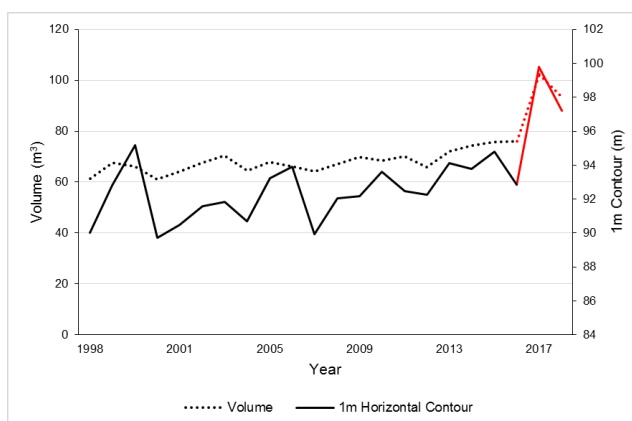
## Site: KCK2575



A: Annotated cross-sectional beach profile for Environment Canterbury site KCK2575 in South Bay, Kaikōura. Profile lines include 1997 Survey (Black dashed line); 2015 Survey (Solid black line); 2015 elevation profile (Grey dashed line); 2017 Survey (Dashed red line) and 2018 Survey (Solid red line).



B: Picture of KCK2575, facing South West. Picture taken 22<sup>nd</sup> August 2018.



C: Beach profile horizontal width change at the MSL contour between 1997 and 2015 for Environment Canterbury site KCK2575.

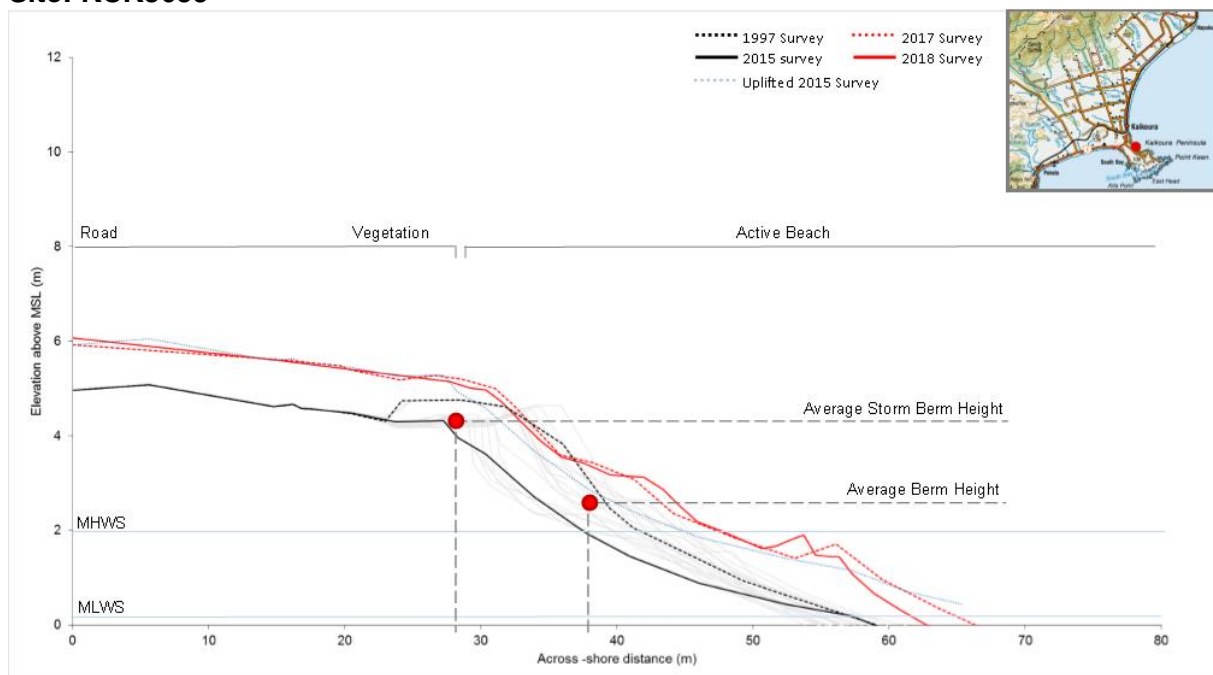
### Site description:

KCK2575 is located in central South Bay, and is the last mixed sand and gravel beach site before the coastline turns to rock shore platforms and cliffs. The profile is aligned in a WSW to ENE orientation, sheltered from storm events coming from the north. The profile is very steep and does not follow the typical MSG beach morphology seen in the other sites, as the foreshore is usually steepened and flat, with no development of berms. The annotated diagram (A) shows that over time the profile has accreted, however the long term trend exhibited at the MSL contour (C) shows a more stable long term trend at this site.

| Site Statistics (Pre Quake):     |                   |                              |                          |
|----------------------------------|-------------------|------------------------------|--------------------------|
| <b>Active beach width</b>        | 40 m              | <b>Beach Slope</b>           | 0.145                    |
| <b>Average berm height</b>       | 2.5 m             | <b>Overall profile trend</b> | Stable/Weak accretion    |
| <b>Average storm berm height</b> | 4.5 m             | <b>Geomorphic group:</b>     | Narrow and steep beaches |
| <b>Average beach volume</b>      | 68 m <sup>3</sup> | <b>Subcategory:</b>          | Swash dominated          |



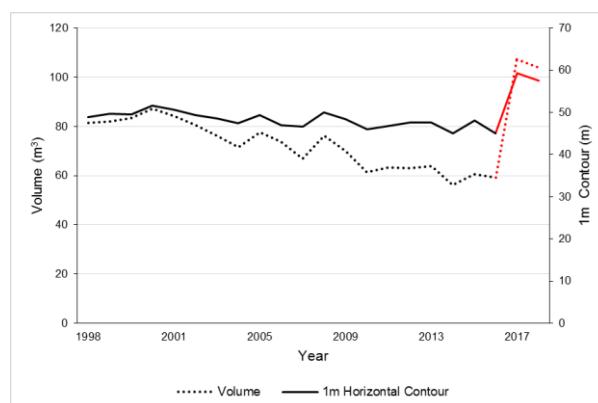
## Site: KCK3659



A: Annotated cross-sectional beach profile for Environment Canterbury site KCK3659, at Gooch's Beach, Kaikōura. Profile lines include 1997 Survey (Black dashed line); 2015 Survey (Solid black line); 2015 elevation profile (Grey dashed line); 2017 Survey (Dashed red line) and 2018 Survey (Solid red line). Inset (top right) shows location of the profile in the study area.



B: Picture of KCK3659 facing South East. Picture taken 23<sup>rd</sup> August 2018.



C: Beach profile horizontal width change at the MSL contour between 1997 and 2015 for Environment Canterbury site KCK3659.

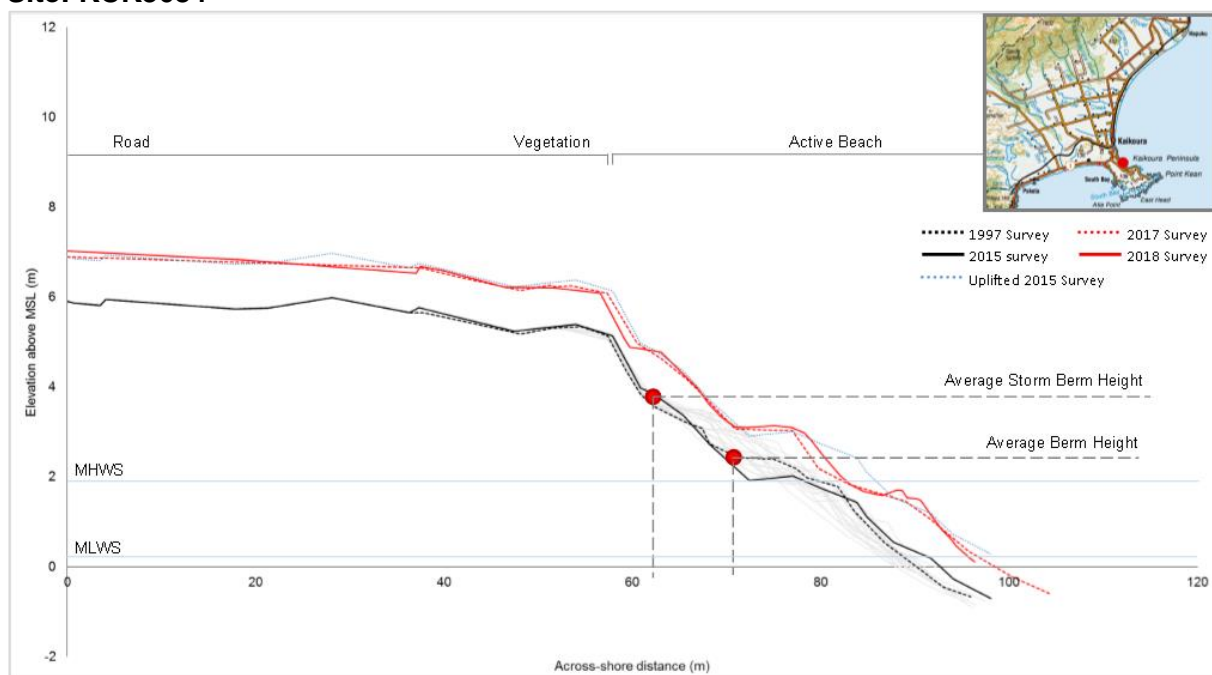
### Site description:

KCK3659 is located at the end of Ramsgate Street on the northern side of the peninsula. The profile is aligned in a NE to SW orientation. It is exposed to storms from the north, however is sheltered from the peninsula to storms from the south. The beach is narrow and steep, and in the past has exhibited typical MSG beach morphology with developed berms. The annotated diagram (A) shows that the whole profile has accreted and eroded over time. The MSL excursion plot shows a cyclical, slightly erosional long term trend. This site was also affected by the re-nourishment efforts undertaken north of the peninsula, and therefore would likely have a long term erosional trend without modification.

| Site Statistics (Pre Quake):     |                   |                              |                          |
|----------------------------------|-------------------|------------------------------|--------------------------|
| <b>Active beach width</b>        | 35 m              | <b>Beach Slope</b>           | 0.159                    |
| <b>Average berm height</b>       | 2.5 m             | <b>Overall profile trend</b> | Erosional                |
| <b>Average storm berm height</b> | 4.5 m             | <b>Geomorphic group:</b>     | Narrow and steep beaches |
| <b>Average beach volume</b>      | 71 m <sup>3</sup> | <b>Subcategory:</b>          | Renourished              |



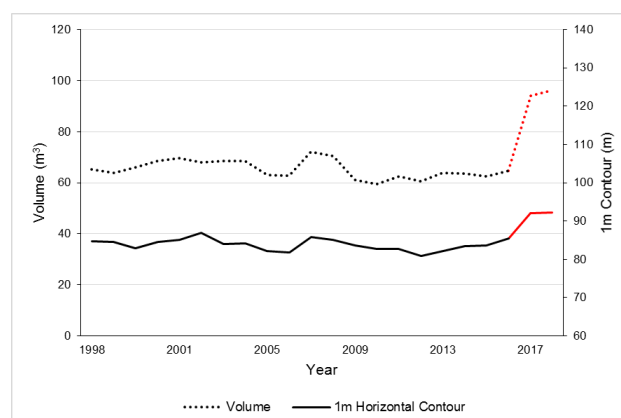
## Site: KCK3684



A: Annotated cross-sectional beach profile for Environment Canterbury site KCK3684, at Gooch's Beach, Kaikōura. Profile lines include 1997 Survey (Black dashed line); 2015 Survey (Solid black line); 2015 elevation profile (Grey dashed line); 2017 Survey (Dashed red line) and 2018 Survey (Solid red line). Inset (top right) shows the location of the profile in the study area.



B: Picture of KCK3684 facing North. Picture taken 23<sup>rd</sup> August 2018.



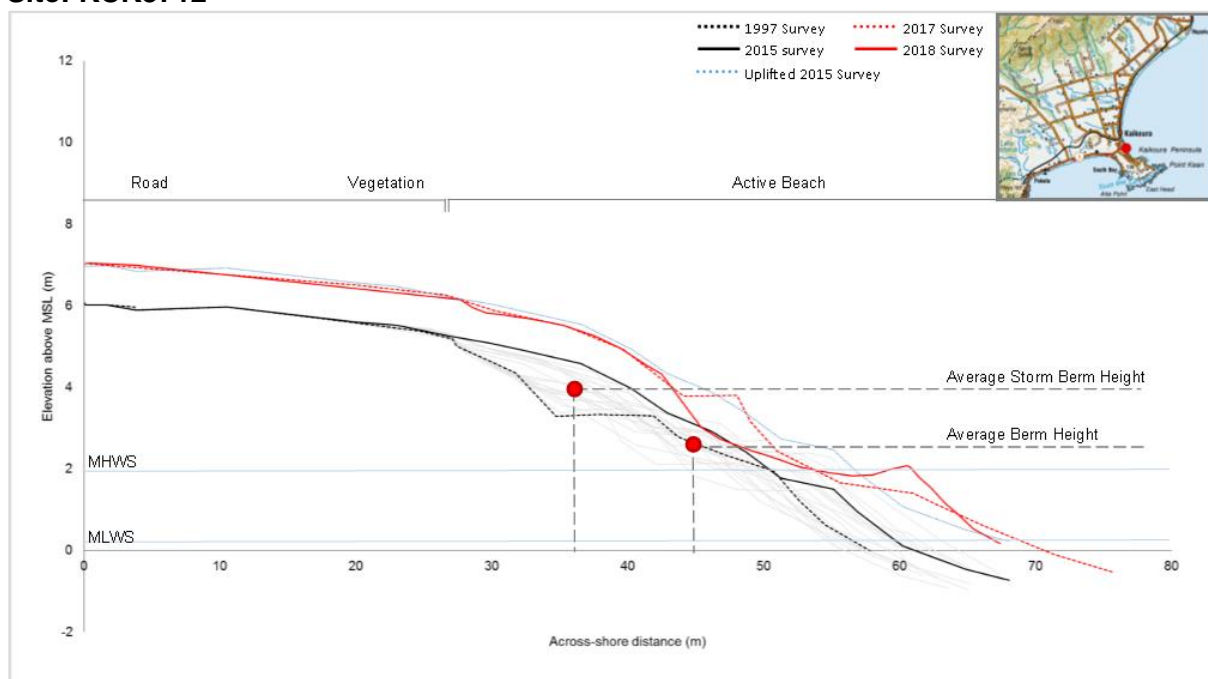
C: Beach profile horizontal width change at the MSL contour between 1997 and 2015 for Environment Canterbury site KCK3684.

### Site description:

KCK3684 is located at the end of Brighton Street on the northern side of the peninsula. The beach profile is aligned in a NE to SW direction, and is sheltered to storms coming from the south. The profile has an active beach width of 30 m. It has several defined berms. The site has been effected by re-nourishment put in place over the past two decades. The annotated diagram (A) shows a slightly eroded profile, while the MSL excursion plot (C) shows a long term cyclical but stable trend. Without the re-nourishment, it is likely this profile would have a long term erosional trend.

| Site Statistics:                 |                   |                              |                          |
|----------------------------------|-------------------|------------------------------|--------------------------|
| <b>Active beach width</b>        | 30 m              | <b>Beach Slope</b>           | 0.14                     |
| <b>Average berm height</b>       | 2.5 m             | <b>Overall profile trend</b> | Stable/weak erosional    |
| <b>Average storm berm height</b> | 3.5m              | <b>Geomorphic group:</b>     | Narrow and steep beaches |
| <b>Average beach volume</b>      | 65 m <sup>3</sup> | <b>Subcategory:</b>          | Renourished              |

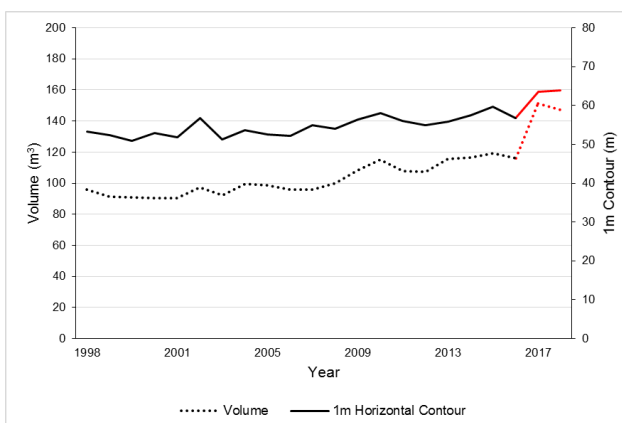
## Site: KCK3712



A: Annotated cross-sectional beach profile for Environment Canterbury site KCK3712, at Gooch's Beach, Kaikōura. Profile lines include 1997 Survey (Black dashed line); 2015 Survey (Solid black line); 2015 elevation profile (Grey dashed line); 2017 Survey (Dashed red line) and 2018 Survey (Solid red line). Inset (top right) shows the location of the profile in the study area.



B: Picture of KCK3712 facing north. Picture taken August 23<sup>rd</sup> 2018.



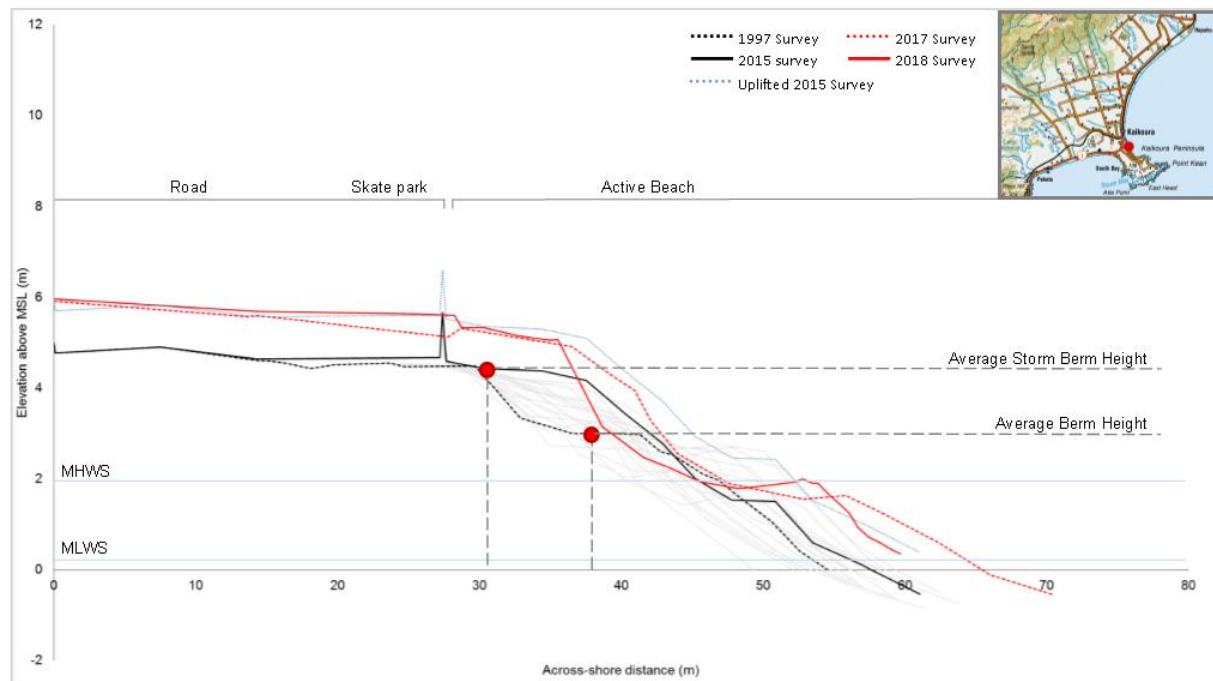
C: Beach profile horizontal width change at the MSL contour between 1997 and 2015 for Environment Canterbury site KCK3712.

### Site description:

KCK3712 is located at the end of Yarmouth Street. The profile is orientated in a north east direction, and is sheltered from storms coming from the south by the peninsula. The profile has an active beach width of 35 m, of which the storm berm and the berm positions have been extremely dynamic over the analysed period. The annotated diagram (A) shows that over time the profile has followed cyclical behaviour, with periods of erosion and accretion. The MSL excursion plot (C) has showed that the MSL contour has remained stable with a slight accretionary trend. This site was affected by the re-nourishment scheme which has effected the long term trend at this site.

| Site Statistics (Pre Quake): |                    |                       |                          |
|------------------------------|--------------------|-----------------------|--------------------------|
| Active beach width           | 35 m               | Beach Slope           | 0.172                    |
| Average berm height          | 2.5 m              | Overall profile trend | Stable/weak accretion    |
| Average storm berm height    | 4 m                | Geomorphic group:     | Narrow and steep beaches |
| Average beach volume         | 102 m <sup>3</sup> | Subcategory:          | Renourished              |

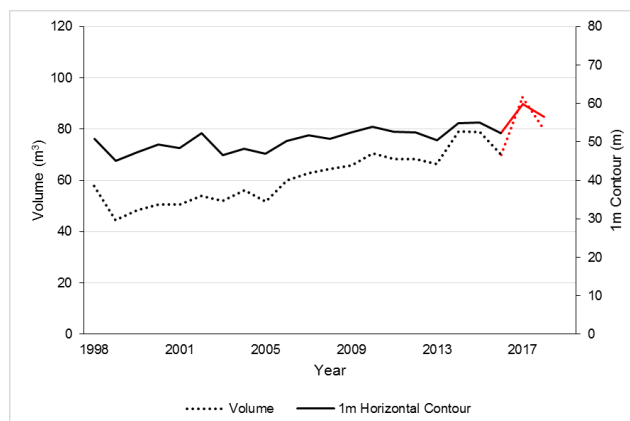
## Site: KCK3737



A: Annotated cross-sectional beach profile for Environment Canterbury site KCK3737, at Gooch's Beach, Kaikōura. Profile lines include 1997 Survey (Black dashed line); 2015 Survey (Solid black line); 2015 elevation profile (Grey dashed line); 2017 Survey (Dashed red line) and 2018 Survey (Solid red line). Inset (top right) shows the location of this profile in the study area.



B: Picture of KCK3737 facing north. Picture taken August 23<sup>rd</sup> 2018.



C: Beach profile horizontal width change at the MSL contour between 1997 and 2015 for Environment Canterbury site KCK3737.

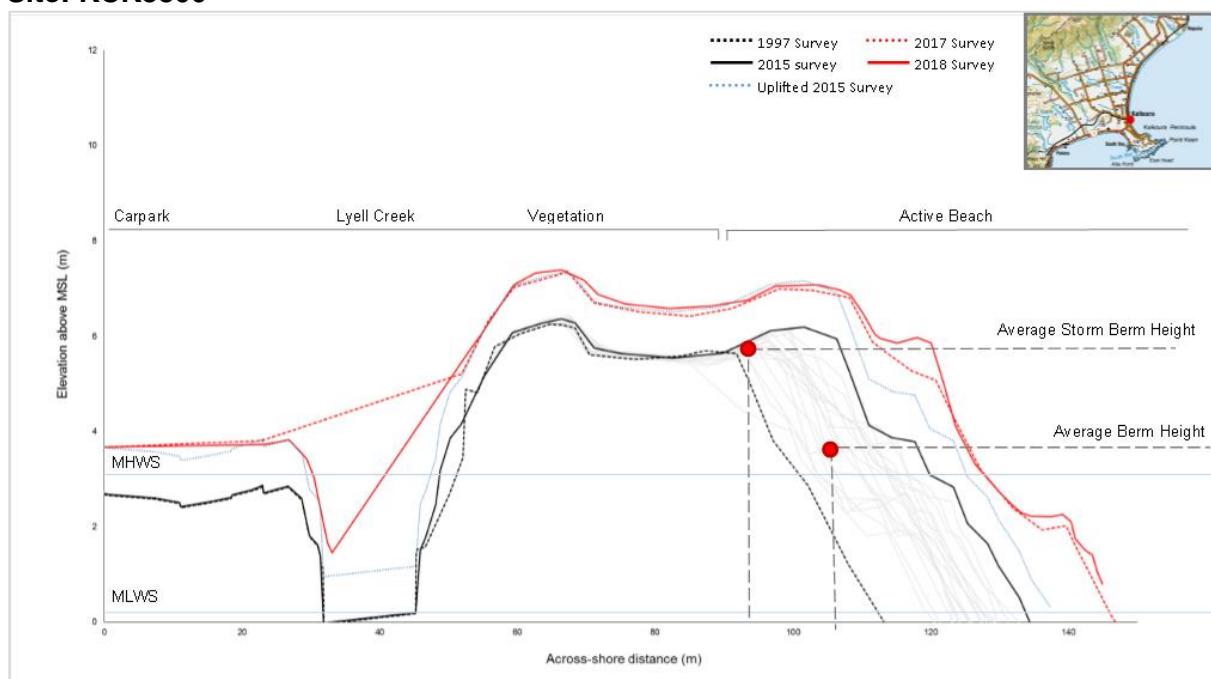
### Site description:

KCK3737 is located just north of Killarney Street, across from the Takahanga Domain, approximately 250 m north of KCK3712. The beach is orientated in a north east direction. It has a narrow active beach width of 30 m, and was also affected by the renourishment scheme which took place throughout the analysed period. The annotated diagram (A) shows that berm is very dynamic and over time has both eroded and accreted. The storm berm has stayed in a relatively similar position throughout the analysed period, restricted by the building and road behind the storm berm. The MSL excursion plot (C) shows the MSL contour exhibits cyclical behaviour, but overall has a stable/slight accretionary trend.

| Site Statistics:                 |                   |                              |                          |
|----------------------------------|-------------------|------------------------------|--------------------------|
| <b>Active beach width</b>        | 30 m              | <b>Beach Slope</b>           | 0.176                    |
| <b>Average berm height</b>       | 3 m               | <b>Overall profile trend</b> | Stable/weak accretion    |
| <b>Average storm berm height</b> | 4.5 m             | <b>Geomorphic group:</b>     | Narrow and steep beaches |
| <b>Average beach volume</b>      | 61 m <sup>3</sup> | <b>Subcategory:</b>          | Renourished              |



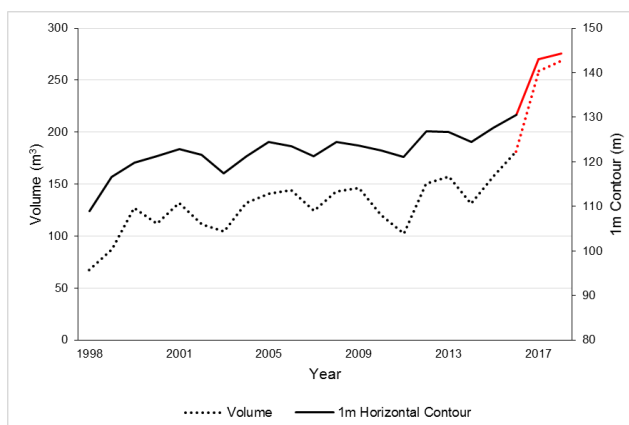
## Site: KCK3800



A: Annotated cross-sectional beach profile for Environment Canterbury site KCK3800, at the town centre, Kaikōura. Profile lines include 1997 Survey (Black dashed line); 2015 Survey (Solid black line); 2015 elevation profile (Grey dashed line); 2017 Survey (Dashed red line) and 2018 Survey (Solid red line). Inset (top right) shows the location of the profile in the study area.



B: Picture of KCK3800 facing North. Picture taken August 23<sup>rd</sup> 2018.



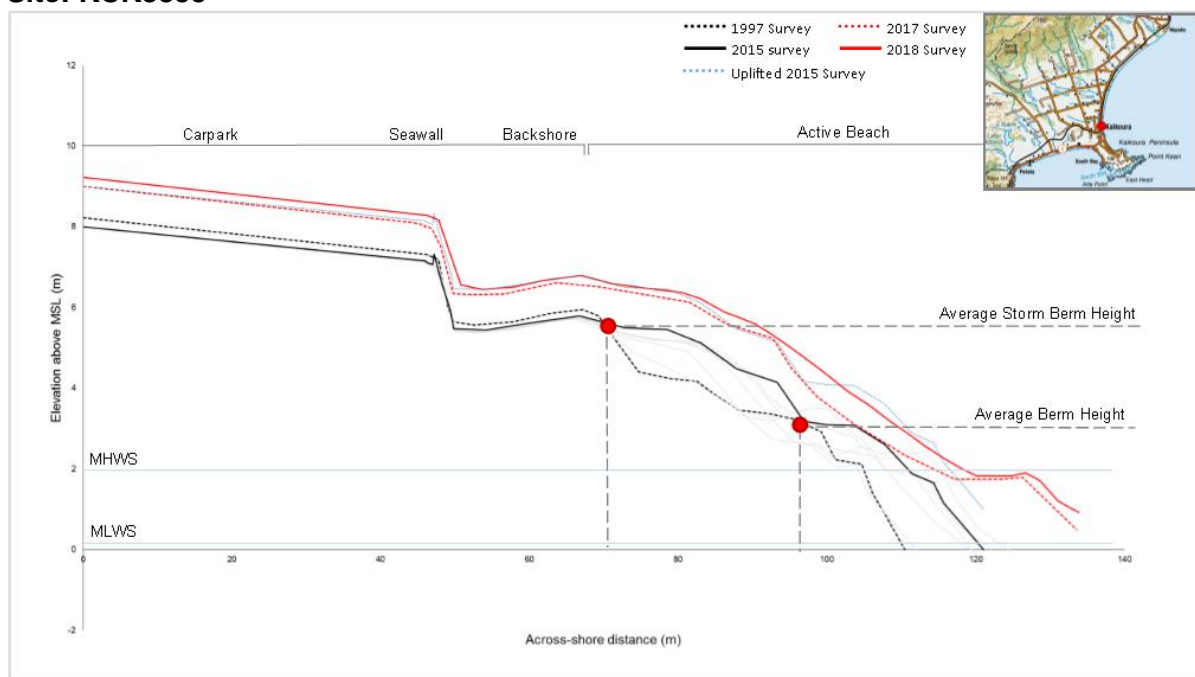
C: Beach profile horizontal width change at the MSL contour between 1997 and 2015 for Environment Canterbury site KCK3800.

### Site description:

KCK3800 is located across the carpark near the Kaikōura I-Site, across Lyell Creek, and through to the beach. The beach is aligned in a NE to SW orientation. The beach has an active profile of 45 m, but its backshore is restricted by Lyell Creek and the township located directly behind it. As seen in the annotated diagram (A), the profile has overall accreted, but the foreshore is very dynamic. The MSL excursion plot (C) shows the beach has cyclical behaviour at the MSL contour, but overall follows a long term accretional trend.

| Site Statistics:          |                    |                       |                  |
|---------------------------|--------------------|-----------------------|------------------|
| Active beach width        | 45 m               | Beach Slope           | 0.187            |
| Average berm height       | 3 m                | Overall profile trend | Accretionary     |
| Average storm berm height | 5.5 m              | Geomorphic group:     | Narrow and steep |
| Average beach volume      | 128 m <sup>3</sup> | Subcategory:          | Accretionary     |

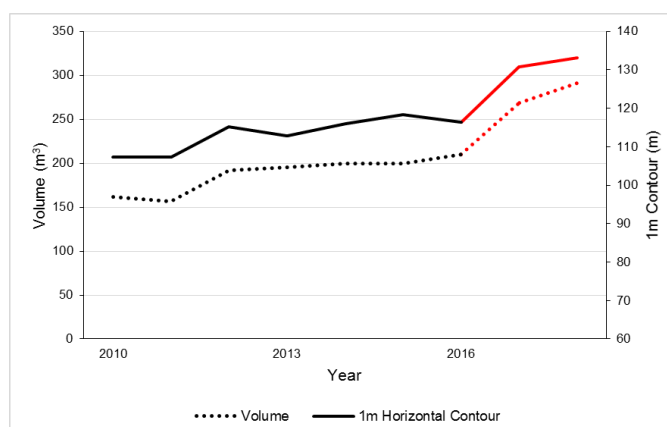
## Site: KCK3855



A: Annotated cross-sectional beach profile for Environment Canterbury site KCK3855, at the Whale Watch, Kaikōura. Profile lines include 1997 Survey (Black dashed line); 2015 Survey (Solid black line); 2015 elevation profile (Grey dashed line); 2017 Survey (Dashed red line) and 2018 Survey (Solid red line). Inset (top right) shows the location of the profile in the study area.



B: Picture of KCK3855 facing north. Picture taken 23<sup>rd</sup> August 2018.



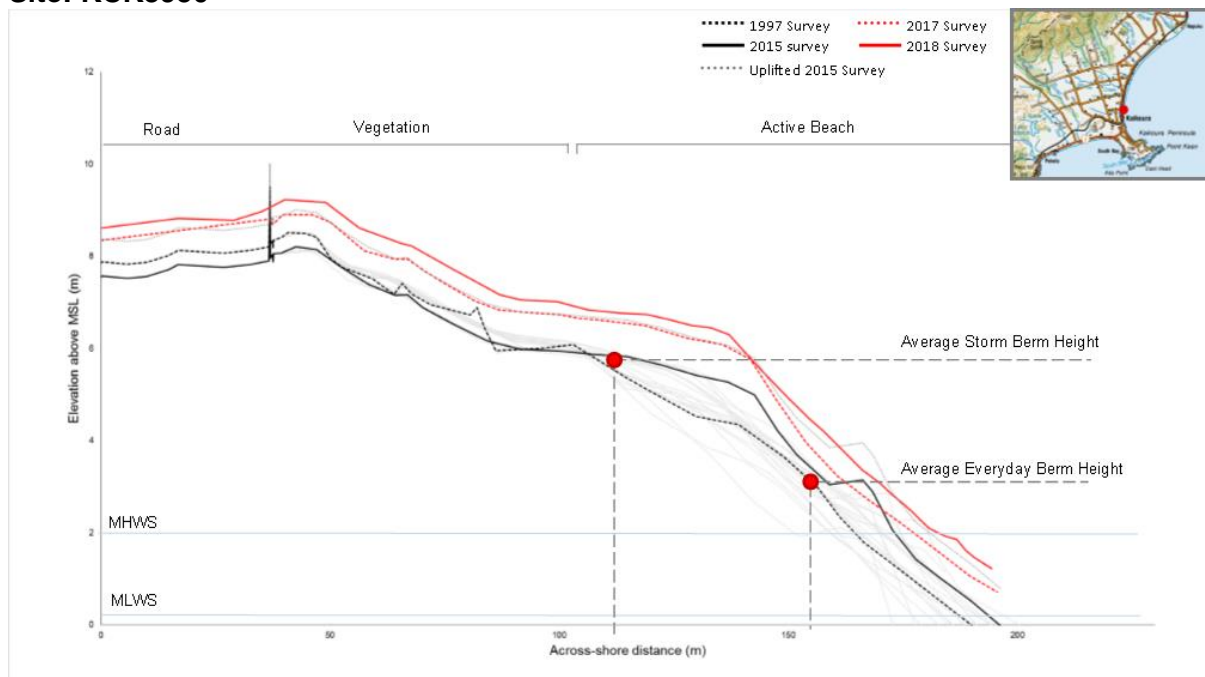
C: Beach profile horizontal width change at the MSL contour between 1997 and 2015 for Environment Canterbury site KCK3855.

### Site description:

Site KCK3855 is located approximately 500 m north of KCK3800, by Whale Watch Kaikōura. The site has only been monitored since 2009. The profile is aligned in an E to W orientation, and has an active beach width of 60 m. The beach is restricted landward at this site by a seawall protecting the whale watch building, carpark and railway station. The annotated diagram (A) shows that overall the profile has accreted, but the foreshore is dynamic. The MSL excursion plot (C) shows an accretionary trend at the MSL contour. Sediment supply is transported to this site alongshore south from the Hāpuku River.

| Site Statistics:                 |                    |                              |                  |
|----------------------------------|--------------------|------------------------------|------------------|
| <b>Active beach width</b>        | 60 m               | <b>Beach Slope</b>           | 0.111            |
| <b>Average berm height</b>       | 3 m                | <b>Overall profile trend</b> | Accretionary     |
| <b>Average storm berm height</b> | 6 m                | <b>Geomorphic group:</b>     | Narrow and steep |
| <b>Average beach volume</b>      | 188 m <sup>3</sup> | <b>Sub category:</b>         | Accretionary     |

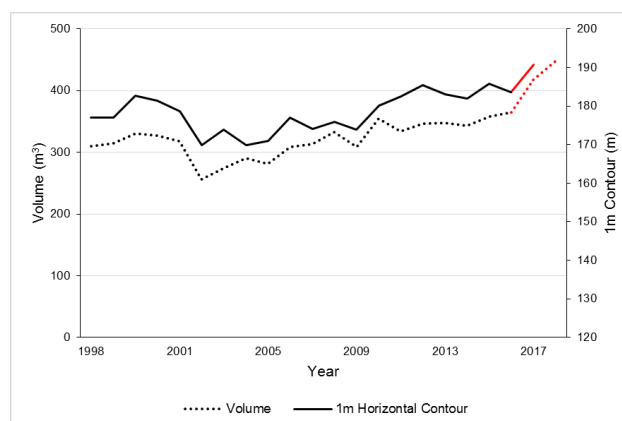
## Site: KCK3950



A: Annotated cross-sectional beach profile for Environment Canterbury site KCK3950, north of the township, Kaikōura. Profile lines include 1997 Survey (Black dashed line); 2015 Survey (Solid black line); 2015 elevation profile (Grey dashed line); 2017 Survey (Dashed red line) and 2018 Survey (Solid red line). Inset (top right) shows the location of the profile in the study area.



B: Picture of KCK3950, facing north. Picture taken 19<sup>th</sup> August 2018.



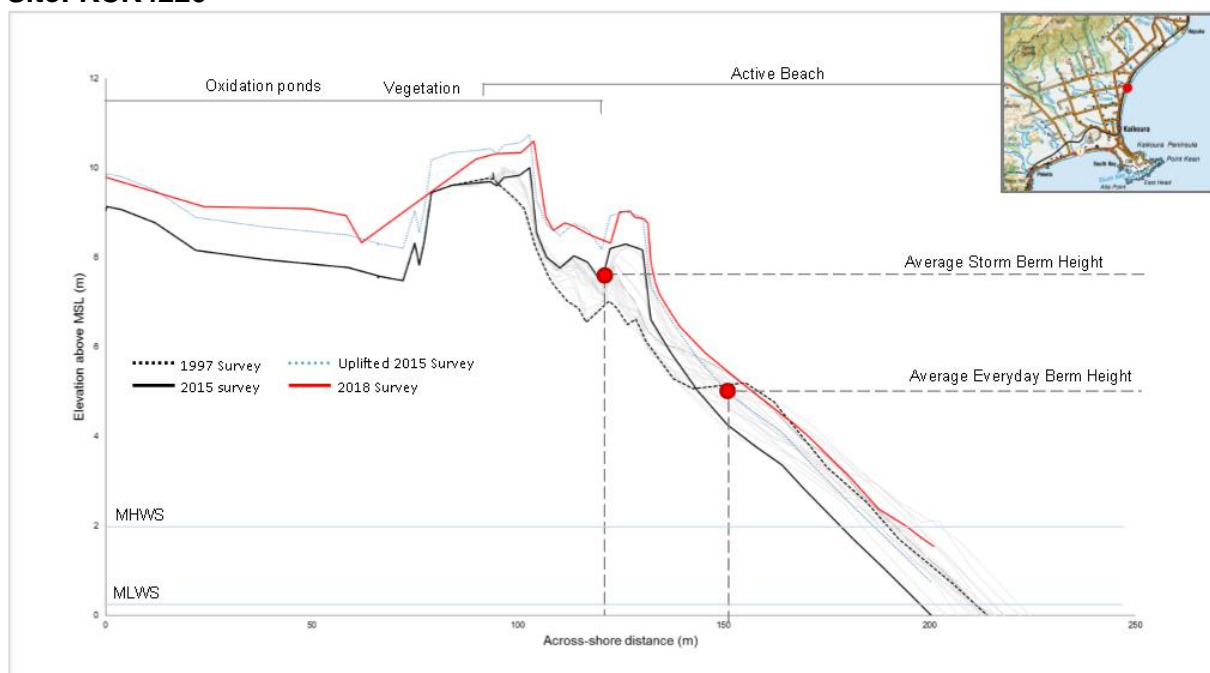
C: Beach profile horizontal width change at the MSL contour between 1997 and 2015 for Environment Canterbury site KCK3950.

### Site description:

KCK3950 is located at the end of Hawthorne Road. The profile is aligned in an E to W orientation. It has an active beach width of 100 m, and a backshore which is also sediment rich, but stable. The annotated diagram (A) shows that the beach profile has an overall accretionary trend, however the foreshore is very dynamic in the swash zone. The MSL excursion plot (C) shows that the site follows an overall accretionary trend, however the MSL contour is extremely dynamic and its position in the past has changed significantly in some events from year to year. Sediment is transported alongshore to this site south from the Hāpuku River.

| Site Statistics:                 |                    |                              |                        |
|----------------------------------|--------------------|------------------------------|------------------------|
| <b>Active beach width</b>        | 100 m              | <b>Beach Slope</b>           | 0.075                  |
| <b>Average berm height</b>       | 3 m                | <b>Overall profile trend</b> | Dynamic/weak accretion |
| <b>Average storm berm height</b> | 6 m                | <b>Geomorphic group:</b>     | Wide and flat          |
| <b>Average beach volume</b>      | 320 m <sup>3</sup> | <b>Subcategory:</b>          | Open coast             |

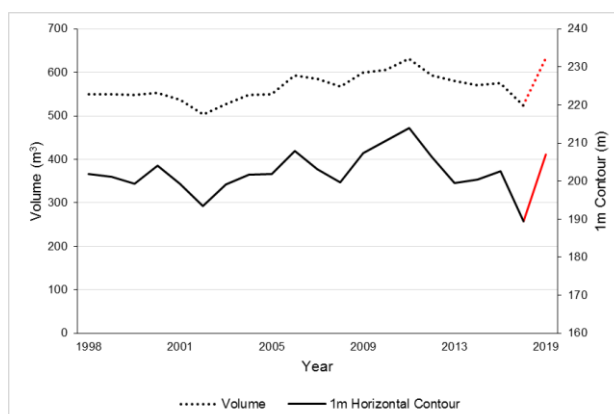
## Site: KCK4220



A: Annotated cross-sectional beach profile for Environment Canterbury site KCK4220, near the oxidation ponds, Kaikōura. Profile lines include 1997 Survey (Black dashed line); 2015 Survey (Solid black line); 2015 elevation profile (Grey dashed line); and 2018 Survey (Solid red line). Inset (top right) shows the location of the profile in the study area.



B: Picture of KCK4220 facing south. Picture taken August 23<sup>rd</sup> 2018.



C: Beach profile horizontal width change at the MSL contour between 1997 and 2015 for Environment Canterbury site KCK4220.

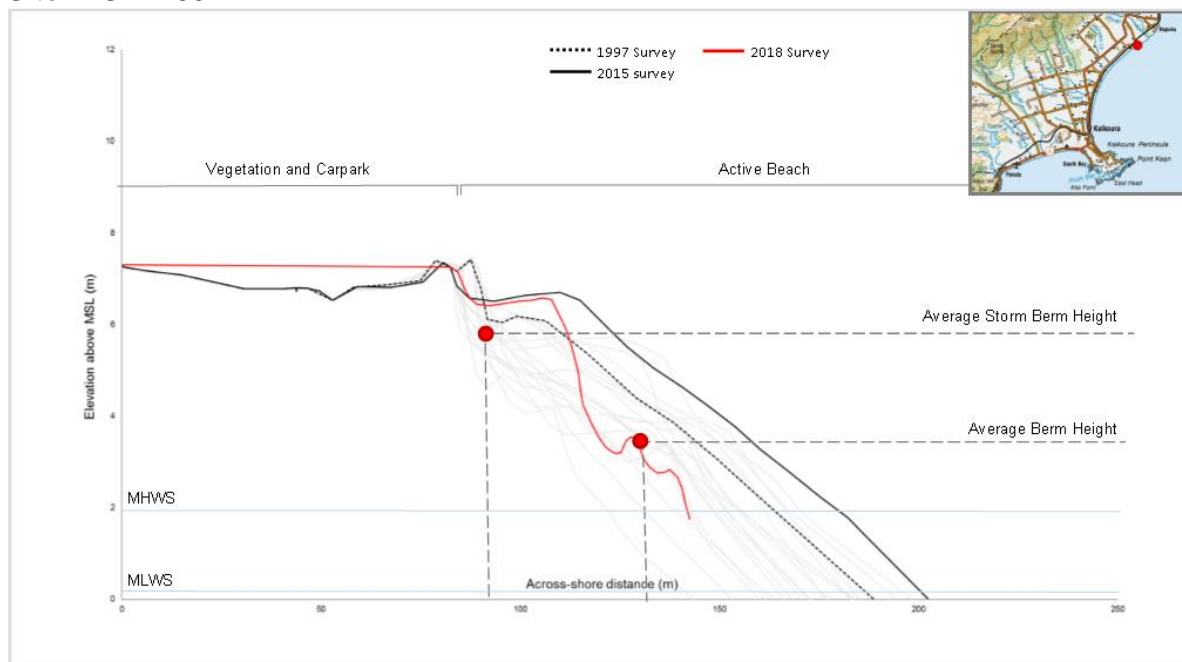
### Site description:

KCK4220 is located near the oxidation ponds, approximately 2.75 km north of KCK3950. The profile is orientated in a SE to NW direction, and has an active beach width of 105 m. Over time, as shown on the annotated diagram (A), the foreshore is very dynamic, but since 1997 has eroded, while the storm berm has accreted since 1997. The profile is very dynamic and exhibits only a slight accretionary trend at the MSL horizontal contour (C), however shows the foreshore does not continuously erode or accrete. The main sediment supply to this site is from longshore transport of sediment from the Hāpuku River.

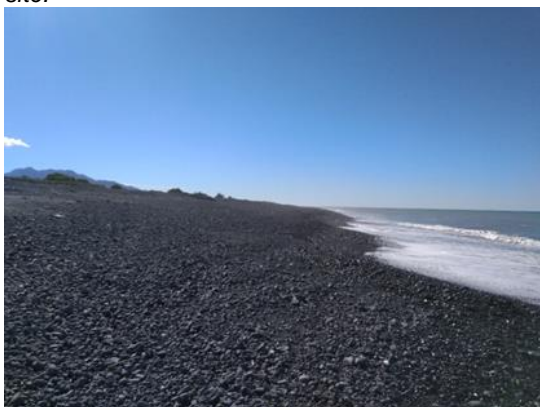
| Site Statistics:                 |                    |                              |                        |
|----------------------------------|--------------------|------------------------------|------------------------|
| <b>Active beach width</b>        | 105 m              | <b>Beach Slope</b>           | 0.080                  |
| <b>Average berm height</b>       | 5 m                | <b>Overall profile trend</b> | Dynamic/weak accretion |
| <b>Average storm berm height</b> | 7.5 m              | <b>Geomorphic group:</b>     | Wide and flat          |
| <b>Average beach volume</b>      | 564 m <sup>3</sup> | <b>Subcategory:</b>          | Open coast             |



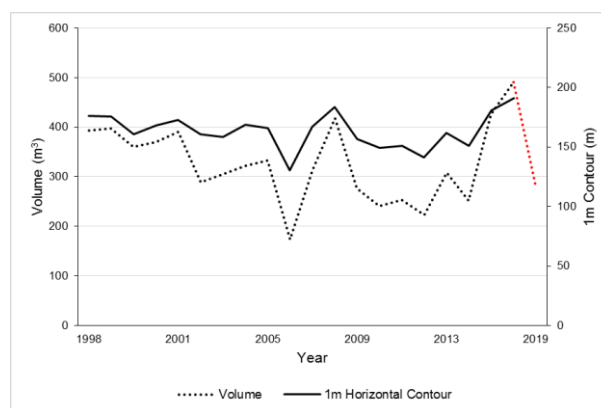
## Site: KCK4700



A: Annotated cross-sectional beach profile for Environment Canterbury site KCK4700, south of the Hāpuku River mouth, Kaikōura. Profile lines include 1997 Survey (Black dashed line); 2015 Survey (Solid black line); and 2018 Survey (Solid red line). The inset (top right) shows the location of the profile in the study area. There is no uplifted 2015 profile as it was recorded in this study there was no uplift at this site. There was also no 2017 survey at this site.



B: Picture of KCK4700 profile facing north. Picture taken April 19<sup>th</sup> 2018.



C: Beach profile horizontal width change at the MSL contour between 1997 and 2015 for Environment Canterbury site KCK4700.

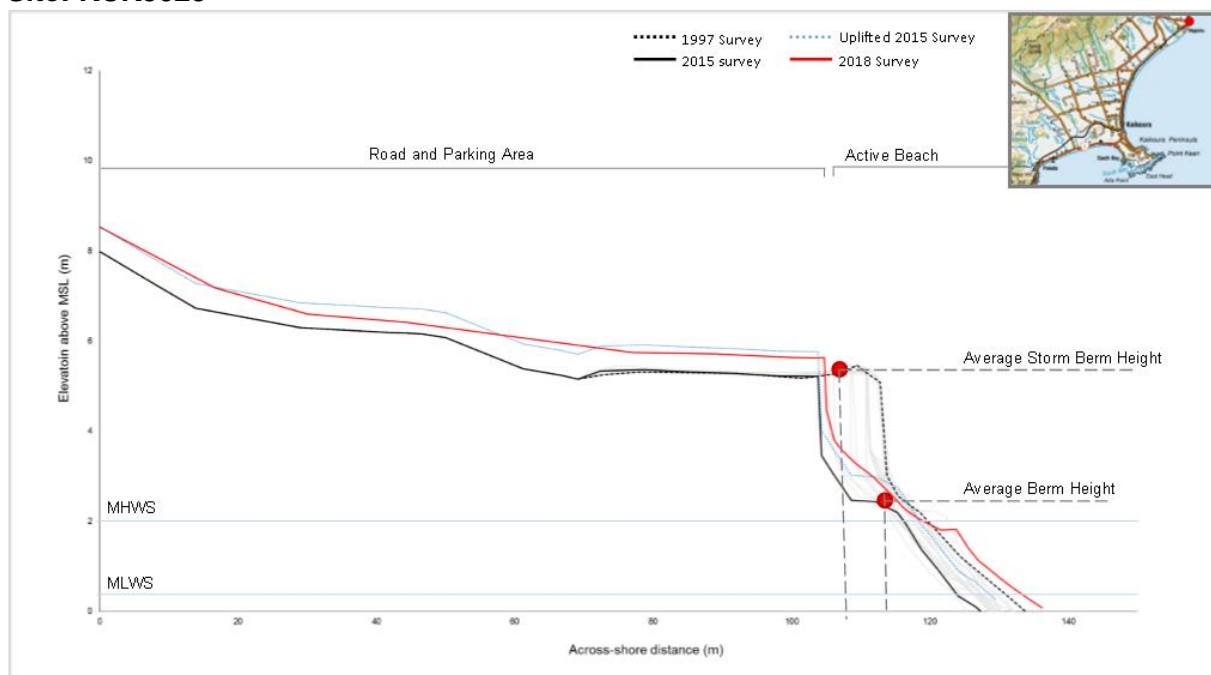
### Site description:

KCK4700 is located out the southern edge of the Hāpuku River flood plain. It has a wide active beach profile of 110 m. The foreshore is extremely dynamic, as shown in the annotated diagram (A). The profile is orientated in a SE to NW direction, and is on the open coastline. The horizontal extent of the berm and storm berm are very dynamic, and as shown in the excursion plot (C), the foreshore is extremely dynamic at the MSL contour, and has the ability to erode and accrete at significant rates between surveys. The close proximity to the Hāpuku River means there is a close sediment source, however the close proximity to the flood plain means the changes in the river levels can also affect the beach profile. Overall the MSL excursion shows there is a slight erosional trend, however the site is very dynamic.

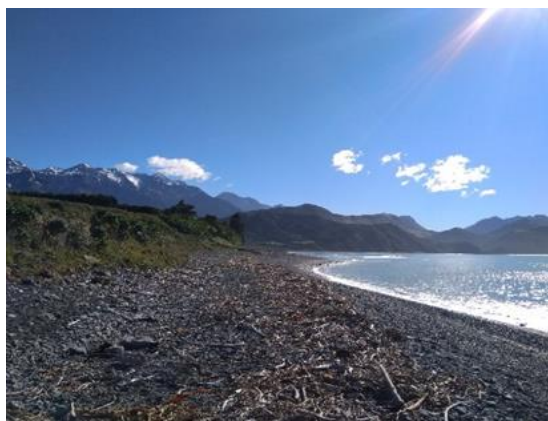
| Site Statistics:                 |                    |                              |                        |
|----------------------------------|--------------------|------------------------------|------------------------|
| <b>Active beach width</b>        | 110 m              | <b>Beach Slope</b>           | 0.072                  |
| <b>Average berm height</b>       | 3.5 m              | <b>Overall profile trend</b> | Dynamic/weak erosional |
| <b>Average storm berm height</b> | 5.5 m              | <b>Geomorphic group:</b>     | Wide and flat          |
| <b>Average beach volume</b>      | 326 m <sup>3</sup> | <b>Subcategory:</b>          | Open coast             |



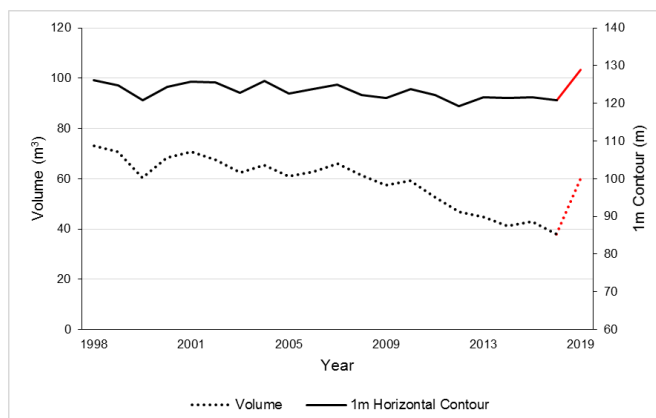
## Site: KCK5025



A: Annotated cross-sectional beach profile for Environment Canterbury site KCK5025, north of the Hāpuku River mouth, Kaikōura. Profile lines include 1997 Survey (Black dashed line); 2015 Survey (Solid black line); 2015 elevation profile (Grey dashed line); and 2018 Survey (Solid red line). The inset (top right) shows the location of the site within the study area. There was no 2017 survey at this site.



B: Picture of KCK5025 facing North. Picture taken April 20<sup>th</sup> 2018.



C: Beach profile horizontal width change at the MSL contour between 1997 and 2015 for Environment Canterbury site KCK5025.

### Site description:

KCK5025 is located approximately 1.5 km north of the Hāpuku River. The profile is orientated in an E to W direction. The beach here is restricted by a carpark located behind the scarp, and SH1 further north. The beach has a narrow active width of 30 m, with large scarp face at its landward extent. The beach profile here follows a stable, cyclical trend, in which overall the whole profile has accreted, but from year to year undergoes periods of erosion and accretion, as seen in the MSL excursion plot (C).

| Site Statistics:                 |                   |                              |                          |
|----------------------------------|-------------------|------------------------------|--------------------------|
| <b>Active beach width</b>        | 30 m              | <b>Beach Slope</b>           | 0.205                    |
| <b>Average berm height</b>       | 2.5 m             | <b>Overall profile trend</b> | Erosional                |
| <b>Average storm berm height</b> | 5.5m              | <b>Geomorphic group:</b>     | Narrow and steep beaches |
| <b>Average beach volume</b>      | 58 m <sup>3</sup> | <b>Subcategory:</b>          | Eroding                  |

## B Methods for calculating geomorphic parameters

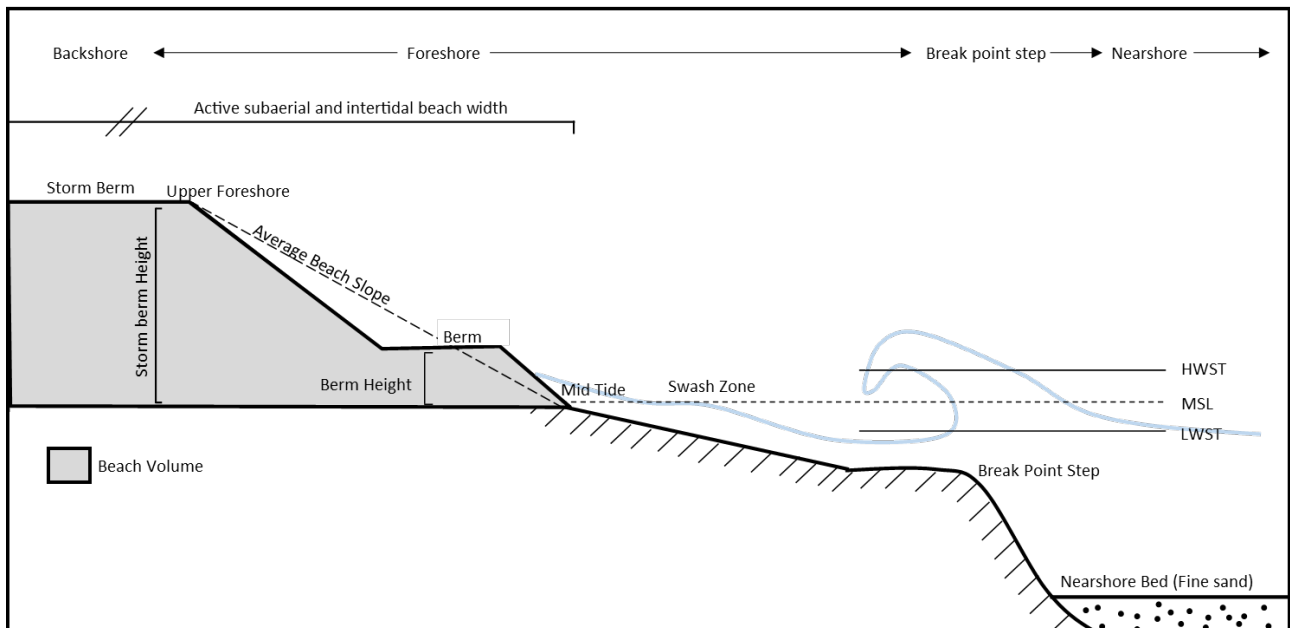


(Figure 4.3) Schematic of a MSG beach profile showing the extent and occurrence of the geomorphic parameters used in the classification of this study in a simplified MSG environment. Adapted from Kirk (1980). Repeated here from Chapter 4 for convenience.

### Beach width

The parameter for beach width in this study was taken from beach profile data collected by ECan from 1997 to 2015. As shown in Figure 4.3, the measurement is taken from the landward edge of the beach profile where there was continuous change over the 18 year analysed period to the mean sea level contour (MSL). The landward extent of this parameter was often similar to the position of the storm berm.

### Beach volume

As shown in Figure 4.3, the volume of sediment at a profile can be calculated using the area underneath the active beach profile, from the landward extent of the active beach profile to the MSL contour.

### Graphic mean clast size

Mean clast size data was taken from ECan survey data collected in 1997. The graphic mean is a standard measure of size used for determining overall size, calculated by Folk (1980) equa-

tion where  $M_z$  is measured in phi ( $\Phi$ ) by taking the phi size at the 16<sup>th</sup>, 50<sup>th</sup> and 84<sup>th</sup> percentile.

$$M_z = \frac{\Phi_{16} + \Phi_{50} + \Phi_{84}}{3} \quad (1)$$

The sedimentology data was collected at the mid tide mark to represent the hydraulic mixing controls on the foreshore, and another sample collected at the upper foreshore mark to represent long swashes of storm waves and wind action (McLean and Kirk, 1969).

## Sorting

This parameter was determined using the sedimentology data collected by ECan in 1997, taken from the mid tide and the upper foreshore areas. Inclusive graphic standard deviation was used to describe the sorting of the samples (Dawe, 1997). The scale used is as described in Folk (1980), as shown in the table below.

Sorting classification scheme (Folk, 1980)

| Inclusive graphic standard deviation ( $\phi$ ) | Sorting texture         |
|---|-------------------------|
| < 0.35  | Very well sorted        |
| 0.35—0.50                                       | Well sorted             |
| 0.50—0.71                                       | Moderately well sorted  |
| 0.71—1.0  | Moderately sorted       |
| 1.0—2.0   | Poorly sorted           |
| 2.0—4.0   | Very poorly sorted      |
| > 4.0   | Extremely poorly sorted |

## Beach slope

The beach slope was calculated using the ratio of change of the elevation and across-shore distance from the average storm berm position, to the MSL contour, and averaging this out across all years for each profile.

## Long-term trend

Long-term trends of the beach profiles were calculated using the MSL excursion points and beach volume changes from 1997 to 2015, with a linear trend line analysis allied to the resultant

plot to determine whether the beaches were eroding (negative trend line slopes), stable (flat trend line), or accreting (positive trend line slopes) over the 18.5 year period.

### **Berm height**

Berm height has been calculated by determining the average berm across-shore and elevation position for the berm, and taking the elevation of these positions of both the berm and the storm berm. These elevations were averaged across the 18.5 year period, and the average was used.

## **C Methods for calculating environmental parameters**

### **Grouping using environmental parameters**

Determining the environmental parameters to use in this study was a mixture of previous literature regarding the Kaikōura coastal environment, discussed in Chapter 3. Arbitrary numbers were applied to each profile based on how they responded to an environmental parameter.

### **Hinterland type**

Hinterland type was determined based on visual field observations of what was occurring in the backshore of the profile, and what was occurring on a broad scale within the catchment. The hinterland types attributed to profiles were:

1. Limestone mudstone peninsula
2. Urban area on fluvial plain
3. Fluvial plain
4. Hapua/River

### **Sediment supply**

Sediment supply was determined based on what the main source of sediment to the profiles, and how extensive that supply is. As shown in the literature, the main sediment supply comes from the Kahutara, Kowhai and Hāpuku Rivers. The sediment supply types attributed to profiles were:

1. Renourishment
2. Rivers and Creeks (1 main river)
3. Rivers and Creeks (2 main rivers)

### **Sediment transport**

Sediment transport was determined based on the literature, wave refraction modelling and remote sensing data to determine for each profile what the primary processes was that was

moving sediment from the main source to the profile. The sediment transport types attributed to profiles were:

1. Renourishment (artificial)
2. Long shore drift (with wave refraction and swell direction)
3. Long shore drift (with swell direction)
4. Long shore drift (with current and swell direction)

### **Sheltering from Southerlies and North Easterlies**

Sheltering from the southerlies and north easterlies was determined based on where the profile was located relative to the Peninsula and prevailing wind direction. The sheltering types attributed to the profiles were:

1. Exposed
2. Some sheltering
3. Sheltered

### **Distance to natural sediment source**

Distance to a natural sediment source was calculated using ArcGIS, measuring the alongshore distance from a profile to its closest respective main sediment source. Profiles north of the Peninsula are measured to the Hāpuku River, and profiles south of the Peninsula are measured to its closest river between the Kowhai and the Kahutara River.

### **Distance from the central Peninsula**

Distance from the central Peninsula was calculated by measuring from the most eastern point of the Peninsula, alongshore to each profile using ArcGIS.

## D Sedimentology results

Sedimentology results carried out using DGS analysis in September 2018, showing comparisons between 2018 and 1997 for both Mean Grain Size and Sand/ Gravel composition.

| Site    | Zone | Mean grain size 2018 (mm) | Mean grain size 1997 (mm) |
|---------|------|---------------------------|---------------------------|
| KCK1870 | MT   | Granule (2.9)             | Very coarse sand (1.2)    |
|         | UF   | Granule (2.37)            | Very coarse sand (1.2)    |
| KCK2200 | MT   | Granule (2.6)             | Granule (3.1)             |
|         | UF   | Granule (3.02)            | Coarse sand (0.86)        |
| KCK2470 | MT   | Very small pebble (5.2)   | Small pebble (9.5)        |
|         | UF   | Very small pebble (4.67)  | Small pebble (13.3)       |
| KCK2486 | MT   | Very small pebble (4)     | Very small pebble (4.4)   |
|         | UF   | Very small pebble (4.17)  | Very small pebble (6.4)   |
| KCK2496 | MT   | Granule (2.1)             | Granule (2.8)             |
|         | UF   | Very small pebble (4.28)  | Granule (3.38)            |
| KCK2510 | MT   | Granule (2.2)             | Very small pebble (6.9)   |
|         | UF   | Very small pebble (4.42)  | Small pebble (8.75)       |
| KCK2550 | MT   | Very small pebble (6.0)   | Very small pebble (5.2)   |
|         | UF   | Very small pebble (4.34)  | Very small pebble (5.8)   |
| KCK2575 | MT   | Granule (3.6)             | Granule (3.3)             |
|         | UF   | Granule (3.81)            | Granule (2.91)            |
| KCK3659 | MT   | Granule (3.8)             | Granule (2.6)             |
|         | UF   | Very small pebble (4.98)  | Very small pebble (4.9)   |
| KCK3684 | MT   | Very small pebble (5.9)   | Very small pebble (6.5)   |
|         | UF   | Very small pebble (5.98)  | Small pebble (12.9)       |
| KCK3712 | MT   | Very small pebble (5.9)   | Small pebble (13)         |
|         | UF   | Small pebble (8.38)       | Medium pebble (16.7)      |
| KCK3737 | MT   | Very small pebble (6.9)   | Small pebble (8.6)        |
|         | UF   | Very small pebble (6.4)   | Medium pebble (18.04)     |
| KCK3800 | MT   | Very small pebble (4.4)   | Medium pebble (16)        |
|         | UF   | Very small pebble (4.05)  | Large pebble (45.7)       |
| KCK3855 | MT   | Very small pebble (7.8)   |                           |
|         | UF   | Granule (3.82)            |                           |
| KCK3950 | MT   | Small pebble (8.6)        | Granule (3.1)             |
|         | UF   | Granule (3.06)            | Very small pebble (6.09)  |
| KCK4220 | MT   | Very small pebble (5.3)   | Very coarse sand (1.3)    |
|         | UF   | Granule (2.12)            | Coarse sand (0.8)         |
| KCK4700 | MT   | Very small pebble (7.7)   | Medium pebble (28)        |
|         | UF   | Very small pebble (5.67)  | Granule (2.27)            |
| KCK5025 | MT   | Very small pebble (4.0)   | Granule (3.7)             |
|         | UF   | Granule (3.92)            | Large pebble (36)         |